



HAL
open science

Unraveling development and ageing dynamics of the rodent dentition

Pauline Marangoni

► **To cite this version:**

Pauline Marangoni. Unraveling development and ageing dynamics of the rodent dentition. Populations and Evolution [q-bio.PE]. Ecole normale supérieure de lyon - ENS LYON, 2014. English. NNT : 2014ENSL0965 . tel-01674158v1

HAL Id: tel-01674158

<https://theses.hal.science/tel-01674158v1>

Submitted on 2 Jan 2018 (v1), last revised 2 Jan 2018 (v2)

HAL is a multi-disciplinary open access archive for the deposit and dissemination of scientific research documents, whether they are published or not. The documents may come from teaching and research institutions in France or abroad, or from public or private research centers.

L'archive ouverte pluridisciplinaire **HAL**, est destinée au dépôt et à la diffusion de documents scientifiques de niveau recherche, publiés ou non, émanant des établissements d'enseignement et de recherche français ou étrangers, des laboratoires publics ou privés.

THÈSE

en vue de l'obtention du grade de

Docteur de l'Université de Lyon, délivré par l'École Normale Supérieure de Lyon

Discipline : Sciences de la vie

Laboratoire : Institut de Génomique Fonctionnelle de Lyon

École Doctorale : Biologie Moléculaire Intégrative et Cellulaire

présentée et soutenue publiquement le 05 décembre 2014

par Madame Pauline MARANGONI

**Unraveling development and ageing dynamics
of the rodent dentition**

Directeur de thèse : M. Laurent VIRIOT

Devant la commission d'examen formée de :

Mme. Ariane BERDAL	Rapporteur
M. Cyril CHARLES	Co-encadrant
M. Yann HERAULT	Examineur
M. Ophir D. KLEIN	Examineur
M. Frédéric MICHON	Rapporteur
M. Laurent VIRIOT	Directeur

*« La science, mon garçon, est faite d'erreurs, mais d'erreurs
qu'il est bon de commettre parce qu'elles mènent peu à peu à la vérité »*

Jules Verne (in *Voyage au centre de la Terre*, 1864)

As it is the tradition, I would like to start by thanking my two supervisors... Laurent, you made me enter the research world working on a biological question I did not even know I could be interested in. And here I am, about six years after you first talked to me about the importance of the fossil record in evolutionary biology. And then Cyril, we met in San Francisco where you let the chatty French intern crush on your coach. If I recall well, Laurent told me that it would be difficult to make you talk. I guess I am contagious. Thank you both for supervising me during this PhD, I really appreciated the independence you let me have, and I value the advices you gave me on the road.

I am also very grateful to the members of my jury, for having agreed to be part of this adventure. Ophir, thank you for coming such a long way just for my defense, it means a lot to me. Fred, thank you for having a nice word to say every single time, and for asking me questions that make me re-think entire parts of my projects in the blink of an eye. Yann, you monitored closely this PhD project, thank you for your advices during my PhD committee meetings, and thank you for being part of this jury to complete the circle! Ariane, I am very grateful that you agreed on coming, and I am looking forward to hearing your questions and remarks.

I am honored to have been part of the IGFL. During all the internships I performed at the old LR4, and in our shiny and new building, I have met and worked with amazing people. Starting with the team Evo-Devo of the Vertebrate Dentition. Béatrice, I am so sad that you will not be at my defense. It has been a pleasure sharing your office, talking about dance, cooking, theater, music, and occasionally about science! Johan, you are the PhD student in charge now, thanks for supporting me even in my poor sport choices ☺ Ana Rosa, this has been a real pleasure having you around, I will miss your accent for sure. Florence, you are officially my qPCR role-model. Thank you for being so kind with me. And of course, thanks to those who have already left the team, but are still present in our minds: Antoine, for the insightful discussions we have had, Helder, especially for the pep talk before my PhD funding examination, Manu, for the amazing ride to La Londe in that van, Maïtena, for your contagious laugh... I shall not forget Henry and Marie-Lise: your kindness is beyond words, and I really enjoyed working next to you. We all make a hell of a team, not quite conventional I have to admit, but who cares?

I value the time I spent with Guillaume, Mélisandre, Juli, and Julie. We all came here for various reasons, but at least we got to create friendships that will hopefully last longer

than our respective PhDs... Cyrielle & Domi (and of course Kévin & Jeff^o), please know that you're missed every single day, and that I cannot wait to be on the same continent than you! One last thing: when I grow up, I want to be just like you 😊 Delphine, thank you for being an active member of my PhD follow up committee. You have been incredibly supportive, and you helped me more than you can imagine. Thank you Sandrine and Benjamin for letting me be part of the sequencing platform experience, I really enjoyed working with you. Of course, I shall not forget our local Charlie's Angels: Martine, Joanne, Sarah, Sonia, Fabienne, you make our lives in the lab easier. Christian, thank you for being so kind with us. Roxane and Myriam, thanks for kindly answering all my PhD-related questions, we are lucky to have you. Kerstin, Adriane, Alice and Chunying, I am super impatient to be back, working with you the 1st time was great, so I have amazing expectations for the 2nd time to come! I also would like to thank Violaine Nicolas (MNHN) and Wim Wendelen (MRAC), for kindly letting me access collection specimens. Lastly, I am perfectly aware that I am here now because I have met amazing biology teachers who passed on their love for their subject to me: Mrs Gueth, Mr Vidal, thanks for supporting my crazy idea to become a researcher and helping me get there.

Of course, there are also people outside of the working sphere that I want to acknowledge, because despite a tight schedule, I have managed to meet, dance, sing, or just have fun with them. Lisou, Julie, Kévin, Guillaume, Nor', Nathalie, Cyrielle, Morgane, Greg, Camille, Wiki, Valentin, Léo, Loïc, Agnès, Sarah, Jérémy, Ellen, Hélène, MJ, Flo, Paulinette, Lise, Bibine, Bérénice, Férouze, Muriel, Sandra, Aurélien, Poulpi, Diane, Sam, Anneke, Jana, Eloïse, Manue, Estelle, you are the most wonderful friends anyone could ever ask for. Alberto, thank you for reminding me that what I love the most is to surpass myself; I cannot wait to be able to dance with you again. And of course, my sincerest apologies to those of you I might have forgotten while writing this, it's definitely harder than it seems...

Before closing this happy chapter of my thesis, let's be emotional for a little bit longer. Martin, thank you for going through my mood swings with a smile on your face. We don't know exactly what the future holds, but we will find a way. Mum and Dad, I am blessed to be your daughter. You taught me to work hard to get where I wanted to be, and I hope I did not disappoint. Thank you for always being so comprehensive with me. Anne-Claire, going through our PhD together was, for sure, the craziest experience we have ever had! Congrats again on your defense earlier this year, and a million thanks for all your help.

Now, back to work...

UNRAVELING DEVELOPMENT AND AGEING DYNAMICS OF THE RODENT DENTITION

The evolution of the vertebrate dentition is among the most exciting topics in the evo-devo field, with particular attention being drawn to the mouse model. The mouse dentition includes four ever-growing incisors and twelve molars with a specific cusp pattern. Incisors and molars develop according to a tightly regulated molecular network.

The ERK-MAPK cascade is involved at various stages of tooth development. Molar tooth phenotype comparisons in mutant mice for genes acting at various levels of the cascade highlighted a dental phenotype signature, which consists in the presence of a supernumerary tooth and shared cusp pattern defects. Some of these recall characters present in fossil rodents, supporting the ERK-MAPK as a good candidate to explain some evolutionary trends of the rodent dentition. By working on a mouse line over-expressing one of this pathway inhibitor in the oral epithelium, I perfect our understanding of Fgf gene role in specifying signaling center formation at the right stage, and in achieving correct mineralization.

When considering evergrowing incisors, mouse dentition is also dynamic at the lifetime scale. I monitored the ageing process of the mouse upper incisors, and provided a chronology of occurrence of the variety of age-related defects display. These defects are set up from the six months on, the most frequent abnormality being the presence of an enamel groove along the surface of the incisor. Using Next Generation Sequencing technologies, I detected transcriptomic changes in the stem cell niches affecting cell proliferation and metabolism, as well as the stem cell niche functioning. The correlation found between the groove occurrence and a large immune response in dental tissues expands our concern for dental stem cell ageing.

KEY WORDS

Rodent dentition, ERK-MAPK pathway, comparative dental anatomy, incisor
stem cell niches, ageing, gene expression profile

TABLE OF CONTENTS

List of the tables and figures

Introduction & objectives	1
Part A: Tooth evo-devo and the RTK/ ERK-MAPK pathway	iii 7
A.1 <i>Rsk2</i> is a modulator of tooth development	12
A.1.1 Material and methods	13
A.1.2 Results	
A.1.3 Discussion	13
A.1.4 Conclusions	16
	18
A.2 Unraveling the evolutionary potential of the ERK-MAPK pathway .	19
<u>Article</u> : Phenotypic and evolutionary implications of modulating the ERK-MAPK cascade using the dentition as a model	20
A.3 Modulations of tooth development in K14-<i>Spry4</i> mice .	48
<u>Article</u> : Implications of FGF signaling pathway in tooth shape and mineralization: insights from the K14- <i>Spry4</i> transgenic mice	50
A.4 Conclusions	73
	75
Part B: Rodent incisors: evolution, diversity & ageing	
B.1 Inter- and intra-specific variation of the rodent incisors	79
B.1.1 Morphometrics	80
B.1.2 Incisor ornamentation	
B.1.3 Color	81
	85
B.2 Phenotypic disruptions of the upper incisors in ageing mice	87
<u>Article</u> : Disruption of the incisor stem cell niches in ageing mice	89
	110
B.3 Transcriptomic disruptions of the upper incisor in ageing mice	
<u>Article</u> : Independent transcriptomic analyses reveal gene expression changes in ageing mouse incisor stem cell niches	111
B.4 Conclusions	154
General conclusion & Perspectives	157
References	161

Annexes	179
Annex 1: Continuous dental replacement in mammals .	179
Annex 2: <i>Rsk2</i> and the mouse craniofacial development	191
Annex 3: Control of the incisor number by Sprouty genes	213
Annex 4: Collection numbers of the rodent specimens coming from natural history museums	231

List of the Tables and Figures

Introduction & objectives

- FIG. 1: Simplified view of dental evolution in mammals 3
- FIG. 2: X-ray microtomographic view of a mouse skull 5

Part A: Tooth evo-devo and the RTK/ ERK-MAPK pathway

- FIG. A.1: Mouse first lower molar development 9
- TAB. A.1: The expression of RTK-activated MAPK-ERK cascade members, modulators and effectors during mouse tooth development 10
- FIG. A.2: Simplified view of the ERK-MAPK cascade . 11

A.1 *Rsk2* is a modulator of tooth development

- FIG. A.3: Variation of molar shape and number in *Rsk2*^{-Y} and *Rsk1,2,3* null mice analyzed by X-ray microtomography 14
- FIG. A.4: Comparison of molar length (mesio-distal distance) and width (vestibulo-lingual distance) in the *Rsk2*^{-Y} sample 15
- FIG. A.5: Variation of M¹ root slope in *Rsk2*^{-Y} mice 16

A.2 Unraveling the evolutionary potential of the ERK-MAPK pathway

Article: Phenotypic and evolutionary implications of modulating the ERK-MAPK cascade using the dentition as a model

- Fig. 1: Dental character matrix. 27
- Fig. 2: Molar tooth proportions in the *Spry1*^{-/-}, *Spry2*^{-/-}, *Spry4*^{-/-} and *Rsk2*^{-Y} mutant mice 30
- Fig. 3: Abnormal phenotype in the *Spry1*^{-/-}, *Spry2*^{-/-}, *Spry4*^{-/-} and *Rsk2*^{-Y} mutant mice 31
- Fig. 4: ST phenotype and surface in the *Spry2*^{-/-}, *Spry4*^{-/-} and *Rsk2*^{-Y} mutant mice 33
- Suppl. Fig. 1: Details of some shared mutant features in the *Rsk2*^{-Y} mice 35
- Fig. 5: Mutant dentition recapitulates the evolution of murine tooth characters 41

A.3 Modulations of tooth development in K14-*Spry4* mice

Article: Implications of FGF signaling pathway in tooth shape and mineralization: insights from the K14-*Spry4* transgenic mice

Fig. 1: Most prevalent phenotypes in the K14- <i>Spry4</i> mice compared to the phenotype of their WT littermates	57
Fig. 2: Additional cusp defects in the transgenic M ¹ and M ₁	58
Fig. 3: Comparison of the molar surface in the transgenic to the molar surface of their WT littermates	59
Fig. 4: Comparison of transgenic and WT first molar histo-morphogenesis from the bud to prior to the bell stage	60
Fig. 5: Abnormal shape of the transgenic molar germ cervical loops	61
Tab. 1: Evolution of both the proportion of transgenic embryos in the collected litters, and the mean number of embryos per stage	62
Fig. 6: <i>Shh</i> gene expression variations in the lower tooth germ	63
Fig. 7: Fusion of the upper and lower jaws in the transgenic mice	64

A.4 Conclusions

Part B: Rodent incisors: evolution, diversity & ageing

FIG. B.1 Development of the mouse lower incisor	75
FIG. B.2 Incisors are asymmetric teeth	76

B.1 Inter- and intra-specific variation of the rodent incisors

FIG. B.3: Differential insertion of the upper incisors in various rodent species	81
FIG. B.4 Presence of enamel groove across the rodent phylogeny	83
FIG. B.5 Diversity of grooved incisor phenotype among the order Rodentia	84
FIG. B.6 Inter- and intra-specific variation in the color of the rodent incisor enamel	86

B.2 Phenotypic disruptions of the upper incisors in ageing mice

Article: Disruption of the incisor stem cell niches in ageing mice

Fig. 1: Mouse incisors are asymmetric teeth that continuously grow throughout the lifespan of the animal	91
Fig. 2: Mouse upper incisors display various age-related abnormalities from about 6 months of age onwards	95
Fig. 3: Enamel grooves are reversible age-related abnormalities	96
Suppl. Fig. 1: Grooves are traceable to the growth region	97
Fig. 4: X-ray microtomography allows a better characterization of the possible age-related abnormalities found in mice	98
Fig. 5: <i>Psammomys obesus</i> also displays age-related abnormalities on its upper incisors	99
Fig. 6: Upper incisor elongation continuously progresses as the mouse ages	100
Fig. 7: A fold in the ameloblast layer causes enamel groove	102

Fig. 8: Abnormalities of tissue organization can be detected in the growth region and the ameloblast layer even when the protruding phenotype appears normal 103

B.3 Transcriptomic disruptions of the upper incisor in ageing mice

Article: Independent transcriptomic analyses reveal gene expression changes in ageing mouse incisor stem cell niches

Fig. 1: Schematized organization of the upper incisor growth region, and age- related defects. 114

Fig. 2: Comparison of the two experimental strategies 117

Suppl. Tab. 1: List of the primers used for RT-qPCR validation of the candidate gene expression levels 121

Tab. 1: Number of differentially expressed genes in the growth region transcriptomic analysis 123

Fig. 3: Genetic variation and differentially expressed genes depending on the specimen age 125

Tab. 2: Number of differentially expressed genes in the entire incisor transcriptomic analysis 127

Fig. 4: Genetic variation and differentially expressed genes depending on the specimen age and phenotype 128

Tab. 3: Genes of interest to understand the molecular impact of ageing on the stem cell niches, and the setting of the aplastic groove 130

Suppl. Tab. 2: List of the differentially expressed genes between two age conditions from the growth region transcriptomic analysis 131

Suppl. Tab. 3: List of the genes differentially expressed between two age conditions from the entire incisor transcriptomic analysis 132

Suppl. Tab. 4: List of the genes differentially expressed in the presence or the absence of aplastic groove 133

B.4 Conclusions

General conclusion & Perspectives

References

Annexes

INTRODUCTION & OBJECTIVES

Since the very first steps of vertebrate paleontology (Cuvier, 1812), the comparative anatomy of teeth and dentitions occupies a very important position in mammal paleobiology. This status stands for several reasons: firstly because teeth are made of the hardest mineralized tissues of the body and as a consequence often become selectively preserved in comparison with other parts of the skeleton during fossilization; secondly because teeth – and especially postcanine teeth (premolars and molars) – provide appropriate characters to study mammalian diet, taxonomy and evolution (Gregory, 1934; McKenna, 1975). Given the morphological diversity among extant species and the available fossil record, biologists and paleobiologists have started to address the question of the mechanisms underlying the setting up of the mammalian dental diversity.

To understand the basis of mammal dental evolution, it is necessary to consider mammals in the larger framework of the synapsid evolution, thus supplementing the living species with many extinct taxa with no current descendants. The earliest members of the lineage leading to mammals lived about 300 million years (Ma) ago (Pough *et al.*, 2005). They displayed a dentition made up of numerous simple, conical and pointed teeth (haplodonty), which were almost identical along the tooth row (homodonty), and which were continuously replaced throughout their life (polyphyodonty) (Ungar, 2010). The earliest mammals *sensu lato*, known at about 200 Ma, had a dentition made of teeth with various shapes (heterodonty) including tricuspid postcanine teeth (plexodonty) that were replaced

once during their lifetime (diphyodonty) (Luo *et al.*, 2004). Further evolutionary trends of the dentition from these earliest mammals *sensu lato* to the placental mammals (eutherians) is characterized by a reduction of the dental formula coupled with a specialization of postcanine teeth leading to the acquisition of the mammalian mastication (Weijjs, 1994). Basal eutherians had a fixed maximal number of teeth (FIG. 1A) and this number continuously decreased over the evolution of most modern eutherian groups such as euarchontoglires (FIG. 1B). Along with this decrease, a higher specialization of the postcanine teeth (especially the molars) was achieved.

Mammals thus progressively acquired a limited dentition replacement, a sectorization of the dentition into three dental types (incisor, canine and postcanine), as well as an increased complexity of their postcanine crown pattern. Because the various steps of these evolutionary processes are only documented by fossils, the evolution of the mammalian dentition has first mainly interested paleontologists, and for the past two decades this interest has expanded to the evo-devo community.

Evo-devo is a dual discipline that compares individual development with phenotypic changes during evolution (Müller, 2007). In order to understand how evolution acted on the biological properties of extinct and extant species, investigations aim at understanding how developmental processes are set up and modulated in extant species. Established correlations allow us to infer that similar processes were acting in the course of evolution (Carroll, 2008). Besides being a major tool to study mammalian evolution, teeth are also a well-studied example of ectodermal organs arising from the interaction of an epithelial layer with the underlying mesenchyme, similarly to many exocrine glands, feathers, scales, nails, and hair (Pispa and Thesleff, 2003).

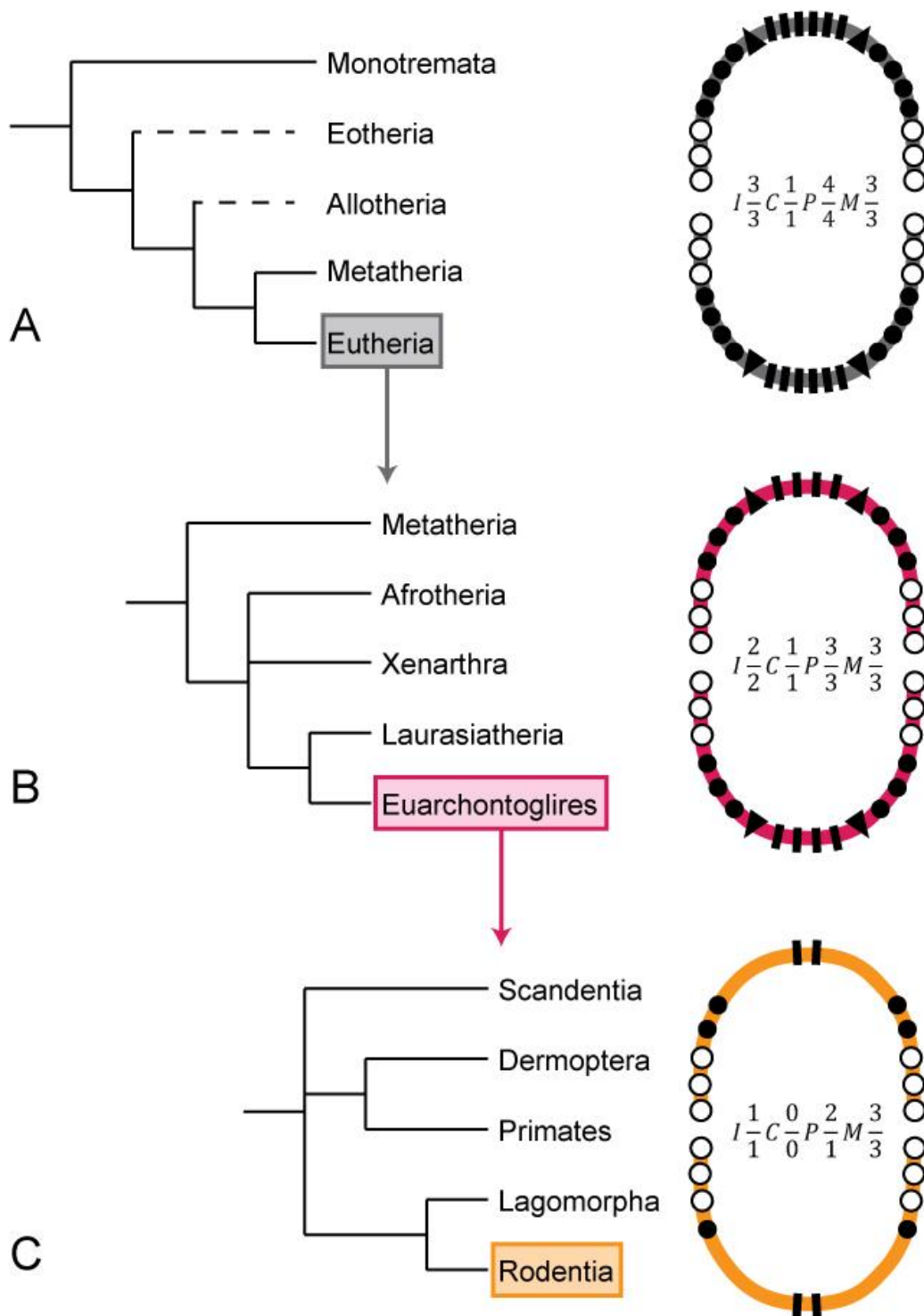


FIG. 1: Simplified view of dental evolution in mammals. Phylogenies are simplified from Bininda-Edmonds *et al.* 2007. (A) Phylogeny and maximal dental formula in mammalian infraclasses. (B) Phylogeny and maximal dental formula of the various eutherian superorders. (C) Euarchontoglire order Phylogeny and maximal dental formula in the various euarchontoglire orders. I – rectangles: incisors, C – triangles: canines, P – black circles: premolars, M – white circles: molars.

Historically, the evo-devo community first asserted itself by comparing various body plans and analyzing the importance of toolkit genes in setting them (Duboule and Dollé, 1989). Dental evo-devo rapidly grew as a major focus of the discipline. As the field developed, a new interest arose on the genetic and epigenetic determination of odontogenesis (Maas and Bei, 1997; Peters and Balling, 1999; Jernvall and Thesleff, 2000; Thesleff, 2003; Tucker and Sharpe, 2004; Catón and Tucker, 2009; Jheon et al., 2011), and computational tools helped to better understand the evolution of dentition features (Salazar-Ciudad and Jernvall, 2010). Since there are about 5,500 species of mammals (Wilson and Reeder, 2005), researchers have to focus on a few species and use them as proxies to collect data (Minelli and Baedke, 2014). A classic extrapolation has been to work on rodents. Indeed, the order Rodentia is a rather large order encompassing about 40% of all mammal species diversity (Wilson and Reeder, 2005). This order – and especially murine rodents – shows a reduction of the maximal dental formula compared to the euarchontoglires (FIG. 1C). Rodents gained the status of well-established mammal representatives within the “tooth community” because of the very interesting dental diversity they display, but also because one of their members, the mouse (*Mus musculus*) has been used as a model for mammalian development for decades (Hedrich, 2004).

Mice are extremely derived in terms of dentition properties. They display only one highly specialized continuously growing incisor, as well as three complex molars that are not replaced per jaw quadrant (FIG. 2). If rare mammalian species display continuous dental replacement (see annex 1: Rodrigues *et al.*, 2011), monophyodonty marks the final limitation in tooth renewal, and is observed in many taxa including muroid rodents, bats or shrews (Jernvall and Thesleff, 2012). Mouse dentition recapitulates the evolutionary trends that are characteristic of mammalian dental evolution, and as a consequence, the understanding of this evolutionary dynamics is of prime interest.

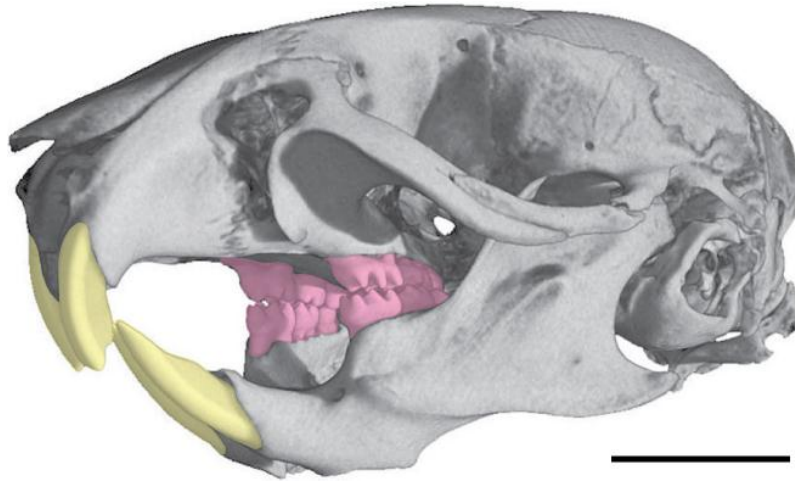


FIG. 2: X-ray microtomographic view of a mouse skull. Incisors (yellow) and molars (pink) are separated by a toothless gap called diastema. Scale bar: 0.5 mm.

The present work aims at addressing two levels of mouse dentition dynamics: (1) the evolutionary dynamics of tooth number determination and shape setting in the postcanine area, and (2) the lifespan dynamics of the continuously growing incisors. Using a classic evo-devo approach on postcanine tooth number and shape, I first tackle the evolutionary potential of the well-documented FGF-activated ERK-MAPK pathway. This is an example of huge signaling pathway modulating most of the cellular processes, also involved at various stages of tooth development (Laugel-Haushalter *et al.*, 2014). By scrutinizing the dentition of mice bearing mutation for various genes expressed in the same signaling pathway, I address the effects of genes acting at different steps of the pathway. From the mineralized tooth phenotype, I draw conclusions regarding the plausible evolutionary relevance of these genes. In a second part, I focus on the mouse continuously growing incisors. By looking at the diversity they display in terms of ornamentation, color and shape, I highlight their importance in the evo-devo field. Switching focus to the modification of their phenotype during the animal lifetime, I address the question of stem cell ageing in combining traditional *in vivo* monitoring and histological studies with cutting-edge transcriptomics to provide a further insight into the use of the mouse model.

PART A

TOOTH EVO-DEVO & THE
RTK/ERK-MAPK
PATHWAY

Organogenesis is one major step achieved during the development of a given organism. It is a dynamic and complex succession of molecular and cellular events leading to the organ identity, properties and functions. The mechanisms involved are well-conserved in all vertebrates. The organs undergoing budding and branching morphogenesis develop according to a series of morphogenetic changes similar to what has been well-documented in the mouse molars.

Tooth development (odontogenesis) is ruled by specific time-space interactions between the oral epithelium of the first branchial arch and the underlying mesenchyme deriving from the neural crests (Peters and Balling, 1999). Odontogenesis begins with a succession of histo-morphogenetical transformations named from the shape of the dental epithelium (FIG. A.1). Mouse gestation lasts around 20 days, and tooth development is initiated around Embryonic day 9.5 (Tucker and Sharpe, 2004). The secretion of growth factors combined with the activity of transcription factors in both upper and lower cheek teeth presumptive areas induces cell proliferation in both odontogenic epithelium and underlying mesenchyme (Thesleff, 2003). The first histo-morphogenetical sign of tooth development is the thickening of the dental epithelium until it reaches the placode stage. Then the placode grows toward the mesenchyme to form a bud (E13). At that stage, two distinct populations of epithelial cells can be observed: (1) a well-organized basal epithelium which remains at the interface with the odontogenic mesenchyme, and (2) a loosely arranged group of cells located towards the mouth cavity called *stellate reticulum*. Later on, the basal surface of the bud invaginates at its lingual and vestibular ends (cervical loops) as the underlying dental mesenchyme condenses. At the cap stage, the primary enamel knot (pEK, dark blue in FIG. A.1) forms in the basal dental

epithelium (Jernvall *et al.*, 1994; Jernvall *et al.*, 1998; Vaahtokari *et al.*, 1996a; Vaahtokari *et al.*, 1996b). The pEK is a dense non-proliferative group of cells secreting many molecules including Sonic Hedgehog (SHH), Fibroblast Growth Factors (FGFs), Bone Morphogenetic Proteins (BMPs) and WNTs (Thesleff *et al.*, 2001). The combination of these molecules plays a major role in inducing the proliferation of surrounding cells, and thus in initiating the presumptive crown shape (Coin *et al.*, 1999). From that stage on, odontogenesis is ruled by this epithelial signaling center.

Then, the cervical loops continue to expand into the mesenchyme, and the cap takes a bell shape. As the cytodifferentiation goes further, secondary enamel knots (sEKs, light blue in FIG. A.1) are formed at the top of the presumptive cusps (Tucker and Sharpe, 2004). At the late bell stage, the dimensions of the presumptive crown are set and the mineralization of the secreted dentin and enamel matrixes starts (Tucker and Sharpe, 1999). These matrixes are respectively secreted by odontoblasts and ameloblasts, two cell types which constitute the epithelio-mesenchymal interface (Arana-Chavez and Massa, 2004; Goldberg *et al.*, 2002). Ameloblasts derive from the basal epithelial layer, while odontoblasts derive the mesenchymal dental papilla (Thesleff *et al.*, 2001). By the end of this sequence, the crown formation is achieved. After the eruption (starting at about postnatal day 10 for the first molar) is achieved, the mouse possesses one incisor separated from three molars by a toothless gap called diastema in each dental quadrant (Nanci, 2007). Incisor development follows the same overall developmental series, the specificities of which will be discussed below.

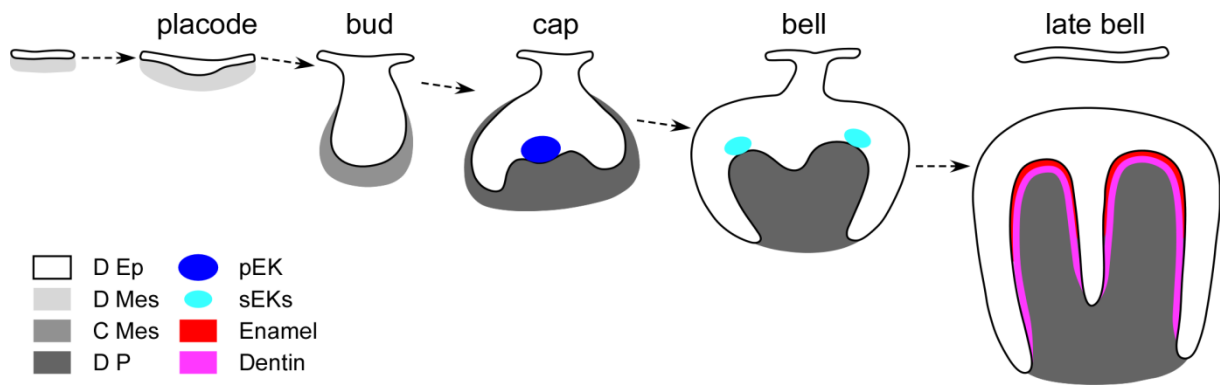


FIG. A.1: Mouse first lower molar development. The dental germ undergoes successive histomorphogenetical modifications leading to formation of a mineralized matrixes-covered tooth ready to erupt. D Ep: dental epithelium; D Mes: dental mesenchyme; C Mes: condensed mesenchyme; D P: dental papilla; pEK: primary enamel knot; sEKs: secondary enamel knots.

This sequence of morphological changes is driven by precise molecular networks acting together to tightly regulate its successive steps (Bei, 2009). One example of important network is the extracellular signal-regulated kinase/mitogen-activated protein kinase (ERK-MAPK) signaling pathway that can be triggered by receptor tyrosine kinase (RTK) activation. This cascade has the specificity of encompassing two signaling pathways necessary for proper tooth development: FGF signaling pathway (Li et al., 2014), and the ERK signaling pathway (Corson et al., 2003). Numerous RTK-activated ERK-MAPK members are expressed in dental tissues. They have been demonstrated to act during tooth development (TAB. A.1).

In Part A, I address the developmental and the evolutionary potential of this RTK-activated ERK-MAPK cascade during odontogenesis. The fixation of a growth factor (GF) on its RTK triggers the phosphorylation of successive kinases down to the final activation of effective kinases, as well as the expression of transcription factors (Sebolt-Leopold and Herrera, 2004, see FIG. A.2).

	MOLAR						INCISOR																					
	in.		placode		bud		cap		bell		diff.		in.		placode		bud		cap		bell		diff.					
	E	M	E	M	E	M	E	M	E	M	E	M	E	M	E	M	E	M	E	M	E	M	E	M				
<i>Egf</i>																												
<i>Egr1</i>	-	-	-	-	-	+	+	+	+	+	+	+	+															
<i>Fgf1</i>			+	+	+	+	+	+	+	+	+	+	+															
* <i>Fgf2</i>			+	+			+	-	+	+	+	-																
<i>Fgf3</i>	-	-	-	-	+	+	+	+	-	+	-	-																
<i>Fgf4</i>	-	-	-	-	+	-	+	-	+	-	-	-	-	-	-	-	+	-	+	-	-	-	-	-				
<i>Fgf7</i>	-	-	-	-	-	-	-	-	-	-	-	-												-	+			
<i>Fgf8</i>	+	-	+	-	-	-	-	-	-	-	-	-	+	-	+	-	-	-	-	-	-	-	-	-				
<i>Fgf9</i>	+	-	+	-	+	-	+	+	+	-	+	-	+	-	+	+	+	+	+	+	-	-	+	-				
<i>Fgf10</i>	+	+	-	+	-	+	-	-	-	+	-	-																
<i>Fgf15</i>	-	-	+	-	-	-	+	-	-	+	-	-																
<i>Fgf16</i>	-	-	-	-	-	-	+	+	+	-	+	-																
<i>Fgf17</i>	+	-	-	-	-	-	+	+	-	-	-	-																
<i>Fgf18</i>	-	-	-	+	-	+	-	+	-	-	-	-																
<i>Fgf20</i>	-	-	+	-	+	-	+	-	+	-	-	-																
<i>Fgfr1IIIb</i>	-	-	-	-	-	-	+	-	+	+	+	+												+	+			
<i>Fgfr1IIIc</i>	-	+	-	+	-	+	+	+	+	+	+	+													+	+		
<i>Fgfr2IIIb</i>	+	-	+	-	+	-	-	-	-	-	-	-													+	-		
<i>Fgfr2IIIc</i>	-	-	-	-	-	+	+	+	-	+	-	-													+	-		
<i>Fgfr3IIIb</i>																									-	+		
<i>Fgfr3IIIc</i>	-	-	-	-	-	-	-	-	-	-	-	-													-	+		
<i>Fgfr4</i>	-	-	-	-	-	-	-	-	-	-	-	-																
° <i>Tgfb1</i>			-	-	+	+	+	-	-	+	+	+																
<i>Tgfb2</i>					-	-				-	+																	
<i>Tgfb3</i>					-	-	+	-	+	-	+	+																
<i>Tgfbr2</i>					-	+	-	+																				
<i>Rasa3</i>																										+	+	
<i>Hras1</i>																										+	-	
<i>Rsk1</i>					+	+	+	-	+	-	+	-	+	-	+	-	+	-	+	+	+	+	+	+	+	+	+	
<i>Rsk2</i>					-	+	-	+	-	+	-	+	-	+	-	+	-	+	-	+	-	+	-	+	-	+	+	
<i>Rsk3</i>					+	+	-	+	-	+	-	+	-	+	-	+	-	+	-	+	-	+	-	+	-	+	-	
<i>Rsk4</i>					+	-	+	-	+	-	+	-	+	-	+	-	+	-	+	-	+	-	+	-	+	-	+	
<i>Spry1</i>					-	-	+	+																			+	+
<i>Spry2</i>							+	-																			+	-
<i>Spry4</i>							-	+																			-	+

TAB. A.1: The expression of RTK-activated MAPK-ERK cascade members, modulators and effectors during mouse tooth development. The table summarize the detection (+) or absence (-) of gene expression during molar and incisor development. in.: initiation; diff.: differentiation; E: epithelium; M: mesenchyme; *: the fixation method used might impair the results reported; °: discrepancies can be found in the literature. Table compiled from Snead *et al.*, 1989; Pelton *et al.*, 1991; Vahtokari *et al.*, 1991; Cam *et al.*, 1992; Karavanova *et al.*, 1992; Wang *et al.*, 1995; Vahtokari *et al.*, 1996; Peters *et al.*, 1992; Orr-Urtreger *et al.*, 1993; Jernvall *et al.*, 1994; Bei and Maas 1998; Jernvall *et al.*, 1998; Kettunen and Thesleff 1998; Kettunen *et al.*, 1998; Xu *et al.*, 1998; Kettunen *et al.*, 2000; Zeniou *et al.*, 2002; Kohn *et al.*, 2003; Åberg *et al.*, 2004; Klein *et al.*, 2006; Porntaveetus *et al.*, 2011; Laugel-Haushalter *et al.*, 2014; Li *et al.*, 2014; and the Eurexpress project website www.eurexpress.org/ee/ (Diez-Roux *et al.*, 2011). In black are members of the pathway, and in gray some of their modulators.

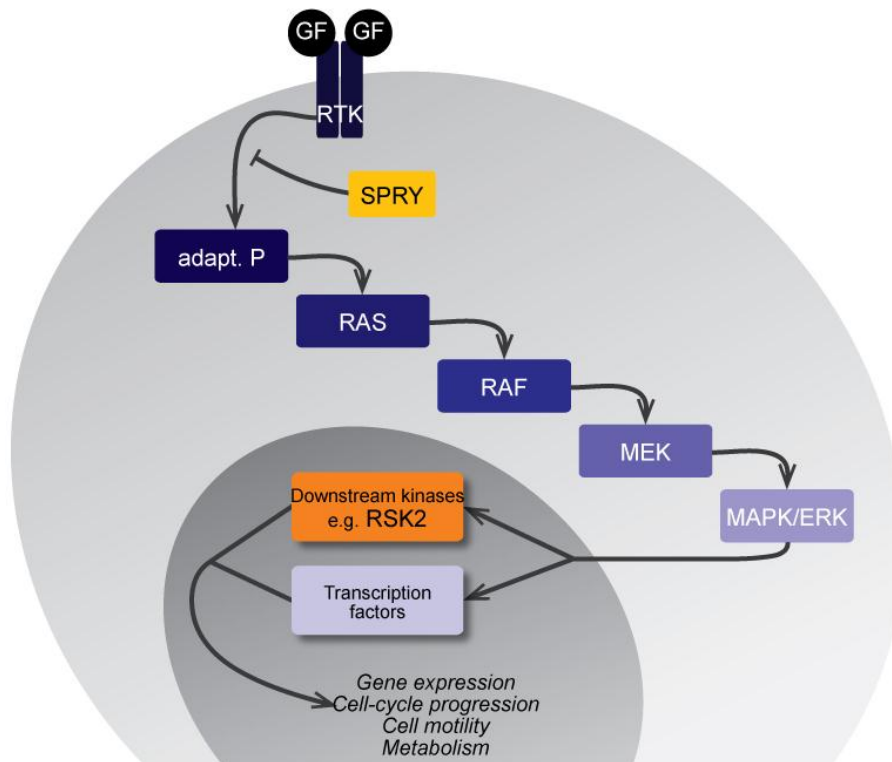


FIG. A.2: Simplified view of the ERK-MAPK cascade. Growth factors binding their receptor (RTK) trigger the activation of the phosphorylation cascade down to the final activation of the pathway effectors. This pathway regulates most of the cellular processes, including gene expression, cell cycle progression, cell motility and metabolism. Our interest is drawn to the Sprouty family (Spry) of RTK inhibitors (yellow), and to one of the effector kinase RSK2 (orange).

I take advantage of the availability of mutant mice for upstream regulator of RTKs (SPRY, yellow in FIG. A.2), and for a downstream effector kinase (RSK2, orange in FIG. A.2) to compare their adult dental phenotypes. By examining the presence of common phenotypes, I address plausible evolutionary role of the cascade in building the dentition of modern mice. I start with a conventional approach on knockout (KO) mice to characterize *Rsk2* action on craniofacial development, and more specifically on tooth formation. Then, I compare the *Spry1*, *Spry2*, and *Spry4* mutant molar phenotypes to the one of *Rsk2*^{-Y} mice. In order to perfect our understanding of the role of ERK-MAPK cascade members, I lastly investigate molar phenotype in transgenic mice over-expressing the *Spry4* gene in the oral epithelium.

A.1 *RSK2* IS A MODULATOR OF TOOTH DEVELOPMENT

This part of my work focuses on a study realized in collaboration with a team of the Developmental Biology and Stem Cells department from the IGBMC (Illkirch, France) published earlier this year in *PLoS One* (see annex 2: Laugel-Haushalter *et al.*, 2014). The study aims at addressing the role of *Rsk2* gene in mouse craniofacial development in order to question the relevance of *Rsk2*^{-Y} and *Rsk1,2,3* null mutants as models for the X-linked craniofacial disorder called Coffin-Lowry syndrome (OMIM #303600). Mutations in *RSK2* gene are responsible for the development of this syndrome in human (Trivier *et al.*, 1996; Jacquot *et al.*, 1998; Delaunoy *et al.*, 2001). The disorder has an estimated prevalence of 1 in 40,000 to 50,000 people, with females displaying a higher feature variability than males (Hanauer and Young, 2002). Clinically, some defects resulting from this syndrome are detectable at birth, while others will progressively be established until the patient reaches the age of 2 (Hunter, 2002). Growth defects, skeletal and craniofacial *dysmorphia*, as well as mental retardation make up the wide range of features associated with the syndrome (Hanauer and Young, 2002; Herrera-Soto *et al.*, 2007).

Our collaborators analyzed the skull phenotype of the two *Rsk* mutant mice, and they designed a microarray experiment to address molecular changes in the regulatory network. I aimed at documenting adult molar phenotype in *Rsk2*^{-Y} as well as triple *Rsk1,2,3* KO mutants in order to complete the description of *Rsk2* gene role in craniofacial development.

A.1.1 Material and methods

A first cohort of 6 *Rsk2*^{-Y} male mice and 6 WT littermates has been studied. They have been bred at the IGBMC mouse breeding facility (Illkirch, France). A second cohort including 7 *Rsk1,2,3*^{-/-} compound mutants was also provided to us. Molar rows were imaged using high-resolution X-ray microtomography with the Nanotom S (GE) equipment available at the UMS3444 (Lyon). A cubic voxel of 3µm was used. 3D-reconstructions from the acquired 2,000 projections were obtained using datavox software and algorithm with a beam hardening correction. Pictures of the reconstructed molar row were taken in occlusal view to observe dental features of each specimen. Measures of the tooth length (mesio-distal distance) and width (vestibule-lingual distance) have been made on occlusal-oriented pictures of the molar rows. Statistical significance of the measures has been verified using the Student t-test for 2 group comparisons, with a *p-value* threshold of 0.05.

A.1.2 Results

Despite the absence of abnormal phenotype in incisors, defects are seen in the molar rows. The most striking abnormality observed in both *Rsk2*^{-Y} and *Rsk1,2,3* null mutant mice is the presence of a ST in both upper and lower jaws (arrowheads, FIG. A.3). This extra tooth is erupted in alignment with the molar row, in a mesial position. The upper ST occurs in 65% of *Rsk2*^{-Y} mice and in 83% of the compound mutant mice. The lower ST occurs in 31% of the simple mutant mice and in 11% of the *Rsk1,2,3* null mice. Overall, the shape of the ST ranges

from a moncuspid tooth to complex molar-like tooth. The inactivation of *Rsk2* alone is sufficient to generate the abnormal ST-displaying phenotype. It is also sufficient to alter tooth proportions (FIG A.4). In compound mutants, the M^3 is absent in 39% of the specimens (e.g. 1283 in FIG. A.3). The absence of any tooth socket calls for agenesis, which is a missing tooth due to a developmental failure.

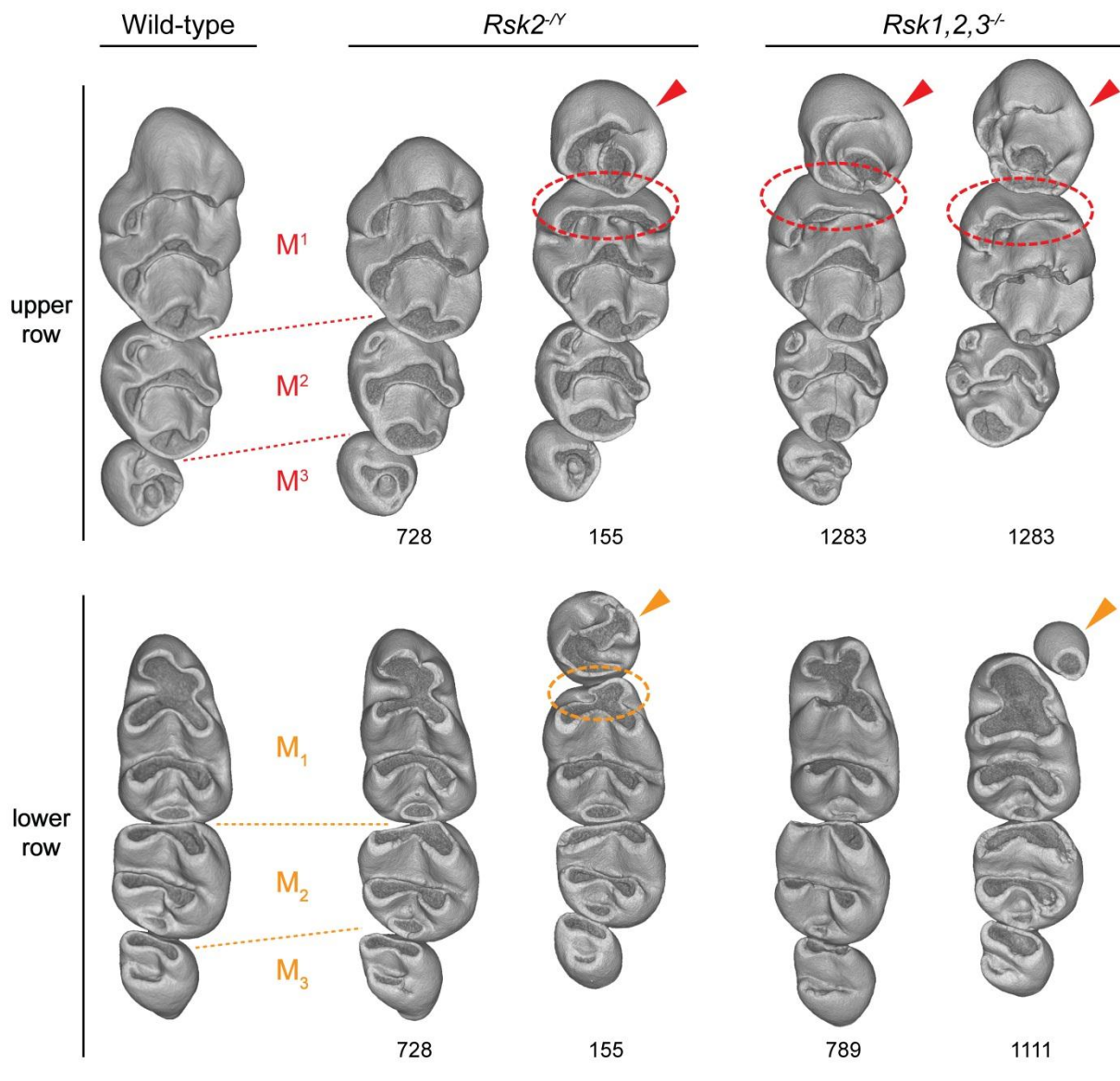


FIG. A.3: Variation of molar shape and number in *Rsk2*^{-/-} and *Rsk1,2,3* null mice analyzed by X-ray microtomography. All molar rows are similarly oriented (top corresponds to mesial, and left to lingual side). On the left are WT molars, other rows are mutant molars as indicated. Arrowheads point to ST; dotted ellipses show the reduction of the mesial-most affected cusp. Numbers refer to specimen ID. Scale bar: 0.7 mm.

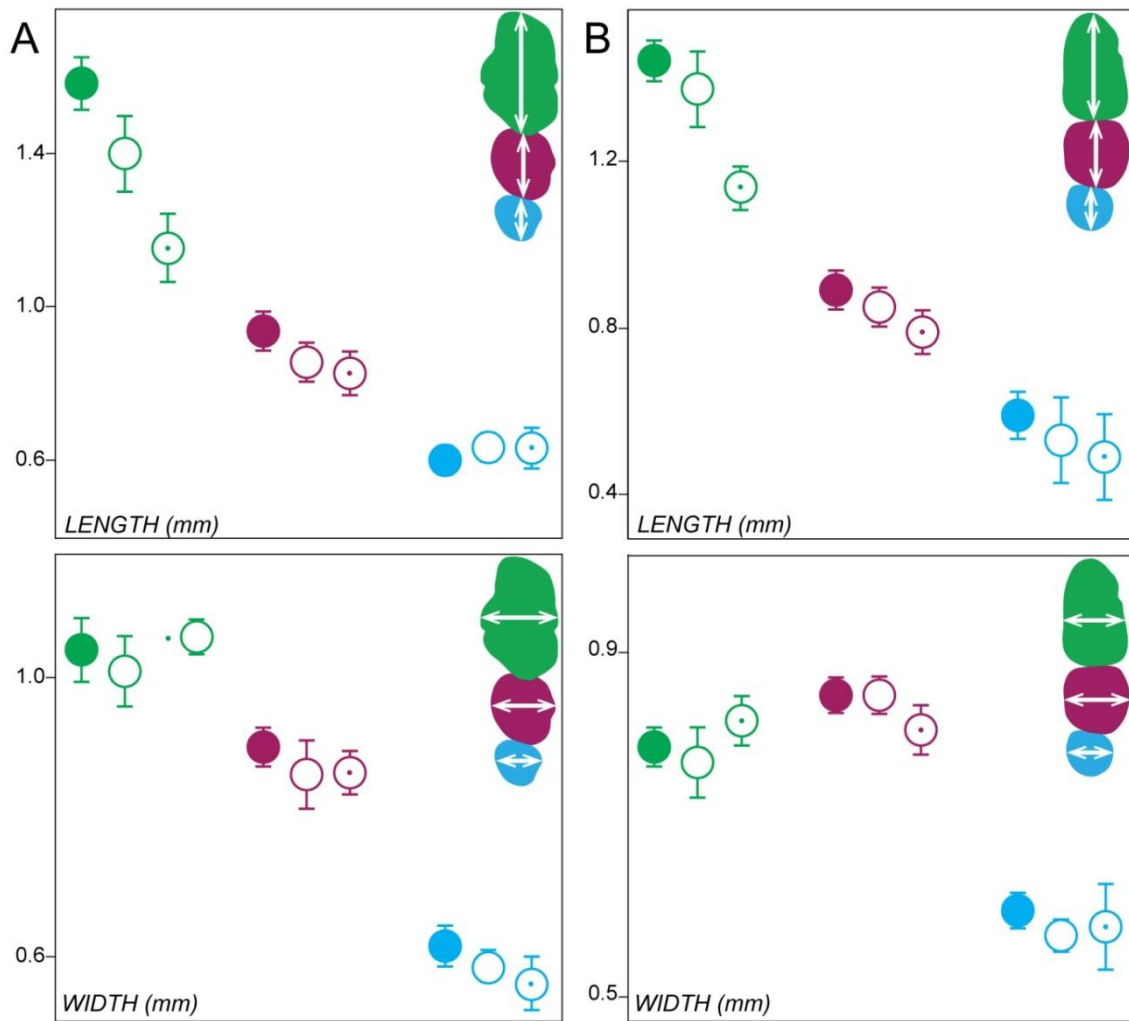


FIG. A.4: Comparison of molar length (mesio-distal distance) and width (vestibulo-lingual distance) in the *Rsk2*^{-Y} sample. A: measurements in the upper rows; B: measurements in the lower rows. WT tooth are depicted with filled circles, *Rsk2*^{-Y} without ST with blanked circles, and *Rsk2*^{-Y} with ST with blanked circles with a dot. Overall, the biggest changes in tooth proportions occur on both M¹ and M₁. Error bars represent the measurement standard deviation.

Shape abnormalities mainly occur in the mesial-most chevron of both M¹ and M₁. Indeed, in both mutant backgrounds, the first chevron appears flattened when a ST occurs (dotted ellipses, FIG. A.3). In the upper jaw, a similar yet less pronounced flattening is also observed in some specimens that do not display any ST (e.g. 728 in FIG. A.3). I found this character to be correlated with the inclination of the M¹ main root (FIG. A.5). Only *Rsk2*^{-Y} mutants display the 3 phenotypes depicted. When the root tends to be set vertically, the first

chevron appears straighter, reducing its size in occlusal view. In the lower molar rows, flattening is only seen when a complex-shaped ST occurs (e.g. 155 in FIG.A.3).

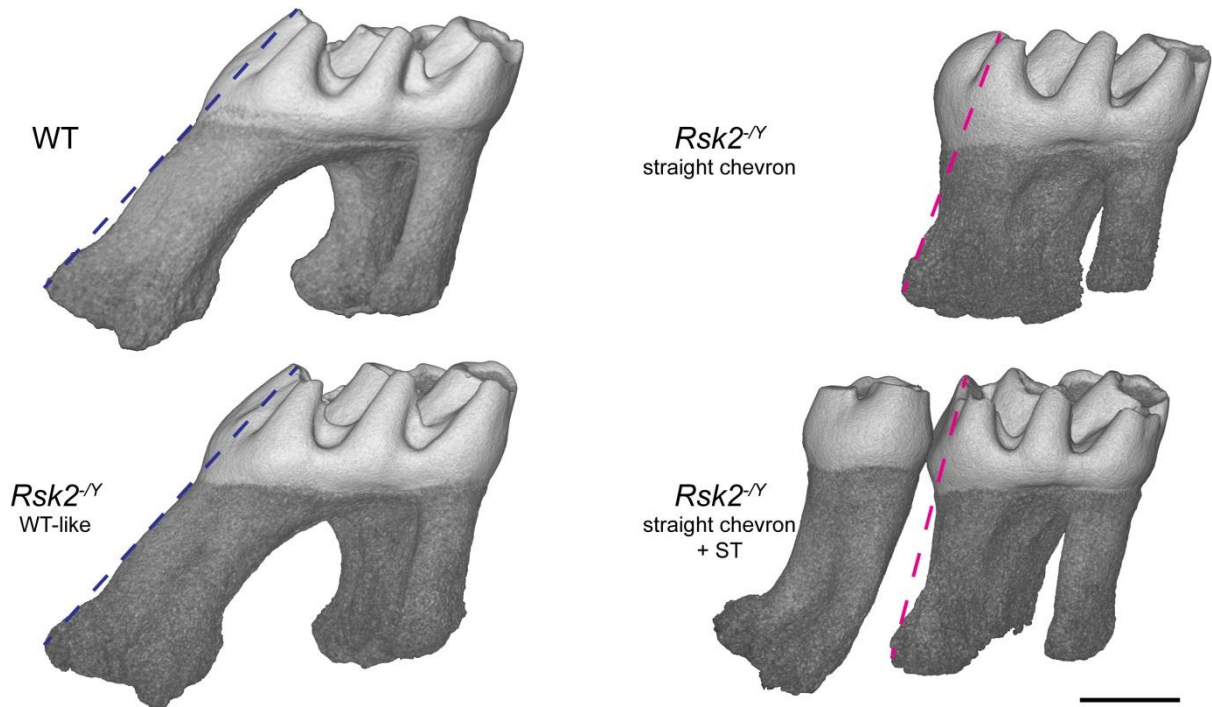


FIG. A.5: Variation of M¹ root slope in *Rsk2*^{-/-} mice. Vestibular side of the molars is facing. On the top is a WT M¹, then the gradient of slope is presented in the mutants. Dotted lines help visualizing the inclination from the tip of the first chevron to the basis of the main root. Scale bar: 0.5mm

A.1.3 Discussion

Coffin-Lowry syndrome orodental features do not relate to *Rsk*-KO mutant phenotype

Coffin-Lowry syndrome is characterized by psychomotor and growth retardation, digit abnormalities, progressive skeletal malformations, as well as craniofacial dysmorphism (Temtamy *et al.*, 1974; Temtamy *et al.*, 1975; Hanauer and Young, 2002). Focusing on those craniofacial dysmorphism, cases report a high narrow palate, a midline lingual furrow, malocclusion, peg-shaped incisors, and hypodontia (Young, 1988). Due to rare availability of

the triple *Rsk1,2,3* null mutants, the complete craniofacial and dental characterization has only been performed here on *Rsk2^{-Y}* mutants (see Annex 1 for details). The study shows an overall length reduction from the nasal to the occipital bone (the frontal bone being the most affected), as well as a strong nasal deviation for the most severe phenotypes seen. In the dental field, ST occurs in both *Rsk2^{-Y}* mutant and in the few compound mutants available, while tooth agenesis only occurs in the triple mutants. Comparing the human abnormalities to the ones highlighted in the murine model, it is clearly difficult to relate them, the only overlap remaining the occurrence of tooth agenesis.

Modulation of *Rsk2* dosage in mouse mirrors evolution of mammalian dentition

Mice are the most common mammalian model used in tooth evo-devo field. The inactivation of *Rsk2* gene only is sufficient to generate a dental phenotype of interest when looking at the evolution of dentition. The maximal dental formula found in Eutheria is $I \frac{3}{3} C \frac{1}{1} P \frac{4}{4} M \frac{3}{3}$, meaning that modern mice lost 2 incisors, 1 canine and 4 premolars along their evolutionary history. In our mutants, the ST occurs in a position corresponding to a 4th premolar, at the back of the diastema. A rudimentary tooth primordium was reported to develop in that same distal part of the diastema though it is aborted by the cap stage (E14) (Peterka *et al.*, 2000; Viriot *et al.*, 2000; Peterková *et al.*, 2003). The ST found in *Rsk2^{-Y}* and *Rsk1,2,3* null mutants is likely to be erupting from the completed development of this rudimentary primordium. This finding recalls another mutant studied in the light of human craniofacial syndrome that finally revealed its evolutionary potential: the *Tabby* mice. Heterozygous *Tabby* mice display ST in their upper molar rows, while K14-*Eda* mice display ST in their lower molar rows (Pispa *et al.*, 1999; Kangas *et al.*, 2004; Charles *et al.*, 2009a). But these mice also display a lot of cusp defects, which do not seem to occur in *Rsk*-knockout mutants. However, the specimens in our sample were not collected at the same age. Due to

the different wear state of the molar rows, it is thus difficult to rule out the existence of such cusp defects.

A.1.4 Conclusions

Rsk2^Y and *Rsk1,2,3* null mice were screened to test whether their craniofacial phenotypes match the clinical picture of the Coffin-Lowry syndrome. Only two of the displayed phenotypes mimic what is observed in human patients. The occurrence of tooth agenesis has indeed been addressed, but the mice are also displaying variable skull phenotype ranging from WT-like to severe dysmorphism associated with nasal bone deviation. Thus, these mutant mice cannot be considered as the best models to address the Coffin-Lowry syndrome.

Interestingly, the occurrence of ST mesially to the molar rows reveals the evolutionary potential of *Rsk2*. The small size of the sample and the variation in the mouse age prevent us from scrutinizing the exact extent of dental abnormalities and the precise evolutionary relevance.

A.2 UNRAVELING THE EVOLUTIONARY POTENTIAL OF THE ERK-MAPK PATHWAY

The occurrence of ST in mesial position to the molar row is a feature that is displayed in several mutant mice already published. Mice carrying mutant for *Gas1*, *Shh*, *Wnt1*, *Wise*, *Lrp4*, *Eda* or *Edar*, *Spry2* and *Spry4* are – among other dental characters – characterized by the similar presence of a ST (respectively Ahn *et al.*, 2010; Charles *et al.*, 2009a; Kangas *et al.*, 2004; Ohazama *et al.*, 2009; Klein *et al.*, 2006; Lagronova-Churava *et al.*, 2013). Among this list, *Spry2* and *Spry4* mutant drew our attention, because of the molecular role of Sprouty proteins. Sprouty proteins are indeed general Receptor Tyrosine Kinase (RTK) inhibitors (Reich *et al.*, 1999), and as so, they can inhibit FGFR-mediated activation of the ERK-MAPK cascade.

Taking advantage of the availability of *Spry1*^{-/-}, *Spry2*^{-/-}, *Spry4*^{-/-} and *Rsk2*^{-Y} mutant mice, we conduct a comparative analysis to address the relative role of these components in the building of the mouse postcanine dentition. Eventually, this study helps us perfecting the analysis of *Rsk2* mutant dental phenotype, and addressing the role of the entire pathway in the course of muroid rodent evolution. This study is currently submitted to *Scientific Reports*.

**Phenotypic and evolutionary implications of modulating
the ERK-MAPK cascade using the dentition as a model**

Pauline Marangoni^{1*}, Cyril Charles^{1*}, Paul Tafforeau², Virginie Laugel-Haushalter³, Adriane Joo⁴, Agnès Bloch-Zupan^{3,5,6}, Ophir D. Klein^{4,7}, and Laurent Viriot^{1§}

¹: Evo-Devo of the Vertebrate Dentition, Institute of Functional Genomics of Lyon, ENS de Lyon, CNRS UMR 5242, Université de Lyon 1, 46 allée d'Italie, 69364 Lyon cedex 07, France

²: European Synchrotron Radiation Facility, 6 rue Jules Horowitz, 38043 Grenoble Cedex, France

³: Development and Stem Cells Department, Institute of Genetics and Molecular and Cellular Biology, Inserm U 964, CNRS UMR 7104, Université de Strasbourg, BP 10142, 67404 Illkirch, France

⁴: Department of Orofacial Sciences and Program in Craniofacial and Mesenchymal Biology, University of California, San Francisco, CA 94143-0442, USA

⁵: Faculty of Dentistry, University of Strasbourg, 8 rue St Elisabeth, 67000 Strasbourg, France

⁶: Reference Centre for Orofacial Manifestations of Rare Diseases, Pôle de Médecine et Chirurgie Bucco-Dentaires, Hôpitaux Universitaires de Strasbourg (HUS), 1 place de l'Hôpital, 67000 Strasbourg, France

⁷Department of Pediatrics and Institute for Human Genetics, University of California San Francisco, San Francisco, California 94143, USA

§ Corresponding author: laurent.viriot@ens-lyon.fr

SUMMARY

The question of phenotypic convergence across a signaling pathway has important implications for both developmental and evolutionary biology. The ERK-MAPK cascade is known to play a significant role in dental development, but the relative roles of its components remain unknown. Here we show that premolar teeth reappear in *Spry2*^{-/-}, *Spry4*^{-/-}, and *Rsk2*^{-Y} mice while premolars have been lost in the mouse lineage 45 million years ago (Ma). In addition, Sprouty-specific anomalies mimic a phenotype absent in extant mice, but present in mouse ancestors prior to 9 Ma. Although the four mutants display convergent phenotypes, each gene has a specific role in tooth number setting up and tooth crown patterning. The similarities found between teeth in fossils and mutants highlight the pivotal role of the ERK-MAPK cascade during the evolution of the dentition in rodents.

KEY WORDS

MAPK signalling pathway, dentition evolution, dental formula,

INTRODUCTION

The extracellular signal-regulated kinase/mitogen-activated protein kinase (ERK-MAPK) pathway is a central regulator of tooth development. This cascade is typically initiated by the binding of a growth factor to a receptor tyrosine kinase (RTK), which triggers the phosphorylation of successive kinases and culminates in activation of effector kinases and the transcription of target genes (Sebolt-Leopold and Herrera, 2004). The MAPK signaling pathway has been intensively studied by cancer biologists because of its effects on regulation of cell proliferation and survival (Downward, 2003; Sebolt-Leopold and Herrera, 2004), but this pathway is also important throughout mouse embryogenesis (Massague, 2003). The pathway has been investigated in numerous embryonic processes, including development of the central nervous system and mesodermal derivatives (Campos *et al.*, 2004), skeletal development (Ge *et al.*, 2007), and tooth development (Thesleff and Mikkola, 2002; Klein *et al.*, 2006; Tompkins, 2006; Xu *et al.*, 2008; Laugel-Haushalter *et al.*, 2014).

Tooth development is a well-documented example of ectodermal organ development. It is a tightly regulated process arising from the crosstalk between dental epithelium and its underlying mesenchyme (Tucker and Sharpe, 2004). The signaling networks responsible for properly building the dentition have been heavily investigated, and numerous members of the ERK-MAPK signaling pathway are known to play a role in tooth development. Early studies examined the fibroblast growth factors (FGFs) that are FGFR ligands, and thus trigger the ERK-MAPK phosphorylation cascade (Neubüser *et al.*, 1997; Thesleff, 2003). Investigations then moved to further steps of the cascade in order to determine which components were involved in tooth development (Goodwin *et al.*, 2013; Laugel-Haushalter *et al.*, 2014). An exciting current challenge is to understand the complexity of feedback regulation in this signaling pathway that can be time- and/or tissue-specific. In the present study, we compare

the phenotype of molar teeth in mice carrying mutations in *Sprouty1*, *Sprouty2*, *Sprouty4*, and *Rsk2* genes, which are involved at various levels in the MAPK cascade.

The Sprouty (*Spry*) family of genes encodes general RTK inhibitors (Hacohen *et al.*, 1998; Reich *et al.*, 1999). After stimulation by growth factors, the Sprouty proteins are thought to translocate to the plasma membrane where their phosphorylation prevents the formation of an FGFR adaptor complex, thus having a negative effect on the activation of the rest of the cascade (Hanafusa *et al.*, 2002). *Spry1* is expressed in both the epithelium and the mesenchyme, with exception of a cluster of non-proliferating epithelial cells that serve as a signaling center called the enamel knot. *Spry2* is expressed only in the epithelium adjacent to the dental mesenchyme, including the enamel knot, and *Spry4* is expressed in the dental mesenchyme (Zhang *et al.*, 2001; Klein *et al.*, 2006). Whereas the morphogenesis of molar teeth in *Spry1*^{-/-} mice has not yet been examined, *Spry2*^{-/-} and *Spry4*^{-/-} mice are known to have abnormal dentition, which sometimes includes ST located immediately in front of the first lower molar (Klein *et al.*, 2006). These supernumerary teeth, which occur at differing frequencies depending on the genetic background (Klein *et al.*, 2006; Ohazama *et al.*, 2009; Lagronova-Churava *et al.*, 2013) are believed to derive from evolutionary vestigial tooth buds that normally undergo apoptosis in wild-type embryos (Peterková *et al.*, 1998; Viriot *et al.*, 2000; Viriot *et al.*, 2002). Lagronova-Churava and colleagues (2013) showed that although all *Spry2*^{-/-} and *Spry4*^{-/-} embryos present a revitalization of tooth rudiments at ED13.5, only 2% of *Spry4*^{-/-} and 27% of *Spry2*^{-/-} specimens had a lower ST. However, the role of *Spry1*, *Spry2* and *Spry4* in the development of upper molars is not known, and the adult molar morphology has not been scrutinized in these mutants.

RSKs (90kDa ribosomal S6 kinases) are effector kinases belonging to the eponymous family of highly conserved serine/threonine kinases (Frödin and Gammeltoft, 1999; Romeo *et al.*, 2012). Out of the four isoforms found in vertebrates, *Rsk2* has been recently demonstrated

to be involved in craniofacial development. *Rsk2*^{-Y} mice display a deformation of the nasal bone, as well as diastemal ST which affect the mesial part of both upper and lower first molars (Laugel-Haushalter *et al.*, 2014). Mutations in the *RSK2* gene have been associated with Coffin-Lowry syndrome (OMIM #303600), a condition characterized by mental and growth retardation along with craniofacial and other skeletal abnormalities (Temtamy *et al.*, 1974; Temtamy *et al.*, 1975; Hanauer and Young, 2002).

Phenotypic convergence across the ERK-MAPK signaling pathway remains poorly documented. By studying the dental phenotype resulting from mutations in genes located upstream (Sprouty) and downstream (*Rsk2*) of the ERK-MAPK cascade, we address the question of whether an ERK-MAPK signature phenotype exists. To answer this question, (1) we have characterized the molar phenotype in several mutant populations in order to evaluate the distribution of the various changes affecting both upper and lower molar rows; (2) precisely quantified the occurrence of supernumerary teeth (ST) as well as their impact on the other teeth of the row, and finally; (3) addressed the evolutionary role of the ERK-MAPK cascade by comparing specific dental traits of mutants with dental traits of other extant or extinct rodents.

MATERIAL AND METHODS

Sprouty mutant mice

All the studied Sprouty mutant mice were generated in backgrounds resulting from crossing between several lineages. The three mutants and the wild type mice were generated by inbreeding at UCSF. The sample set was composed of homozygous mice as indicated: 25 *Spry1*^{-/-}, 50 *Spry2*^{-/-}, 50 *Spry4*^{-/-}, and 60 WT individuals (littermates of the various mutants). For each specimen, left and right, upper and lower tooth rows were studied independently. The age of the specimens ranged from 1 month to 2.5 months. Animal experimentation was carried out in compliance with the policies and procedures established by the UCSF Institutional Animal Care and Use Committee.

***Rsk2*^{-Y} mice**

The *Rsk2* mutant mouse line was generated as previously described (Yang *et al.*, 2004). Since *Rsk2* is located on the X chromosome, analyses were performed on *Rsk2*^{-Y} males, on a C57BL/6J background. The sample set was composed of 45 *Rsk2*^{-Y} and 45 WT littermates (*Rsk2*^{+Y}). Mouse protocols were complied with the 2010/63/UE directive and the 2013/02/01 French decree, and were thus approved by the CERBM-GIE: ICS/IGBMC Ethical Research Board.

Observation and imaging of dental rows

All the heads were prepared in order to remove all non-mineralized tissues to allow good observation and measurement of the dental rows. They were examined and photographed using a Leica stereomicroscope. The measurements were obtained by following the outline of each tooth from the photos of occlusal view of the row. Thus, the length, width, and area of the tooth were produced by Leica software. Some Sprouty mutant dental rows were imaged using X-ray-synchrotron Radiation Facility (ESRF, Grenoble, France), beamline

ID 19 and BM5, with a monochromatical beam at energy of 25 keV. X-ray synchrotron microtomography has been demonstrated to bring high-quality results for accurate imaging of small teeth (Tafforeau *et al.* 2006). A cubic voxel of 7.46 μ m was used. Some *Rsk2^{-Y}* mutant dental rows were imaged using the X-ray cone-beam computed microtomography with a Nanotom machine (GE) at an energy of 100keV with a cubic voxel of 3 μ m. All 3D renderings were performed using VGStudiomax software.

Statistics

Student's t-tests were used to verify the significance of differences in tooth size between the mutant mice but also between the mutant and the WT mice. A threshold value of 0.05 (*p-value*) was used to assess the significance of the observed differences.

RESULTS

The mouse (*Mus musculus*) is a muroid rodent. Like all the members of this superfamily, mice have a simplified dentition composed only of incisors and molars separated by a long toothless gap called diastema. Three lower (M_1 M_2 M_3) and three upper (M^1 M^2 M^3) molar teeth are present in each mouth quadrant. The crowns of molar teeth bear a relatively stable number of cusps that are: 8 for M^1 , 6 for M^2 , 4 for M^3 , 7 for M_1 , 5 for M_2 , and 4 for M_3 . Crowns of upper molars are made of rows of 3 cusps arranged in linguo-vestibular chevrons pointing mesially (except the third one, which is incomplete), whereas crowns of lower molars are made of rows of 2 cusps linked by linguo-vestibular and rather straight crests called lophs (Fig. 1, first column). The two mesial lophs of the M_1 are also linked together by a mesio-distal connection.

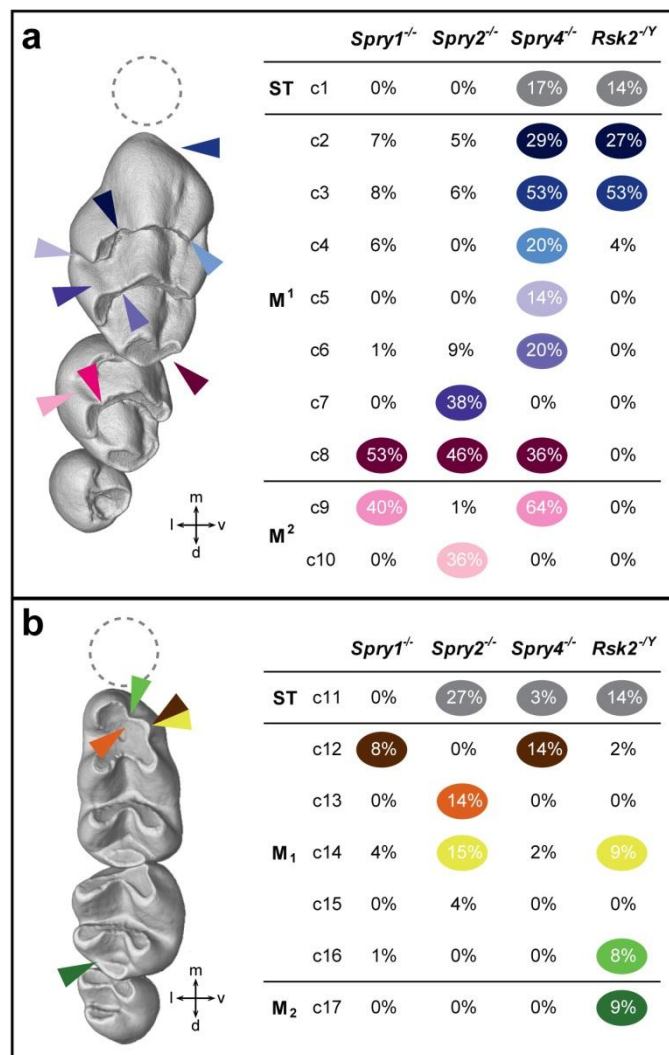


Fig. 1: Dental character matrix. [previous page] On the first column are displayed WT upper (top) and lower (bottom) molar rows, with coloured arrowheads pointing to the localization of the most frequent defects seen in the 4 mutant backgrounds. Each character is listed with the occurrence frequency in all the mutant mice observed. (c1-10) are defects of the upper mutant postcanine teeth. (c1) is the occurrence of a ST; (c2-4) are M¹ 1st chevron defects, respectively lingual cusp disconnection, straight mesial cusp and absence of the vestibular cusp; (c5) is the presence of an extra lingual cusp between the 1st and 2nd chevrons; (c6) is the disconnection of the lingual cusp of the M¹ 2nd chevron; (c7) is the occurrence of a lingual crest; (c8) is the occurrence of an extra distal cusp; (c9) is the disconnection of the mesio-lingual cusp of the M²; (c10) is the connection of distal cusps. (c11-17) are defects of the lower mutant postcanine teeth. (c11) is the occurrence of a ST; (c12) is the absence of the mesio-vestibular cusp; (c13) is the display of very symmetric mesial-most cusps; (c14) is the split of the mesio-vestibular cusp; (c15) is the occurrence of an extra mesial cusp; (c16) is the strong disconnection of the mesial cusps of the M₁; (c17) is the abnormal connection of the 2nd and 3rd teeth of the M₁.

Diversity of the dental phenotypes in *Sprouty* mutants

We examined the arrangement and shape of the postcanine dentition in four populations comprising 25 *Spry1*^{-/-}, 50 *Spry2*^{-/-}, and 50 *Spry4*^{-/-} mice. Area measurements showed that the occlusal surface of molars in *Spry1*^{-/-} and *Spry4*^{-/-} mice is larger than in the WT mice, whereas the molar occlusal surface in *Spry2*^{-/-} mice is smaller than in the WT mice (t test, *p* value<0.05, Fig. 2).

The molar teeth of *Spry1*^{-/-} and WT mice are globally similar in shape, and 51% of the *Spry1*^{-/-} dental rows display a WT-like phenotype. The defects are numbered as character# (c#) from the mesial to the distal part of the row. The main defects of the *Spry1*^{-/-} postcanine dentition are: (c8) the occurrence of a supplementary distal cusp on the M¹ (53%); (c9) the disconnection of the mesio-lingual cusp from the first chevron of the M² (40%); and (c12) the absence of the mesio-vestibular cusp of the M₁ (8%) (Fig. 1, Fig. 3B, Suppl. Fig. 1A). The postcanine dentition in *Spry2*^{-/-} mice had stronger differences compared to WT samples, and only 21% of *Spry2*^{-/-} dental rows still display a WT-like phenotype. The main changes of the *Spry2*^{-/-} postcanine dentition are: (c7) the connection between the two lingual cusps of the M¹

(38%); (c8) the occurrence of a supplementary distal cusp on the M¹ (46%); (c10) the connection between the two lingual cusps of the M² (36%); (c11) the occurrence of a lower ST (27%); and (c13-14) an abnormal shape, number, and/or interconnection of the mesial cusps of the M₁ (29%) (Fig. 1, Fig. 3C). *Spry4*^{-/-} molar tooth phenotype is the most variable among the 3 Sprouty mutants. These teeth ranged from a WT-like phenotype (24%) to relatively severe anomalies, especially in the M¹. The main defects of the *Spry4*^{-/-} postcanine dentition are: (c1) the occurrence of an upper ST (17%); (c2-3-4) the presence of lingual cusp disconnection, straight mesial cusp and absence of the vestibular cusp affecting the first chevron of the M¹ (66% combined); (c5) the occurrence of a supplementary lingual cusp between the first and the second chevron (14%); (c6) the disconnection of the lingual cusp from the second chevron of the M¹ (20%); (c8) the occurrence of a supplementary distal cusp on the M¹ (36%); (c9) the disconnection of the mesio-lingual cusp from the first chevron of the M² (64%); (c11) the occurrence of a lower ST (3%); (c12-14) an abnormal number and/or interconnection of the mesial cusps of the M₁ (16%) (Fig. 1, Fig. 3D).

Except for three characters, the dentition of *Spry1*^{-/-} mice thus resembles that of WT mice, whereas *Spry2*^{-/-} and *Spry4*^{-/-} mice show extra cusps and crest disconnections, as well as severe reductions and defects in the mesial parts of the M¹ (*Spry4*^{-/-} only) and in the M₁ (rarely in *Spry4*^{-/-}, frequently in *Spry2*^{-/-}). *Spry4*^{-/-} mutants develop ST in both upper and lower jaws, whereas *Spry2*^{-/-} only display lower ST. Lower ST have been observed in *Spry2*^{-/-} and *Spry4*^{-/-} molar rows, whereas upper ST only occurred in *Spry4*^{-/-} molar rows. *Spry1*^{-/-} mutants thus never develop any ST, and only *Spry4*^{-/-} mutants display ST in both upper and lower tooth rows. These findings suggest a potential relationship between the occurrence of ST and abnormal arrangement of the mesial parts of the first molars.

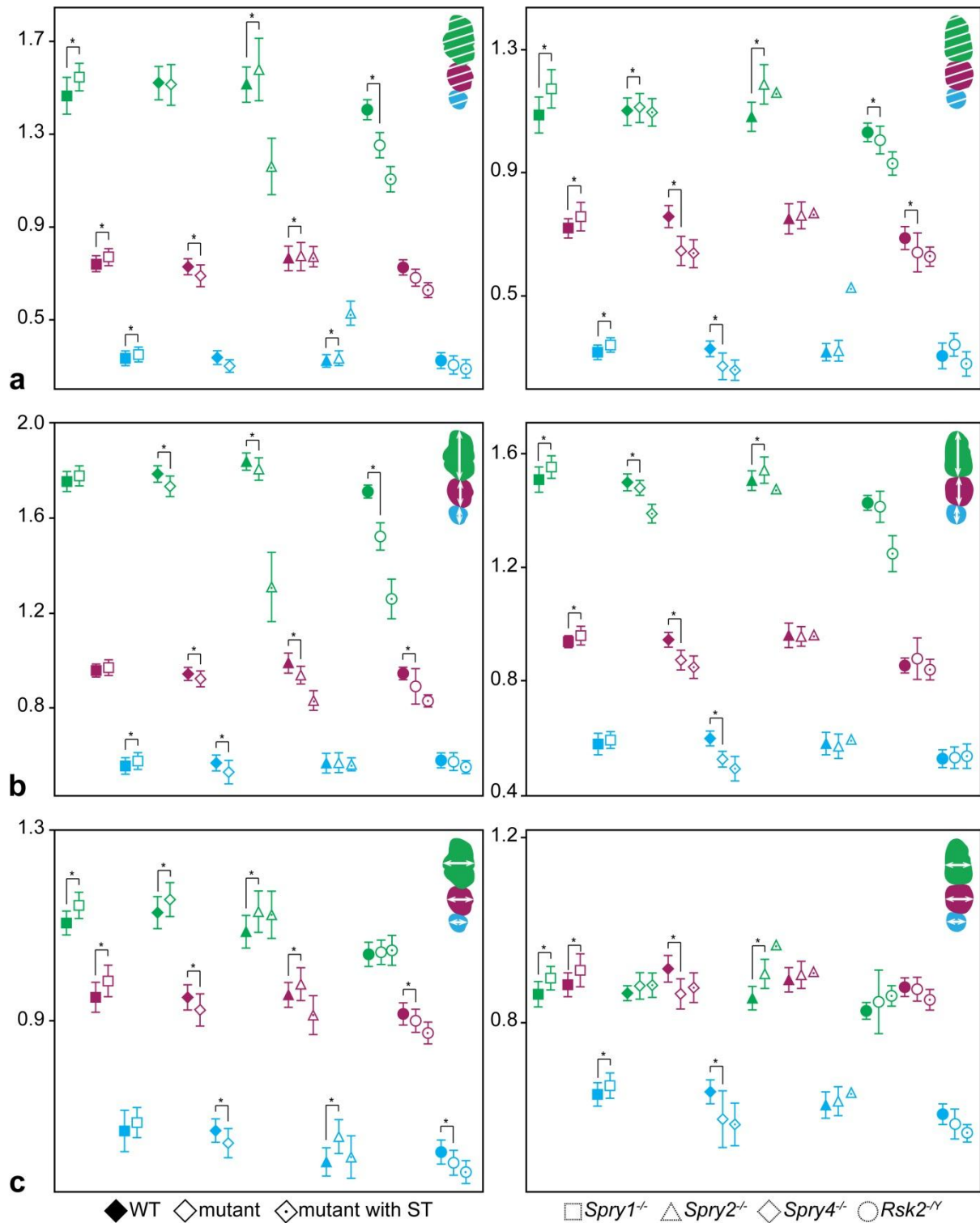


Fig. 2: Molar tooth proportions in the *Spry1*^{-/-}, *Spry2*^{-/-}, *Spry4*^{-/-} and *Rsk2*^{-/-} mutant mice. First molars are coloured in green, second molars in pink, and third molars in blue. Filled forms represent the WT for each background, squares represent the *Spry1*^{-/-} mutants, *Spry2*^{-/-} mutants without (blanked) or with (dot) ST, *Spry4*^{-/-} mutants without (blanked) or with (dot) ST and *Rsk2*^{-/-} mutants without (blanked) or with (dot) ST.

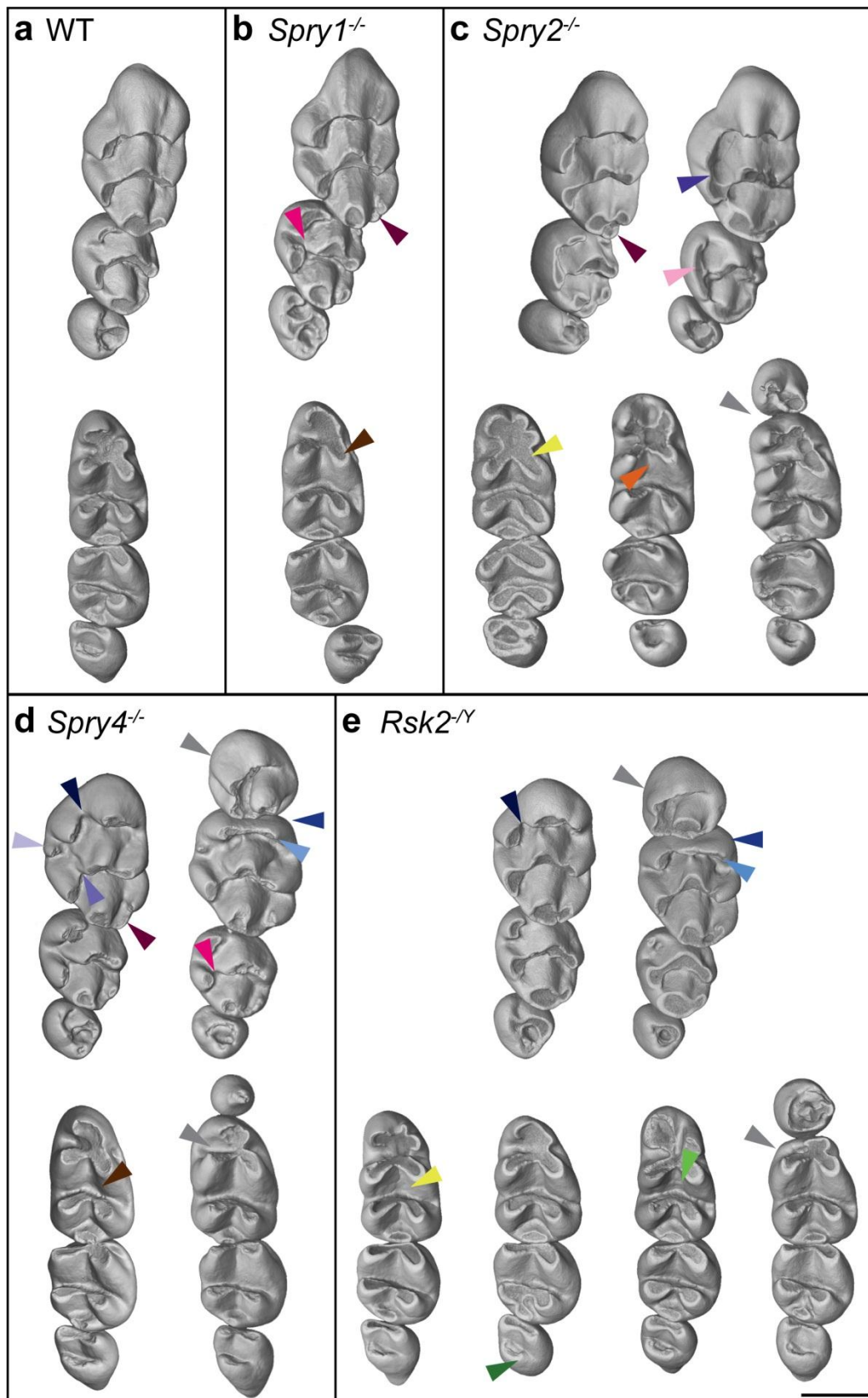


Fig. 3: Abnormal phenotype in the *Spry1*^{-/-}, *Spry2*^{-/-}, *Spry4*^{-/-} and *Rsk2*^{-/-} mutant mice. (A) WT dental rows; (B) *Spry1*^{-/-} dental rows; (C) *Spry2*^{-/-} dental rows; (D) *Spry4*^{-/-} dental rows; (E) *Rsk2*^{-/-} dental rows. Coloured arrowheads correspond to the features displayed in the Fig. 2

Similarities and differences of *Rsk2* dental phenotype as compared to Sprouty dentitions

We next examined a cohort of 45 *Rsk2*^{-Y} mice. The postcanine occlusal surface area in *Rsk2*^{-Y} mice is smaller than in WT mice (M^1 and $M_{1,2}$ being significantly smaller, p -value < 0.05, Fig. 2). Although many *Rsk2*^{-Y} specimens display relatively severe dental defects, 45% of the examined dental rows display a WT-like phenotype. The main defects of the *Rsk2*^{-Y} postcanine dentition are: (c1) the occurrence of an upper ST (14%); (c2-3-4) the presence of many defects on the first chevron of the M^1 (71%); (c11) the occurrence of a lower ST (14%); (c12+14+16) an abnormal number and/or interconnection of the mesial cusps of the M_1 (19%); (c17) abnormal mesio-distal connections between the second and the third lophs of the M_2 (9%) (Fig. 1, Fig. 3E). The frequency of ST occurrence is lower than what has been previously reported (Laugel-Haushalter *et al.*, 2014), and this may be explained by the examination of a larger sample or by shifts in the genetic background over time.

The comparison of the postcanine dental phenotypes between *Rsk2*^{-Y} and the 3 Sprouty mutant mice shows that *Rsk2*^{-Y}, *Spry2*^{-/-} and *Spry4*^{-/-} mice all develop ST, at varying frequencies. *Spry2*^{-/-} mice never have an upper ST, but they frequently have a lower ST (27%). *Spry4*^{-/-} mice frequently have an upper ST (17%), but they rarely have a lower ST (3%). *Rsk2*^{-Y} mice develop both upper and lower ST relatively frequently (14%). In addition to developing lower and upper ST, *Rsk2*^{-Y} and *Spry4*^{-/-} postcanine dentitions share many similar defects affecting the mesial parts of both M^1 and M_1 . The occurrence of defects on mesial parts of the M^1 is much more frequent than the occurrence of an upper ST, but the defects in the mesial parts of the M^1 and M_1 are also associated with a shortening in length of both teeth (Fig. 2). Finally, *Rsk2*^{-Y} mutants do not develop the supplementary distal cusp of the M^1 common to all Sprouty mutants, nor do they share with *Spry1*^{-/-} and *Spry4*^{-/-} mutants the trend towards having larger teeth than the WT mice.

The presence of ST impacts both the shape and size of the other teeth in the row

The size and shape of ST range from small rounded moncuspid teeth to large complex multicuspoid teeth that can comprise up to five cusps (Fig. 4). In complex upper ST, a large central cusp is always present surrounded by a variable number of cusps linked by an almost circular crest. The most complex upper ST tend to have a mesial chevron pointing mesially (especially in *Spry4*^{-/-}) whereas the lower ST mainly have a bicuspid shape (especially in *Spry2*^{-/-}). These features show that ST have a clear murine shape identity.

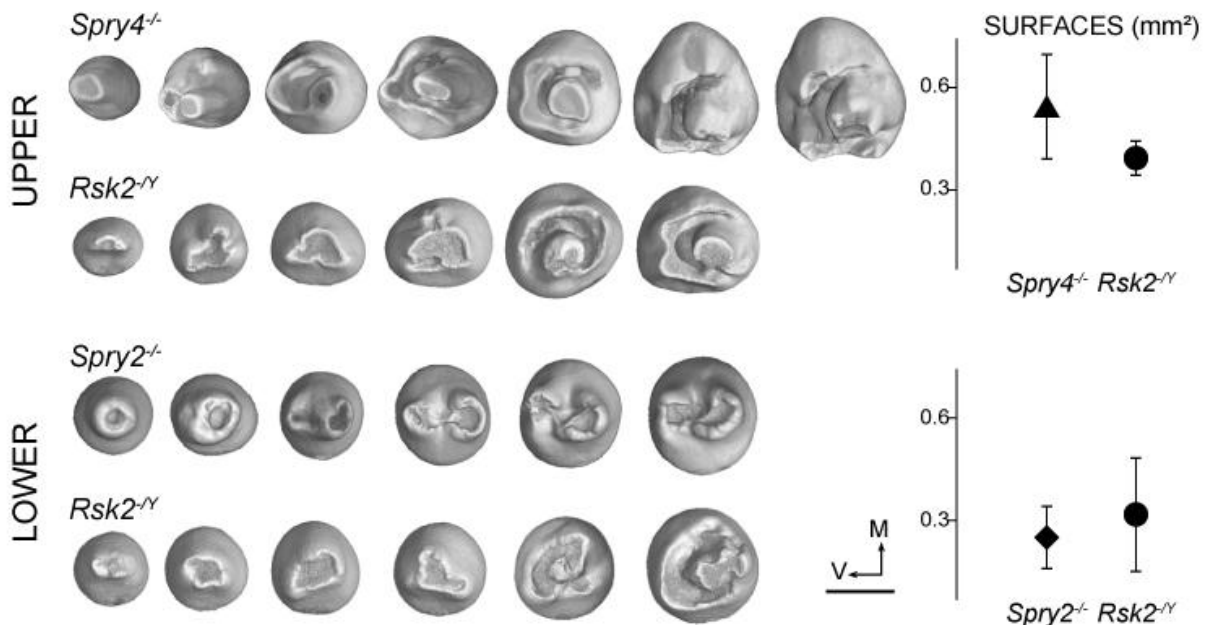
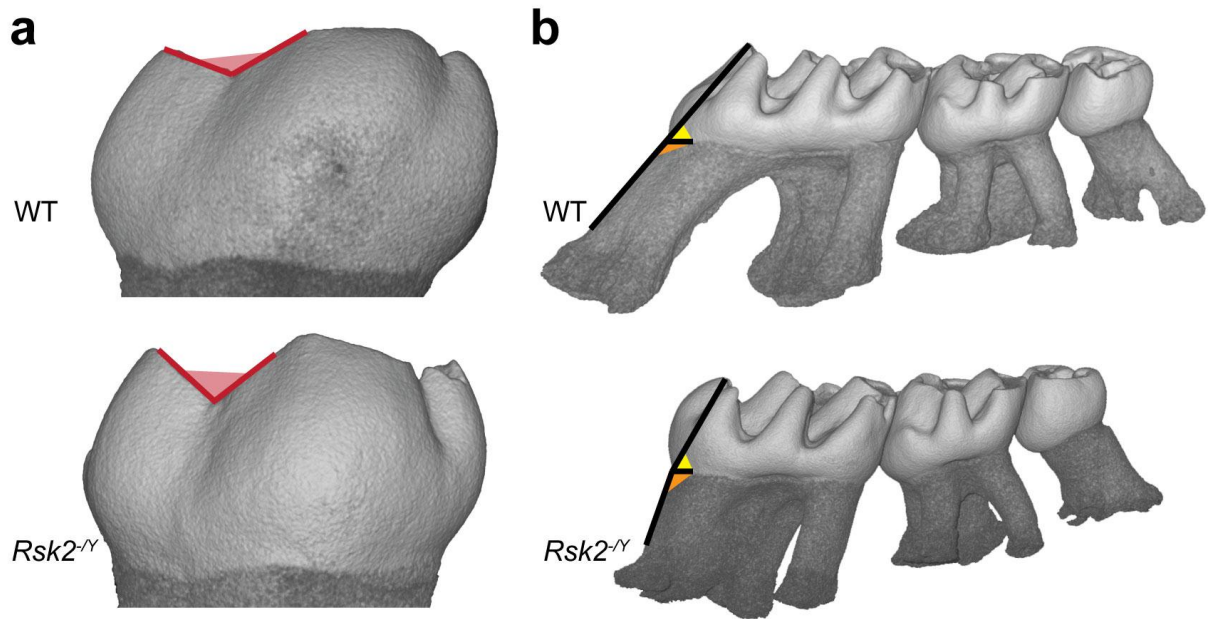


Fig. 4: ST phenotype and surface in *Spry2*^{-/-}, *Spry4*^{-/-} and *Rsk2*^{-/-} mutants. ST range from small rounded moncuspid teeth to large multicuspoid teeth. Right column indicates the mean surface in all the ST-displaying mutant mice, error bars represent the standard deviation. V and M respectively point towards the vestibular and mesial directions. Scale bar: 0.4mm.

The larger the ST is, the more the mesial parts of the neighbouring M¹ and M₁ are impacted. The occurrence of a ST leads to compression and flattening of the mesial part of the following tooth. This is particularly visible on M¹ of *Spry4*^{-/-}, and on both M¹ and M₁ of *Rsk2*^{-/-} mutants. As a consequence, the overall occlusal area of the molar row is smaller in mutants

displaying a ST, with the exception of the *Spry4*^{-/-} upper row in which the area of the M³ seems to increase in compensation for the decrease of M¹ area (Fig. 2).

In the most severely impacted phenotypes, the mesial contour of the M¹ becomes rounded, whereas it is triangular in WT mice (e.g. Fig. 3E without ST). In addition, the two mesial-most cusps of the first chevron become extremely reduced into a simple crest (53% *Spry4*^{-/-} and in *Rsk2*^{-/Y}), and the mesio-vestibular cusp may completely disappear (20% *Spry4*^{-/-} and 4% in *Rsk2*^{-/Y}). Interestingly, the mesial shrinkage of the M₁ is associated with a change in the tilt angle of both cusps and roots of the first chevron (Suppl Fig. 1B). In WT mice, the slope of the M¹ mesial root is in continuity with the tilt of 50° that makes the central cusp of the first chevron with the dental neck. In mutants having a ST, as well as in some mutants that do not display any ST, the tilt between the root axis and the tooth neck tends to be more vertical (about 70°), as does the slope of the first chevron central cusp (about 60°). The same type of defects can be seen when M₁ is preceded by a ST in the three mutants: the first loph of the M₁ is shortened and cusps appear as crushed by the presence of the ST.



Suppl. Fig. 1: Details of some shared mutant features depicted in the *Rsk2*^{-/-} mice. (A) The disconnection of the lingual-most cusp of the M1 1st chevron. (B) Variation of the M1 mesial root inclination in mutant mice. Note the straightening of the slope in *Rsk2*^{-/-} mutants. Yellow angle is 50° in WT mice, and 60° in mutant mice. The root orientation itself is also modified, as depicted in orange.

DISCUSSION

Similar yet distinct dental phenotypes in *Sprouty* and *Rsk2* mutants

Morphological comparisons show that the occurrence of a supplementary cusp at the distal extremity of the M¹ can be considered as a phenotypic signature of the *Sprouty* mutant dentitions, and *Rsk2* mutants never develop this supplementary cusp. These comparisons also highlight that *Spry4*^{-/-} and *Rsk2*^{-Y} mutants share many phenotypic features, such as the occurrence of upper and lower ST as well as abnormal arrangements in the mesial parts of the first molars. Although these mesial abnormalities in these teeth appear to be caused by the occurrence of ST, a question remains concerning the higher frequency of modifications of the M¹ first chevron in *Spry4*^{-/-} and *Rsk2*^{-Y} mutants (66-71%) when compared to the frequency of occurrence of ST (14-17%). It has already been shown in *Eda*^{Ta} mice that a supplementary dental germ can develop mesially to the M¹ until advanced stages without necessarily giving rise to a mineralized tooth (Charles et al., 2009a). In these cases, the development of a supplementary dental germ may be sufficient to cause disorders in the development of the mesial part of the following tooth. We can thus infer that about 70% of the specimens develop a supplementary upper tooth germ that will impact on the phenotype of the M¹.

Roles of *Sprouty* and *Rsk2* genes within the ERK-MAPK cascade

Sprouty genes are thought to encode proteins that inhibit signaling through the FGFR pathway (Hacohen *et al.*, 1998; Hanafusa *et al.*, 2002; Kim and Bar-Sagi, 2004). Examination of the dental phenotypes in mutant mice led to the discovery of shared features. All three *Sprouty* mutants share the presence of a supernumerary distal cusp, arguing in favor of shared functions. But distinct characters were also observed in each mutant, pointing to some specific functions of these genes in tooth morphology. The phenotypic diversity in the

Sprouty mutants may be ascribed to differences in spatial and temporal expression patterns of these genes. Our data complement previous findings concerning the generation of similar phenotypes with the loss of function of *Spry2* and *Spry4* genes. We have previously reported that the *Spry4*^{-/-} phenotype penetrance was lower than the one in *Spry2* null mutants (Klein et al., 2006). Our results show that the differences between the two proportions are even larger than previously reported. This trend is reversed for the upper rows, for which we did not observe ST in *Spry2*^{-/-} mice, whereas these were found in 17% in *Spry4*^{-/-} mice. The proportion of ST in mutant dental rows was comparable to what Lagronova-Churava et al. (2013) reported, but lower than our first publication on the topic (Klein et al. 2006). Such a change in penetrance could be explained by a shift in the genetic background over generations. Finally, neither of our previous reports (Klein et al., 2006; Lagronova-Churava et al., 2013) studied the effect of loss of function of *Spry1*. Our work shows that *Spry1*^{-/-} mice also display modifications in the shape of the M¹ and M², as well as in overall size of the dental row.

RSK2 is an effector kinase that functions downstream of the MAPK cascade, whereas Sprouty genes modulate the cascade through their inhibitory effect on the pathway. The possible negative feedback regulation from *Rsk2* on the adaptor protein SOS, which recruits Ras (Frödin and Gammeltoft, 1999), may lead to similarities in the phenotypes of Sprouty and *Rsk2* mutants. Both *Spry4* and *Rsk2* are expressed during odontogenesis in the dental papilla (Zhang et al., 2001; Corson et al., 2003; Laugel-Haushalter et al., 2014), which may explain the high degree of similarity in the phenotypes associated with their loss of function. Our study thus provides an example of molecular and phenotypic convergence of various steps in the same signaling pathway.

Mutations in Sprouty genes and *Rsk2* lead to more teeth and more cusps, which is the opposite trend of mutations in the *Fgf* genes which lead to phenotypes with fewer cusps (e.g.

Fgf3, Wang *et al.*, 2007; Charles *et al.*, 2009b). This contrast in phenotypic impacts of the mutations between *Rsk2* and *Fgf3* is concordant with the current knowledge of regulatory feedbacks acting on the whole pathway.

Molecular basis of ST development

In addition to Sprouty and *Rsk2* null mice, other mutants have been described with ST mesially to the first molars. Some of these mutations are in genes encoding proteins that interact with the ERK-MAPK pathway. The balance between SHH and Wnt signals has been demonstrated to be crucial for the development of the diastemal rudimentary tooth germ. The link between the two pathways involves regulation of expression of Fgf pathway members by the Wnt signalling pathway. Mice mutant for *Gas1*, *Shh*, *Wnt1*, *Wise*, *Lrp4*, *Apc*, *Ctnnb1*, *Eda* or *Edar* genes are characterized by a disruption of this important molecular equilibrium and display ST (respectively Ahn *et al.*, 2010; Charles *et al.*, 2009a; Kangas *et al.*, 2004; Ohazama *et al.*, 2009; Wang *et al.*, 2009). Apart from the *Apc* and *Ctnnb1* null mutants, the ST occurs very similarly to what is observed in Sprouty and *Rsk2* mutants. Thus, modulation of the Wnt signaling pathway upstream of the ERK-MAPK pathway could mimic the effect of loss of Sprouty gene or *Rsk2* function, which might explain phenotypic similarities in the occurrence of ST in both pathways.

The *Apc* and *Ctnnb1* null mutants display many more ST located in the vicinity of the incisor region (Wang *et al.*, 2009). Authors hypothesized that incisor stem cells might be migrating, generating odontogenesis-competent *foci*. The difference between one ST being displayed in a mesial position (compared to the molar row), and multiple ST being displayed in a disordered manner is likely to be caused by the direct interaction with Ras and ERK. Indeed, such interactions have been demonstrated in the context of multiple cancer models in the mouse (Luo *et al.*, 2009; Moon *et al.*, 2014).

Potential roles of Sprouty and Rsk2 gene in the evolution of rodent dentition

The most striking phenotypic trait of *Spry2*^{-/-}, *Spry4*^{-/-} and *Rsk2*^{-Y} mutants is the occurrence of ST located in front of the first molars at both the lower and the upper jaws. It has long been known that the rodent dentition has evolved towards a reduction in the number of teeth over the course of evolution in parallel with a specialization of the molar teeth (HersHKovitz, 1980). Basal rodents had lower and upper premolars and it is only since the rise of muroid rodents that premolars have been completely lost in the lineage leading up to the murine rodents. It has however been demonstrated that rudimentary dental germs are maintained in both the upper and the lower diastema during mouse early dental development (Peterková *et al.*, 1998; Viriot *et al.*, 2000). Because these rudimentary germs are located in the vicinity of the first molar germs, they have been considered to be rudiments of premolar germs lost over evolution (Viriot *et al.*, 2002). These rudimentary germs rapidly abort by apoptosis and do not become autonomous mineralized teeth. It has been demonstrated that they can contribute to the development of the M₁ by merging with the M₁ germ (Viriot *et al.*, 2002). Although it has not yet been formally demonstrated, it is likely that the same mechanism occurs with the upper rudimentary germ immediately adjacent to the M¹ (Peterková *et al.*, 1996) for participation in the development of the first chevron.

Here we deliver new insights into the role of the MAPK signaling pathway members beyond what has been previously reported (Klein *et al.*, 2006; Lagronova-Churava *et al.*, 2013; Laugel-Haushalter *et al.*, 2014). The loss of function of *Spry2*, *Spry4* or *Rsk2* allows the continuation of the development of some rudimentary premolar germs until the formation of autonomous mineralized teeth. The segmentation of the postcanine dental row is thus impacted because it comprises four teeth instead of three and the mesial parts of the first molars are accordingly reduced (Fig. 3). We can thus assign the supplementary teeth located immediately in front of the first molars to deciduous fourth premolar teeth (dP⁴ and dP₄) that

will not be replaced. Teeth located at the fourth premolar position are known in the earliest muroid rodents (Li *et al.*, 2012) as well as in some extant dipodoids such as *Sicista* and *Zapus* (Pucek *et al.*, 1982; Rodrigues *et al.*, 2011), the sister group of muroids. Fourth premolars are present in the squirrel- and in the guinea pig-related clades, which arose earlier in the history of rodents than the mouse-related clade (Fabre *et al.*, 2012). The loss of function of *Spry2*, *Spry4* or *Rsk2* involves developmental mechanisms that revitalize autonomous premolar teeth and that simplify accordingly the mesial parts of the first molars. The dental phenotype in *Spry2*^{-/-}, *Spry4*^{-/-}, and *Rsk2*^{-/Y} mutants thus represents a reversal in the evolutionary trends of the dental phenotype through the transition from pre-muroid to muroid rodents (Fig. 5A), which is documented within the fossil record (Tong, 1992; Li *et al.*, 2012;) to have probably happened between 50 and 45 million years ago (Ma).

As discussed above, many other mouse mutants display ST mesially to first molars, but both the phenotypical and the developmental aspects of the postcanine row segmentation has solely been scrutinized in mutants of the EDA pathway (Charles *et al.*, 2009a). From these studies, it is clear that dental phenotypes in *Eda*^{Ta} (Tabby) and *Edar*^{dl-J} (Downless) mice radically differ from those of *Spry2*^{-/-}, *Spry4*^{-/-}, and *Rsk2*^{-/Y} mice. Tabby and Downless mice have postcanine teeth with simplified occlusal patterns characterized by the absence of many cusps, as well as by abnormal arrangements of the lophs and the chevrons respectively in the lower and upper molars (Charles *et al.*, 2009a). In contrast, *Spry2*, *Spry4*, or *Rsk2* losses of function provoke rearrangements of the M¹ and M₁ mesial parts, but minimally impact the rest of the dental rows. From these arguments, we propose that *Spry2*, *Spry4* or *Rsk2* are candidate genes for a major role in the evolutionary trend towards reduction of the dental formula in muroid rodents 45 Ma.

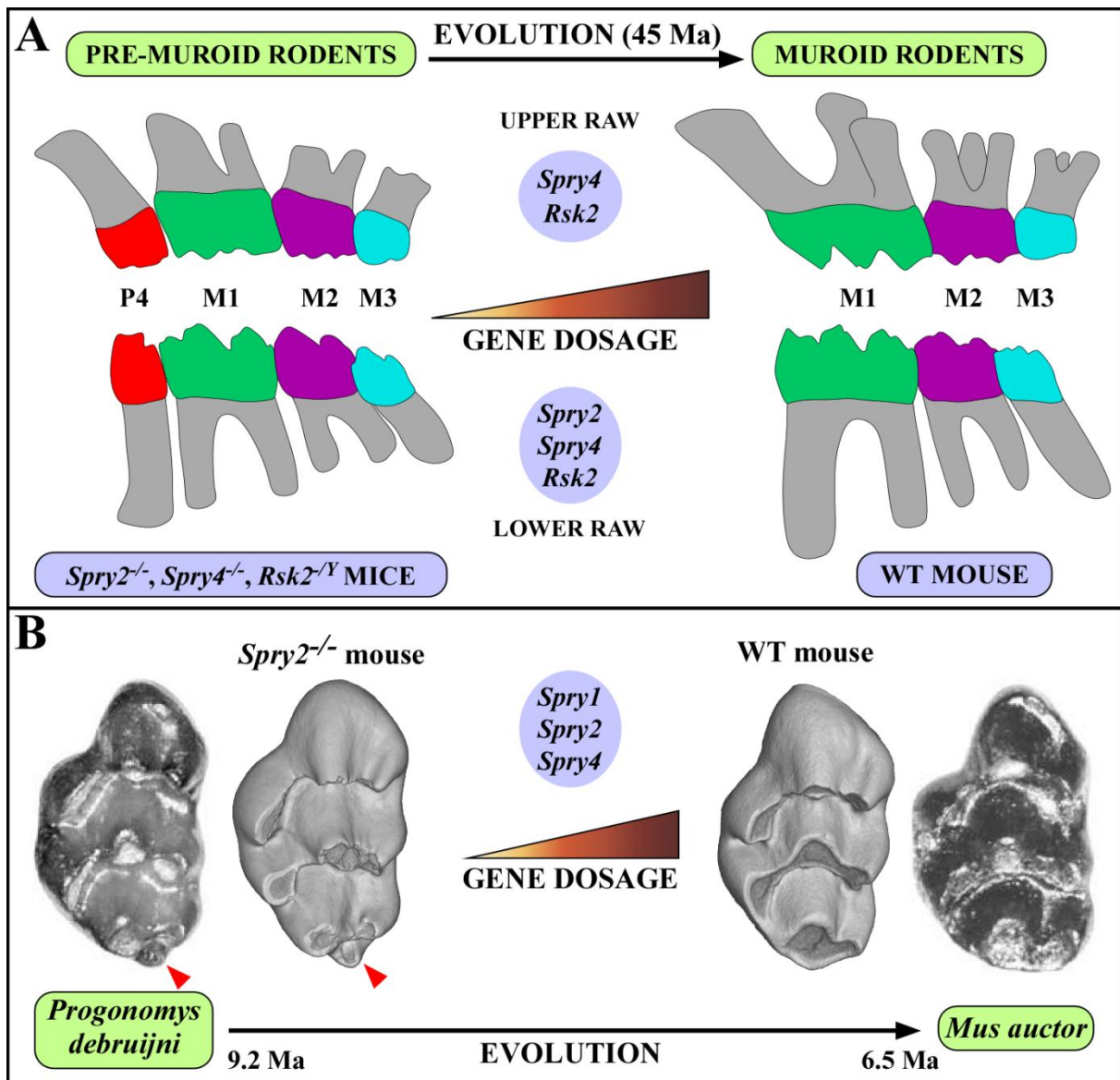


Fig. 5: Mutant dentition recapitulates the evolution of murine tooth characters. (A) The dental phenotype arising from the loss of function of *Spry2*, *Spry4* and *Rsk2* genes mimics the reduction of tooth number in muroid rodent evolution. (B) *Spry2^{-/-}* M¹ mimics *Progonomys debruijni* M¹.

Interestingly, a character that stands out from the mutant mice is the occurrence of a supplementary distal cusp, named the posterocone, on the M¹ of the three Sprouty mutants (arrowhead in Fig. 5B). The posterocone is rarely present in extant species of murine rodents, whereas this cusp or the equivalent crest located at the same location, the posteroloph, were almost always present in the basal fossil murine genera such as *Potwarmus*, *Antemus*, and

Progonomys. However, neither the modern mouse (*Mus musculus*) nor its oldest ancestor (*Mus auctor*) display an individualized posterocone (Fig. 5B). In the lineage leading to the modern mouse, the posterocone has been lost during the transition from *Progonomys debuijini* to *Mus auctor*, and this transition is documented by the fossil record in the Siwaliks of Pakistan to have occurred between 9.2 and 6.5 Ma (dating from Kimura *et al.*, 2013). Apart from the presence of a posterocone, *Spry1*^{-/-}, *Spry2*^{-/-}, and *Spry4*^{-/-} mice share other dental features with these basal murine genera such as the trend of the lingual cusps of the M¹ to be least connected to the central cusps. All of these similarities indicate that *Spry1*, *Spry2*, or *Spry4* could have played a major role during the transition from *Progonomys* to *Mus*, which constitutes a major transition in the history of murine rodents.

CONCLUDING REMARKS

Spry1, *Spry2*, *Spry4*, and *Rsk2*, which encode components of the ERK-MAPK signalling pathway are identified here as putative major actors in the evolution of the dentition in rodents. These genes could have played a pivotal role in the reduction of the dental formula and in the rearrangement of the mesial parts of the first molars during the transition from pre-muroid to muroid rodents prior to 45 Ma. They also might have acted in the disappearance of the posterocone and in the connections of the lingual cusps to the chevrons during the transition from basal murines to *Mus auctor* between 9.2 and 6.5 Ma. Both morphological transformations happened independently, separated by about 35 Ma, suggesting that the premolar loss might have been triggered by *Rsk2* gene dosage augmentation. The posterocone would then have been triggered by an increase in Sprouty gene expression. Finally, an interesting issue remains open, which is the potential role of Sprouty or Fgf genes in the morphogenesis of the connections between lingual cusps and central cusps of the M¹ chevrons. Charles *et al* (2009) reported that *Fgf3*^{-/-} mice have M¹ with lingual cusps that are

completely disconnected from the central cusps. Here we report that Sprouty mice, especially *Spry2*^{-/-} and *Spry4*^{-/-} mice, often have M¹ with disconnected lingual cusps. As Sprouty and Fgf genes are known to play antagonist roles during tooth morphogenesis, it is interesting to note that the loss of function of the two antagonist results in an equivalent impact on the lingual cusps of the M¹.

ACKNOWLEDGEMENTS

We thank E. Maître for her help in the morphological description of the teeth. We thank A. Hanauer, V. Fraulob and B. Schuhbaur for providing, expanding and genotyping respectively the *Rsk2*^{-Y} mouse colony, and Nicolas Strauli and Sarah Alto for help with the Sprouty mouse breeding. We are grateful to A. Langer and P. Dolle. We also thank V. Lazzari for his critical reading of the manuscript.

This work was funded by grants from the University of Strasbourg, the Hôpitaux Universitaires de Strasbourg (API, 2009-2014, Development of the oral cavity: from gene to clinical phenotype in Human to ABZ), the IFRO, and EU-ERDF A27 (Oro-dental manifestations of rare diseases to ABZ), the ENS de Lyon (to LV), and the NIH (R01 DE021420 to ODK). Support for this research was also provided by the RMT-TMO Offensive Sciences initiative, INTERREG IV Upper Rhine program <http://www.genosmile.eu>.

CONTRIBUTIONS

L.V and O.D.K conceived the project. P.M and C.C designed the analyses, which P.M and C.C performed. P.T conducted the ESRF imaging of Sprouty mouse dental rows. V.L.H and A.B-Z provided the *Rsk2*^{-Y} mice, while A.J bred the Sprouty null mice. P.M, C.C, A.B-Z, O.D.K and L.V wrote the manuscript.

- Åberg, T., Wang, X. P., Kim, J. H., Yamashiro, T., Bei, M., Rice, R., Ryoo, H. M. and Thesleff, I.** (2004). Runx2 mediates FGF signaling from epithelium to mesenchyme during tooth morphogenesis. *Dev. Biol.* **270**, 76–93.
- Ahn, Y., Sanderson, B. W., Klein, O. D. and Krumlauf, R.** (2010). Inhibition of Wnt signaling by Wise (Sostdc1) and negative feedback from Shh controls tooth number and patterning. *Development* **137**, 3221.
- Aouadi, M., Binetruy, B., Caron, L., Le Marchand-Brustel, Y. and Bost, F.** (2006). Role of MAPKs in development and differentiation: lessons from knockout mice. *Biochimie* **88**, 1091–1098.
- Campos, L. S., Leone, D. P., Relvas, J. B., Brakebusch, C., Fässler, R., Suter, U. and others** (2004). β 1 integrins activate a MAPK signalling pathway in neural stem cells that contributes to their maintenance. *Development* **131**, 3433–3444.
- Charles, C., Pantalacci, S., Tafforeau, P., Headon, D., Laudet, V. and Viriot, L.** (2009a). Distinct impacts of Eda and Edar loss of function on the mouse dentition. *PLoS One* **4**, e4985.
- Charles, C., Lazzari, V., Tafforeau, P., Schimmang, T., Tekin, M., Klein, O. and Viriot, L.** (2009b). Modulation of Fgf3 dosage in mouse and men mirrors evolution of mammalian dentition. *Proc. Natl. Acad. Sci.* **106**, 22364.
- Corson, L. B., Yamanaka, Y., Lai, K.-M. V. and Rossant, J.** (2003). Spatial and temporal patterns of ERK signaling during mouse embryogenesis. *Development* **130**, 4527–4537.
- Downward, J.** (2003). Targeting RAS signalling pathways in cancer therapy. *Nat. Rev. Cancer* **3**, 11–22.
- Fabre, P.-H., Hautier, L., Dimitrov, D. and Douzery, E. J.** (2012). A glimpse on the pattern of rodent diversification: a phylogenetic approach. *BMC Evol. Biol.* **12**, 88.
- Frödin, M. and Gammeltoft, S.** (1999). Role and regulation of 90 kDa ribosomal S6 kinase (RSK) in signal transduction. *Mol. Cell. Endocrinol.* **151**, 65–77.
- Ge, C., Xiao, G., Jiang, D. and Franceschi, R. T.** (2007). Critical role of the extracellular signal-regulated kinase–MAPK pathway in osteoblast differentiation and skeletal development. *J. Cell Biol.* **176**, 709–718.
- Goodwin, A. F., Oberoi, S., Landan, M., Charles, C., Groth, J., Martinez, A., Fairley, C., Weiss, L. A., Tidyman, W. E., Klein, O. D., et al.** (2013). Craniofacial and dental development in cardio-facio-cutaneous syndrome: the importance of Ras signaling homeostasis. *Clin. Genet.* **83**, 539–544.
- Hacohen, N., Kramer, S., Sutherland, D., Hiromi, Y. and Krasnow, M. A.** (1998). sprouty encodes a novel antagonist of FGF signaling that patterns apical branching of the Drosophila airways. *Cell* **92**, 253–263.
- Hanafusa, H., Torii, S., Yasunaga, T. and Nishida, E.** (2002). Sprouty1 and Sprouty2 provide a control mechanism for the Ras/MAPK signalling pathway. *Nat. Cell Biol.* **4**, 850–858.
- Hanauer, A. and Young, I. D.** (2002). Coffin-Lowry syndrome: clinical and molecular features. *J. Med. Genet.* **39**, 705–713.
- HersHKovitz, P.** (1980). *Evolution of Neotropical Cricetine Rodents (Muridae): With Special Reference to the Phyllotine Group*. University Microfilms International.

- Kangas, A. T., Evans, A. R., Thesleff, I. and Jernvall, J.** (2004). Nonindependence of mammalian dental characters. *Nature* **432**, 211–214.
- Kim, H. J. and Bar-Sagi, D.** (2004). Modulation of signalling by Sprouty: a developing story. *Nat. Rev. Mol. Cell Biol.* **5**, 441–450.
- Kimura, Y., Jacobs, L. L. and Flynn, L. J.** (2013). Lineage-Specific Responses of Tooth Shape in Murine Rodents (Murinae, Rodentia) to Late Miocene Dietary Change in the Siwaliks of Pakistan. *PLoS ONE* **8**, e76070.
- Klein, O. D., Minowada, G., Peterkova, R., Kangas, A., Yu, B. D., Lesot, H., Peterka, M., Jernvall, J. and Martin, G. R.** (2006). Sprouty genes control diastema tooth development via bidirectional antagonism of epithelial-mesenchymal FGF signaling. *Dev. Cell* **11**, 181–190.
- Lagronova-Churava, S., Spoutil, F., Vojtechova, S., Lesot, H., Peterká, M., Klein, O. D. and Peterková, R.** (2013). The Dynamics of Supernumerary Tooth Development Are Differentially Regulated by Sprouty Genes. *J. Exp. Zool. B Mol. Dev. Evol.*
- Laugel-Haushalter, V., Paschaki, M., Marangoni, P., Pilgram, C., Langer, A., Kuntz, T., Demassue, J., Morkmued, S., Choquet, P., Constantinesco, A., et al.** (2014). RSK2 Is a Modulator of Craniofacial Development. *PLoS One* **9**, e84343.
- Li, Y.-X., Yun-Xiang, Z. and Xiang-Xu, X.** (2012). The composition of three mammal faunas and environmental evolution in the last glacial maximum, Guanzhong area, Shaanxi Province, China. *Quat. Int.* **248**, 86–91.
- Luo, J., Solimini, N. L. and Elledge, S. J.** (2009). Principles of cancer therapy: oncogene and non-oncogene addiction. *Cell* **136**, 823–837.
- Massague, J.** (2003). Integration of Smad and MAPK pathways: a link and a linker revisited. *Genes Dev.* **17**, 2993–2997.
- Moon, B.-S., Jeong, W.-J., Park, J., Kim, T. I., Choi, K.-Y. and others** (2014). Role of Oncogenic K-Ras in Cancer Stem Cell Activation by Aberrant Wnt/ β -Catenin Signaling. *J. Natl. Cancer Inst.* **106**, djt373.
- Neubüser, A., Peters, H., Balling, R. and Martin, G. R.** (1997). Antagonistic interactions between FGF and BMP signaling pathways: a mechanism for positioning the sites of tooth formation. *Cell* **90**, 247–255.
- Nie, X., Luukko, K. and Kettunen, P.** (2006). FGF signalling in craniofacial development and developmental disorders. *Oral Dis.* **12**, 102–111.
- Ohazama, A., Haycraft, C. J., Seppala, M., Blackburn, J., Ghafoor, S., Cobourne, M., Martinelli, D. C., Fan, C.-M., Peterkova, R. and Lesot, H.** (2009). Primary cilia regulate Shh activity in the control of molar tooth number. *Development* **136**, 897–903.
- Peterková, R., Lesot, H., Vonesch, J. L., Peterka, M. and Ruch, J. V.** (1996). Mouse molar morphogenesis revisited by three dimensional reconstruction. I. Analysis of initial stages of the first upper molar development revealed two transient buds. *Int. J. Dev. Biol.* **40**, 1009–1016.
- Peterková, R., Peterka, M., Vonesch, J. L., Turecková, J., Viriot, L., Ruch, J. V. and Lesot, H.** (1998). Correlation between apoptosis distribution and BMP-2 and BMP-4 expression in vestigial tooth primordia in mice. *Eur. J. Oral Sci.* **106**, 667–670.

- Pucek, Z., Niethammer, J. and Krapp, F.** (1982). *Sicista betulina* (Pallas, 1778)-Waldbirkenmaus. *Handb. Säugetiere Eur. Bd 2*, 516–538.
- Reich, A., Sapir, A. and Shilo, B.** (1999). Sprouty is a general inhibitor of receptor tyrosine kinase signaling. *Development* **126**, 4139.
- Rodrigues, H. G., Charles, C., Marivaux, L., Vianey-Liaud, M. and Viriot, L.** (2011). Evolutionary and developmental dynamics of the dentition in Muroidea and Dipodoidea (Rodentia, Mammalia). *Evol. Dev.* **13**, 361–369.
- Romeo, Y., Moreau, J., Zindy, P. J., Saba-El-Leil, M., Lavoie, G., Dandachi, F., Baptissart, M., Borden, K. L. B., Meloche, S. and Roux, P. P.** (2012). RSK regulates activated BRAF signalling to mTORC1 and promotes melanoma growth. *Oncogene* **32**, 2917–2926.
- Sebolt-Leopold, J. S. and Herrera, R.** (2004). Targeting the mitogen-activated protein kinase cascade to treat cancer. *Nat. Rev. Cancer* **4**, 937–947.
- Temtamy, S. A., Miller, J. D., Dorst, J. P., Hussels-Maumenee, I., Salinas, C., Lacassie, Y. and Kenyon, K. R.** (1974). The Coffin-Lowry syndrome: a simply inherited trait comprising mental retardation, faciodigital anomalies and skeletal involvement. *Birth Defects Orig. Artic. Ser.* **11**, 133–152.
- Temtamy, S. A., Miller, J. D. and Hussels-Maumenee, I.** (1975). The Coffin-Lowry syndrome: an inherited faciodigital mental retardation syndrome. *J. Pediatr.* **86**, 724–731.
- Thesleff, I.** (2003). Epithelial-mesenchymal signalling regulating tooth morphogenesis. *J. Cell Sci.* **116**, 1647.
- Thesleff, I. and Mikkola, M.** (2002). The role of growth factors in tooth development. *Int. Rev. Cytol.* **217**, 93–135.
- Tompkins, K.** (2006). Molecular mechanisms of cytodifferentiation in mammalian tooth development. *Connect. Tissue Res.* **47**, 111–118.
- Tong, Y. S.** (1992). *Pappocricetodon*, a pre-Oligocene cricetid genus (Rodentia) from central China. *Vertebr. Palasiat.* **30**, 1–16.
- Tucker, A. and Sharpe, P.** (2004). The cutting-edge of mammalian development; how the embryo makes teeth. *Nat. Rev. Genet.* **5**, 499–508.
- Viriot, L., Lesot, H., Vonesch, J. L., Ruch, J. V., Peterka, M. and Peterková, R.** (2000). The presence of rudimentary odontogenic structures in the mouse embryonic mandible requires reinterpretation of developmental control of first lower molar histomorphogenesis. *Int. J. Dev. Biol.* **44**, 233–240.
- Viriot, L., Peterková, R., Peterka, M. and Lesot, H.** (2002). Evolutionary implications of the occurrence of two vestigial tooth germs during early odontogenesis in the mouse lower jaw. *Connect. Tissue Res.* **43**, 129–133.
- Wang, X. P., Suomalainen, M., Felszeghy, S., Zelarayan, L. C., Alonso, M. T., Plikus, M. V., Maas, R. L., Chuong, C. M., Schimmang, T. and Thesleff, I.** (2007). An integrated gene regulatory network controls stem cell proliferation in teeth. *PLoS Biol.* **5**, e159.
- Wang, X. P., O'Connell, D. J., Lund, J. J., Saadi, I., Kuraguchi, M., Turbe-Doan, A., Cavalleco, R., Kim, H., Park, P. J., Harada, H., et al.** (2009). *Apc* inhibition of Wnt signaling regulates

supernumerary tooth formation during embryogenesis and throughout adulthood. *Development* **136**, 1939.

Wilkie, A. O. and Morriss-Kay, G. M. (2001). Genetics of craniofacial development and malformation. *Nat. Rev. Genet.* **2**, 458–468.

Xu, X., Han, J., Ito, Y., Bringas Jr, P., Deng, C. and Chai, Y. (2008). Ectodermal Smad4 and p38 MAPK are functionally redundant in mediating TGF- β /BMP signaling during tooth and palate development. *Dev. Cell* **15**, 322–329.

Yang, X., Matsuda, K., Bialek, P., Jacquot, S., Masuoka, H. C., Schinke, T., Li, L., Brancorsini, S., Sassone-Corsi, P., Townes, T. M., et al. (2004). ATF4 is a substrate of RSK2 and an essential regulator of osteoblast biology: implication for Coffin-Lowry syndrome. *Cell* **117**, 387–398.

Zhang, S., Lin, Y., Itaranta, P., Yagi, A. and Vainio, S. (2001). Expression of Sprouty genes 1, 2 and 4 during mouse organogenesis. *Mech. Dev.* **109**, 367–370.

A.3 MODULATIONS OF TOOTH DEVELOPMENT IN K14-SPRY4 MICE

Work on direct knock-out mutants for FGF signaling pathway has provided strong evidence of their importance during tooth development, but so has the work on the FGFR inhibitors. Sprouty genes have been established for the past 10 years as major modulators of tooth development. Li and colleagues (2014) recently reviewed the implication of the pathway during odontogenesis. FGFs and their receptors are necessary to initiate the right type of tooth at the right time and place (Tucker and Sharpe, 1999). They regulate the invagination of the dental epithelium, and are needed for the dental papilla to be condensed (Kettunen *et al.*, 2000; Wang *et al.*, 2004). Specific expression patterns in the pEK and sEKs of some *Fgf* genes are indispensable for correct tooth shape and cusp formation (Tucker and Sharpe, 2004), as well as to set proper ameloblast and odontoblast differentiation (Ruch *et al.*, 1995; Wang *et al.*, 2004). In adult mice, they play a crucial role in the maintenance of the incisor stem cell niche (Klein *et al.*, 2008; Chang *et al.*, 2013).

In the following article, I aim at addressing the global role of FGF signaling pathway in the dental epithelium. When tooth development is initiated, the competence to form a tooth germ lies in the mesenchyme, which induces the thickening of dental epithelium. After that first step, the odontogenic competence is shifted back to the epithelium (Maas and Bei, 1997). I take advantage of the existence of a transgenic mouse line to polish our understanding of the role of *Fgf* genes in shaping dental epithelium. Mice carrying the Tg(KRT14-Spry4)#Krum transgene (<http://www.informatics.jax.org/javawi2/servlet/WIFetch?page=alleleDetail&id=MGI:5466567>)

were designed to overexpress the *Spry4* gene in the oral epithelium leading thus to a down-regulation of FGF signaling pathway in this region. By linking erupted tooth morphology and histology of the developing tooth germ, I review the importance of Fgf genes in correctly shaping dental epithelium.

**Implications of FGF signaling pathway in tooth shape and mineralization:
insights from the K14-*Spry4* transgenic mice**

Pauline Marangoni¹, Cyril Charles¹, Youngwook Ahn², Kerstin Seidel³, Andrew Jheon³,
Sarah Alto³, Robb Krumlauf², Laurent Viriot¹, and Ophir Klein^{3,4}§

¹: Evo-Devo of Vertebrate Dentition, Institute of Functional Genomics of Lyon, ENS de Lyon, CNRS UMR 5242, University of Lyon 1, 46 allée d'Italie, 69364 Lyon cedex 07, France

²: Stowers Institute for Medical Research, 1000E 50th Street, Kansas City, MO 64110, USA

³: Department of Orofacial Sciences and Program in Craniofacial and Mesenchymal Biology, University of California San Francisco, San Francisco, CA 94143, USA

⁴: Department of Pediatrics and Institute for Human Genetics, University of California San Francisco, San Francisco, CA 94143, USA

§ Corresponding author: ophir.klein@ucsf.edu

ABSTRACT

The role of Fgf genes in tooth development has been gradually addressed to unravel the full extent of their involvement. Aiming at refining the current view on the FGF signaling pathway, we characterized the phenotype of erupted molars, and linked it with changes in the tooth developmental sequence, in mice carrying the Tg(KRT14-Spry4)#Krum transgene. The global down-regulation of the pathway in these mice led to the setting of mineralization defects affecting the enamel layer, which were highly penetrant. Other modifications in cusp shape tackle the developmental delay observed in embryos. The impaired formation of the molar primary enamel knot resulting from the delay affects the molecular regulation of tooth development. Lastly, the rare occurrence of a fusion between upper and lower provide additional information to approach *syngnathia*. This study thus further delineates the role of FGF signaling pathway in the development of the oral region.

KEY WORDS

FGF signaling pathway, tooth shape, enamel mineralization, syngnathia

INTRODUCTION

FGF signaling pathway is a major actor of tooth development. For the past decade, the role of Fgf genes in setting the very specific developmental sequence of tooth development has been investigated (Li *et al.*, 2014). Given the number of available mouse mutants for this specific signaling pathway, research has also been able to hypothesize on their evolutionary implications in setting the complex mouse molar cusp pattern (Kavanagh *et al.*, 2007; Charles *et al.*, 2009; Harjunmaa *et al.*, 2014). Most of our knowledge on FGF signaling pathway and tooth evo-devo has been provided by loss of function mice that were simple or double mutants for Fgf genes or for Sprouty (Spry) genes. The latter are very important when looking at the tight time- and tissue-specific regulation of tooth development.

Indeed, Spry genes were first identified as inhibitors of FGF receptors (FGFR) in *Drosophila* (Hacohen *et al.*, 1998), and their inhibitory effects were extended to the mouse (Mason *et al.*, 2006). Four Spry orthologs are found in *Mus musculus* (de Maximy *et al.*, 1999). *Spry1*, *Spry2* and *Spry4* are expressed during tooth development (Klein *et al.*, 2006). Their expression is induced by the stimulation of growth factors, and they inhibit in FGFR-mediated activation of the ERK-MAPK signaling pathway (Hanafusa *et al.*, 2002). In terms of their implication during tooth development, *Spry2* and *4* genes are known to prevent the development of diastemal buds and to restrict the ameloblast differentiation in the lingual side of the incisor (Klein *et al.*, 2006; Klein *et al.*, 2008; Lagronova-Churava *et al.*, 2013, Marangoni, Charles *et al.* in prep.). In addition, along with *Spry1*, all three are important for setting the right murine cusp pattern (*ibidem*).

Here we focus on a transgenic mouse line carrying a transgene that has newly been implemented in the JAX allele database – the Tg(KRT14-Spry4)#Krum transgene – in which the expression of *Spry4* mouse cDNA is driven under the control of the keratin-14 human

promoter (<http://www.informatics.jax.org/javawi2/servlet/WIFetch?page=alleleDetail&id=MGI:5466567>).

This line will be referred to as K14-*Spry4* line in the following article. It was designed to mimic a global down-regulation of epithelial FGF signaling pathway. Although in the course of tooth development *Spry4* gene is normally expressed in the dental mesenchyme (Klein *et al.*, 2006), the transgene is expressed in the whole oral epithelium which includes dental epithelium. The erupted molar morphology in the transgenic specimens displays numerous signs of enamel layer irregularities. Histologic analyses of the developing tooth germs highlights a developmental delay that affects the formation of the tooth primary signaling center: the primary enamel knot (pEK). Preliminary gene expression pattern study reveals a shrinking of the lower tooth germ pEK that make *Shh* expression hardly detectable. Finally, the defects are not only seen in the developing tooth region, but a rare fusion of the upper and lower jaws also occurs in that genetic background.

MATERIAL AND METHODS

Transgenic mice

K14-*Spry4* mice were designed and produced in the Stowers Institute for Medical Research, Kansas City (USA). The mouse *Spry4* cDNA (904b) was inserted downstream of a human KRT14 promoter (2.2kb) preliminary amplified from a BAC clone (RP11-434D2) using the following primers: 5'-AAGATCTAGG-TGCGTGGGGTTGGGATG-3' and 5'-GAAGCTTGAGCGAGCAG-TTGGCTGAGTG-3'. The gene was then subcloned into the pCMS-EGFP vector (Clontech) replacing the CMV promoter. After linearization and gel-purification, the 3772 bp-long pKRT14-*Spry4* construct was injected into a CBA/J x C57BL/10J one-cell zygote.

The line was maintained since 2008 by breeding transgenic males with CBA/J x C57BL/10J females. The transgenic offspring displays a less furnished fur and abnormal and/or shorter tail. Embryos for the present study were generated by breeding transgenic males with C57BL/6J females. In those embryos, the transgene displayed a mosaic expression pattern detectable from the embryonic day 14 (E14). Mice were housed at the UCSF.

Characterization of erupted dentition

A sample of 25 transgenic adults, and 15 WT littermates was generated in the LARC (UCSF, USA) by breeding C57BL/6J females with K14-*Spry4* males. At five weeks, animals were sacrificed by CO₂ asphyxia and cervical dislocation. Their heads were placed in a *Dermestes maculatus* colony to clean the skulls, which were then imaged using X-ray microtomography (cubic voxel size of 3µm). Crown surface was measured on the occlusal-oriented pictures of the scanned volumes by drawing the outline of the molars with Canvas.

Histological analyses

Noon of the day on which the vaginal plug was detected was considered as the E0.5. Whole litters (125 embryos in total) were collected every 12 hours from E13 to E18.5. Littermates were genotyped using the following primers: 5'-CTGGGCAGGTAAGTATCAAGG-3' and 5'-TGGTCAATGGGTAAGATGGTG-3'. PCR was performed according to: 2 min at 94°C, 25 cycles of 30 s at 94°C – 30 s at 54.8°C – 1 min at 72°, and 5 min at 72°C. K14-*Spry4* transgenic embryos display a 354bp fragment specific to the construct. Embryos were collected in 1X PBS and fixed overnight in 4% PFA. After dehydration in graded ethanol, embryos were processed in paraffin and serially sectioned (7 µm thick) using a Leica Autocut 2055 microtome. Masson's trichrome was used to conduct the histological analyses of the sectioned dental germs (hemalum, 8 min; fushine, 2 min; aniline blue, 1 min). Pictures were taken with an Olympus microscope equipped with a CCD camera and Cell F™.

Gene expression patterning

DIG-labeled probes for *Sonic hedgehog* gene (*Shh*) were generated from a plasmid (Molecular Zoology team, IGFL). Plasmid linearization was carried out with HindIII restriction enzymes (New England Biolabs) at a concentration of 5 units for 1µg DNA. The linearized DNA fragments were transcribed *in vitro* using T3 RNA polymerase (Invitrogen) and labeled with a digoxigenin labeling mix (Roche). *In situ* hybridizations were performed on E14.5, and E15.5 beforehand sectioned WT and transgenic embryos according to standard protocols. Samples were deparaffinized with xylene, rehydrated in graded ethanol and treated with 10 µg/mL proteinase K (Roche) before being hybridized with probe overnight at 70°C. Staining was repeated on serial sections. Pictures were taken with a Leica microscope equipped with a CCD camera and Cell F™.

RESULTS

Fgf gene down-regulation leads to strong enamel irregularities, mild cusp defects, and smaller teeth

We investigated the arrangement and shape of the molar rows in a population of 25 transgenic mice and compared it to what 15 of their WT littermates display. The mice were collected at 5-week-old to study fully erupted but still only slightly worn molars.

Analysis of molar tooth phenotype shows that the transgenic molar rows display a great diversity of cusp defects, but also defects in the tooth neck. The latter marks the anatomic separation between the crown covered with enamel and the roots covered with cementum. The most prevalent defects in the upper molar rows are (1) the presence of indentations of the tooth neck (62%), which are especially visible on the mesial side of the M¹ (35%), and (2) the presence of pits and irregularities on the crown enamel surface (50%) (Fig.1A, B). On the lower molar rows, the presence of indentations of the tooth neck is visible in the entire transgenic population, the vestibular side being often the most severely affected (vestibular and lingual views, Fig.1B, C). Moreover, in 50% of the transgenic cohort, the distal-most part of both M₁ and M₂ is reduced or absent, while the mesio-vestibular cusp of the M₁ is reduced in 30% of the transgenic specimens (occlusal views, Fig.1B, C).

A variable series of cusp defect affects both M¹ and M₁ transgenic molars to a lesser extent (Fig.2). Indeed, M¹ occasionally display (1) an ectopic connection linking the lingual cusps of both 1st and 2nd chevrons (4%), (2) a disconnection of the lingual-most cusp of the 1st chevron (2%), (3) an ectopic crest linking the vestibular cusps of both 1st and 2nd chevrons (2%), and (4) a splitted and individualized 1st chevron central cusp (2%) (Fig.2B). M₁ occasionally display ectopic connection of the distal-most part of the tooth (4%), a bigger mesio-lingual cusp (4%), a splitted mesio-lingual cusp (2%), and cingular cusps (2%) (Fig.2D).

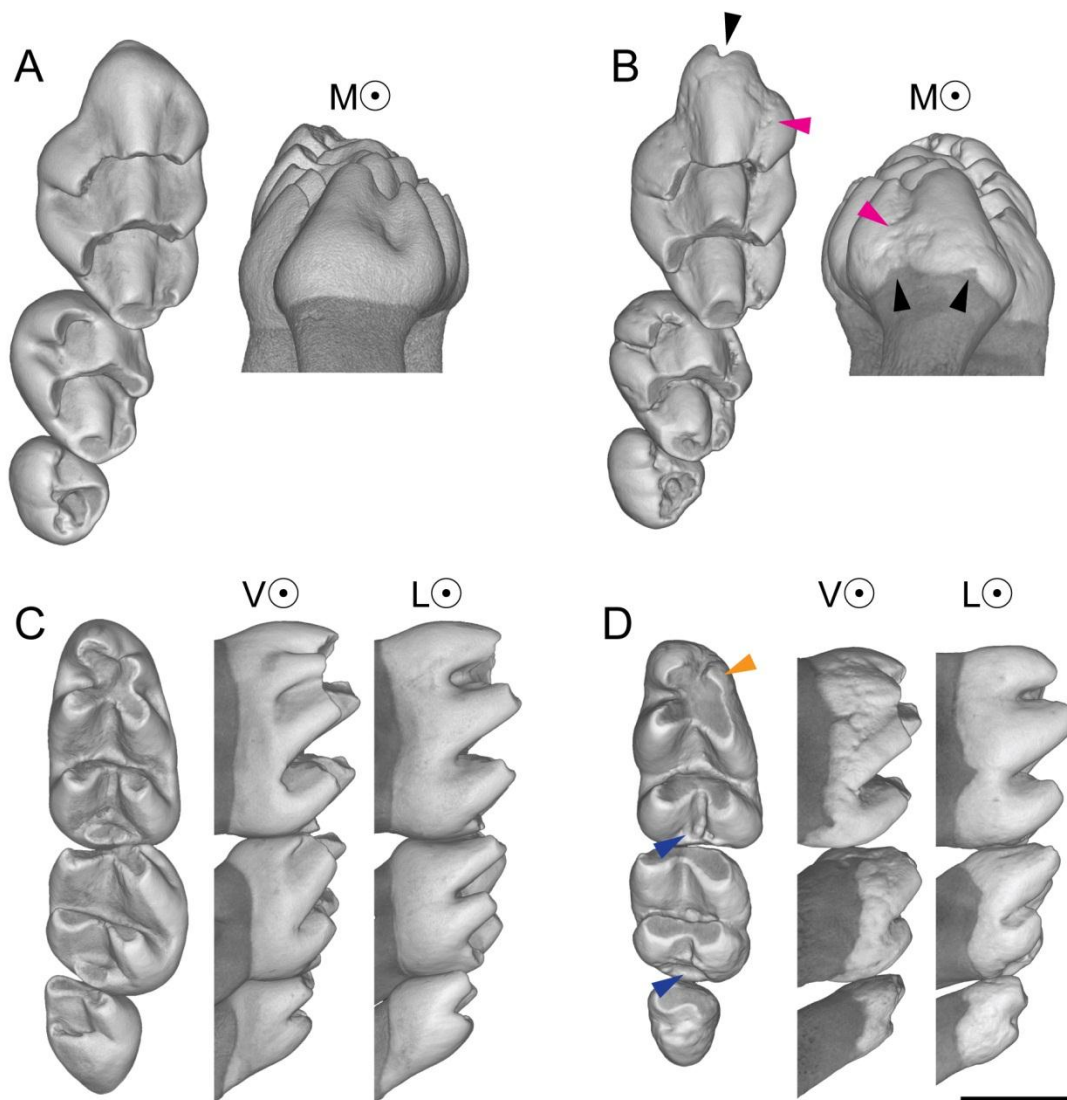


Fig. 1: Most prevalent phenotypes in the K14-*Spry4* mice compared to the phenotype of their WT littermates. M (mesial), V (vestibular), and L (lingual) refer to the orientation of the molar row. (A) Upper WT molar row, occlusal (left) and mesial (right) views. (B) Upper transgenic molar row, occlusal (left) and mesial (right) views. Black arrowhead points to the irregularities of the tooth neck, pink arrowhead to small enamel pits or irregularities. (C) Lower WT molar row, occlusal (left), vestibular (center), and lingual (right) views. Note the very smooth tooth neck displayed at the limit of the enamel layer. (D) Lower transgenic molar row, occlusal (left), vestibular (center), and lingual (right) views. Orange arrowhead points the reduction of the mesio-vestibular cusp, while blue arrowheads show the reduction of the distal-most cusps of both M_1 and M_2 . On the vestibular and lingual view, note the indentations of the tooth neck. Scale bar: 0.75 mm.

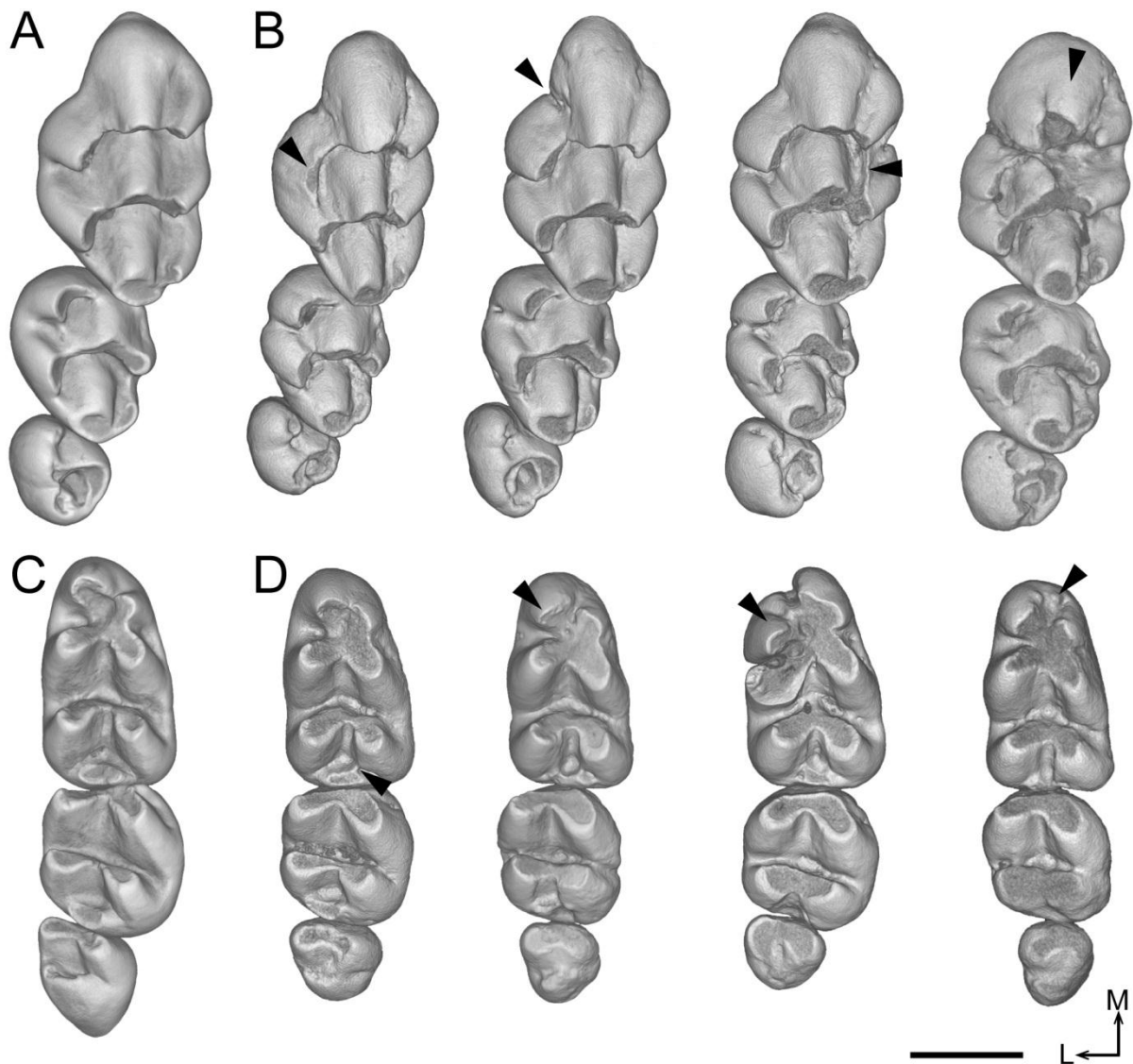


Fig. 2: Additional cusp defects in the transgenic M^1 and M_1 . (A) Upper WT molar row phenotype. (B) From left to right, transgenic M^1 also display a connection between the two lingual-most cusps (4%), a disconnection of the lingual cusp of the 1st chevron (2%), a partial vestibular crest (2%), and a splitted and individualized 1st chevron central cusp (2%). (C) Lower WT molar row phenotype. (D) From left to right, transgenic M_1 also display a ectopic connection of the distal-most part of the tooth (4%), a bigger mesio-lingual cusp (4%), a splitted mesio-lingual cusp (2%), and cingular cusps (2%). Scale bar: 0.75 mm. M and L arrows respectively points towards the mesial and lingual directions.

Tooth surface measurements confirmed that both the upper and lower transgenic molars are smaller than the WT molars (Fig.3). The range of tooth surface displayed in the transgenic cohort is wider than the WT one, once again illustrating the variability of the phenotypes obtained in the transgenic mice.

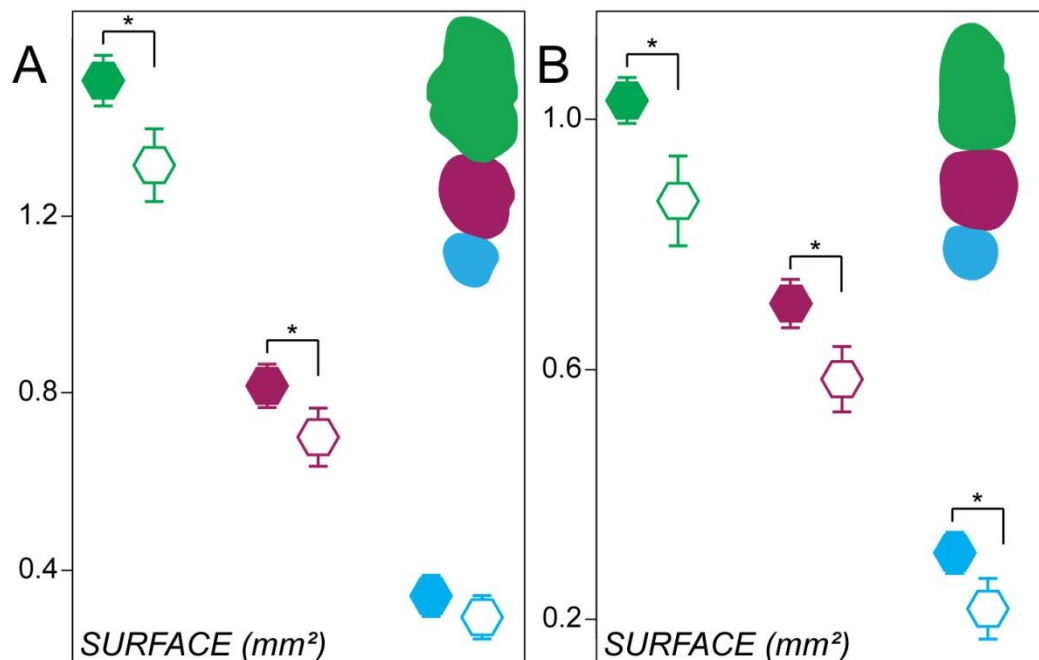


Fig. 3: Comparison of the molar surface in the transgenic to the molar surface of their WT littermates. The tooth surface was measured in occlusal views. WT tooth are depicted with filled hexagons, transgenic molars with blanked hexagons; error bars represent the measurement standard deviation. (A) Measurements in the upper rows show that transgenic M¹ and M² display a smaller surface (t-test, *p*-value<0.05). (B) Measurements in the lower rows show all three transgenic molars have a surface smaller than the WT one (t-test, *p*-value<0.05).

FGFs are essential to ensure the pEK formation and the right dental epithelium shape

In the tooth developmental sequence, the formation of a group of non-dividing cells called the primary enamel knot (pEK) at the cap stage is necessary to drive the next steps (Jernvall *et al.*, 1994). The pEK is a cluster of cells specifically expressing some genes among which is *Fgf4*. The secreted FGF4 protein will direct further invagination of the epithelium, thus playing a role in the crown patterning (Jernvall *et al.*, 1998; Vaahtokari *et al.*, 1996). We

firstly focused on the cap stage which starts at about E14.0 in WT mice, and on the immediate surrounding stages (Fig.4). At the bud stage, the transgenic upper and lower first molar buds look similar to the WT ones (E13.0 and E13.5 in Fig.5). At E14.0, observations reveal a developmental delay with the absence of invagination of the transgenic cervical loops (black arrowheads in the WT). The delay is confirmed at E14.5 with the absence of a fully formed pEK in about 50% the transgenic mice. Sections also reveal that the developmental delay appears caught up by E15.5, the transgenic molar germs remaining only smaller.

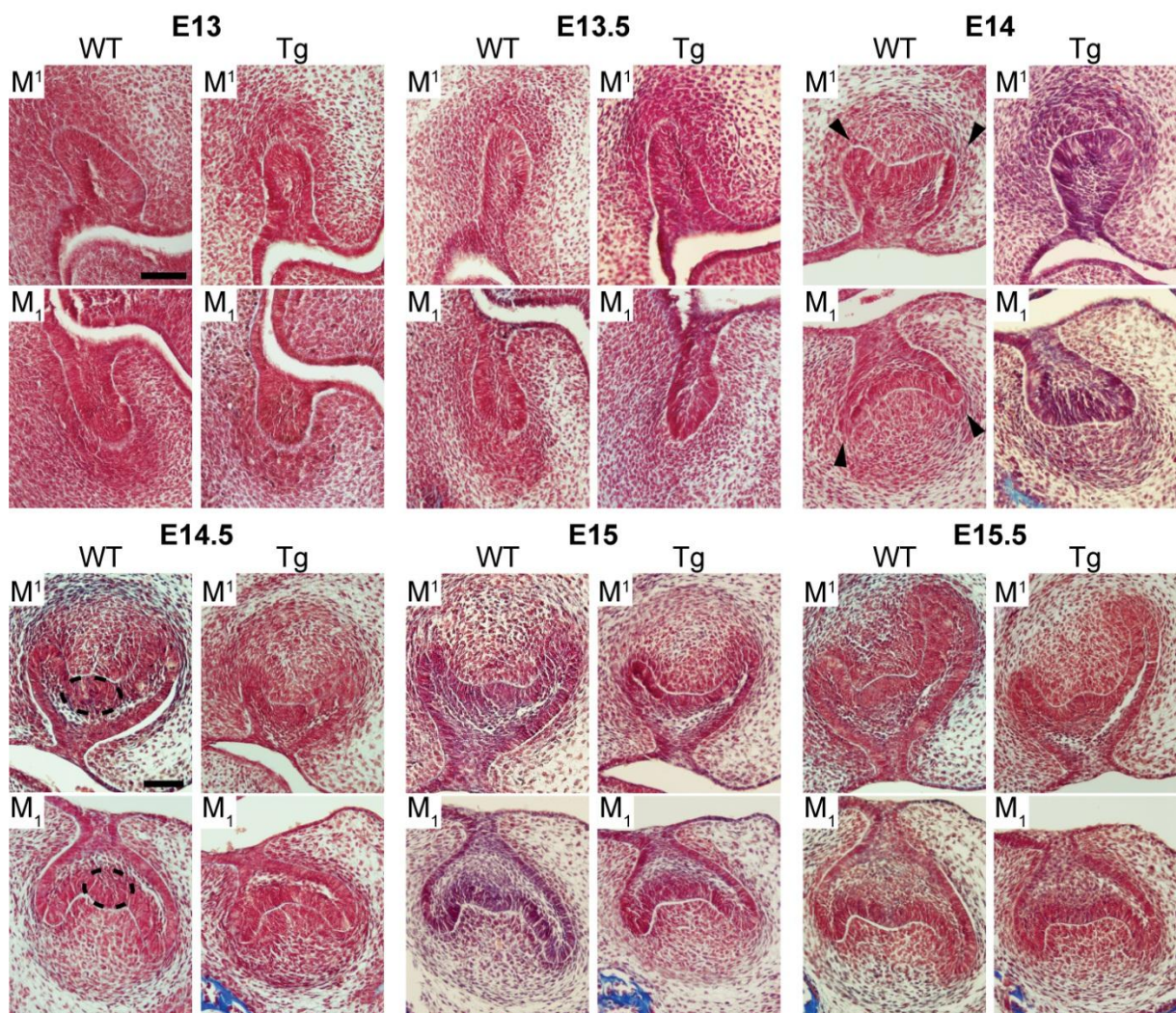


Fig. 4: Comparison of transgenic and WT first molar histo-morphogenesis from the bud to prior to the bell stage. CL invagination (black arrowheads) and pEK (dotted circles) formation are delayed in the transgenic cohort. First picture row is displayed at the same scale than in E13.0 WT M¹; second picture row is displayed at the same scale than in E14.5 WT M¹. Scale bars: 100 μ m.

Focusing on late bell stage (E16.5 onwards), we tried to find an histological explanation to the irregular surface of the crown enamel and to the indentations. Overall, the transgenic dental germs, and especially the lower ones, display a rather irregular shape of their inner enamel epithelium in the sectioned embryos, with abnormal cell morphology being mostly visible on the cervical loops (dotted line, Fig.5).

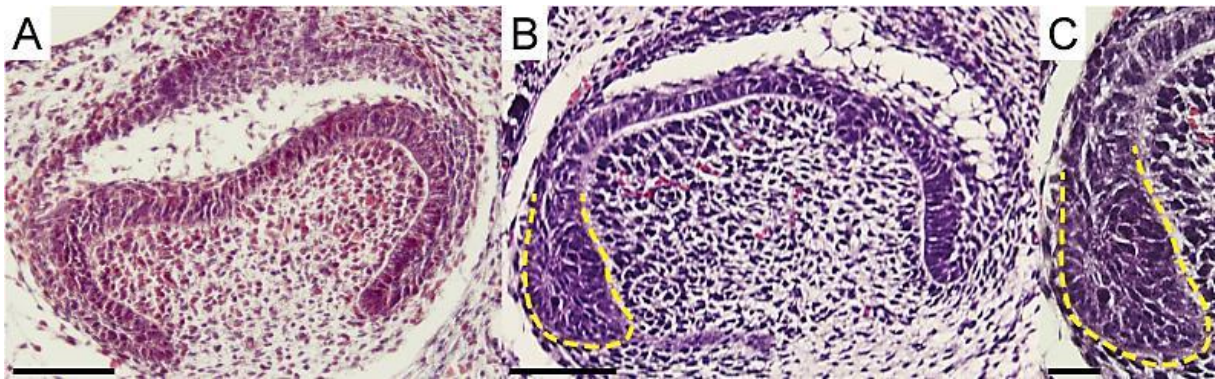


Fig. 5: Abnormal shape of the transgenic molar germ cervical loops. (A) WT embryo at E16.5. (B) Transgenic embryo at E16.5. Note the irregularly large aspect of the cervical loop. (C) Close up on the defect. Scale bars: 100 μ m.

Our analysis of the late bell tooth germ histology was confronted to the relative difficulty of harvesting transgenic embryos. Given the crossbreeding realized, we expected to get an approximate transgenic vs. WT embryos ratio of 0.5 per litter. However, we noticed during our embryo collection a decrease in the transgenic embryo proportion (Mann-Whitney Wilcoxon sum rank test, p -value <0.05). This decrease starts to occur at E16.5, while the size of the litters stays in the range of what is described in WT laboratory mice (Tab.1).

	E13	E13.5	E14	E14.5	E15	E15.5	E16	E16.5	E17	E17.5	E18	E18.5
transgenic ratio	0.53	0.53	0.47	0.50	0.52	0.50	0.44	0.40	0.37	0.38	0.31	0.22
litter mean size	7.5	7.5	7.5	9	7	9	7	7.5	6.5	8	6	6.5

Tab. 1: Evolution of both the proportion of transgenic embryos in the collected litters and the mean number of embryos per stage. The proportion of transgenic embryos drops starting E16.5 (Mann-Whitney Wilcoxon sum rank test, p -value<0.05), while the number of embryos collected in every litter remains consistent (no statistically significant difference detected, p -value=0.1).

FGF signaling pathway down-regulation impacts the expression *Shh* gene

As pEK is a major signaling center that sends morphogenesis signals to perfect tooth formation, we focused on this structure to tackle the question of possible deregulation of the molecular networks involved. Some genes are already known to be expressed in these rounded structures. The list includes *Fgf3*, *4* and *9*, some *Bmps*, *Edar*, a couple of *Wnts* and *Shh* (Jernvall *et al.*, 1998; Kettunen and Thesleff, 1998; Yamashiro *et al.*, 2003). Our attention was drawn to *Shh* because it is a member of the eponymous SHH pathway, because its expression is restricted to EKs only, and because *in vitro* addition of exogenous SHH resulted in abnormal epithelial invagination (Hardcastle *et al.*, 1998). Investigating the expression pattern of the candidate gene *Shh*, we observed at E14.5 and E15.5 that *Shh* expression was located in a smaller area in the lower dental germs, making it hardly detectable in the lower tooth germs (Fig.6).

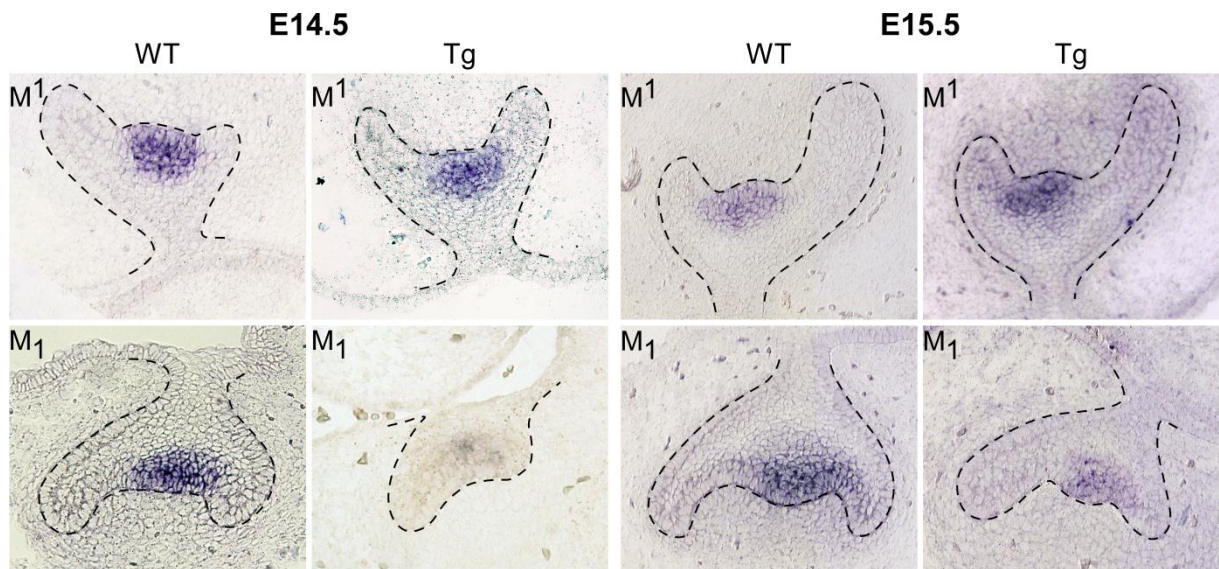


Fig. 6: *Shh* gene expression variations in the lower tooth germ. Note the apparent weaker staining in the lower transgenic genes, likely due to the smaller region identified as pEK. Dotted lines help visualizing the tooth germ.

FGF signaling pathway down-regulation can lead to a defect in maintaining the upper and lower jaws separated

Along with this, a rare but severe defect affects 8% of the transgenic cohort. It consists in the failure to keep the upper and lower jaws properly separated (Fig.8). This failure results in a fusion of the upper and lower jaws. The fusion ranges from a simple juxtaposition and sealing of the upper and lower dental epithelium in the region where teeth develop (Fig.7A), to a severe sealing associated with cell proliferation between the two initial layers (Fig.7B).

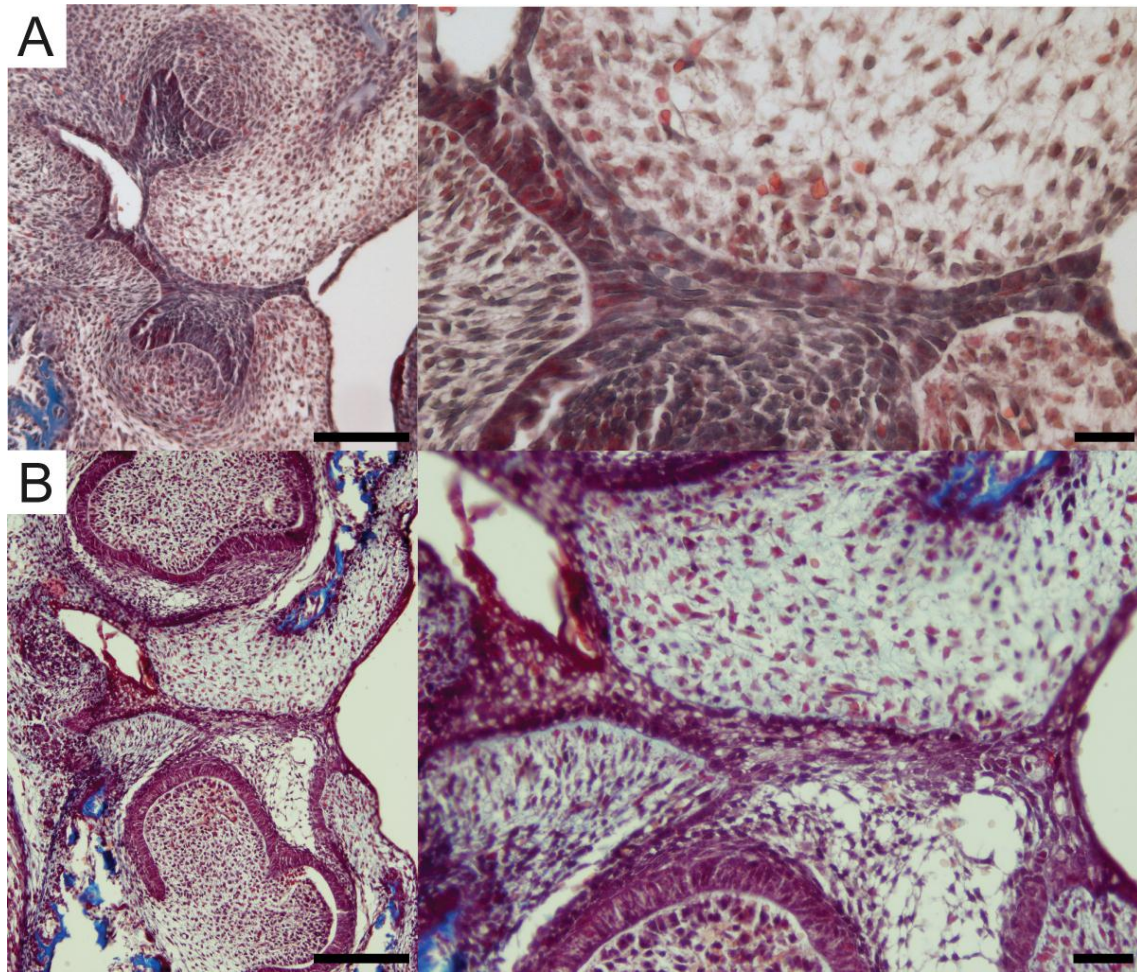


Fig. 8: Fusion of the upper and lower jaws in the transgenic mice. The penetrance of the phenotype is 8%. (A) Milder fusion phenotype, with the maxillary and mandibular shelves still visible. (B) More severe fusion with a proliferating event sealing the upper and lower jaws together. Scale bars: 500 μm .

DISCUSSION

Fgf gene importance in setting tooth shape and proportions is confirmed

The global down-regulation of FGF signaling pathway in mice carrying the Tg(KRT14-Spry4) transgene causes a reduction in the tooth surface. This result is highly similar to what is observed in other Fgf mutant mice (namely in *Fgf3*^{-/-} mice, Charles *et al.*, 2009). However, the transgenic mice also display strong irregularities of the enamel layer in both upper and lower molars, as well as a reduction of the distal-most parts of the M₁ and M₂. Ameloblasts are responsible for enamel secretion, and they are specifically polarized cells (Zeichner-David *et al.*, 1995). Abnormalities observed at the histological scale in the morphology of the inner enamel epithelium and the cervical loop cells could result in an abnormal enamel secretion and mineralization. Because the mineralization defects are the most prevalent defects overall, the role of Fgf genes in that process can be addressed in *in vivo* models, which will help specifying the conclusions obtained from cultured tooth germs (Tsuboi *et al.*, 2003).

The reduction or absence of the distal-most parts of the M₁ and M₂ raises the interesting question of the sequence of cusp addition. The molar developmental sequence progresses from the mesial to the distal part of the presumptive row (Viriot *et al.*, 2002), but the sequence of cusp formation has not been characterized yet. In that context, it is difficult to link the delayed formation of the pEK to this reduction, which both occur in 50% of the transgenic cohort (embryo or adults).

The K14-Spry4 line displays a great phenotypic variability

The display of highly variable cusp defects in both M¹ and M₁, as well as much more frequent defects, is interesting. This might be imputable to transgene expression variations,

resulting in gene dosage changes. When a gene is translocated or a transgene inserted into a *locus*, it is not rare to witness *cis* inactivation when the final locus is in or next heterochromatin. This effect is called variegation, and was described first in *Drosophila melanogaster* (Muller, 1930). It is also well-known in plants, in which it is responsible for the differential color sometimes displayed in the leaves (Chen *et al.*, 2000). This same phenomenon could be the cause of the mosaicism in the transgene expression observed, resulting in highly variable phenotype on top of the signature phenotypes of the transgenic line.

More generally, given the increase in transgenic embryo lethality, the adult morphologies we observe are likely to be only a subset of the tooth defects that could be developed. We should not forget that the transgene ectopically expresses a general RTK inhibitor in a developmental context where teeth are not the only organ forming. Tooth development is not the only process affected by the transgene expression, as is evidenced by the presence of an abnormal hair phenotype on these mice. *Spry* genes are known to antagonize Endothelial Growth Factor (EGF) signaling, and given the role of Vascular EGFs (VEGFs) in patterning the cardiovascular system, we can hypothesize that the embryonic lethality would be associated with defects in this developmental process (Ferrara, 2005).

Fgf genes are major actor of the tooth development regulation

Preliminary results on the expression pattern of Fgf gene interactors in the pEK reveal that *Shh* gene expression is hardly detectable in lower transgenic germs, the size of pEK being apparently smaller. According to the established model of signaling in the molar pEK, epithelial FGFs stimulate SHH signaling pathway thanks to a dialog with mesenchymal FGFs (Klein 2006). The absence of modulation of *Shh* gene expression in the upper transgenic

molar germ suggests the existence of a compensatory regulation specific to the upper molar germ.

The upper and lower jaws, and their respective derivatives, do not share the same embryonic origin (Tucker and Sharpe 2004). Neither are they formed under the same molecular control (Tucker and Sharpe 1999, Cobourne and Sharpe 2003). This so-called 'odontogenic homeobox code' could explain the differences in the phenotypes observed between upper and lower transgenic molars. Given that the majority of the studies investigating tooth development molecular regulation have been conducted in KO mutants, we expect from future analyses in this transgenic mouse line to perfect our understanding of those upper vs. lower tooth development differences.

FGF signaling pathway down-regulation leads to congenital defects

The epithelial fusion is certainly rare in the transgenic mouse line studied here, but it has a promising implication in better understanding the development of a craniofacial syndrome. Equivalent cases of partial closing of the oral cavity (syngnathia) have been reported in fewer than sixty cases in human patients (e.g. Dawson *et al.*, 1997; Fallahi *et al.*, 2010). A recent study elegantly demonstrated that *Fgf8* was implicated in the setting of the fusion in a dosage-dependent manner (Inman *et al.*, 2013). *Fgf8* is expressed in the early tooth development, as well as in the 1st pharyngeal arch (Maas and Bei, 1997). The defects we see in the tooth developmental sequence occur from E14.0 on, but we cannot rule out that the development of the syngnathia in our transgenic mice actually starts earlier, which might indicate that *Fgf8* down-regulation is involved here.

Syngnathia also occurs in other mutant mice, especially in the *Jag2*^{-/-} mouse embryos that display a similar fusion (Mitsiadis *et al.*, 2005). JAG2 is one of NOTCH ligand. NOTCH signaling pathway is involved in what is called lateral inhibition which is one of the

mechanisms controlling cell differentiation (Kopan and Ilagan, 2009). *Jag2* null mice die at birth and display abnormal morphology of dental germs as well as fusion between the palatal and mandibular shelves. The penetrance of the fusion in *Jag2* null mutants seems to be more important and the histology of the defect looks similar in every reported case. However, it has not been used yet to address the human pathology, and our results point towards the existence of convergent molecular mechanisms leading to this defect.

The upper and lower jaws do not originate in the same embryonic annex. The upper jaw is formed with cells from the fronto-nasal process and from the first branchial arch, whereas the lower jaw is formed with 1st branchial arch cells (Cobourne and Sharpe, 2003). The observed sealing and fusion of the epithelia is due to a defect in maintaining the jaws separated. A change in the cellular junction patterning is likely to cause the sealing of the two epithelial layers. FGFs are known to interact with the actin cytoskeleton (Chihara *et al.*, 2003; Wheelock and Johnson, 2003). This interaction is mediated by the regulation of the Rac kinase activity. The more phosphorylated the actin is, the less stable it is, preventing it from polymerizing. When FGF signaling is reduced, so is Rac activity, leading to the stabilization of actin. It might result in the polymerization of actin filaments that is likely to increase the cellular junctions interacting with actin cytoskeleton.

CONCLUDING REMARKS

In summary, the K14-*Spry4* mouse line has put the focus on the importance of Fgf genes to form a smooth and regular enamel layer. Epithelial Fgf genes were found essential to develop the pEK in the correct time frame. This project highlighted how specific the regulation of odontogenesis, especially when unravelling the molecular networks affected by the transgene expression. The modifications seen at embryonic stages will generate modifications of the mineralized molar row, but given the embryonic lethality, and the transgene variegation effects,

the exact causality of the defects on the mineralized teeth are not completely clear. The implication of this family of genes in syngnathia reinforces the beneficial association often existing between developmental biology and clinical work.

ACKNOWLEDGEMENTS

We thank Nicolas Strauli and Sarah Alto for help with the Sprouty mouse breeding. We also thank S. Pantalacci for sharing *Shh* plasmid with us. We are grateful to J. Richman for critical discussions over the project. This work was funded by grants from the ENS de Lyon (to LV), and the NIH (R01 DE021420 to ODK).

- Chang, J. Y. F., Wang, C., Liu, J., Huang, Y., Jin, C., Yang, C., Hai, B., Liu, F., D'Souza, R. N., McKeehan, W. L., et al.** (2013). Fibroblast growth factor signaling is essential for self-renewal of dental epithelial stem cells. *J. Biol. Chem.* **288**, 28952–28961.
- Charles, C., Lazzari, V., Tafforeau, P., Schimmang, T., Tekin, M., Klein, O. and Viriot, L.** (2009). Modulation of Fgf3 dosage in mouse and men mirrors evolution of mammalian dentition. *Proc. Natl. Acad. Sci.* **106**, 22364.
- Chen, M., Choi, Y., Voytas, D. F. and Rodermel, S.** (2000). Mutations in the Arabidopsis VAR2 locus cause leaf variegation due to the loss of a chloroplast FtsH protease. *Plant J.* **22**, 303–313.
- Chihara, T., Kato, K., Taniguchi, M., Ng, J. and Hayashi, S.** (2003). Rac promotes epithelial cell rearrangement during tracheal tubulogenesis in Drosophila. *Development* **130**, 1419.
- Cobourne, M. T. and Sharpe, P. T.** (2003). Tooth and jaw: molecular mechanisms of patterning in the first branchial arch. *Arch. Oral Biol.* **48**, 1–14.
- Dawson, K. H., Gruss, J. S. and Myall, R. W. .** (1997). Congenital bony syngnathia: a proposed classification. *Cleft Palate. Craniofac. J.* **34**, 141–146.
- De Maximy, A. A., Nakatake, Y., Moncada, S., Itoh, N., Thiery, J. P. and Bellusci, S.** (1999). Cloning and expression pattern of a mouse homologue of Drosophila sprouty in the mouse embryo. *Mech. Dev.* **81**, 213–216.
- Fallahi, H. R., Naeini, M., Mahmoudi, M. and Javaherforoosh, F.** (2010). Congenital zygomatico-maxillo-mandibular fusion: a brief case report and review of literature. *Int. J. Oral Maxillofac. Surg.* **39**, 930–933.
- Ferrara, N.** (2005). The role of VEGF in the regulation of physiological and pathological angiogenesis. In *Mechanisms of angiogenesis*, pp. 209–231. Springer.
- Hacohen, N., Kramer, S., Sutherland, D., Hiromi, Y. and Krasnow, M. A.** (1998). sprouty encodes a novel antagonist of FGF signaling that patterns apical branching of the Drosophila airways. *Cell* **92**, 253–263.
- Hanafusa, H., Torii, S., Yasunaga, T. and Nishida, E.** (2002). Sprouty1 and Sprouty2 provide a control mechanism for the Ras/MAPK signalling pathway. *Nat. Cell Biol.* **4**, 850–858.
- Hardcastle, Z., Mo, R., Hui, C. and Sharpe, P. T.** (1998). The Shh signalling pathway in tooth development: defects in Gli2 and Gli3 mutants. *Development* **125**, 2803.
- Harjunmaa, E., Seidel, K., Häkkinen, T., Renvoisé, E., Corfe, I. J., Kallonen, A., Zhang, Z.-Q., Evans, A. R., Mikkola, M. L., Salazar-Ciudad, I., et al.** (2014). Replaying evolutionary transitions from the dental fossil record. *Nature* **512**, 44–48.

- Inman, K. E., Purcell, P., Kume, T. and Trainor, P. A.** (2013). Interaction between Foxc1 and Fgf8 during Mammalian Jaw Patterning and in the Pathogenesis of Syngnathia. *PLoS Genet.* **9**, e1003949.
- Jernvall, J., Kettunen, P., Karavanova, I., Martin, L. B. and Thesleff, I.** (1994). Evidence for the role of the enamel knot as a control center in mammalian tooth cusp formation: non-dividing cells express growth stimulating Fgf-4 gene. *Int. J. Dev. Biol.* **38**, 463–463.
- Jernvall, J., Aberg, T., Kettunen, P., Keranen, S. and Thesleff, I.** (1998). The life history of an embryonic signaling center: BMP-4 induces p21 and is associated with apoptosis in the mouse tooth enamel knot. *Development* **125**, 161.
- Kavanagh, K. D., Evans, A. R. and Jernvall, J.** (2007). Predicting evolutionary patterns of mammalian teeth from development. *Nature* **449**, 427–432.
- Kettunen, P. and Thesleff, I.** (1998). Expression and function of FGFs-4,-8, and-9 suggest functional redundancy and repetitive use as epithelial signals during tooth morphogenesis. *Dev. Dyn.* **211**, 256–268.
- Kettunen, P., Laurikkala, J., Itäranta, P., Vainio, S., Itoh, N. and Thesleff, I.** (2000). Associations of FGF-3 and FGF-10 with signaling networks regulating tooth morphogenesis. *Dev. Dyn.* **219**, 322–332.
- Klein, O. D., Minowada, G., Peterkova, R., Kangas, A., Yu, B. D., Lesot, H., Peterka, M., Jernvall, J. and Martin, G. R.** (2006). Sprouty genes control diastema tooth development via bidirectional antagonism of epithelial-mesenchymal FGF signaling. *Dev. Cell* **11**, 181–190.
- Klein, O. D., Lyons, D. B., Balooch, G., Marshall, G. W., Basson, M. A., Peterka, M., Boran, T., Peterkova, R. and Martin, G. R.** (2008). An FGF signaling loop sustains the generation of differentiated progeny from stem cells in mouse incisors. *Development* **135**, 377.
- Kopan, R. and Ilagan, M. X. G.** (2009). The canonical Notch signaling pathway: unfolding the activation mechanism. *Cell* **137**, 216–233.
- Lagronova-Churava, S., Spoutil, F., Vojtechova, S., Lesot, H., Peterká, M., Klein, O. D. and Peterková, R.** (2013). The Dynamics of Supernumerary Tooth Development Are Differentially Regulated by Sprouty Genes. *J. Exp. Zoolog. B Mol. Dev. Evol.*
- Li, C.-Y., Prochazka, J., Goodwin, A. F. and Klein, O. D.** (2014). Fibroblast growth factor signaling in mammalian tooth development. *Odontol. Soc. Nippon Dent. Univ.* **102**, 1–13.
- Maas, R. and Bei, M.** (1997). The genetic control of early tooth development. *Crit. Rev. Oral Biol. Med.* **8**, 4.

- Mason, J. M., Morrison, D. J., Albert Basson, M. and Licht, J. D.** (2006). Sprouty proteins: multifaceted negative-feedback regulators of receptor tyrosine kinase signaling. *Trends Cell Biol.* **16**, 45–54.
- Mitsiadis, T. A., Regaudiat, L. and Gridley, T.** (2005). Role of the Notch signalling pathway in tooth morphogenesis. *Arch. Oral Biol.* **50**, 137–140.
- Muller, H. J.** (1930). Types of visible variations induced by X-rays in *Drosophila*. *J. Genet.* **22**, 299–334.
- Ruch, J. V., Lesot, H. and Begue-Kirn, C.** (1995). Odontoblast differentiation. *Int. J. Dev. Biol.* **39**, 51.
- Tsuboi, T., Mizutani, S., Nakano, M., Hirukawa, K. and Togari, A.** (2003). Fgf-2 regulates enamel and dentine formation in mouse tooth germ. *Calcif. Tissue Int.* **73**, 496–501.
- Tucker, A. S. and Sharpe, P. T.** (1999). Molecular genetics of tooth morphogenesis and patterning: the right shape in the right place. *J. Dent. Res.* **78**, 826.
- Tucker, A. and Sharpe, P.** (2004). The cutting-edge of mammalian development; how the embryo makes teeth. *Nat. Rev. Genet.* **5**, 499–508.
- Vahtokari, A., Aberg, T. and Thesleff, I.** (1996). Apoptosis in the developing tooth: association with an embryonic signaling center and suppression by EGF and FGF-4. *Development* **122**, 121.
- Viriote, L., Peterková, R., Peterka, M. and Lesot, H.** (2002). Evolutionary implications of the occurrence of two vestigial tooth germs during early odontogenesis in the mouse lower jaw. *Connect. Tissue Res.* **43**, 129–133.
- Wang, X. P., Suomalainen, M., Jorgez, C. J., Matzuk, M. M., Werner, S. and Thesleff, I.** (2004). Follistatin regulates enamel patterning in mouse incisors by asymmetrically inhibiting BMP signaling and ameloblast differentiation. *Dev. Cell* **7**, 719–730.
- Wheelock, M. J. and Johnson, K. R.** (2003). Cadherins as modulators of cellular phenotype. *Annu. Rev. Cell Dev. Biol.* **19**, 207–235.
- Yamashiro, T., Tummers, M. and Thesleff, I.** (2003). Expression of Bone Morphogenetic Proteins and Msx Genes during Root Formation. *J. Dent. Res.* **82**, 172–176.
- Zeichner-David, M., Diekwisch, T., Fincham, A., Lau, E., MacDougall, M., Moradian-Oldak, J., Simmer, J., Snead, M. and Slavkin, H. C.** (1995). Control of ameloblast differentiation. *Int. J. Dev. Biol.* **39**, 69–92.

A.4 Conclusions

Evo-devo stands for evolutionary developmental biology. Dental evo-devo takes advantage of the well-documented tooth germ developmental sequences, and uses the molecular assumptions built by developmental biologists to test evolutionary hypotheses. The use of molar shape and postcanine tooth number to address evolutionary transitions is well-accepted in the community (Harjunmaa *et al.*, 2014).

In this part of my PhD work, I aimed at further expanding our knowledge of the ERK-MAPK signaling pathway involvement in tooth evolution and development. After confirming the role of *Rsk2* in craniofacial development, I focused on its postcanine dentition, and compared it with the one of *Spry1*^{-/-}, *Spry2*^{-/-}, and *Spry4*^{-/-} mutant mice. The high interest of this comparison relies on the fact that they are both members of the pathway, but that they act at various steps.

Similarities are observed between the dentitions, with several features being commonly displayed in Sprouty and *Rsk2* mutant mice. Notably, the occurrence of a ST in the equivalent of a 4th premolar position in *Spry2*^{-/-}, *Spry4*^{-/-} and *Rsk2*^{-Y} mice, along with the Sprouty-specific display of a posterocone – which is a dental feature that disappeared from the *Mus* lineage 9.2 to 6.5 Ma ago – led us to hypothesize that the premolar loss might have been triggered by *Rsk2* gene dosage augmentation, while the posterocone loss might be imputable to Sprouty gene dosage augmentation. Overall, these results emphasize that vestigial tooth buds located in the diastemal region can be reactivated to form ST by genetic modifications, thus contributing to our understanding of the dental formula control in the order Rodentia.

Stepping back to the actors that can activate the ERK-MAPK cascade, my work on the K14-*Spry4* mice confirmed the role of epithelial Fgf genes in the enamel mineralization process. If my conclusions regarding this part are mainly developmental, they also enlighten the role that complementary models of genetically engineered mice have to play in understanding tooth evo-devo.

If mouse molars are traditionally used in the field, it does not mean that they are the only type of tooth that will help us catch a glimpse at the complex evolutionary history of teeth. Indeed, mouse incisors have sometimes also been used to address the question of tooth number control, notably by addressing the Sprouty-mediated modulation of RTK pathway (see annex 3, Charles *et al.*, 2011). More globally, the work on rodent hypsodont –high-crowned teeth – and hypselodont teeth – ever-growing teeth – has also helped scientists raise the questions of the adaptation to differential diets and of prolonged growth (Renvoisé and Michon, 2014).

PART B

**RODENT INCISORS:
EVOLUTION, DIVERSITY,
& AGEING**

Adult stem cells are necessary for the organism to ensure tissue homeostasis. One original feature of rodents (and lagomorphs) is that their incisors are continuously growing throughout the animal's lifespan thanks to the presence of stem cell niches located in their growing zone (Meng *et al.*, 2004). In return, the protruding tips of the incisors continuously wear down when the animal gnaws. Because of their easy access, mouse incisors constitute a pivotal model to address the maintenance of such a dynamic balance.

The development of mouse incisor follows the well-known developmental sequence of ectodermal organs. In terms of histo-morphogenesis, it is highly similar to what is observed for molar development, except that the incisor cap rotates towards distal direction, leading to its specific orientation (FIG B.1). The distal extremity of the invaginating epithelium, called cervical loops (in 2D sections), encompasses epithelial stem cell niches (ESCs) (Harada *et al.*, 1999).

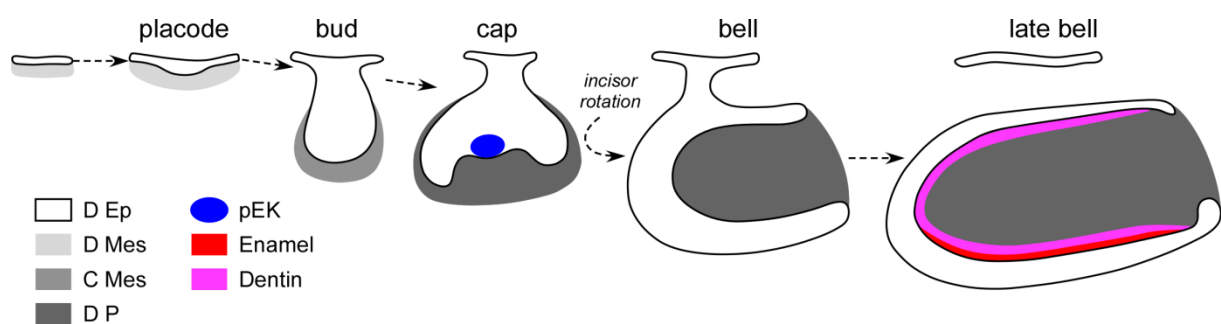


FIG. B.1: Development of the mouse lower incisor. The dental germ undergoes successive histo-morphogenetic stages, similar to what is observed during molar development, except that the incisor germ rotates towards distal direction. D Ep: dental epithelium; D Mes: dental mesenchyme; C Mes: condensed mesenchyme; D P: dental papilla; pEK: primary enamel knot.

The epithelial stem cell niches are asymmetric (Harada *et al.*, 2002a; Harada *et al.*, 2002b; Klein *et al.*, 2008). The labial cervical loop (laCL) is bigger, and contains a consequent population of stem cells located in the stellate reticulum (SR, between the inner and outer epithelium layers). The lingual cervical loop (liCL) however only contains a few stem cells (Thesleff *et al.*, 2007; Juuri *et al.*, 2012). The loops and the inner and outer dental epithelium project in 3D and define a sheath in which the incisor will grow (Harada and Ohshima, 2004). Label-retaining and lineage tracing experiments have demonstrated that the cervical loop acts as a reservoir for epithelial stem cells which will drive the continuous growth of the incisor (Seidel *et al.*, 2010; Juuri *et al.*, 2012). This asymmetry results in the asymmetry of the incisor (FIG. B.2).

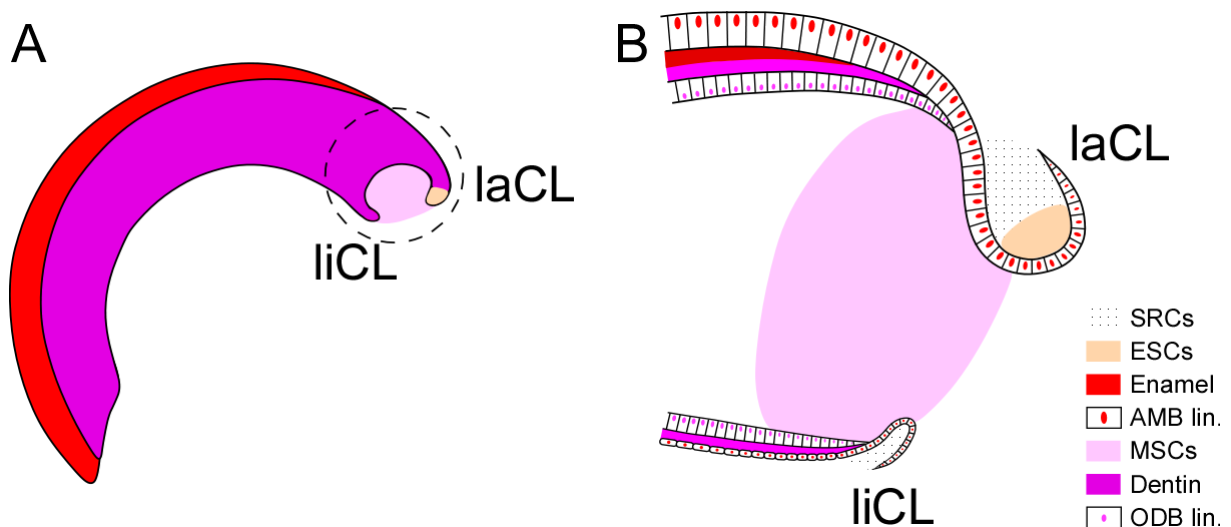


FIG. B.2: Incisors are asymmetric teeth.. Enamel is only displayed on the vestibular (or labial) side. The asymmetry results from histological asymmetry between the labial cervical loop (laCL) and the lingual cervical loop (liCL). Epithelial stem cells (ESCs) are located in the laCL, next to the loosely arranged stellate reticulum cells (SRCs), while mesenchymal stem cells (MSCs) are more dispersed within the pulp. Ameloblast lineage (AMB lin.) derives from ESCs which will differentiate as they exit the niche. Odontoblast lineage (ODB lin.) arises from the MSCs found in the pulp, more precisely from the neurovascular bundle.

Incisors display enamel only on their vestibular side (also known as labial side), where functional ameloblasts arise from the ESC pool and start secreting this mineralized matrix at E19.5. On the lingual side, ameloblasts fail to develop leading to a side where only dentin can

be found (Klein *et al.*, 2008; Seidel *et al.*, 2010). Dentin is secreted by odontoblasts, which dynamic turnover is supported by mesenchymal stem cells (MSCs). In a recent study, the neurovascular bundle – located in the pulp cavity of the incisor – was acknowledged as the likely niche of MSCs (Zhao *et al.*, 2014). Finally, the lingual side of mouse incisors is covered with a thin layer of cementum and is thus considered as the root analog whereas the vestibular side is considered as the crown analog (Tummers and Thesleff, 2003; Juuri *et al.*, 2013). The presence of enamel only on vestibular sides and differences in both curvature and size generate a beveled wear pattern at the occlusal contact between upper and lower incisors. The acquisition of features allowing this bevel-cut shape attests to complex coordinated changes.

Studies of the genetic networks report that members of the TGF β , BMP, Wnt, FGF, Hedgehog and Eda pathways as well as their modulators (Follistatin, Ectodin, Spry) are involved in incisor development (Begue-Kirn *et al.*, 1992; Tucker *et al.*, 1998; Tummers and Thesleff, 2003; Wang *et al.*, 2004; Seidel *et al.*, 2010; Suomalainen and Thesleff, 2010; Chang *et al.*, 2013; Li *et al.*, 2014). Stem cell maintenance has been a crucial topic in the field, and the role of Fgf signaling pathway – and especially FGF10 – is constantly specified (Chang *et al.*, 2013; Renvoisé and Michon, 2014).

Despite the interest of the mouse incisor model in terms of regeneration potential, which constitutes an active field in dental research, incisors are usually considered as very simple teeth, and the problem of the diversity in shape, size and color of incisors at the scale of the order Rodentia has never been properly tackled. In this part of my thesis, I intend to focus on various aspects of the diversity of rodent incisors in relation to their evolutionary history. Beyond a relatively simple-looking circular shape, incisor displays a high degree of

specialization, stability and variability at various scales, from age-related individual variations to intra-order variations.

B.1 INTRA- AND INTER-SPECIFIC VARIATION OF THE RODENT INCISORS

Glires is a taxonomic grouping encompassing the living Rodentia and Lagomorpha as well as all their extinct relatives. The acquisition of continuously growing incisors is a synapomorphy of Glires, including the extinct orders Miotonida and Mixodontia (McKenna and Bell, 1997). Rodents and the mixodonts together form the Mirorder Simplicidentata, so-called because simplicidentates only possess two upper and two lower enlarged continuously growing incisors, which have been assigned to the second decidual incisors (dI^2 and dI_2) (Lockett, 1985). Lagomorphs and the miotonids together form the Mirorder Duplicidentata, so-called because duplicidentates have four upper and two lower continuously growing incisors. The upper dentition of duplicidentates includes two tiny continuously growing third permanent incisors (I^3), which are located immediately behind the dI^2 (Ooë, 1980; Lockett, 1985). Within Glires, the position of *Gomphos* remains problematic because this genus has four upper and four lower continuously growing incisors. After being considered as a stem rodent, it has been reassigned to stem lagomorphs (Kraatz et al., 2009).

Because they protrude out their oral cavity, incisors are the most obviously visible teeth of both rodents and lagomorphs. Their vestibular surface, covered with enamel is facing the observer. Upper incisors are especially visible because they partially hide the lower ones. In lagomorphs, upper incisors are very alike across the phylogeny with a clear vestibular groove being displayed on the vestibular surface. In rodents however, it is not rare to observe a great variability.

B.1.1 Morphometrics

Incisors are asymmetric teeth displaying a beveled wear pattern at the occlusal contact between upper and lower incisors. The absence of enamel on the lingual side of both upper and lower incisors also confers flexibility on the rodents when they gnaw. The risk of breakage is minimized, but not completely avoided, what remains an issue for the animal. Also on the down-side of the system are the opposite cases of malocclusion. Indeed, when incisors are not properly occluding, they grow out without being worn down, and eventually inward, running through the rodent jaws. Laboratory mice are for example exposed to this issue because of the hardness of their food or trauma from fighting or improper chewing of the cages. There might also be a genetic predisposition to malocclusion, but this has only been demonstrated in rabbits (Fox and Crary, 1971; Petznek *et al.*, 2002).

On their proximal end, rodent lower incisors growth region is located distally to the molar row (Harada *et al.*, 1999). As a consequence, their curvature radius is higher than in the upper incisors, which growth region is located more mesially (Lin, 2010). Interestingly, there is an inter-specific variability in the localization of the growth region in the upper jaws: muroid rodents tend to have an insertion mesially to the upper molar row (FIG. B.3A), whereas some subterranean rodents like the Bathyergidae have their growth region set more distally (FIG. B.3B, C).

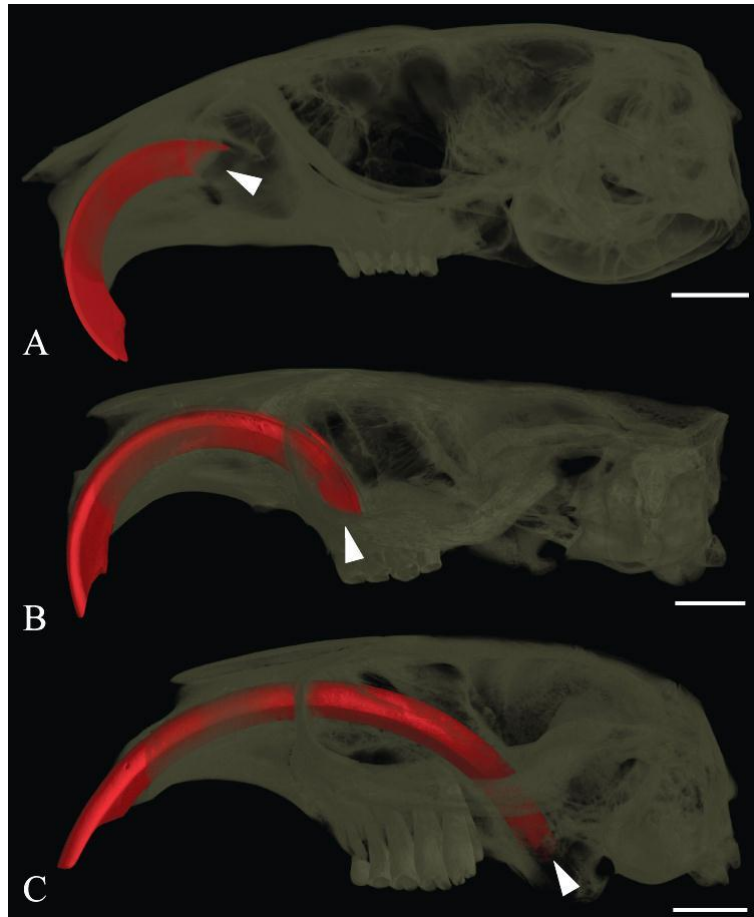


FIG. B.3: Differential insertion of the upper incisors in various rodent species. Sagittal view of 3 rodent skulls, with the upper incisors colored in red, and the growth region pointed with a white arrowhead. (A) *Psammomys obesus* (Myomorpha, Muridae, Gerbillinae; specimen from the livestock of Deakin University, Australia); (B) *Bathyergus suillus* (Hystricomorpha, Hystricognathi, Bathyergidae, Bathyerginae; MNHN); (C) *Heliophobius argentiocinereus* (Hystricomorpha, Hystricognathi, Bathyergidae, Bathyerginae; MNHN). Scale bars: 5mm. For the MNHN specimen collection number, please refer to the annex 4.

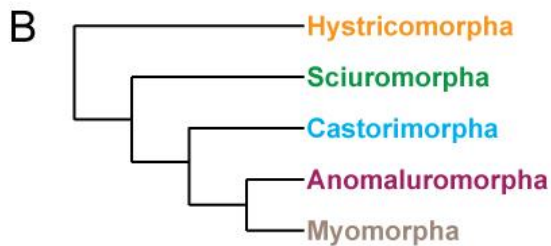
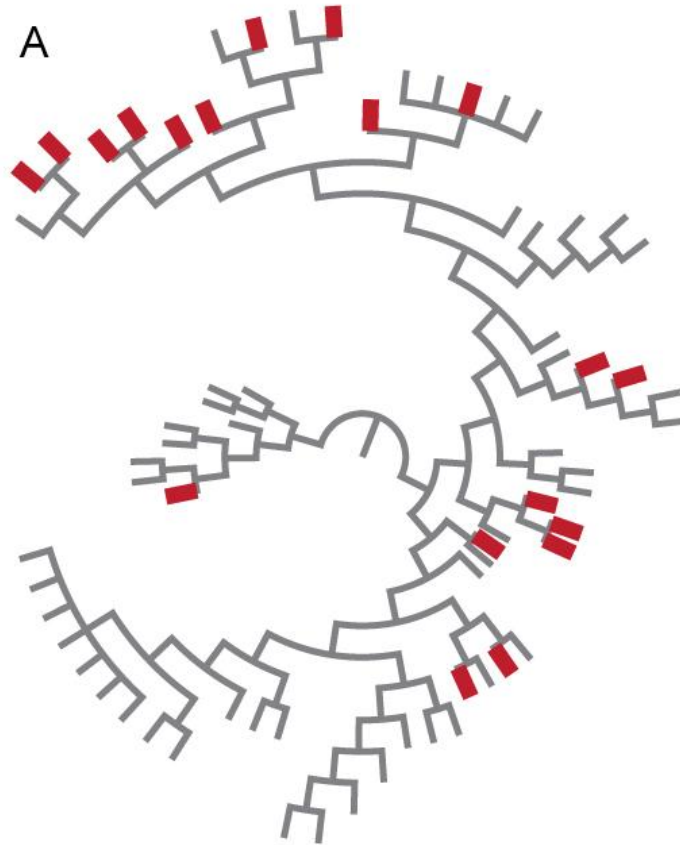
B.1.2 Incisor ornamentation

The five suborders Anomaluromorpha, Castorimorpha, Hystricomorpha, Myomorpha, and Sciuromorpha together make up the order Rodentia. The myomorph “mouse-like” rodents represent about 70% of the living rodent species and almost a quarter of all living mammalian

species (Wilson and Reeder, 2005). The presence of vestibular grooves on incisors is a widely spread character within the order Rodentia. The distribution of this character within the rodent phylogeny clearly shows that it has independently appeared several times (FIG. B.4A). Vestibular grooves almost exclusively occur on upper incisors, and the unbalanced distribution constitutes an important issue for understanding the morphological function of this character.

Within the suborder Sciuromorpha, only two out of the 61 genera, namely *Aeretes* and *Rheithrosciurus*, have been documented as displaying grooves (Nowak, 1999). In the four other suborders, grooved incisors are a common phenotype (FIG. B.4B-G). There is no phylogenetic signal in the presence of this feature, which argues for its convergent occurrence. Attesting to this, the Gerbillinae subfamily (encompassing gerbil species) stably displays one groove on the upper incisor at the exception of the *Psammomys* genus that does not display any (FIG. B.5A). The number of grooves displayed varies between the genera (FIG. B.5, no groove: *Psammomys obesus*, one groove: *Geomys bulleri*, *Gerbillus sp.*, *Myotomys unisulcatus*, *Parotomys brantsii*, *Otomys irroratus*; two grooves: *Geomys bursarius*; three grooves: *Thryonomys swinderianus*).

FIG. B.4 (following page): Presence of enamel groove across the rodent phylogeny. (A) Schematized phylogeny of the three most representative rodent suborders (Sciuromorpha, Myomorpha and Hystricomorpha) at the subfamily level (adapted from Fabre *et al.*, 2012). It shows in red the convergent occurrence of the grooved enamel surface. (B) Rodent phylogeny at the suborder level (from Fabre *et al.*, 2012). (C-G) Inventory of the presence of smooth enamel surface (smooth), grooved enamel surface (grooved), and unscrutinized genera (unknown). Numbers in brackets indicate the total number of genera within the rodent suborders, or within the rodent families.



C

	<i>smooth</i>	<i>grooved</i>	<i>unknown</i>
Hystricomorpha (77)			
Ctenodactylidae (4)	1	3	0
Bathyergidae (5)	4	1	0
Hystricidae (3)	3	0	0
Petromuridae (1)	1	0	0
Thryonomyidae (1)	1	0	0
Erethizontidae (5)	3	0	2
Chinchillidae (3)	3	0	0
Dinomyidae (1)	1	0	0
Caviidae (6)	4	0	2
Dasyproctidae (2)	1	0	1
Cuniculidae (1)	1	0	0
Ctenomyidae (1)	1	0	0
Octodontidae (8)	1	0	7
Abrocomidae (2)	0	0	2
Echimyidae (21)	8	0	16
Myocastoridae (1)	1	0	0
Capromyidae (8)	2	0	6
Heptaxodontidae (4)	0	0	4

D

	<i>smooth</i>	<i>grooved</i>	<i>unknown</i>
Sciuromorpha (61)			
Aplodontiidae (1)	1	0	0
Sciuridae (51)	36	2	13
Gliridae(9)	7	0	1

E

	<i>smooth</i>	<i>grooved</i>	<i>unknown</i>
Castorimorpha (13)			
Castoridae (1)	1	0	0
Heteromyidae (6)	2	4	0
Geomyidae (6)	1	5	0

F

	<i>smooth</i>	<i>grooved</i>	<i>unknown</i>
Anomaluromorpha (4)			
Anomaluridae (3)	3	0	0
Petetidae (1)	1	0	0

G

	<i>smooth</i>	<i>grooved</i>	<i>unknown</i>
Myomorpha (326)			
Dipodidae (16)	5	6	5
Platacanthomyidae (2)	2	0	0
Spalacidae (6)	6	0	1
Calomyscidae (1)	0	0	1
Nesomyidae (21)	14	4	3
Cricetidae (130)	64	9	57
Muridae (150)	49	27	74

The vast majority of grooved-tooth rodent display only one groove, but some species display up to 10 thin grooves (*Rheithrosciurus* genus, Wilson and Reeder, 2005). Grooves found in the Otomyinae subfamily depict the differential position of the groove, as well as its depth (FIG.B.5C). It is important to note that none of those natural grooves are aplastic, meaning that there is always a continuous layer of enamel on the vestibular side of the incisor (see the example of *Thryonomys swinderianus*, FIG. B.5D).

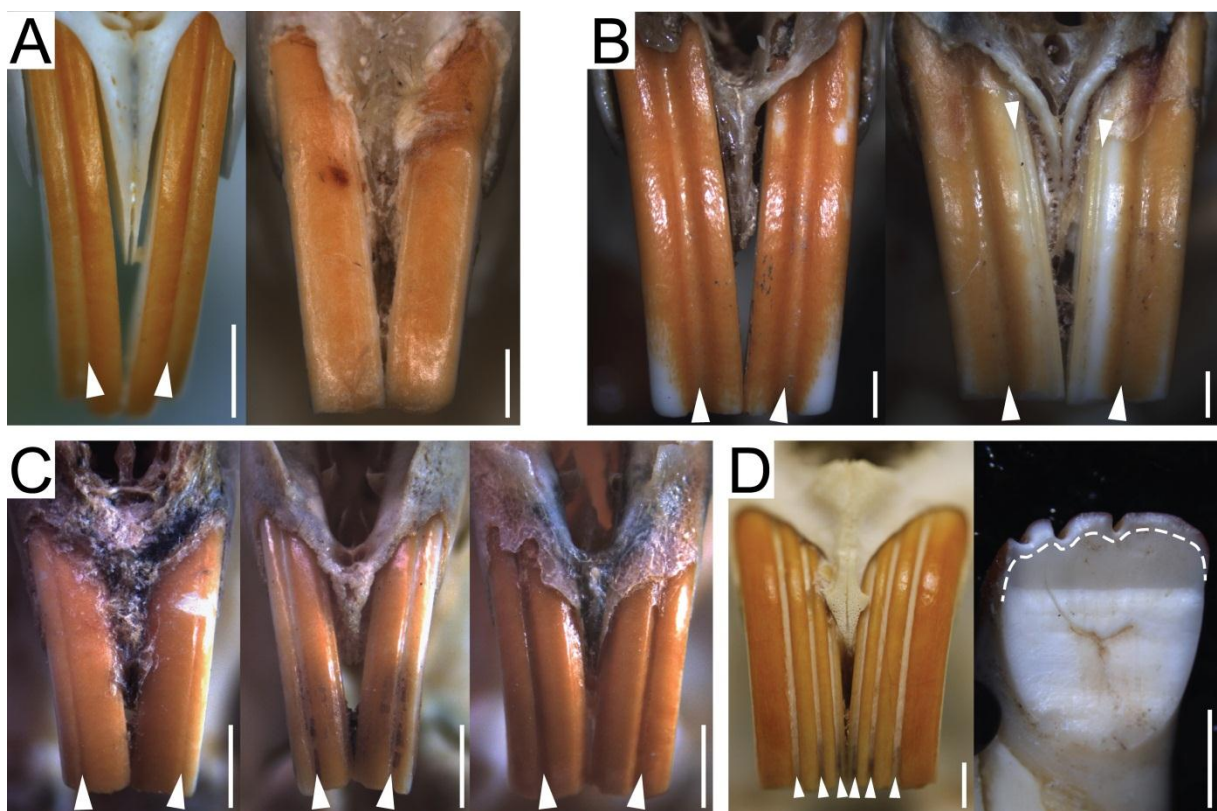


FIG. B.5: Diversity of grooved incisor phenotype among the order Rodentia. (A) *Gerbillus* sp. displays one central groove whereas *Psammomys obesus* does not display any. (B) *Geomys bulleri* (left) and *Geomys bursarius* (left) do not display the same number of grooves. (C) In the Otomyinae subfamily, the groove displayed in not localized at the same place (from left to right *Myotomys unisulcatus*, *Paratomys brantsii*, and *Otomys irroratus*). (D) The vestibular grooves are never aplastic, as it is well visible in *Thryonomys swinderianus*. Arrowheads point out the presence of grooves, the white dotted line draws the limit between the enamel and dentin layers. Scale bars: 1 mm (except in D 2.5 mm). All specimens except *Psammomys obesus* and *Thryonomys swinderianus* (personal collections) come from the MNHN (Paris), the NHL (London) or the MRAC (Tervuren) collections. For collection numbers, please refer to annex 4.

B.1.3 Color

Tooth pigmentation is quite common in nature. Several vertebrate taxa have been used as model to study this diversity, including shrews, salamanders and fish (Motta, 1987; Sparks *et al.*, 1990; Clemen, 1988; Suga *et al.*, 1992; Anderson and Miller, 2011). In rodent dentition, this natural variability is especially visible on incisors. Depending on the species, the enamel displays a color ranging from white to dark orange (FIG. B.6A). This variability can also be observed intra-specifically, for example between young and older *Mus musculus* littermates (FIG. B.6B). Lastly, it is common to see color variation between the upper and lower incisors (FIG. B.6C).

Wen and Paine (2013) have demonstrated that the enamel layer specific pigmentation is linked to the incisor capacity to incorporate iron. The more colored the tooth is, the higher the iron enrichment is. Working on *Blarina bricauda* heavily pigmented teeth, Dumont and colleagues (2014) have resolved the structural and chemical organization of the pigments within the enamel layer. The pigments have thus been shown to be concentrated in a thin layer of aprismatic enamel at the surface of the incisor. In this study, pigmented teeth have also been shown to be 30% harder than less pigmented teeth, which is likely to represent an asset against very abrasive diets. Thus, even without a specific cusp pattern like in molars, incisors might also have played a role in the diversification of rodent food intake.



FIG. B.6: Inter- and intra-specific variation in the color of the rodent incisor enamel. (A) Inter-specific color variation in the suborder Myomorpha, from left to right: *Psammomys obesus*, *Microtus arvalis*, *Eliurus minor*, *Nesomys rufus*. Scale bars: 1 mm. (B) Intra-specific color variation between two *Mus musculus* littermates, left is 22 days-old, right is 54 days-old. (C) Intra-individual color variation between the upper and the lower incisors of a same *Mus musculus* specimen. Scale bars: 0.5 mm. *Mus musculus* specimens were collected from our livestock, other specimens (except *Psammomys obesus*) come from the MNHN collections. For collection numbers, please refer to annex 4.

An important source of variation in incisor phenotype, at least for the mouse, is the age of the specimen. The littermates photographed in FIG. B.6B lived in the same cage, ate the same food, but they were euthanized for further experiments at various time points. I will now further investigate incisor ageing.

B.2 PHENOTYPIC DISRUPTIONS OF THE UPPER INCISORS IN AGEING MICE

Rodent incisors share very conserved and stable features across their phylogeny, as well as much more variable properties. Their ever-growing capacity has been focused on, especially to understand the importance of stem cell environment and the decision between self-renewal and differentiation. But when an organism ages, acquired and inherited factors affect its cells, and especially its stem cells (Sharpless and DePinho, 2007). Consequently, an organism is considered to be “as old as its stem cells” (Ho *et al.*, 2005). Because of their role in continuous growth, tissue repair, and regeneration, the age-related decrease in adult stem cell competence is a crucial issue.

Working on the phenotypic aspect of rodent incisors, we have already stated that features like the enamel pigmentation vary within a species depending on the age of the observed specimen. Incisor ornamentation also varies along the mouse lifespan. In the wild, mice live less than a year. However in the absence of predation in laboratory conditions, scientists are able to breed and maintain mice for a longer time period. The current longevity record is 1819 days (almost 5 years) for a dwarf mouse whose growth hormone receptor had been inactivated (Bartke and Brown-Borg, 2004), and 4 years for a laboratory WT mouse (Miller *et al.*, 2002). In 1971, Robins and Rowlatt first reported the existence of dental abnormalities in the upper incisors of 22- to 36-month-old mice including the display of a discolored and grooved enamel surface, as well as the increase in the proportion of broken teeth. They also noticed the rare overgrowth of the mandibular incisors which occurred when

they did not enter in contact with the maxillary incisors, which had been known in other rodents for decades (e.g. in the beaver: Bland Sutton, 1884; in the porcupine: Shadle *et al.*, 1944). The defects they saw on the upper incisors remind of the variable features discussed above: the occurrence of a vestibular groove and the difference in enamel color.

Despite the physiological interest in age-related pathologies attested by the WHO 2013 Global Forum on Innovation for Ageing Populations (WHO | WHO Global Forum on Innovations for Ageing Populations), and more generally the scientific interest in stem cell ageing (Liu and Rando, 2011; Signer and Morrison, 2013), the case of age-related defects of the mouse upper incisors has remained poorly focused on. Indeed, because of the continuous growth, incisors constitute a relatively easy model to work on how stem cells react to face ageing. I address here this phenomenon in WT mice to perfect our understanding of dental stem cell ageing and to scrutinize the dynamics of the defect occurrence.

Disruption of the incisor stem cell niches in ageing mice

Pauline Marangoni, Ludivine Bertonnier-Brouty, Cyril Charles, Laurent Viriot^{1*}

Team Evo-Devo of Vertebrate Dentition, Institute of Functional Genomics of Lyon, ENS de Lyon, CNRS UMR
5242, University of Lyon 1, 46 allée d'Italie, 69364 Lyon cedex 07, France

§ Corresponding author: laurent.viriot@ens-lyon.fr

ABSTRACT

Rodent incisors continuously grow throughout their lifespan due to the presence of adult stem cells at their proximal end. The addition of new tissues from this growth region balances the abrasion generated when the animal gnaws. Although the surface of mouse incisors is normally smooth, upper incisors tend to display irregularities originating from the growth region as the animal gets older than its life expectancy in the wild. Performing *in vivo* monitoring on CD1 “swiss” mice and C57Bl/6N mice, we provided a live phenotypic analysis of some of these defects. X-ray microtomography, morphometrical tools and histological staining were used to assess incisor morphology. We detected mineralized tissue anomalies from about six months of age, most frequently vestibular enamel grooves. The abnormality proportion only increases from that point onwards. Upper incisors were shown to continuously widen as mice age. A fold in the enamel secreting layer was linked with enamel irregularities, and hyperplastic epithelial stem cell niche with modifications of incisor geometry. Our work provides an accurate description of the abnormality setting up to address age-related stem cell niche disruption.

KEY WORDS

Stem cell ageing, incisor, groove, mouse, sand rat, chrono-morphology, histology

INTRODUCTION

The majority of organs and tissues that constitute a given organism are continuously renewed. It is not rare to see these life-long renewing organs affected by ageing. In rodents for example, neural stem cells lose part of their proliferative capacities with ageing, resulting in the decline of the number of newly formed neurons (Kuhn *et al.*, 1996). Likewise, mouse melanocyte stem-cell maintenance decreases with ageing has been partly responsible for hair graying (Nishimura *et al.*, 2005). The quiescent state of the muscle stem cell niche has also been shown to be disrupted by ageing (Chakkalakal *et al.*, 2012). The existence of age-related defects like discolored and/or grooved enamel surface of the upper incisors, as well as the occasional overgrowth of the lower incisors prove that incisor stem cells are no exception to the rule (Robins and Rowlett, 1971).

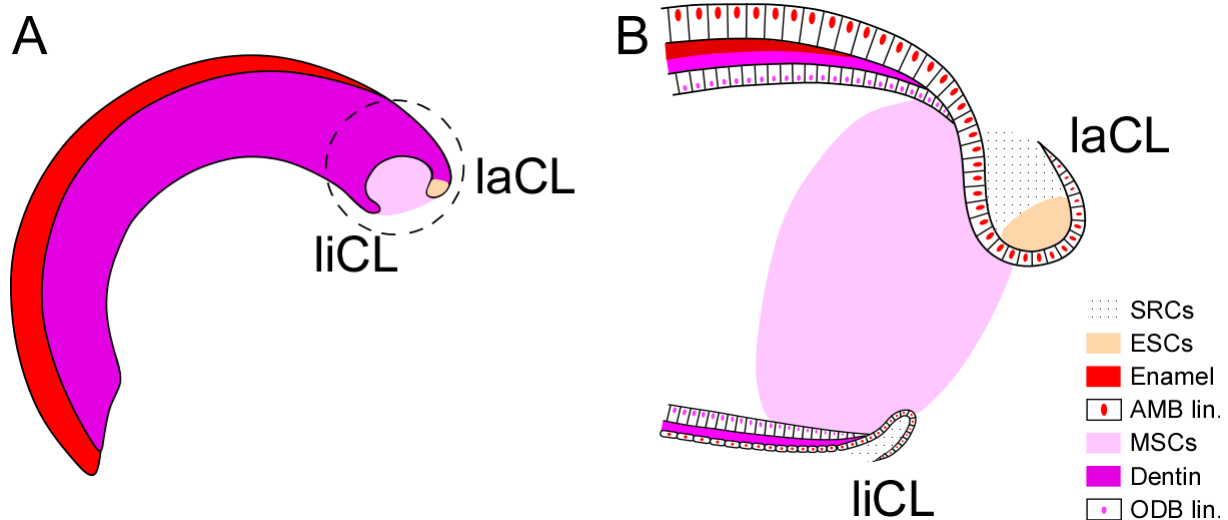


Fig. 1. Mouse incisors are asymmetric teeth that continuously grow throughout the lifespan of the animal. (A) Incisors are asymmetric teeth displaying enamel only on their vestibular (labial) side. The growth region is circled, and usually spotted by the presence of two cervical loops on the labial (laCL) and the lingual (liCL) sides of the tooth. (B) Epithelial stem cells (ESCs) are contained within the stellate reticulum population (SRCs) in the laCL. As the ESCs move out from the niche, they differentiate into the ameloblast lineage (AMB lin.). Mesenchymal stem cells (MSCs) are dispersed within the pulp, and they form the odontoblast lineage (ODB lin.) as they differentiate.

Rodent incisors continuously grow throughout their lifespan, and wear continuously as the animal gnaws. The dynamic equilibrium is allowed by the presence of stem cells persisting into the mouse adulthood which are located in the incisor growth region (Fig.1). Epithelial stem cells are located within specific histological structures called cervical loops (Harada *et al.*, 1999), whereas mesenchymal stem cells are scattered in the pulp in-between (Zhao *et al.*, 2014). Both are necessary to ensure incisor proper formation.

The characterization of upper incisor age-related phenotype has only been sporadically addressed in WT mice (Robins and Rowlatt, 1971), in ^{224}Ra -treated mice (Humphreys *et al.*, 1985), and in the Senescence Accelerated Mouse line (Sashima *et al.*, 1987). Only one rodent species has been shown to display the same kind of age-related abnormalities: the sand rat *Psammomys obesus* (Ulmansky *et al.*, 1984). If phenotypic descriptions were provided, the studies lack the dynamic aspect of ageing. The mouse incisors grow at a rate of 365 $\mu\text{m}/\text{day}$ and the visible tissues are worn out and replaced in approximately 12 days, highlighting the necessity of a repeated monitoring to perfect the characterization (Hwang and Tonna, 1965; Li *et al.*, 2012).

Here, we focus on the effects of incisor stem cell ageing in a WT context, in order to provide a chrono-morphological study of age-related defects occurrence. By monitoring *in vivo* mouse cohorts and further supplementing our histological analyses with classical tissue staining and X-ray microtomography, we specify that age-defects most frequently affect the enamel of upper incisors, and that they are set up earlier than expected. By conducting histological analyses on serial sections of the growth region, we highlight the disruption of the tissue arrangement and we show that the most frequent defect, the presence of an enamel groove, is due to the deep folding of the ameloblast layer. Finally, we verify that *Psammomys obesus* upper incisors are also affected by ageing, and we described new age-related defects.

MATERIAL & METHODS

Mice

We performed *in vivo* monitoring on two cohorts of WT mice housed in the PBES facility (ENS de Lyon, UMS3444). We started with 30 female mice from the CD1 “swiss” line (an outbred line), and with 30 female mice from the C57Bl/6N line (an inbred line). Our protocol consisted in (1) a daily monitoring of the mouse cohorts, and (2) picture taking every 2 weeks (ethics protocol #ENS-2012-015). For that matter, mice were anesthetized using Vetflurane and pictures of their upper incisors were taken with a Leica stereomicroscope equipped with a CCD camera. What is observed on the visible enamel surface at any given week has been formed about 2 weeks before. 10 mice of each background were euthanized by cervical dislocation at the age of 6 months, 10 more of each background at the age of 12 months, and the rest of the colony (10 mice each) was euthanized at the age of 18 months.

A total of 6 CD1 “swiss” and 15 C57Bl/6N mice not included in the *in vivo* monitoring of age-related modifications were also collected from PBES users to increase our dataset on tissue histology. These mice were euthanized according to the protocol previously described. Similarly, a total of 15 C57Bl/6J and 24 B6BCA (C57Bl/6J-derived mice) male mouse heads were collected from the CDTA facility (Orléans, UPS44) to increase our dataset on X-ray microtomographic phenotypic characterization. Age ranking was the following: 7 mice of 11 months, 3 mice of 12 months, 5 mice of 13 months, 10 mice of 16 months, 9 mice of 17 months, 3 mice of 18 months, and 2 mice of 24 months.

Sandrats

Specimens of the sandrat species *Psammomys obesus* were provided by the University of Deakin (Australia). The dataset consists in 12 samples as following: two newborns, two 1-month-old specimens, one 3-month-old specimen, two 12-month-old specimens, one 14-

month old specimen, three 18-month-old specimens, and one 24-month-old specimen. Heads were retrieved from ethanol, dried and phenotyped using X-ray microtomography.

Tissue histology

Freshly dissected mouse incisors were fixed overnight in 4% PFA. Then, they were decalcified for 4 weeks in a solution of 2% PFA and 12.5% EDTA or for 3 weeks in 0.5 M EDTA, washed and dehydrated in graded ethanol, and finally processed overnight in HistoClear (Leica) and paraffin using Leica tissue processor TP1020. Samples were embedded in paraffin blocs and kept at +4°C to be later sectioned (7 µm thick) using the Leica RM2255 microtome. Paraffin was removed from the slides using xylene, and samples were rehydrated using graded EtOH. Most of the samples were stained in hematoxylin (4 min), Scott's water for blue nuclei (3 min) and eosin (1 min 15 s). Slides were mounted using Cytoseal 60 (Thermo scientific). Two specimens with aplastic enamel grooves were stained with Masson's trichrome (hemalum, 8 min; fushine, 2min; aniline blue, 1min) to ensure a better discrimination between tissues.

X-ray microtomography analyses

C57Bl/6J-derived mouse heads retrieved from the CDTA facility were imaged using an X-ray cone-beam computed microtomography with a Nanotom machine (GE) at an energy of 100 keV with a cubic voxel of 5 µm. All 3D renderings were performed using VGStudiomax software. *Psammomys obesus* heads were similarly imaged, with a cubic voxel size of 5 to 8 µm depending on the skull size.

To obtain transverse sections of the mouse upper incisors, the 3D renderings were oriented sagittally along the medial plan of the tooth. A VGStudiomax algorithm allowed the virtual section of the incisor around the axis that is perpendicular to the plan defined by the circle subscribed to the tooth.

RESULTS

Multiple age-related abnormalities affect the mouse upper incisors

Focusing on defects affecting the visible part of the upper incisors that is the enamel layer covering their vestibular side, we have addressed the specific *in vivo* chronology of occurrence of age-related defects. Five abnormalities have been observed in total: enamel dysplasias, a single enamel groove, hair growing out of the dental cavity, an aplastic groove, two aplastic grooves, all of them found in the C57Bl/6N cohort (from left to right in Fig.2A). However, only three of them (enamel dysplasia, a single enamel groove and hair growing out of the dental cavity) have been observed in the CD1 “swiss” cohort.

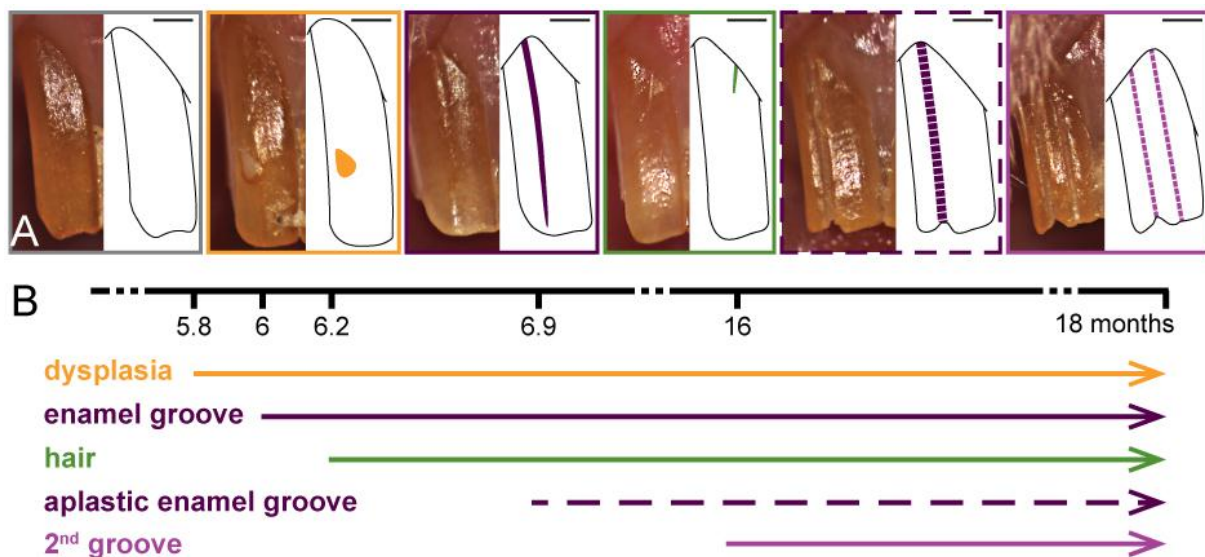


Fig. 2. Mouse upper incisors display various age-related abnormalities from about six months of age onwards. (A) Phenotypic aspect of the visible part of upper incisors in the mice that were monitored *in vivo*. From left to right, incisors display: a smooth enamel surface, an enamel dysplasia (green patch), a groove in the enamel layer, a hair growing out of the tooth cavity, a large and aplastic groove, two aplastic grooves. The last two defects were only found in inbred mice. Scale bars: 250 μm . (B) Chronology of the occurrence of the defects. 1/3 of the mice end up with a combination of defects, which are most frequently defects on the enamel layer.

We show an earlier onset comparing to what has been published by Robins and Rowlett (1971). Indeed, the detection of enamel dysplasia is possible from 6 months on in both CD1 “swiss” and C57Bl/6J cohorts (Fig.2B). A week later, the first grooves start to be displayed,

followed by the detection of hair growing out of the cavity. The presence of this thin air growing out of the dental cavity does not come from littermate grooming because the texture and color do not match the mouse fur. Aplastic enamel grooves start to be seen later on, followed by the occurrence of a 2nd groove only in our C57Bl/6J cohort.

The persistence of the defects varies. Given the quick continuous growth of the incisor, enamel dysplasias are worn out relatively quickly and can be traced for more than two weeks. The hair growing out of the dental cavity looks very thin and fragile. It could thus be easily pulled out when the mouse grooms its littermates, feeds or chews on the cage. As for the enamel groove, which are the most frequent defect seen during the entire in vivo monitoring (in 43% of both the CD1 “swiss” and the C57Bl/6N cohorts), a reversion of the phenotype can be observed in 50% of the case (Fig.3). In the example depicted, the reversion of one large and aplastic 2nd groove in a C57Bl/6N mouse is observed 2 weeks after it has been set up.

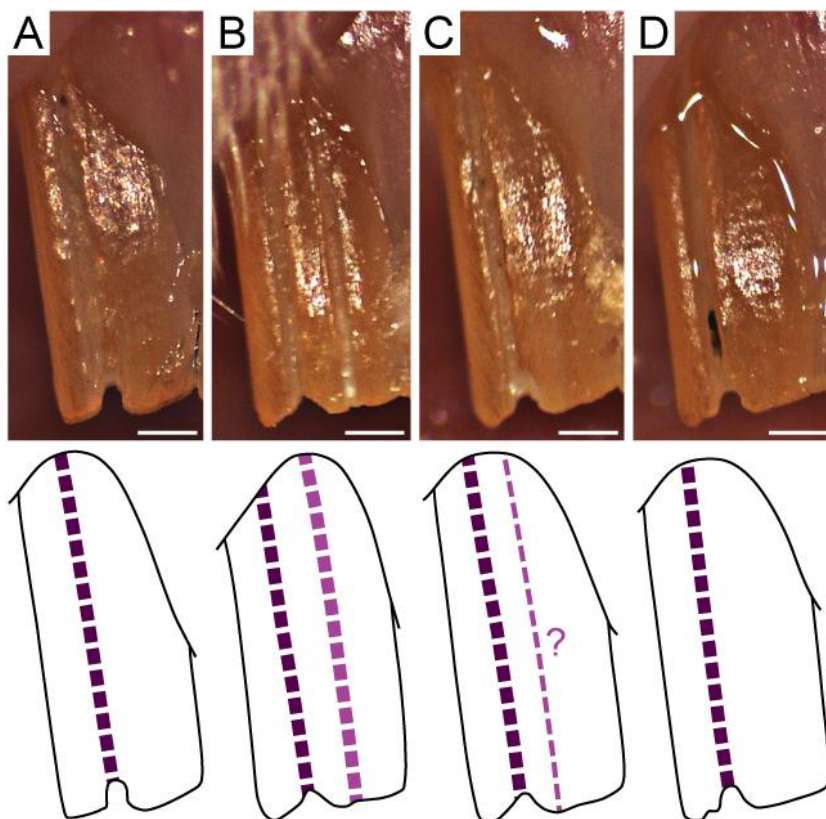


Fig. 3. Enamel grooves are reversible age-related abnormalities. The possible reversion of enamel grooves has been documented on a C57Bl/6N mouse from 60 to 66 weeks (15 to 16.5 months). Upper row displays the pictures of the living mouse; lower row displays the schematic phenotype. (A) 60 weeks: one aplastic groove is observed, (B) 62 weeks: two aplastic grooves are observed; (C) 64 weeks: the 1st aplastic groove is still visible, but the 2nd one is not clear; (D) 66 weeks: the 2nd aplastic groove set has disappeared. Scale bars: 250 μ m.

Age-related defects also affect other areas of the mouse upper incisors

Using X-ray computed microtomography, we further characterize the age-related abnormalities using a complementary dataset we collected. Phenotypic analysis of the 3D-renderings of the specimens coming from the CDTA facility corroborates that the proportion of defects increases with the age of the specimen (Fig.4A). However in this static dataset, defects have not been observed in the younger class (11-month-old mice). The sequence of abnormality occurrence is similar to our *in vivo* findings. This analysis helps describing a new defect that is the presence of a fold in the dentin (uni- or bilateral) starting 13 months (blue, Figure 4B). It affects between 5 and 18% of the incisors between 13 and 17 months of age. In the last three age classes, dentin fold is present in 50% of the defect combination, along with enamel dysplasia and *dens in dentes* (yellow, Fig.4B). The occurrence of one or more enamel grooves still stands out as being the most frequent defect displayed. Interestingly, the gradual increase in the proportion of age-related defects reach a maximum in the oldest class (24-month-old mice), where no normal incisor is displayed anymore. Given rodent incisor specific growth pattern, what is seen on the protruding part of the incisor has been generated in the growth region and has progressed away from it. This is especially visible when looking at enamel grooves, because the folding is observable in the less mineralized part of the incisors that corresponds to the growth region (Suppl. Fig.1).



Suppl. Fig. 1. Grooves are traceable to the growth region.(A) 11-month-old specimen with no defect displayed. (B) 17-month-old specimen with two grooves. Note that the grooves visible on the vestibular enamel surface affect the dentine surface as well, because the mineralized tissue visualized here is the dentin.

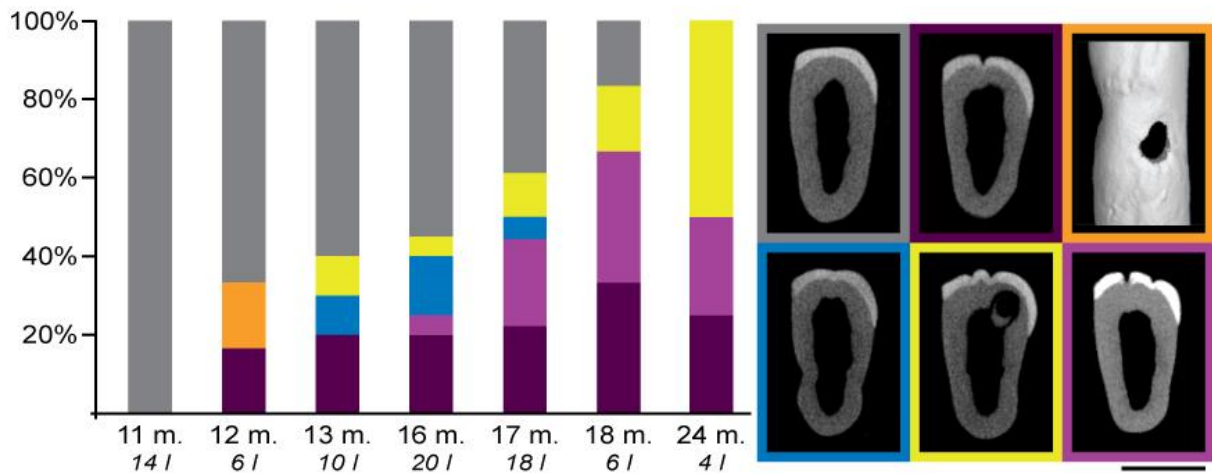


Fig. 4. X-ray microtomography allows a better characterization of the possible age-related abnormalities found in mice. Histogram shows the proportion of incisors showing defects in each age group. Colors correspond to the frame of the phenotypes pictured on the right. Grey: normal incisor; dark purple: one enamel groove; orange: enamel dysplasia; blue: dentin fold; yellow: combination of defects; light purple: two enamel grooves. The proportion of defects increases with the age of the considered group, and the enamel groove are here also the most frequent defect displayed. m. month; I. incisive. Scale bar: 500 μ m.

***Psammomys obesus* also displays age-related abnormalities of its upper incisors**

Mice are not the only rodents starting to display abnormalities on their upper incisors as they age. Abnormalities are displayed in our *Psammomys obesus* samples from 12 months on (Fig.5). From that time point, a single dentin groove is observed centrally in all the upper incisors (yellow arrowheads, Fig.5). Three incisors from 12-month-old specimens, one from a 18-month-old-specimen, and one from the 24-month-old specimen additionally display what we identified as a growth region odontoma (black arrowhead, Fig.5B). Along with this defect come various signs of previous disruption events in the growth system (red arrowheads, Fig.5B).

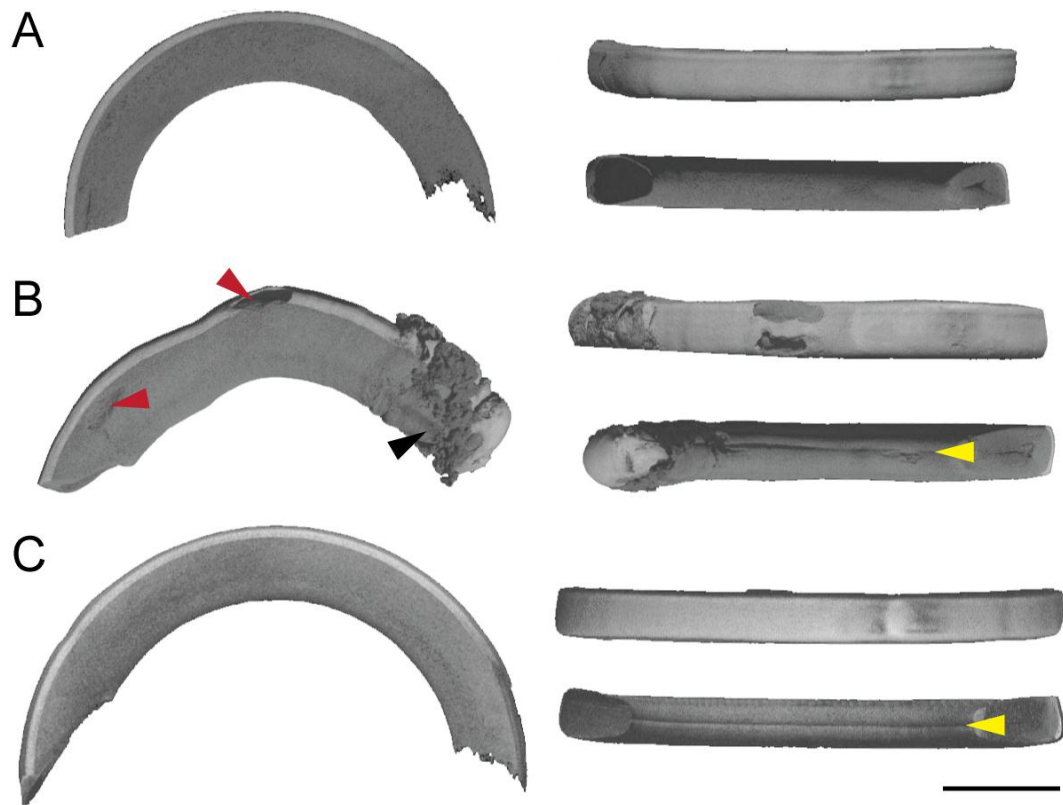


Fig. 5. *Psammomys obesus* also displays age-related abnormalities on its upper incisors. (A) 3-month-old specimen displaying a normal upper incisor phenotype. (B) 12-month-old specimen displaying signs of growth region disruption (red arrowheads), a probable odontoma (black arrowhead), and a dentin groove (yellow arrowhead). (C) 18-month old specimen displaying a dentin groove (yellow arrowhead). Scale bar: 3 mm.

Linear elongation of the upper incisors occurs as the mice age

Mouse incisors start to develop during embryogenesis, and start to erupt ten days after the pup is born. These teeth are fully functional in the juvenile, and since they are continuously growing, they never get replaced over the lifespan of the animal. The incisors of the adult mice are bigger than the ones from the juveniles. We were interested in that constant modification of the incisors, and wanted to test whether or not ageing would impact the phenomenon. By measuring the upper incisors mesio-distal length in our cohorts, we show that the increase is linear in both mouse lines (C57Bl/6N: $y=0.00167x+0.53455$, $R^2=0.9642$, $p\text{-val}<2.2e-16$; CD1 “swiss”: $y=0.001279x+0.542190$, $R^2=0.9698$, $p\text{-val}<2.2e-16$; in Fig.6).

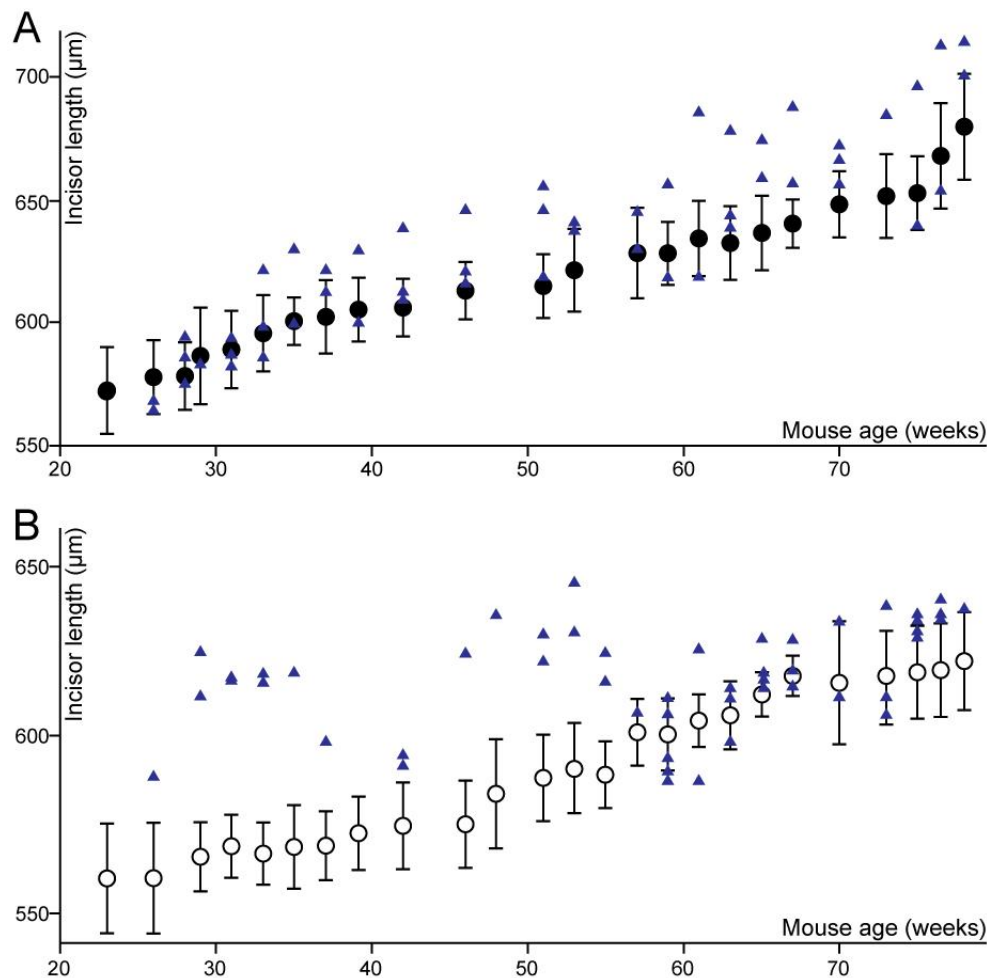


Fig. 6. Upper incisor elongation continuously progresses as the mouse ages. Filled circles represent the evolution of the mesio-distal length of C57Bl/6N depending on the mouse age. Blanked circles show the same progression in CD1 "swiss" mice. Scale bars display the measurement standard deviation. The elongation follows a linear regression in both genetic backgrounds. C57Bl/6N: $y=0.00167x+0.53455$ ($R^2=0.9642$, $p\text{-val}<2.2e-16$); CD1 "swiss": $y=0.001279x+0.542190$ ($R^2=0.9698$, $p\text{-val}<2.2e-16$).

C57Bl/6J upper incisors are significantly longer than CD1 "swiss" upper incisors (Mann-Whitney Wilcoxon, $p\text{-value}<0.05$). The distribution of the mesio-distal length in grooved incisors differs between the two cohorts (blue triangles, Fig.6). These numerical values have not been included in the regression and in the standard deviation calculation. The dispersion of the values remains equivalent at each time point in the C57Bl/6N cohort. In the CD1 "swiss" cohort however, the dispersion is characterized by two phases. Up to 55 weeks (about one year), grooved incisors are significantly longer than smooth incisors (Mann-

Whitney Wilcoxon, $p\text{-value}<0.05$), but in the last six months of the monitoring, there is no significant difference anymore. This might indicate a change in the groove setting in this background.

Grooves occur in the same percentage of mice from both cohorts, but we find that in mouse where only one upper incisor displays a vestibular enamel groove, the smooth incisor shows a lower mesio-distal length when compared to the grooved incisor (Mann-Whitney Wilcoxon, $p\text{-value}<0.05$).

Various histological defects are displayed in the growth region

Mice that were monitored *in vivo* have been sacrificed at three ages (6, 12 and 18 months) in order to address modification of the normal organization of the upper incisor growth region (see also Fig.1B). Histological analyses confirm the occurrence of tissue organization defects and re-state that the age-related abnormalities are set up in the growth region. The serial sections realized on the two upper incisors of a C57Bl/6N mouse of 18 months help comparing tissue organization in the absence and in the presence of enamel grooves (Fig.7). The left incisor still displays the normal smooth enamel surface, but the right incisor displays both a fine groove and a marked groove (green and yellow arrowheads respectively, Fig.7B). Exploring the series of sections reveals that a strong folding of the ameloblast layer is responsible for the phenotype seen protruding out of the mouth, folding that also impact the organization of the odontoblast layer (Fig.7C, D).

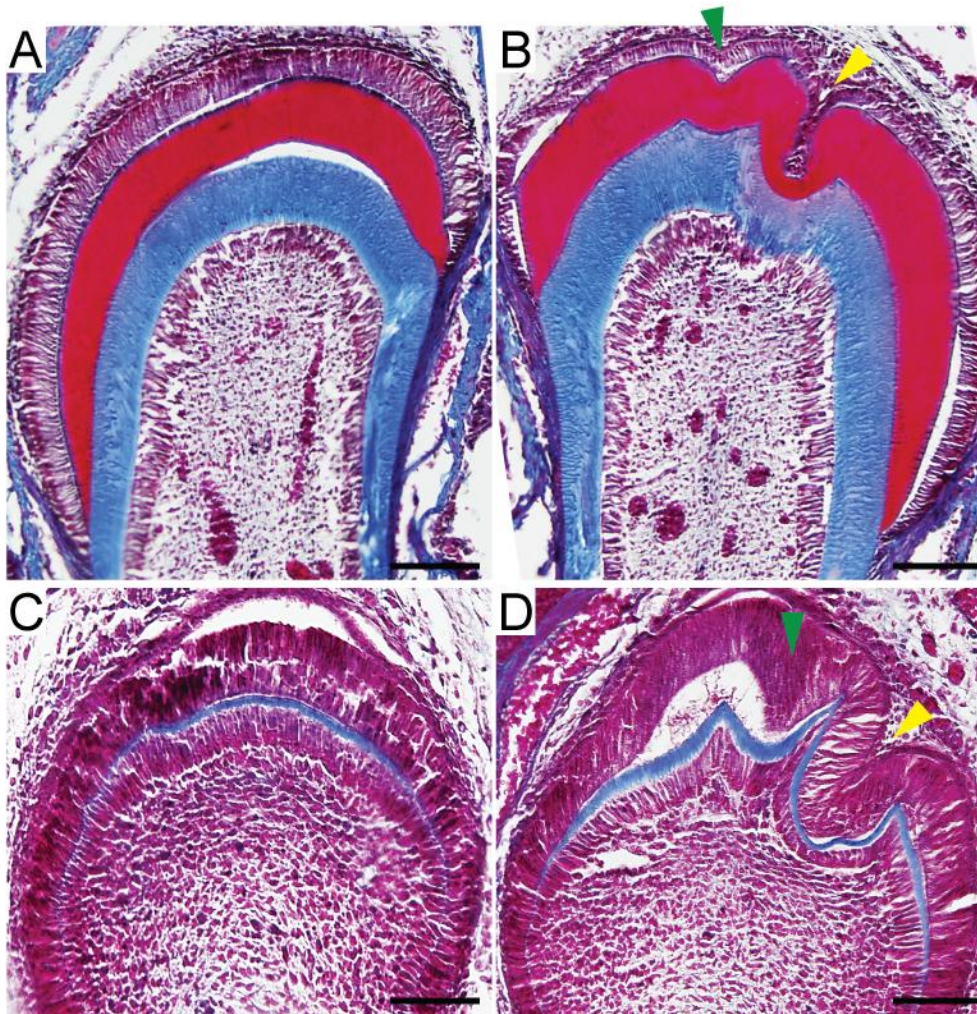


Fig. 7. A fold in the ameloblast layer causes enamel groove. (A, B) Transverse sections in the right and left incisors of a 18-months old C57Bl/6N mouse. (C, D) Transverse sections of the same specimen, only more proximally towards the growth region. All the sections were stained using Masson's trichrome (in red is the enamel, in blue is dentin). Scale bars: 100 μ m.

In a 12-month-old C57Bl/6N, a joint folding of the odontoblast, dentin and ameloblast layer can be traced in successive slices in the transit-amplifying zone (yellow arrowheads Figure 8A). This mouse also displays a hyperplastic laCL when compared to a normal-looking laCL of one littermate (yellow dotted line in Fig.8A). In a 6-month-old CD1 "swiss" mouse, we have been able to observe the duplication of the ameloblast layer which seem to be caused by an erratic cell proliferation event (Fig.8B).

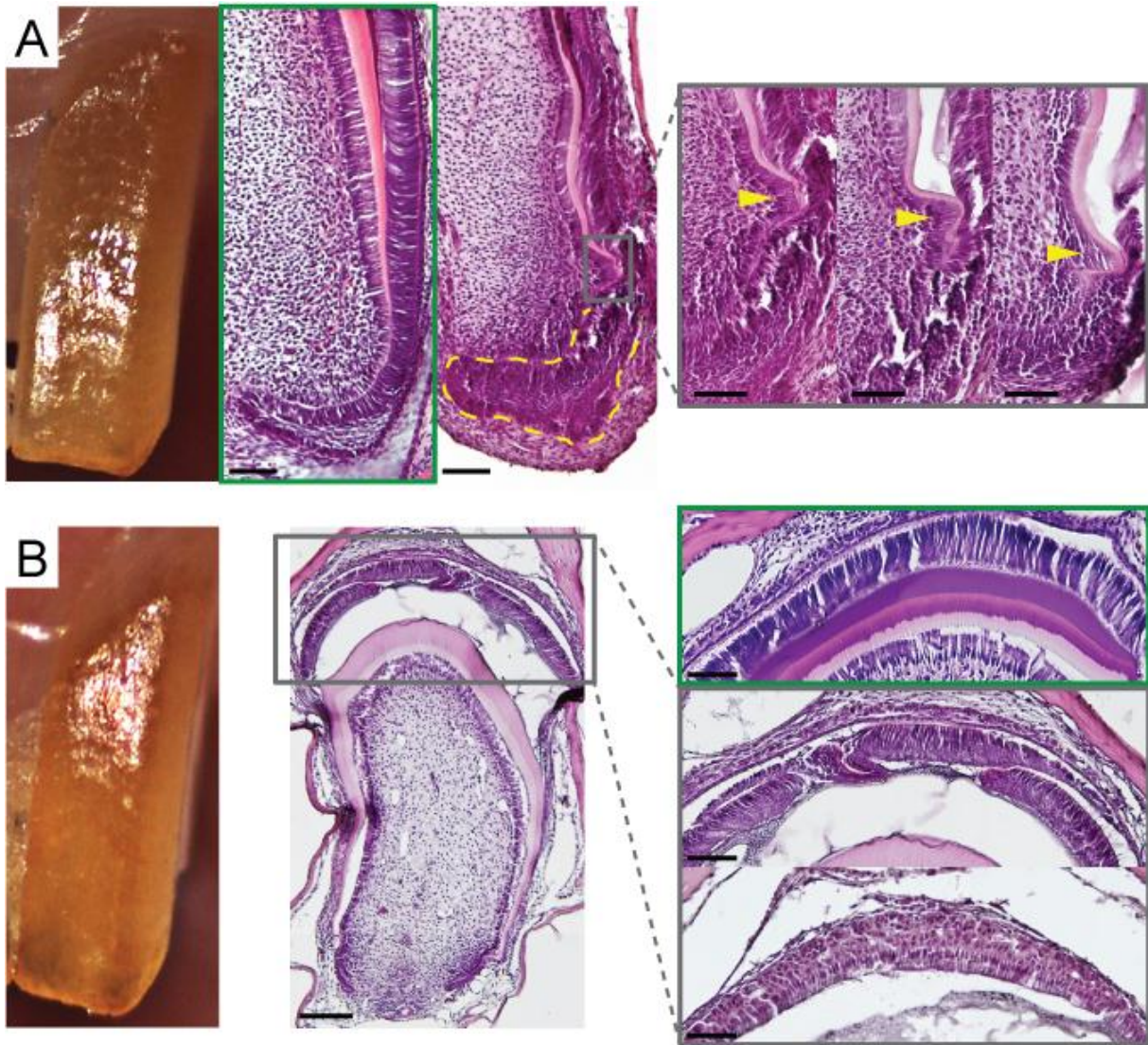


Fig. 8. Abnormalities of tissue organization can be detected in the growth region and the ameloblast layer even when the protruding phenotype appears normal. (A) 12 month-old C57Bl/6N specimen displaying an hyperplastic laCL (yellow dotted curve) and a fold affecting the odontoblast, dentin and ameloblast layers (yellow arrowheads). **(B).** 6-month-old CD1 "swiss" specimen displaying an abnormal duplication of the ameloblast layer originatin from an abnormal cell proliferation (bottom right hand corner). The normal histology is framed in green. Scale bars: 100 μm.

DISCUSSION

An updated chrono-morphology of age-related defects is provided

In 1971, Robins and Rowlatt considered a bigger mouse colony, all animals being from a C57Bl/6J genetic background. Their experimental design aimed at comparing upper incisor phenotypes of numerous mice on three separated occasions, without tracing the becoming of the individuals. Robins and Rowlatt concluded that age-related defects were virtually absent on the incisors of 4 to 16-month-old specimens but present in the 22 to 36-month-old groups. On the contrary, our study provides an individual monitoring of ageing mice. This allows us to understand the quick dynamics of abnormality setting. Furthermore, we show a much earlier onset than what was thought, with mice starting to display enamel mineralization defects from about 6 months of age.

Furthermore, our experimental design allows us to address the persistence of the defects displayed. The reversion of enamel grooves is observed in 50% of the specimens we monitored. Stem cell ageing has often been studied in the light of cancer biology because of a decline in the replicative function of various stem cell types (Signer and Morrison, 2013). When an organism ages, DNA damages indeed accumulate and its genomic instability increases, leading to an increase in tumor formations (Finkel *et al.*, 2007). This phenomenon is usually viewed as irreversible. Although grooves are not tumors, our results prove the existence of correction mechanisms that allow the ageing growth region and the stem cell niches to get back to a normal functioning.

The modifications observed depend on the genetic background

By opting for an *in vivo* comparison between an inbred mouse line (C57Bl/6N) and an outbred mouse line (CD1 “swiss”), we address whether or not the genetic background could influence the apparition of age-related defects. We find that although both lines eventually

develop age-related defects, C57Bl/6N mice end up with the strongest defects (higher number of aplastic vestibular grooves). The genetic identity mirrors the degree of consanguinity obtained by crossing littermates over 20 generations (Hedrich, 2004). Thus, inbred mice can be considered as genetically identical (Charles River's C57Bl/6N model information sheet). Outbred mice are animal in which a certain genetic diversity is maintained. CD1 "swiss" mice display about 28% of diversity in 110 tested loci (Charles River's CD1 model information sheet). Although the effects of consanguinity have never been linked with ageing pathologies or progeria-like syndromes, the disadvantages associated with human inbreeding has already been reviewed in the population genetics field (Bittles and Neel, 1994). The results we obtained here tend to prove that the same trend is displayed in the mouse, with a set of age-related abnormalities that can be extended in consanguine specimens.

Hairy teeth raise the question of stem cell differentiation

Robins and Rowlett (1971) put much emphasis on their finding of a high hair impaction in the gingival tissues of both maxillary and mandibular incisors that is caused by grooming regardless of the age of the mice. They use this finding and the reported presence of cysts in mice aged between 11 and 29 months (van Rijssel and Mühlbock, 1955) to hypothesize that the hair inserted in the gingiva could favor the development of cysts in the maxillary tissues that could disrupt the growth region, thus generating the grooves. Our histological studies did not show any inflammatory infiltration in the case of the enamel groove occurrence, but demonstrated that a folding of the ameloblast layer was the mechanical cause of the grooved phenotype.

Surprisingly, we do not find hair impaction to be characteristic of our mouse colonies. However, we have been able to spot ectopic development of hair in the dental socket. The only organs normally growing out of the dental cavity of a mouse are its teeth. Nonetheless,

the presence of very thin and colorless hair addresses the very interesting question of cellular identity. The stem cell niches of the incisors and of the hair follicle originate from the ectoderm, and share similarities in terms of molecular regulation of the niche maintenance and function (Naveau *et al.*, 2014). If the histological organization of both niches differs, it does not rule out the possibility of a change in the differentiation program of the incisor epithelial stem cells. This change in cell fate would be supported by the action of major signaling pathways in either of the organs discussed here.

Grooved incisors are reminiscent of a convergent feature of rodent dentition

The presence of vestibular grooves is the most frequent defect we found in the cohorts we monitored *in vivo*, as well as in the samples we collected for further characterization of the age-related defects. Interestingly, the mouse is not the only rodent displaying more and more abnormalities as it ages. The Gerbillinae species *Psammomys obesus* also naturally does. In the previous study of the phenomenon on this species, Ulmansky and colleagues (1984) described the occurrence of tooth fracture, frequent overgrowth, and the detection of a gingival inflammatory process. We opted for a X-ray microtomographic approach in order to see whether or not ageing sand rats, like ageing mice, were displaying mineralization defects. The dentin grooves detected on the lingual side of the upper incisors are highly similar to what is observed on the mouse vestibular side. It highlights that the mesenchymal stem cell niche is likely to be affected to ageing as well. However, the presence of odontoma-like masses appears specific to *P. obesus*. This phenotype is interesting because an increase in the occurrence frequency of this defect has been documented in ageing osteopetrotic mice (Amling *et al.*, 2000).

Another slightly different case has been reported in wild-type animals: a specimen of *Zapus princeps* displays a supernumerary groove mesially to the first one that is characteristic

of its species (specimen MVZ-36877, C. Charles' PhD dissertation). Interestingly, the presence of vestibular grooves is a dental features shared by 61 genera out of the 481 that constitute the Rodentia order. The absence of any phylogenetic signal in the repartition of the character highlights its independent and convergent acquisition. Peramorphic developmental heterochronies could explain the diversity of ornamentation in the Rodentia order. Molecularly speaking, modulations of the gene expression profiles in the ageing stem cell niches of the mouse or the sand rat upper incisors might be re-activating the mechanisms leading to groove development.

CONCLUDING REMARKS

In summary, we have showed that two different types of age-related modifications affect the mouse upper incisors. The first one occurs from the day the incisor germ starts to develop, and consists in the continuous modification of the tooth size. Ageing beyond the mouse life expectancy does not modify this property, the mesio-distal length of the incisor linearly increasing over the time of our study. The second type of age-related modifications encompasses all the defects seen in the mineralized tissues: dysplasia, aplasia, vestibular enamel groove (aplastic or not), and dentin folding. Taken together, our findings will be the basis of further transcriptomic studies aiming at understanding the molecular disruption of the upper incisor stem cells caused by ageing, and we will thus be able to fully characterize from the phenotype to the genotype the impact of ageing on our model.

ACKNOWLEDGEMENTS

We are grateful to the PBES animal facility (UMS3444, Lyon, France), and to B. Pain for insightful discussion on the topic. This research was funded by a grant from the ENS de Lyon (to LV and CC).

- Amling, M., Neff, L., Priemel, M., Schilling, A. F., Rueger, J. M. and Baron, R.** (2000). Progressive increase in bone mass and development of odontomas in aging osteopetrotic c-src-deficient mice. *Bone* **27**, 603–610.
- Bartke, A. and Brown-Borg, H.** (2004). Life extension in the dwarf mouse. *Curr. Top. Dev. Biol.* **63**, 189–225.
- Bittles, A. H. and Neel, J. V.** (1994). The costs of human inbreeding and their implications for variations at the DNA level. *Nat. Genet.* **8**, 117–121.
- Bland Sutton, J.** (1884). Comparative dental pathology (1). *Trans. Odontol. Soc. G. B.* **16**, 88–145.
- Chakkalakal, J. V., Jones, K. M., Basson, M. A. and Brack, A. S.** (2012). The aged niche disrupts muscle stem cell quiescence. *Nature*.
- Finkel, T., Serrano, M. and Blasco, M. A.** (2007). The common biology of cancer and ageing. *Nature* **448**, 767–774.
- Harada, H., Kettunen, P., Jung, H. S., Mustonen, T., Wang, Y. A. and Thesleff, I.** (1999). Localization of putative stem cells in dental epithelium and their association with Notch and FGF signaling. *J. Cell Biol.* **147**, 105.
- Hedrich, H.** (2004). The laboratory mouse. Academic Press.
- Ho, A. D., Wagner, W. and Mahlknecht, U.** (2005). Stem cells and ageing. *EMBO Rep.* **6**, S35–S38.
- Humphreys, E. R., Robins, M. W. and Stones, V. A.** (1985). Age-related and ²²⁴Ra-induced abnormalities in the teeth of male mice. *Arch. Oral Biol.* **30**, 55–64.
- Hwang, W. S. S. and Tonna, E. A.** (1965). Autoradiographic analysis of labeling indices and migration rates of cellular component of mouse incisors using tritiated thymidine (H3TDR). *J. Dent. Res.* **44**, 42–53.
- Kuhn, H. G., Dickinson-Anson, H. and Gage, F. H.** (1996). Neurogenesis in the dentate gyrus of the adult rat: age-related decrease of neuronal progenitor proliferation. *J. Neurosci.* **16**, 2027–2033.
- Li, C.-Y., Cha, W., Luder, H.-U., Charles, R.-P., McMahon, M., Mitsiadis, T. A. and Klein, O. D.** (2012). E-cadherin regulates the behavior and fate of epithelial stem cells and their progeny in the mouse incisor. *Dev. Biol.* **366**, 357–366.
- Liu, L. and Rando, T. A.** (2011). Manifestations and mechanisms of stem cell aging. *J. Cell Biol.* **193**, 257–266.
- Miller, R. A., Harper, J. M., Dysko, R. C., Durkee, S. J. and Austad, S. N.** (2002). Longer life spans and delayed maturation in wild-derived mice. *Exp. Biol. Med. Maywood NJ* **227**, 500–508.

- Naveau, A., Seidel, K. and Klein, O. D.** (2014). Tooth, hair and claw: Comparing epithelial stem cell niches of ectodermal appendages. *Exp. Cell Res.*
- Nishimura, E. K., Granter, S. R. and Fisher, D. E.** (2005). Mechanisms of hair graying: incomplete melanocyte stem cell maintenance in the niche. *Science* **307**, 720–724.
- Robins, M. W. and Rowlatt, C.** (1971). Dental abnormalities in aged mice. *Gerontology* **17**, 261–272.
- Sashima, M., Satoh, M. and Suzuki, A.** (1987). Incisor Abnormality of Senescence Accelerated Mouse (SAM) 1. *Gerodontology* **6**, 145–148.
- Shadle, A. R., Ploss, W. R. and Marks, E. M.** (1944). The extrusive growth and attrition of the incisor teeth of *Erethizon dorsatum*. *Anat. Rec.* **90**, 337–341.
- Sharpless, N. E. and DePinho, R. A.** (2007). How stem cells age and why this makes us grow old. *Nat. Rev. Mol. Cell Biol.* **8**, 703–713.
- Signer, R. A. J. and Morrison, S. J.** (2013). Mechanisms that Regulate Stem Cell Aging and Life Span. *Cell Stem Cell* **12**, 152–165.
- Ulmansky, M., Ungar, H. and Adlhr, J. H.** (1984). Dental abnormalities in aging sand rats (*Psammomys obesus*). *J. Oral Pathol. Med.* **13**, 366–372.
- Van Rijssel, T. G. and Mühlbock, O.** (1955). Intramandibular tumors in mice. *J. Natl. Cancer Inst.* **16**, 659–689.
- WHO | WHO Global Forum on Innovations for Ageing Populations WHO.**
- Zhao, H., Feng, J., Seidel, K., Shi, S., Klein, O., Sharpe, P. and Chai, Y.** (2014). Secretion of Shh by a Neurovascular Bundle Niche Supports Mesenchymal Stem Cell Homeostasis in the Adult Mouse Incisor. *Cell Stem Cell* **14**, 160–173.

B.3 TRANSCRIPTOMIC DISRUPTIONS OF THE UPPER INCISORS IN AGEING MICE

Among the abnormal phenotypes developing on the mouse upper incisors, the occurrence of vestibular grooves stands out as being the most frequent defect set up. It also stands out because previous work in the tooth evo-devo field acknowledged the development of similar phenotypes in mutant mice. Indeed, *Lrp4*^{hypo/hypo} mice, as well as *Dcr*^{K14-/-} mice were described as displaying such grooves (respectively in Ohazama *et al.*, 2010; and in Michon *et al.*, 2010). However, based on a large-scale characterization of hematopoietic stem cell ageing (Rossi *et al.*, 2007), a candidate gene-based approach is likely to be too restrictive to get a good overview of the plausible large-scale changes in the gene expression profiles.

Taking advantage of Next-Generation Sequencing (NGS) technologies as a powerful tool for transcriptome analysis, I propose a comparative approach to unravel the existence of age-related changes in gene expression profiles, which consists in focusing on the incisor growth region solely or on the entire incisor. Results prove that the transcriptomic approach was indicated, although sampling questions are raised. I also aim at understanding how enamel grooves can be set up in a WT ageing context by comparing incisors of the same age which do not display the same phenotype.

**Independent transcriptomic analyses reveal gene expression changes
in ageing mouse incisor stem cell niches**

Pauline Marangoni¹, Benjamin Gillet², Sandrine Hughes²,
Florence Carrouel¹, Cyril Charles¹, and Laurent Viriot^{1§}

¹: Evo-Devo of Vertebrate Dentition, Institute of Functional Genomics of Lyon, ENS de Lyon, CNRS UMR 5242, University of Lyon 1, 46 allée d'Italie, 69364 Lyon cedex 07, France

²: Sequencing platform, Institute of Functional Genomics of Lyon, ENS de Lyon, CNRS UMR 5242, University of Lyon, 46 allée d'Italie, 69364 Lyon cedex 07, France

§ Corresponding author: laurent.viriot@ens-lyon.fr

ABSTRACT

Stem cell ageing is a growing concern because of the negative impact it has on organ homeostasis. Mouse incisors are an example of continuously growing organ, what is enabled by the presence of several stem cell niches at their proximal end. From six months on, ageing affects the phenotype of the mouse upper incisors only. By developing two complementary transcriptomic approaches, we address the question of the molecular disruption of the ageing stem cell niches. We show that by analyzing gene expression profiles from the microdissected stem cell niches or from the entire incisor, we manage to detect age-related changes in the gene expression levels. The general rule appears to be a global down-regulation of the genes normally expressed in the incisor and in its growth region. We also show by comparing the transcriptome of incisors at the same age, but displaying a smooth or a grooved vestibular surface, that a large immune response is set up in the grooved incisor cohort. Together, these data confirm that age-related transcriptomic changes are detectable. Further examination of selected candidate genes based on their known implication in various developmental processes or signaling pathways will help establishing a causal link between these defects and the phenotypic defects we previously reported.

KEY WORDS

Stem cell ageing, RNA-seq, micro-dissection, enamel groove

INTRODUCTION

Mouse incisors are continuously growing organs made of two highly mineralized tissues: enamel and dentin (Harada et al., 2002a). These tissues are generated from differentiated cells that display a very precise origin. Enamel is secreted by ameloblasts which differentiate from epithelial stem cells located in the cervical loop structures, while dentin is secreted by odontoblast which derive from mesenchymal stem cells located in the pulp (Arana-Chavez and Massa, 2004; Seidel *et al.*, 2010). All the stem cell containing structures are located at the proximal end of the incisors, referred to as the growth region (Fig.1A, B). Although the system lasts during the mouse lifetime, it is affected by ageing. It has been shown that age-related defects develop on the mouse upper incisors from 6 months on (Robins and Rowlatt, 1971; Marangoni *et al.* in prep, please see Chap. B.2). These defects are set up in the growth region and they become visible to the observer once they reach the protruding part of the tooth. They mostly include abnormalities of the enamel layer covering the vestibular (labial) side of the incisor. The presence of an enamel groove is the most frequent age-related abnormality observed (Fig.1C).

The organization of the incisor growth region is very precise, and allows the special circular shape to develop. Stem cell maintenance, dental cell differentiation, enamel and dentin secretion and mineralization are tightly regulated processes which all involve the growth region (Jussila *et al.*, 2013). But the capacity to ensure the upper incisor specific shape is obviously impacted by ageing through histological rearrangements. In order to better understand the molecular disruption of the stem cell niches resulting in those rearrangements, we performed transcriptomic analyses. We aimed at addressing the plausible age-related changes in the gene expression profiles of the mouse upper incisor growth region and at identifying candidate genes to further study dental stem cell ageing.

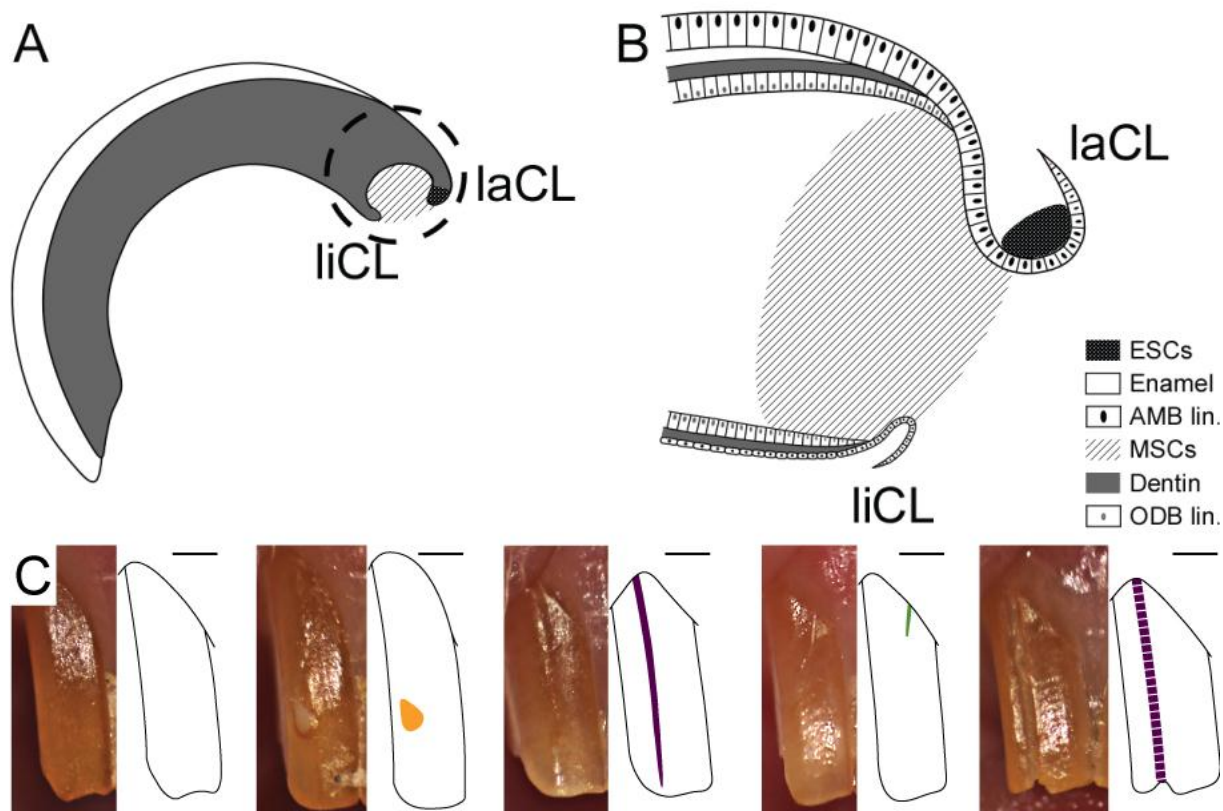


Fig. 1. Schematized organization of the upper incisor growth region, and age-related defects. (A) Incisors are asymmetric teeth displaying enamel only on their vestibular (labial) side. The growth region is circled. (B) The growth region is constituted of the labial and lingual cervical loops (laCL and liCL), and the in-between pulp. Epithelial stem cells (ESCs) are contained within the laCL. As the ESCs move out from the niche, they differentiate into the ameloblast lineage (AMB lin.). Mesenchymal stem cells (MSCs) are dispersed within the pulp, and they form the odontoblast lineage (ODB lin.) as they differentiate. (C) Mouse upper incisors are affected by ageing. Defects are set in the growth region and become visible as the tooth grows. From left to right are displayed a normal (smooth) incisor, one displaying enamel dysplasia (orange), one displaying a vestibular enamel groove (purple), one with a hair growing out of the tooth socket (gray), and one with an aplastic vestibular groove (no enamel left). Scale bars: 0.5 mm.

Because of the organization of the incisor in several areas (growth region, transit-amplifying portion and differentiated zone), we chose a double approach to assess stem cell ageing, analyzing the gene expression profiles of (1) the sole growth region, which was extracted by laser capture, and (2) entire incisors with or without a vestibular groove. By combining the results, we show that both the growth region and the entire incisor transcriptomes vary depending on the age. Most of the genes differentially expressed between age conditions are down-regulated in old samples. We were able to identify a list of 20 genes

which biological function is interesting in the light of ageing, among which *Fgf7*, *Krt7*, *Mmp20* and *Wnt2b* stand out. We also provide an extensive comparative analysis between smooth and grooved incisors of similar age. We show a strong correlation between the presence of an aplastic groove and an immune response with hundreds of genes involved in the NF- κ B innate immune response being up-regulated.

MATERIALS & METHODS

Sample preparation

Two transcriptomic analyses were performed: one specifically focuses on the growth region, while the second addresses entire incisors. For the construction of the 1st dataset, the upper incisors of 5 CD1 “swiss” mice of 6 months (CD1-6) were dissected from the mouse skull tissues in 1X PBS, soaked in 30X sucrose for 4h, and frozen in liquid nitrogen immediately after. The protocol was repeated for 5 CD1 “swiss” mice of 12 months (CD1-12), 5 CD1 “swiss” mice of 18 months (CD1-18), 5 C57Bl6/N mice of 6 months (B6-6), 5 C57Bl6/N mice of 12 months (B6-12), and 5 C57Bl6/N mice of 18 months (B6-18). The choice of the two mouse lines was dictated by the previous study we performed (Marangoni *et al.*, in prep.), in order for us to investigate the importance of the background in the molecular disruption. Samples were stored at -80°C, and were destined for a Laser-Capture Microdissection (LCM) and a RNA-seq experiment.

Secondly, the incisors of 3 C57Bl6/N mice of 6 months (B6-6) were dissected in 1X PBS, and frozen in liquid nitrogen. Dissection was performed under a stereomicroscope to ensure that the collected upper incisors did not display any abnormality. The protocol was repeated for 3 C57Bl6/N mice of 18 months without any defects (B6-18 S for smooth), and for 3 C57Bl6/N mice of 18 months displaying an aplastic groove (B6-18 G for grooved). All samples were stored at -80°C, and destined to a RNA-seq experiment.

A summary of the entire experimental strategy is provided in the Fig.2. All the mice used for the dissection were housed at the PBES facility (ENS de Lyon, UMS3444), and euthanized using cervical dislocation. The animal experimentation procedure was validated by the ethics committee of the PBES (protocol #ENS-2012-015).

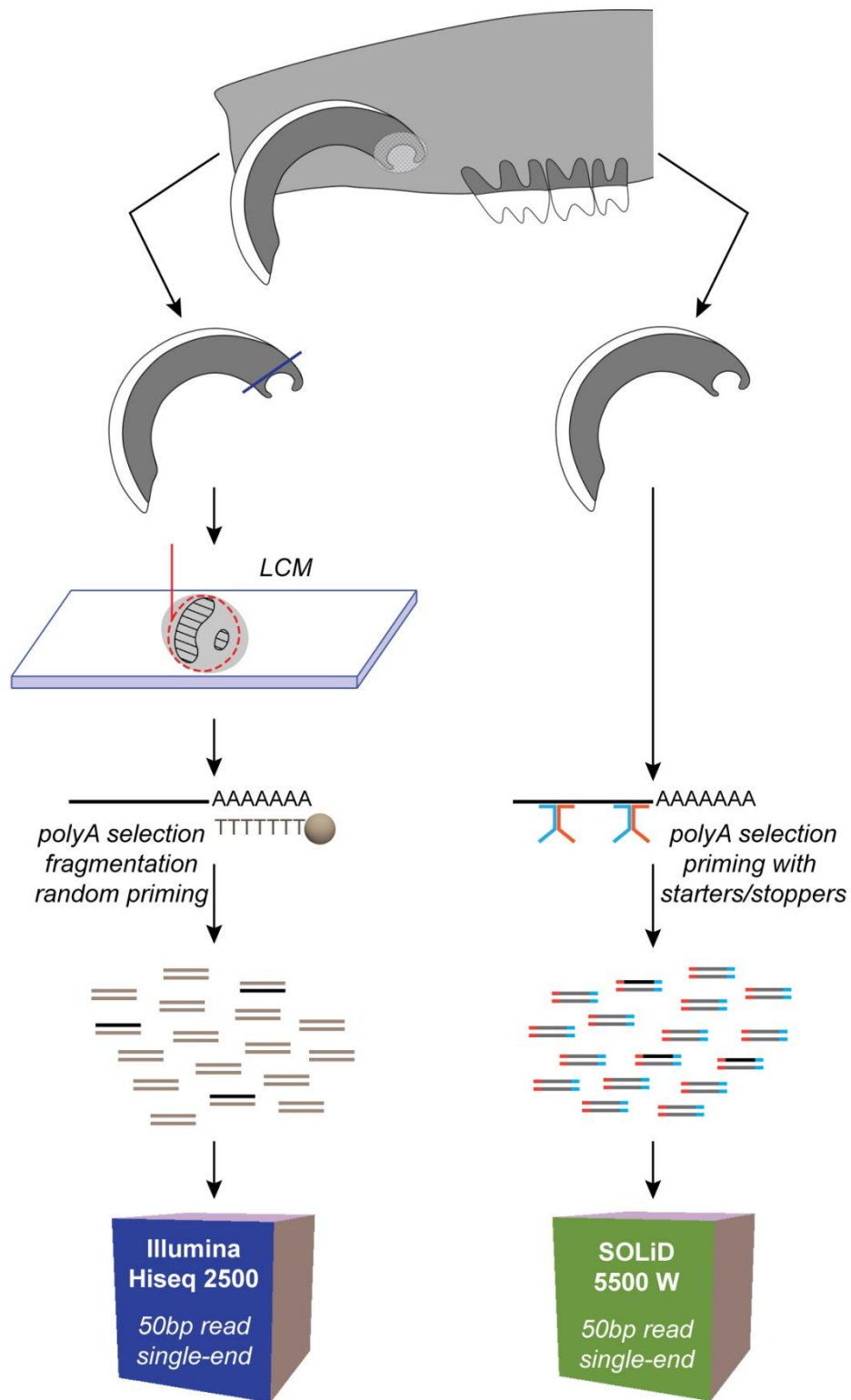


Fig. 2. Comparison of the two experimental strategies. On one hand incisors were dissected, and their growth region (hatched ellipse, top picture) was micro-dissected using Laser Capture Microdissection (LCM). cDNA libraries were obtained with a protocol dedicated to small amount or degraded RNA with cDNA amplification step before fragmentation. Validated banks were then sequenced using a Illumina HiSeq 2500 apparatus. On the other hand, incisors were dissected and total RNA extracted. cDNA libraries were generated using a starter/stopper system developed by Lexogen. Data were sequenced using a

LCM and Illumina library preparation

In order to dissect as precisely as possible the incisor stem cell niches, we designed a LCM approach, performed at the ProfileXpert platform (University of Lyon, IBISA platform). The six groups of frozen incisors (CD1-6, CD1-12, CD1-18, B6-6, B6-12, and B6-18) were embedded using as little Tissue Tech (Fisher) as possible and sectioned using a Leica cryostat (10-12 μm thick). Slides were thawed out at room temperature, dehydrated in graded ethanol and xylene. Slides were dried in a vacuum dome for 10 min. LCM was then performed using PixCell LCM System (Arcturus Engineering) and CapSure® Macro LCM caps (Arcturus Engineering). Actual microdissection was allowed by the application of laser spots (7.5 μm size) through the cap, sealing the transfer film to the region of interest. The region was then removed from the slide by pulling the cap up.

Total RNAs were extracted directly from the caps using the RNeasy extraction kit (Qiagen). RNA quality and quantity were then assessed using a 2100 Bioanalyzer (Agilent Technologies). Due to the results of the test phases, samples of a same age and genotype were pulled together in order to make a single sample per age and background condition. Amplified cDNA was prepared from 5ng of pooled total RNA using the Ovation RNA-seq system V2 and following the manufacturer instructions (NuGEN Technologies, Inc.). 500 ng of amplified cDNA were purified using AMPure XP beads (Agencourt Biosciences Corporation), and fragmented by sonication using a Covaris E210 instrument, and used to construct the Illumina libraries. DNA library quality was assessed using 2100 Bioanalyzer (Agilent Technologies) and quantified using NGS qPCR library quantification kit with EvaGreen (#QUANT-01-0000S, Solis Biodyne). The libraries were loaded in the flow cell at a 14pM concentration and sequenced in the Illumina HiSeq 2500 as single-end 50 base reads. Library preparation and sequencing were performed at the IGBMC Microarray and Sequencing platform (member of *France Génomique* program, Illkirch, France).

SOLiD library preparation and sequencing

Total RNAs were extracted from the incisors of the second dataset consisting in nine mouse upper incisors (three groups: 6 months, 18 months smooth, 18 months grooved). Samples were ground in liquid nitrogen and re-suspended in lysis buffer. Extraction was carried out using RNeasy extraction kit (Qiagen). Samples were treated independently, and RNA concentration was measured using a Qubit 2.0 Fluorometer (Lifetechnologies). Barcoded libraries were prepared from 750 ng of total RNA using the SENSE mRNA-SEQ Library Prep Kits for SOLiD (Lexogen). Then, libraries were converted to be sequenced using SOLiD Wildfire technology using 5500 W conversion primer kit as recommended by Lifetechnologies. Quantification and quality assessment of the libraries was performed on 2200 TapeStation analyzer (Agilent Technologies). Libraries were finally diluted to 4nM, mixed in equimolar proportions and placed in two lines of the flow-cell (four samples on lane 1 and five samples on lane 2) following the Wildfire Template Amplification Protocol for ICS 2.1 provided by Lifetechnologies. Sequencing was performed on the sequencing platform of the IGFL (UMR5242, Lyon, France) using a 5500 W SOLiD sequencer upgraded with the Wildfire technology.

Analysis workflow

After the removal of over-represented sequences using FASTQC (Babrahan Bioinformatics group), Illumina reads were aligned to the USCS_mm10 reference genome using Bowtie2 (Langmead and Salzberg, 2012) available on our local web-interface Galaxy (Goecks *et al.*, 2010). Similarly, after a first step of filtering (to eliminate possible reads from ncRNA, tRNA or ribosomal RNA), SOLiD color-coded reads were aligned in colored space to the USCS_mm10 reference genome (with Ensembl gtf file for annotation) using the LifeScope software with default parameters.

For both Illumina and SOLiD aligned dataset, Galaxy was then used to assess the number of reads per feature with HTSeq count for each sample (Anders *et al.*, 2014, intersection nonempty mode). The differential expression analyses was performed on R software using DESeq2 package (Love *et al.*, 2014) by taking advantage of an in-house program to analyze the output generated (F. Chatonnet). We used the following parameters to determine differentially expressed genes: only genes which had a minimal number of counts of 10 were considered, differences in their expression level were assessed with a $p\text{-value} \leq 0.05$, and finally only those that displayed a Fold Change (FC) superior or equal to 2 in their compared expression level were considered differentially expressed. Gene ontology was assessed using the Gene Ontology enRiChment anaLysis and visuaLizAtion tool (GORILLA, Eden *et al.*, 2009).

Validation of candidate gene expression changes

The validation of changes in gene expression levels detected during both RNA-seq experiments by RT-qPCR is ongoing. For the both types of samples, cDNA has been amplified from the remaining RNA samples using SuperScript II reverse transcriptase (Lifetechnologies). RT-qPCR using the iQ SYBR Green Supermix (BioRad) and a CFX96 apparatus (Biorad) will help prioritizing further studies. Transcript levels were normalized to the housekeeping gene glyceraldehyde-3-phosphate dehydrogenase (GAPDH), results being expressed as normalized expression values (equal to $2^{-\Delta Cq}$). Primers were designed using NCBI Primer-BLAST software, and sequences used are listed in the Suppl. Tab.1.

Gene	Forward primer	Reverse primer
<i>Dspp</i>	AGGCTTTCACACGCTGCTAT	TTTCTGGTGAGGGGTCTGGA
<i>Fgf7</i>	CATGCTTCCACCTCGTCTGT	CAGTTCACACTCGTAGCCGT
<i>Krt6a</i>	AGTAACTGTGACTGCCCCGT	GCCAAGAGCATCAAGGAAAGC
<i>Mmp20</i>	CTGCAGACCCCAACCTACTG	GCAAGGTGGTAGTTGCTCCT
<i>Podn</i>	AACGTACACGTGCTCAAGGT	GTAGAGTTCCCGAAGCTGGG
<i>Sost</i>	TCTGCCTACTTGTGCACGC	GACCTCTGTGGCATCATTCT
<i>Cxcr4</i>	CCATGGAACCGATCAGTGTG	GAAGCAGGGTTCCTTGTTGG
<i>Cyp26a1</i>	CCGACCGCTTTATAGTGCCT	GGAATGAAGCTGAACCGGGA
<i>Gfi1</i>	AGAGGGGCACACAGTTTAGC	CCACATGCCCACCAGATGTT
<i>Glipr2</i>	AGTGTGGAGAGAACCTTGCG	CTGTACCACCTATCGGCCAC
<i>Grem1</i>	CAAACACCAGCCGAAACAG	GGGCATTTCCGACCATCTGA
<i>Hand2</i>	ACGGACACGTTTCTTACAGC	TGGGTTCTTGGGCGCTTATT
<i>Hrh2</i>	AGAGAACACAAAGCCACCGT	TCCACGGTAAACGAAGGCAG
<i>Ibsp</i>	TGACAGCCGGGAGAACAATC	AACCTTCCTTTTCGGCAGTCC
<i>Krt7</i>	GAACCGCTCTATCCAGAGGC	GGACTCTAACTTGGCACGCT
<i>Mmp25</i>	AGTCCCCCGAAAACGACATC	AGCTCGCAGTGACAATCACA
<i>Sfrp4</i>	CCTGGCAACATACCTGAGCA	CACTCCTCTGGACGGCTTTT
<i>Spp1</i>	GGGCAGCCATGAGTCAAGT	CATCCGACTGATCGGCACTC
<i>Wisp</i>	CACCTGTGGGTTGGGCATAG	CTCCAGTTGGCAGAATCGGT
<i>Wnt2b</i>	GTGTCAACGCTACCCAGACA	CACTCTCGGATCCATTCCCG

Suppl. Tab. 1. List of the primers used for RT-qPCR validation of the candidate gene expression levels. Sequences were retrieved using Primer-BLAST software (NCBI).

RESULTS

Micro-dissected incisor growth region compose an heterogeneous dataset

We consider here the 6-month-old mouse cohort as the control for young specimens, and we compare their gene expression profile to the two older cohorts (12- and 18-month-old mice). Our previous analyses showed that mice were impacted by ageing regardless of their background, the most striking difference between CD1 “swiss” and C57Bl6/N being that CD1 mice did not display aplastic grooves for the duration of our monitoring (Marangoni *et al.*, in prep.; please see Chap. B.2). For all our analyses, we have started by working on the raw data. However, in order to minimize the number of differentially expressed genes resulting from a change in the ratio between epithelial and mesenchymal cells imputable to the sample dissection, we decided to also work on normalized data. Because *Sox2* is a known marker for epithelial stem cells (Juuri *et al.*, 2013), and because it is not a differentially expressed gene, we realized a first normalization using *Sox2* count number. For the same reasons, we also normalized the count tables with *Fgf10* count value. Indeed, *Fgf10* is an essential actor that helps maintaining the functioning of the stem cell niche (Harada *et al.*, 2002b), and it is expressed in the mesenchyme surrounding the cervical loops (Klein *et al.*, 2008).

The dataset has the specificity of being generated by pulling 6 micro-dissected growth regions for each of the age cohorts. The most striking finding resulting from the analysis of this data is that the dataset displays heterogeneity that could be due to individual variability and/or to the absence of transcriptomic change along with ageing. The Principal Component Analysis (PCA) (Fig.3A) recapitulates this observation, with no age-dependent clustering of the samples being observed. The heatmaps and dendrograms argue in favor of the sample variability, which could either come from biases in the sampling or from differences between the genetic background of the mice (Fig.3B). However, the detection of differentially

expressed genes matching our conditions (Fig.3D, E; Tab.1) tend to show that age modifications can be found, and that this dataset might benefit from ongoing investigations about the genetic diversity between mouse line.

Growth region analysis		Growth region analysis	
12 months vs. 6 months	DE+FC \geq 2	18 months vs. 6 months	DE+FC \geq 2
raw data	17	raw data	21
<i>Sox2</i> -norm.	0	<i>Sox2</i> -norm.	0
<i>Fgf10</i> -norm.	0	<i>Fgf10</i> -norm.	4

Tab. 1. Number of differentially expressed genes in the growth region transcriptomic analysis. Each sub-table specifies the comparison realized, as well as the number of genes of interest revealed working on raw, *Sox2*-normalized or *Fgf10*-normalized count tables. DE: differentially expressed, FC \geq 2: fold change superior or equal to 2.

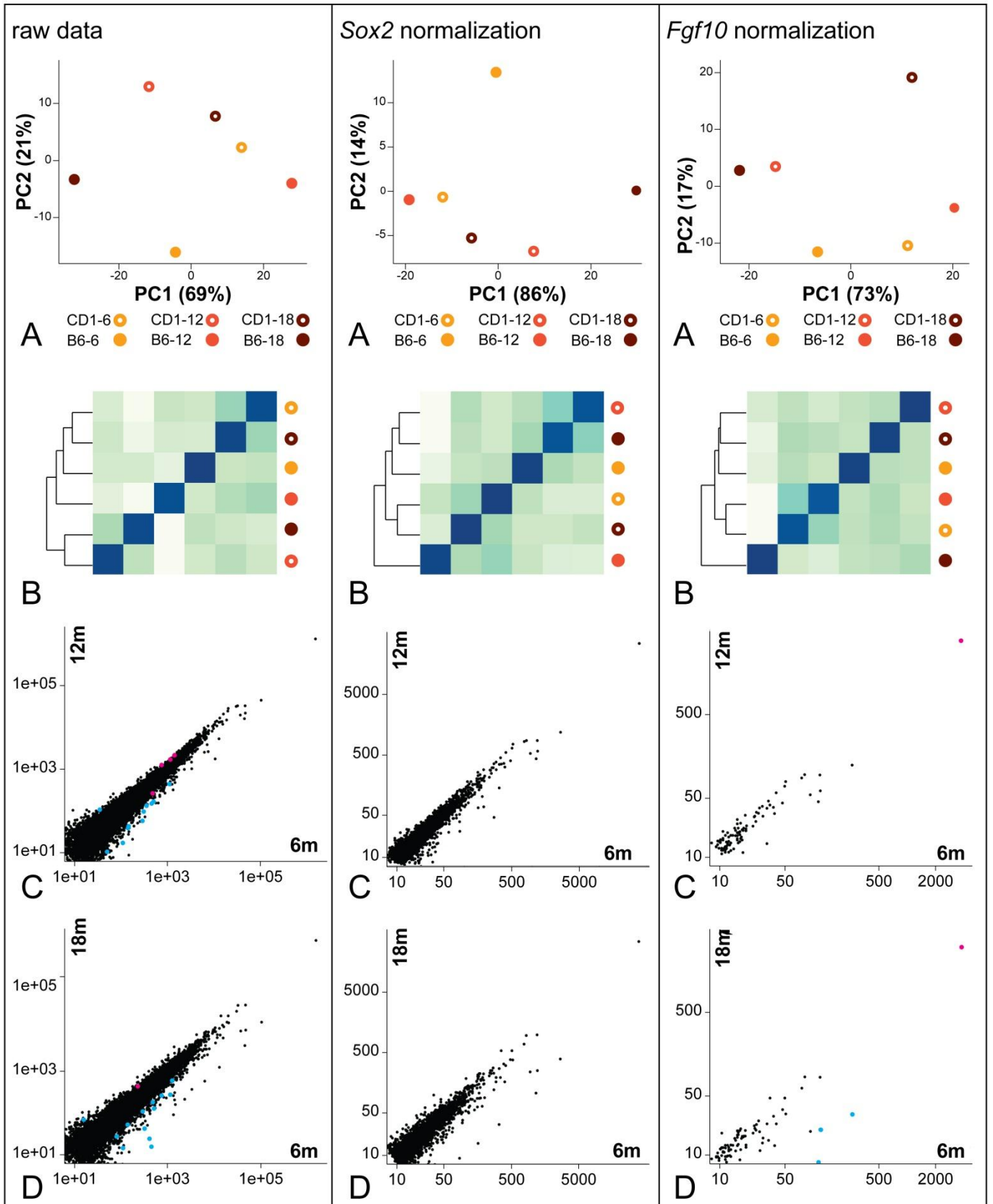
The transcriptome of the mouse incisor growth region varies when the animal ages

The comparison of the number of read per feature reveals that 17 genes are differentially expressed with a FC \geq 2 threshold when comparing 12-month-old mice with 6-month-old mice, regardless of their genetic background (Fig.3C, Tab.1). In all cases, these 17 genes appear down-regulated in the older mice (Suppl. Tab.2). One of them stands out because of its very specific expression pattern. Indeed, *Fgf7* is known for being expressed in the mesenchyme directly surrounding the cervical loops. Similarly, 21 genes are differentially expressed with a FC \geq 2 when comparing 18-month-old mice to our 6-month-old mice (Figure 3D, Tab.1). As previously observed, most of them (18/21) are down-regulated in the older cohort (Suppl. Tab.2). Among them, two are of special interest: *Mmp20* and *Sost*, both strongly down-regulated in the older cohort. *Mmp20* has being associated with *amelogenesis imperfecta* and could play a role in the age-related increase in mineralization defects. *Sost* is a member of Wnt signaling pathway. Incisor mesenchyme is competent to Wnt signaling

pathway, which help regulating the development of the correct number of incisors (Fujimori *et al.*, 2010).

In the *Sox2*-normalized analysis, no gene appears differentially expressed in the two comparisons (2nd column, Fig.3C, D). In the *Fgf10*-normalized analysis, no gene appears differentially expressed when comparing 12- to 6-month old mice (3rd column, Fig.3C, D). However, four genes stand out as being differentially expressed with a $FC \geq 2$ in the 2nd comparison: *Bglap*, *Colla1*, *Colla2*, and *Dspp*. Both collagen genes can be mutated in *dentinogenesis imperfecta*, as well as *Dspp* gene (Sreenath *et al.*, 2003). However, none of these 4 genes were picked in the analysis of the raw data.

Fig. 3. [following page] Genetic variation and differentially expressed genes depending on the specimen age. These data refer to the growth region transcriptomic analysis. Each column is organized similarly with (A) PCA plot of the variability in the specimen gene expression profile, the percentage indicate the contribution of the principal axes of variation; (B) heatmaps and dendrogram indicating the relationships between the samples based on their gene expression; (C) correlation graphs where black dots represent the filtered genes, pink dots represent the differentially expressed genes, and blue dots represent those with a $FC \geq 2$. 1st column is the raw data, 2nd the *Sox2*-normalized data, and 3rd the *Fgf10*-normalized data.



Second RNA-seq confirms the existence of age-related changes in the transcription levels

A second dataset has been designed to compare more easily the gene expression profile of mice of various ages. In an effort to generate a more homogeneous dataset, we opted for an analysis on whole dissected incisors, subdivided in three cohorts: young and smooth (6-month-old mice), old and smooth (18-month-old mice), and finally old and grooved (18-month-old mice) samples. In this dataset, we have three replicates for each condition. We then performed the same analytic workflow on this dataset.

The variation between the samples was assessed by PCA. It shows that samples from the same cohort tend to plot together, regardless of the normalization applied (Fig.4A). The segregation between the young and the old and smooth samples is much finer than the separation between smooth and grooved old specimens. The latter is strongly displayed on PC1 where 2/3 of the ‘old and grooved’ replicates plot completely separately from the rest of the replicates (Fig.4A, all columns). This highlights the huge variability of the gene expression profile in the case of grooved incisors. The heatmap and dendrogram plots provided by the DESeq2 package confirm this repartition, one grooved incisor being retained within the smooth tooth group (Fig.4B).

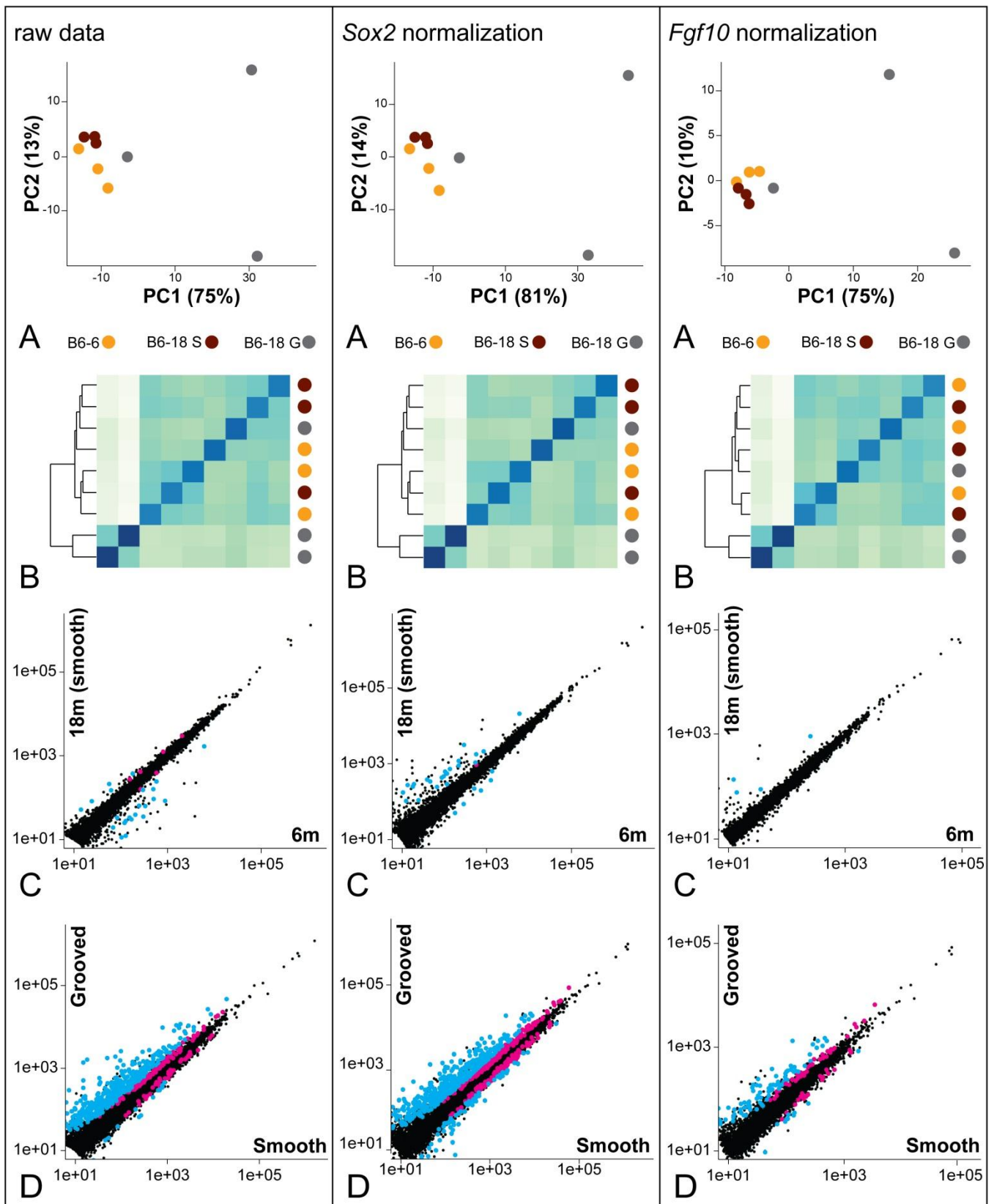
The comparison between ‘young and smooth’ and ‘old and smooth’ specimens indicates that 28 genes are differentially expressed with a $FC \geq 2$. The number is brought to 31 when working with the *Sox2*-normalized count table, and to six when working with the *Fgf10*-normalized count table (Fig.4C, Tab.2). When comparing the gene lists, 24 genes are found in the raw data and the *Sox2*-normalized data, four in the raw data and the *Fgf10*-normalized data, as well as in both normalized data (Suppl. Tab.3). Most of the genes highlighted here are down-regulated in the older specimens (all in raw data and *Fgf10*-normalized data, and 5/31 in *Sox2*-normalized data, Suppl. Tab.3).

If the global down-regulation affects the same proportion of genes that in the study of the growth region transcriptome, none of the genes found in the entire incisor transcriptomic analysis was found differentially expressed in the first analysis. Gene ontology study using GOrilla software does not reveal enrichment in any biological process or function in the case of the two age comparisons from the 1st RNA-seq performed. The same search on the comparison between young and old and smooth incisors shows a detectable enrichment in metabolism regulation, but the signal is lost when entering the list of genes from the two normalized datasets.

Entire incisor		Entire incisor	
18 months vs. 6 months	DE+FC \geq 2	grooved vs. smooth	DE+FC \geq 2
raw data	28	raw data	442
<i>Sox2</i> -norm.	31	<i>Sox2</i> -norm.	502
<i>Fgf10</i> -norm.	6	<i>Fgf10</i> -norm.	145

Tab. 2. Number of differentially expressed genes in the entire incisor transcriptomic analysis. Each sub-table specifies the comparison realized, as well as the number of genes of interest revealed working on raw, *Sox2*-normalized or *Fgf10*-normalized count tables. DE: differentially expressed, FC \geq 2: fold change superior or equal to 2.

Fig. 4. [following page] Genetic variation and differentially expressed genes depending on the specimen age and phenotype. These data refer to the entire incisor transcriptomic analysis. Each column is organized similarly with (A) PCA plot of the variability in the specimen gene expression profile, the percentage indicate the contribution of the principal axes of variation; (B) heatmaps and dendrogram indicating the relationships between the samples based on their gene expression; (C) correlation graphs where black dots represent the filtered genes, pink dots represent the differentially expressed genes, and blue dots represent those with a FC \geq 2. 1st column is the raw data, 2nd the *Sox2*-normalized data, and 3rd the *Fgf10*-normalized data.



Huge differences occur between grooved and smooth incisors

Regarding the defect factor, the number of genes differentially expressed with a $FC \geq 2$ is much bigger. 442 genes fulfill our condition in the raw data, 502 in the *Sox2*-normalized data, and 145 in the *Fgf10*-normalized data (Fig.4D, Tab.2, Suppl. Tab.4). When cross-referencing those genes between the datasets, 96% of the genes are redundantly found in the raw data and the *Sox2*-normalized data, and of 12% when comparing the raw data and the *Fgf10*-normalized dataset.

The biggest finding in terms of gene ontology enrichment comes from this comparison between grooved and smooth incisors. Indeed, we detect a very strong enrichment in immune system response. Going through the list of genes differentially expressed, we find about 35% of them involved in immune processes (Suppl. Tab.4). The vast majority of them are involved in the NF- κ B mediated immune response, with notably many metalloproteases, chemokines, complements, and cytokines stimulated. All these genes of interest are strongly up-regulated in the grooved incisors, thus establishing a strong correlation between the presence of an aplastic groove and a large immune response.

Picking candidate genes to perfect our understanding of the ageing impact of the continuously growing incisors

Documentation of the various lists of differentially expressed genes obtained in our dataset has allowed us to pick several candidate genes to address more precisely dental stem cell ageing. We picked 20 genes of high interest for further examination (Tab.3). *Dspp*, *Fgf7*, *Krt6a*, *Mmp20*, *Podn* and *Sost* are the genes of interest chosen to further address the ageing process within the growth region. *Cxcr4*, *Cyp26a1*, *Gfi1*, *Glipr2*, *Grem1*, *Hand2*, *Hrh2*, *Ibsp*, *Krt7*, *Mmp25*, *Sfrp4*, *Spp1*, *Wisp*, and *Wnt2b* are the genes of interest chosen to further address the setting up of the enamel groove.

AGE FACTOR

GENE	UP/DOWN	GENE	UP/DOWN	GENE	UP/DOWN
<i>Dspp</i>	↘	<i>Krt6a</i>	↘	<i>Podn</i>	↘
<i>Fgf7</i>	↘	<i>Mmp20</i>	↘	<i>Sost</i>	↘

DEFECT FACTOR

GENE	UP/DOWN	GENE	UP/DOWN	GENE	UP/DOWN
<i>Cxcr4</i>	↘	<i>Hand2</i>	↗	<i>Sfrp4</i>	↘
<i>Cyp26a1</i>	↗	<i>Hrh2</i>	↘	<i>Spp1</i>	↘
<i>Gfi1</i>	↘	<i>Ibsp</i>	↘	<i>Wisp</i>	↘
<i>Glpr2</i>	↘	<i>Krt7</i>	↘	<i>Wnt2b</i>	↘
<i>Grem1</i>	↘	<i>Mmp25</i>	↘		

Tab. 3. Genes of interest to understand the molecular impact of ageing on the stem cell niches, and the setting of the aplastic groove. The orientation of the arrow in the UP/DOWN column indicates if there is a higher (up) or a lower (bottom) expression of the gene in the old and smooth or old and grooved groups when compared to their respective

12 months vs. 6 months		18 months vs. 6 months			
GENE	UP/DOWN	GENE	UP/DOWN	GENE	UP/DOWN
<i>AU040972</i>	↘	<i>5730405O15Rik</i>	↗	<i>Bglap</i>	↘
<i>Acpp</i>	↘	<i>9930013L23Rik</i>	↘	<i>Colla1</i>	↘
<i>Bnc2</i>	↘	<i>Ankrd45</i>	↘	<i>Colla2</i>	↘
<i>Celf3</i>	↘	<i>Arhgap4</i>	↗	<i>Dspp</i>	↘
<i>Coll14a1</i>	↘	<i>Bcan</i>	↘		
<i>Col8a1</i>	↘	<i>Cpz</i>	↘		
<i>Cyp2e1</i>	↘	<i>Creb3l1</i>	↘		
<i>Fgf7</i>	↘	<i>Dpf3</i>	↘		
<i>Flt4</i>	↘	<i>Emid2</i>	↘		
<i>Harbi1</i>	↘	<i>Endod1</i>	↘		
<i>Itga11</i>	↘	<i>Fam65c</i>	↘		
<i>Lrrc32</i>	↘	<i>Gabra4</i>	↘		
<i>Ltbp2</i>	↘	<i>Gale</i>	↘		
<i>Rab30</i>	↘	<i>Gpr133</i>	↘		
<i>Smcr7</i>	↘	<i>Itga11</i>	↘		
<i>Susd5</i>	↘	<i>Ltbp2</i>	↘		
<i>Thsd7b</i>	↘	<i>Mmp20</i>	↘		
		<i>Ncam2</i>	↘		
		<i>Sgol2</i>	↗		
		<i>Slc13a5</i>	↘		
		<i>Sost</i>	↘		

Suppl. Tab. 2. List of the differentially expressed genes between two age conditions from the growth region transcriptomic analysis. All the genes listed above are differentially expressed with a $FC \geq 2$. Genes highlighted in yellow are the genes of interest to conduct further studies on the ageing of the incisor growth region. In black are the lists obtained analyzing the raw data, in grey is the list obtained analyzing the *Fgf10*-normalized data.

18 months vs. 6 months

GENE	UP/DOWN	GENE	UP/DOWN	GENE	UP/DOWN
<i>Aqp3</i>	↘	<i>Abpb</i>	↘	<i>Krt6a</i>	↘
<i>Calml3</i>	↘	<i>Aqp3</i>	↘	<i>Lcn13</i>	↘
<i>Cecr6</i>	↗	<i>Calml3</i>	↘	<i>Ltf</i>	↘
<i>Chi3l1</i>	↘	<i>Casp14</i>	↘	<i>Lypd3</i>	↘
<i>Chit1</i>	↘	<i>Cd24a</i>	↗	<i>Obp1a</i>	↘
<i>Fgg</i>	↗	<i>Cecr6</i>	↗	<i>Sprr1a</i>	↘
<i>Fxyd2</i>	↘	<i>Chi3l1</i>	↘		
<i>Inmt</i>	↘	<i>Chit1</i>	↘		
<i>Krt4</i>	↘	<i>Fgg</i>	↗		
<i>Krt6a</i>	↘	<i>Fxyd2</i>	↘		
<i>Lcn11</i>	↘	<i>Gm14744</i>	↘		
<i>Lcn13</i>	↘	<i>Inmt</i>	↘		
<i>Lcn14</i>	↘	<i>Klk13</i>	↘		
<i>Ltf</i>	↘	<i>Krt4</i>	↘		
<i>Ly6g6c</i>	↘	<i>Krt6a</i>	↘		
<i>Lypd3</i>	↘	<i>Lcn11</i>	↘		
<i>Mup4</i>	↘	<i>Lcn14</i>	↘		
<i>Nm1l</i>	↗	<i>Ltf</i>	↘		
<i>Obp1a</i>	↘	<i>Lypd3</i>	↘		
<i>Pdzk1ip1</i>	↘	<i>Mup4</i>	↘		
<i>Pglyrp1</i>	↘	<i>Nrn1l</i>	↗		
<i>Podn</i>	↘	<i>Obp1a</i>	↘		
<i>Psap1l</i>	↘	<i>Pdzk1ip1</i>	↘		
<i>Slc38a3</i>	↗	<i>Pglyrp1</i>	↘		
<i>Spink5</i>	↘	<i>Podn</i>	↘		
<i>Sprr1a</i>	↘	<i>Psap1l</i>	↘		
<i>Tac2</i>	↗	<i>Psors1c2</i>	↘		
<i>Tfap2b</i>	↘	<i>Slc38a3</i>	↘		
		<i>Spink5</i>	↘		
		<i>Tac2</i>	↘		
		<i>Tfap2b</i>	↘		

Suppl. Tab. 3. List of the genes differentially expressed between two age conditions from the entire incisor transcriptomic analysis. All the genes listed above are differentially expressed with a $FC \geq 2$. Genes highlighted in yellow are the genes of interest to conduct further studies on the ageing of the incisor growth region. In black is the list obtained analyzing the raw data, in blue the one obtained analyzing the *Sox2*-normalized data, and in grey is the list obtained analyzing the *Fgf10*-normalized data. In bold are the genes found in at least 2 of the 3 analyses

Grooved vs. Smooth

GENE	UP/DOWN	GENE	UP/DOWN	GENE	UP/DOWN
<i>2010001M09Rik</i>	↗	<i>Aqp9</i>	↗	<i>Ccr7</i>	↗
<i>2210020M01Rik</i>	↗	<i>Arg1</i>	↗	<i>Cd109</i>	↗
<i>2310046A06Rik</i>	↗	<i>Arhgap25</i>	↗	<i>Cd177</i>	↗
<i>2610109H07Rik</i>	↗	<i>Arhgdib</i>	↗	<i>Cd2</i>	↗
<i>2610528A11Rik</i>	↗	<i>Arl11</i>	↗	<i>Cd247</i>	↗
<i>5330426P16Rik</i>	↗	<i>Atf3</i>	↗	<i>Cd300lb</i>	↗
<i>5830416P10Rik</i>	↗	<i>Atp10a</i>	↗	<i>Cd300ld</i>	↗
<i>A4galt</i>	↗	<i>Atp2a3</i>	↗	<i>Cd33</i>	↗
<i>AA467197</i>	↗	<i>Atp6v0d2</i>	↗	<i>Cd37</i>	↗
<i>AB124611</i>	↗	<i>Atp8b1</i>	↗	<i>Cd48</i>	↗
<i>AF251705</i>	↗	<i>Atp8b4</i>	↗	<i>Cd68</i>	↗
<i>AW112010</i>	↗	<i>B2m</i>	↗	<i>Cd72</i>	↗
<i>Abp1</i>	↗	<i>B3galt2</i>	↗	<i>Cd84</i>	↗
<i>Acp5</i>	↗	<i>Batf2</i>	↗	<i>Cd8a</i>	↗
<i>Adam12</i>	↗	<i>Bcl3</i>	↗	<i>Cdh15</i>	↗
<i>Adamts7</i>	↗	<i>BC013712</i>	↗	<i>Cdk6</i>	↗
<i>Adamtsl3</i>	↗	<i>Bdkrb1</i>	↗	<i>Cebpb</i>	↗
<i>Adora3</i>	↗	<i>Birc3</i>	↗	<i>Cebpd</i>	↗
<i>Adra2a</i>	↗	<i>Btla</i>	↗	<i>Chad</i>	↗
<i>Adssl1</i>	↗	<i>Clra</i>	↗	<i>Chi3l1</i>	↗
<i>Aifm3</i>	↘	<i>ClS</i>	↗	<i>Chi3l3</i>	↗
<i>Akna</i>	↗	<i>C3</i>	↗	<i>Chka</i>	↘
<i>Aldh1a1</i>	↗	<i>C5ar1</i>	↗	<i>Cilp</i>	↗
<i>Aldh3a1</i>	↗	<i>Cacna1h</i>	↗	<i>Clec12a</i>	↗
<i>Alox12</i>	↗	<i>Calb2</i>	↗	<i>Clec4n</i>	↗
<i>Alox5ap</i>	↗	<i>Caskin1</i>	↗	<i>Clec5a</i>	↗
<i>Amical</i>	↗	<i>Casp4</i>	↗	<i>Cntfr</i>	↘
<i>Angptl4</i>	↗	<i>Ccl7</i>	↗	<i>Col13a1</i>	↗
<i>Antxr2</i>	↗	<i>Ccl8</i>	↗	<i>Col16a1</i>	↗
<i>Apbb1ip</i>	↗	<i>Ccl9</i>	↗	<i>Col22a1</i>	↗
<i>Apobr</i>	↗	<i>Ccno</i>	↗	<i>Col3a1</i>	↗
<i>Apod</i>	↗	<i>Ccr2</i>	↗	<i>Col5a3</i>	↗

Grooved vs. Smooth

GENE	UP/DOWN	GENE	UP/DOWN	GENE	UP/DOWN
<i>Col8a2</i>	↗	<i>Ecm1</i>	↗	<i>Gbp7</i>	↗
<i>Comp</i>	↗	<i>Egln3</i>	↗	<i>Gcnt4</i>	↗
<i>Coro1a</i>	↗	<i>Ehf</i>	↗	<i>Gda</i>	↗
<i>Coro6</i>	↘	<i>Elf3</i>	↗	<i>Gfi1</i>	↗
<i>Cp</i>	↗	<i>Entpd1</i>	↗	<i>Gfod1</i>	↗
<i>Cryab</i>	↗	<i>Epha3</i>	↗	<i>Gjb2</i>	↗
<i>Csrnp1</i>	↗	<i>Ero1l</i>	↗	<i>Gjb3</i>	↗
<i>Cst7</i>	↗	<i>Evi2a</i>	↗	<i>Gjb4</i>	↗
<i>Ctsc</i>	↗	<i>Evi2b</i>	↗	<i>Glipr1</i>	↗
<i>Ctsk</i>	↗	<i>Eya2</i>	↗	<i>Glipr2</i>	↗
<i>Ctss</i>	↗	<i>F10</i>	↗	<i>Gm11428</i>	↗
<i>Ctsw</i>	↗	<i>F3</i>	↗	<i>Gm266</i>	↗
<i>Cxcl16</i>	↗	<i>F5</i>	↗	<i>Gm6682</i>	↗
<i>Cxcr4</i>	↗	<i>Fam71f2</i>	↗	<i>Gngt2</i>	↗
<i>Cxcr6</i>	↗	<i>Fam83a</i>	↗	<i>Gpr133</i>	↗
<i>Cybb</i>	↗	<i>Fas</i>	↗	<i>Gpr171</i>	↗
<i>Cyp26a1</i>	↗	<i>Fcer1g</i>	↗	<i>Gpr18</i>	↗
<i>Cyth4</i>	↗	<i>Fcrlb</i>	↗	<i>Gpr88</i>	↗
<i>Cytip</i>	↗	<i>Fes</i>	↗	<i>Gpx3</i>	↗
<i>D730048J04Rik</i>	↗	<i>Fgf7</i>	↗	<i>Grap2</i>	↗
<i>Dcstamp</i>	↗	<i>Fgl2</i>	↗	<i>Grem1</i>	↗
<i>Ddit4l</i>	↗	<i>Fgr</i>	↗	<i>Gyk</i>	↗
<i>Ddn</i>	↘	<i>Flt3</i>	↗	<i>H2-Ab1</i>	↗
<i>Dennd1c</i>	↗	<i>Fmnl1</i>	↗	<i>H2-D1</i>	↗
<i>Dgat2</i>	↗	<i>Fos</i>	↗	<i>H2-Eb1</i>	↗
<i>Dock2</i>	↗	<i>Fut7</i>	↗	<i>H2-K1</i>	↗
<i>Dok3</i>	↗	<i>Fxyd2</i>	↗	<i>H2-Q10</i>	↗
<i>Dpt</i>	↗	<i>Fxyd5</i>	↗	<i>H2-Q4</i>	↗
<i>Dram1</i>	↗	<i>Fyb</i>	↗	<i>H6pd</i>	↗
<i>Dtx4</i>	↗	<i>Gabrb3</i>	↗	<i>Hand2</i>	↘
<i>Dusp1</i>	↗	<i>Galr2</i>	↗	<i>Hapln4</i>	↗
<i>E2f8</i>	↗	<i>Gdf10</i>	↗	<i>Hk3</i>	↗

Grooved vs. Smooth

GENE	UP/DOWN	GENE	UP/DOWN	GENE	UP/DOWN
<i>Hmha1</i>	↗	<i>Irf4</i>	↗	<i>Ly9</i>	↗
<i>Hrh2</i>	↗	<i>Isg20</i>	↗	<i>Lyz2</i>	↗
<i>Htra4</i>	↗	<i>Itgae</i>	↗	<i>Mal</i>	↗
<i>Hvcn1</i>	↗	<i>Itgal</i>	↗	<i>Map3k8</i>	↗
<i>Ibsp</i>	↗	<i>Itgax</i>	↗	<i>Mepe</i>	↗
<i>Icam1</i>	↗	<i>Itgb2</i>	↗	<i>Mmp10</i>	↗
<i>Ifi47</i>	↗	<i>Itgb3</i>	↗	<i>Mmp12</i>	↗
<i>Ifitm5</i>	↗	<i>Jdp2</i>	↗	<i>Mmp13</i>	↗
<i>Ifitm6</i>	↗	<i>Junb</i>	↗	<i>Mmp25</i>	↗
<i>Igfbp4</i>	↗	<i>Klf2</i>	↗	<i>Mmp9</i>	↗
<i>Igfbp7</i>	↗	<i>Klk1</i>	↗	<i>Mpo</i>	↗
<i>Igj</i>	↗	<i>Klrk1</i>	↗	<i>Ms4a4d</i>	↗
<i>Igsf6</i>	↗	<i>Krt23</i>	↗	<i>Mst1r</i>	↗
<i>Igtp</i>	↗	<i>Krt7</i>	↗	<i>Mt3</i>	↗
<i>Ikzf1</i>	↗	<i>Laptn5</i>	↗	<i>Muc1</i>	↗
<i>Il10ra</i>	↗	<i>Lat</i>	↗	<i>Muc6</i>	↘
<i>Il13ra2</i>	↗	<i>Lat2</i>	↗	<i>Mxd1</i>	↗
<i>Il17f</i>	↗	<i>Lck</i>	↗	<i>Myo1f</i>	↗
<i>Il18r1</i>	↗	<i>Lcp1</i>	↗	<i>Myo1g</i>	↗
<i>Il1f9</i>	↗	<i>Lcp2</i>	↗	<i>Naip2</i>	↗
<i>Il1r1</i>	↗	<i>Lilrb3</i>	↗	<i>Napsa</i>	↗
<i>Il1rap</i>	↗	<i>Litaf</i>	↗	<i>Ncf1</i>	↗
<i>Il1rl1</i>	↗	<i>Lpl</i>	↗	<i>Ncf4</i>	↗
<i>Il1rn</i>	↗	<i>Lrg1</i>	↗	<i>Nckap11</i>	↗
<i>Il27ra</i>	↗	<i>Lrrc25</i>	↗	<i>Neurl3</i>	↗
<i>Il2rg</i>	↗	<i>Lrrc32</i>	↗	<i>Nfam1</i>	↗
<i>Il4ra</i>	↗	<i>Lrrc55</i>	↗	<i>Nfe2</i>	↗
<i>Il6</i>	↗	<i>Lsp1</i>	↗	<i>Nfkb2</i>	↗
<i>Inpp5d</i>	↗	<i>Ltbp2</i>	↗	<i>Nfkbie</i>	↗
<i>Irak2</i>	↗	<i>Ly6a</i>	↗	<i>Nfkbiz</i>	↗
<i>Irak3</i>	↗	<i>Ly6e</i>	↗	<i>Ngp</i>	↗
<i>Irf1</i>	↗	<i>Ly6i</i>	↗	<i>Nlrc5</i>	↗

Grooved vs. Smooth

GENE	UP/DOWN	GENE	UP/DOWN	GENE	UP/DOWN
<i>Nmb</i>	↗	<i>Plcb2</i>	↗	<i>S100a8</i>	↗
<i>Nnmt</i>	↗	<i>Plcg2</i>	↗	<i>S100a9</i>	↗
<i>Nod2</i>	↗	<i>Pmaip1</i>	↗	<i>Samhd1</i>	↗
<i>Nptx1</i>	↗	<i>Podn</i>	↗	<i>Sash3</i>	↗
<i>Npy</i>	↗	<i>Podnl1</i>	↗	<i>Sele</i>	↗
<i>Ntn1</i>	↗	<i>Ppp1r16b</i>	↗	<i>Selp</i>	↗
<i>Oas3</i>	↗	<i>Ppp1r3d</i>	↗	<i>Selplg</i>	↗
<i>Oasl1</i>	↗	<i>Prss22</i>	↗	<i>Sema4a</i>	↗
<i>Ocstamp</i>	↗	<i>Prtn3</i>	↗	<i>Sept1</i>	↗
<i>Orm1</i>	↗	<i>Psca</i>	↗	<i>Serpina1a</i>	↗
<i>Oscar</i>	↗	<i>Psd4</i>	↗	<i>Serpine1</i>	↗
<i>Otop2</i>	↘	<i>Psmb8</i>	↗	<i>Serpine2</i>	↗
<i>P4ha3</i>	↗	<i>Psmb9</i>	↗	<i>Serping1</i>	↗
<i>Padi2</i>	↗	<i>Pth1r</i>	↗	<i>Sfpi1</i>	↗
<i>Pappa2</i>	↗	<i>Ptpn7</i>	↗	<i>Sfrp2</i>	↗
<i>Parp10</i>	↗	<i>Ptprc</i>	↗	<i>Sfrp4</i>	↗
<i>Parvg</i>	↗	<i>Rab20</i>	↗	<i>Sgms2</i>	↗
<i>Pax3</i>	↗	<i>Rab32</i>	↗	<i>Sh2d3c</i>	↗
<i>Pcsk6</i>	↗	<i>Rac2</i>	↗	<i>Shc2</i>	↗
<i>Pde1b</i>	↗	<i>Ramp1</i>	↗	<i>Shisa3</i>	↗
<i>Pdzk1ip1</i>	↗	<i>Rasal3</i>	↗	<i>Siglece</i>	↗
<i>Pfkfb3</i>	↗	<i>Rasgrp1</i>	↗	<i>Six2</i>	↗
<i>Pglyrp4</i>	↗	<i>Rasgrp4</i>	↗	<i>Sla</i>	↗
<i>Pi16</i>	↗	<i>Rbp4</i>	↗	<i>Slamf7</i>	↗
<i>Pik3ap1</i>	↗	<i>Rel</i>	↗	<i>Slamf8</i>	↗
<i>Pik3cg</i>	↗	<i>Relb</i>	↗	<i>Slc16a3</i>	↗
<i>Pik3r5</i>	↗	<i>Retnlg</i>	↗	<i>Slc2a1</i>	↗
<i>Pilra</i>	↗	<i>Rimklb</i>	↘	<i>Slc2a3</i>	↗
<i>Pim1</i>	↗	<i>Rin3</i>	↗	<i>Slc36a2</i>	↗
<i>Pion</i>	↗	<i>Rinl</i>	↗	<i>Slc37a2</i>	↗
<i>Pla2g7</i>	↗	<i>Rsad2</i>	↗	<i>Slc39a4</i>	↗
<i>Plau</i>	↗	<i>S100a4</i>	↗	<i>Slc45a3</i>	↗

Grooved vs. Smooth

GENE	UP/DOWN	GENE	UP/DOWN	GENE	UP/DOWN
<i>Slc5a1</i>	↗	<i>Tnfrsf1b</i>	↗	<i>2010001M09Rik</i>	↗
<i>Slfn8</i>	↗	<i>Tnfrsf26</i>	↗	<i>2210020M01Rik</i>	↗
<i>Soat2</i>	↗	<i>Tnfsf11</i>	↗	<i>2310046A06Rik</i>	↗
<i>Socs3</i>	↗	<i>Tnfsf14</i>	↗	<i>2610109H07Rik</i>	↗
<i>Sp100</i>	↗	<i>Tnfsf8</i>	↗	<i>2610528A11Rik</i>	↗
<i>Spink5</i>	↗	<i>Tnfsf9</i>	↗	<i>2700038G22Rik</i>	↘
<i>Spn</i>	↗	<i>Tnip1</i>	↗	<i>5330426P16Rik</i>	↗
<i>Spon1</i>	↗	<i>Traf1</i>	↗	<i>5830416P10Rik</i>	↗
<i>Spp1</i>	↗	<i>Trem12</i>	↗	<i>6330406I15Rik</i>	↗
<i>Srpx2</i>	↗	<i>Trim30a</i>	↗	<i>9230116N13Rik</i>	↘
<i>Sst</i>	↗	<i>Trpm2</i>	↗	<i>9430031J16Rik</i>	↗
<i>St6galnac5</i>	↗	<i>Tyrobp</i>	↗	<i>A2m</i>	↗
<i>Stac3</i>	↘	<i>U90926</i>	↗	<i>A4galt</i>	↗
<i>Stambp11</i>	↗	<i>Ubd</i>	↗	<i>A530013C23Rik</i>	↗
<i>Stat4</i>	↗	<i>Upk1b</i>	↗	<i>A930013F10Rik</i>	↘
<i>Steap4</i>	↗	<i>Upp1</i>	↗	<i>AA467197</i>	↗
<i>Stk17b</i>	↗	<i>Vegfc</i>	↗	<i>AB124611</i>	↗
<i>Susd2</i>	↗	<i>Was</i>	↗	<i>AF251705</i>	↗
<i>Svep1</i>	↗	<i>Wisp2</i>	↗	<i>AW112010</i>	↗
<i>Syk</i>	↗	<i>Wnt2b</i>	↗	<i>Abp1</i>	↗
<i>Tac2</i>	↘	<i>Xylt1</i>	↗	<i>Acp5</i>	↗
<i>Tap1</i>	↗	<i>Zbp1</i>	↗	<i>Acs11</i>	↗
<i>Thbs2</i>	↗	<i>Zc3h12a</i>	↗	<i>Actr3b</i>	↗
<i>Thy1</i>	↗			<i>Adam12</i>	↗
<i>Tlr2</i>	↗			<i>Adamts13</i>	↗
<i>Tlr4</i>	↗			<i>Adcy1</i>	↗
<i>Tm4sf19</i>	↗			<i>Adra2a</i>	↗
<i>Tmem119</i>	↗			<i>Adss11</i>	↗
<i>Tmem154</i>	↗			<i>Agt</i>	↗
<i>Tmprss11bnl</i>	↗			<i>Aifm3</i>	↗
<i>Tnfaip8l2</i>	↗			<i>Akna</i>	↗
<i>Tnfrsf11b</i>	↗			<i>Aldh1a1</i>	↗

Grooved vs. Smooth

GENE	UP/DOWN	GENE	UP/DOWN	GENE	UP/DOWN
<i>Aldh3a1</i>	↗	<i>C1s</i>	↗	<i>Cdk6</i>	↗
<i>Alox12</i>	↗	<i>C3</i>	↗	<i>Cebpd</i>	↗
<i>Alox5ap</i>	↗	<i>C5ar1</i>	↗	<i>Celsr3</i>	↗
<i>Angptl4</i>	↗	<i>Cacna1h</i>	↗	<i>Chad</i>	↗
<i>Ankk1</i>	↗	<i>Calb2</i>	↗	<i>Chi3l1</i>	↗
<i>Antxr2</i>	↗	<i>Caskin1</i>	↘	<i>Chi3l3</i>	↗
<i>Apbb1ip</i>	↗	<i>Casp4</i>	↗	<i>Chka</i>	↘
<i>Apobr</i>	↗	<i>Ccl17</i>	↗	<i>Chst7</i>	↗
<i>Apod</i>	↗	<i>Ccl7</i>	↗	<i>Cilp</i>	↗
<i>Apol6</i>	↗	<i>Ccl8</i>	↗	<i>Clca4</i>	↗
<i>Arg1</i>	↗	<i>Ccl9</i>	↗	<i>Clec12a</i>	↗
<i>Arhgap25</i>	↗	<i>Ccno</i>	↗	<i>Clec4n</i>	↗
<i>Arhgap9</i>	↗	<i>Ccr2</i>	↗	<i>Clec5a</i>	↗
<i>Arhgdib</i>	↗	<i>Ccr7</i>	↗	<i>Clec7a</i>	↗
<i>Arl11</i>	↗	<i>Cd109</i>	↗	<i>Cntfr</i>	↘
<i>Atf3</i>	↗	<i>Cd177</i>	↗	<i>Col13a1</i>	↗
<i>Atp10a</i>	↗	<i>Cd247</i>	↗	<i>Col16a1</i>	↗
<i>Atp2a3</i>	↗	<i>Cd28</i>	↗	<i>Col22a1</i>	↗
<i>Atp6v0d2</i>	↗	<i>Cd300lb</i>	↗	<i>Col3a1</i>	↗
<i>Atp8b1</i>	↗	<i>Cd300ld</i>	↗	<i>Col5a3</i>	↗
<i>Atp8b4</i>	↗	<i>Cd33</i>	↗	<i>Col8a2</i>	↗
<i>B2m</i>	↗	<i>Cd37</i>	↗	<i>Comp</i>	↗
<i>B3galt2</i>	↗	<i>Cd48</i>	↗	<i>Coro1a</i>	↗
<i>B430306N03Rik</i>	↗	<i>Cd6</i>	↗	<i>Coro6</i>	↘
<i>Bace2</i>	↗	<i>Cd68</i>	↗	<i>Cp</i>	↗
<i>Batf2</i>	↗	<i>Cd72</i>	↗	<i>Cryab</i>	↗
<i>Bcl3</i>	↗	<i>Cd80</i>	↗	<i>Cst7</i>	↗
<i>Bdkrb1</i>	↗	<i>Cd84</i>	↗	<i>Ctsc</i>	↗
<i>Birc3</i>	↗	<i>Cd8a</i>	↗	<i>Ctsk</i>	↗
<i>Btk</i>	↗	<i>Cd96</i>	↗	<i>Ctss</i>	↗
<i>Btla</i>	↗	<i>Cdc42ep2</i>	↗	<i>Ctsw</i>	↗
<i>Clra</i>	↗	<i>Cdh15</i>	↗	<i>Cxcl16</i>	↗

Grooved vs. Smooth

GENE	UP/DOWN	GENE	UP/DOWN	GENE	UP/DOWN
<i>Cxcr4</i>	↗	<i>Evi2a</i>	↗	<i>Gjb3</i>	↗
<i>Cxcr6</i>	↗	<i>Evi2b</i>	↗	<i>Gjb4</i>	↗
<i>Cyba</i>	↗	<i>Eya2</i>	↗	<i>Glipr1</i>	↗
<i>Cybb</i>	↗	<i>F10</i>	↗	<i>Glipr2</i>	↗
<i>Cyp26a1</i>	↗	<i>F3</i>	↗	<i>Gm11428</i>	↗
<i>Cyp2f2</i>	↗	<i>F5</i>	↗	<i>Gm266</i>	↗
<i>Cyth4</i>	↗	<i>Fam25c</i>	↗	<i>Gm6682</i>	↗
<i>Cytip</i>	↗	<i>Fam26f</i>	↗	<i>Gmip</i>	↗
<i>D730048J04Rik</i>	↗	<i>Fam83a</i>	↗	<i>Gngt2</i>	↗
<i>Dcstamp</i>	↗	<i>Fas</i>	↗	<i>Gpr132</i>	↗
<i>Ddit4l</i>	↗	<i>Fcer1g</i>	↗	<i>Gpr133</i>	↗
<i>Ddn</i>	↗	<i>Fcgr4</i>	↗	<i>Gpr171</i>	↗
<i>Dennd1c</i>	↗	<i>Fcrlb</i>	↗	<i>Gpr18</i>	↗
<i>Dgat2</i>	↗	<i>Fes</i>	↗	<i>Gpr88</i>	↗
<i>Dnahc6</i>	↗	<i>Fgf7</i>	↗	<i>Gpr97</i>	↗
<i>Dock2</i>	↗	<i>Fgl2</i>	↗	<i>Gpre5d</i>	↗
<i>Dok3</i>	↗	<i>Fgr</i>	↗	<i>Gpx3</i>	↗
<i>Dpt</i>	↗	<i>Flt3</i>	↗	<i>Grap2</i>	↗
<i>Dram1</i>	↗	<i>Fmnl1</i>	↗	<i>Grem1</i>	↗
<i>Dtx4</i>	↗	<i>Fos</i>	↗	<i>Gsx1</i>	↘
<i>Dusp4</i>	↗	<i>Fxyd2</i>	↗	<i>Gyk</i>	↗
<i>Dusp5</i>	↗	<i>Fxyd5</i>	↗	<i>H2-Ab1</i>	↗
<i>E2f8</i>	↗	<i>Fyb</i>	↗	<i>H2-D1</i>	↗
<i>Ecm1</i>	↗	<i>Gabrb3</i>	↗	<i>H2-Eb1</i>	↗
<i>Eepd1</i>	↗	<i>Galr2</i>	↗	<i>H2-K1</i>	↗
<i>Egln3</i>	↗	<i>Gbp7</i>	↗	<i>H2-Q10</i>	↗
<i>Ehf</i>	↗	<i>Gcnt4</i>	↗	<i>H2-Q4</i>	↗
<i>Emid1</i>	↗	<i>Gda</i>	↗	<i>H2-T24</i>	↗
<i>Entpd1</i>	↗	<i>Gfi1</i>	↗	<i>H6pd</i>	↗
<i>Epha3</i>	↗	<i>Gfod1</i>	↗	<i>Hand2</i>	↘
<i>Ephb2</i>	↗	<i>Gfra4</i>	↗	<i>Hapln4</i>	↗
<i>Ero1l</i>	↗	<i>Gjb2</i>	↗	<i>Haver2</i>	↗

Grooved vs. Smooth

GENE	UP/DOWN	GENE	UP/DOWN	GENE	UP/DOWN
<i>Hk3</i>	↗	<i>Ipcef1</i>	↗	<i>Litaf</i>	↗
<i>Hmha1</i>	↗	<i>Irak2</i>	↗	<i>Lpl</i>	↗
<i>Hrh2</i>	↗	<i>Irak3</i>	↗	<i>Lrg1</i>	↗
<i>Htra4</i>	↗	<i>Irf1</i>	↗	<i>Lrrc25</i>	↗
<i>Hvcn1</i>	↗	<i>Irf4</i>	↗	<i>Lrrc32</i>	↗
<i>Ibsp</i>	↗	<i>Irf5</i>	↗	<i>Lrrc55</i>	↗
<i>Icam1</i>	↗	<i>Isg15</i>	↗	<i>Lsp1</i>	↗
<i>Ifi2712a</i>	↗	<i>Isg20</i>	↗	<i>Ltbp2</i>	↗
<i>Ifi44</i>	↗	<i>Islr2</i>	↗	<i>Ly6a</i>	↗
<i>Ifi47</i>	↗	<i>Itgae</i>	↗	<i>Ly6e</i>	↗
<i>Ifitm5</i>	↗	<i>Itgal</i>	↗	<i>Ly9</i>	↗
<i>Ifitm6</i>	↗	<i>Itgam</i>	↗	<i>Lyz2</i>	↗
<i>Igfbp4</i>	↗	<i>Itgax</i>	↗	<i>Mal</i>	↗
<i>Igfbp7</i>	↗	<i>Itgb2</i>	↗	<i>Map3k8</i>	↗
<i>Igj</i>	↗	<i>Itgb3</i>	↗	<i>Mepe</i>	↗
<i>Igsf6</i>	↗	<i>Itgbl1</i>	↗	<i>Mfsd4</i>	↗
<i>Ikzf1</i>	↗	<i>Itk</i>	↗	<i>Mmp12</i>	↗
<i>Il10ra</i>	↗	<i>Jdp2</i>	↗	<i>Mmp13</i>	↗
<i>Il13ra2</i>	↗	<i>Junb</i>	↗	<i>Mmp25</i>	↗
<i>Il1f9</i>	↗	<i>Klf2</i>	↗	<i>Mmp8</i>	↗
<i>Il1r1</i>	↗	<i>Klrk1</i>	↗	<i>Mmp9</i>	↗
<i>Il1rap</i>	↗	<i>Krt1</i>	↗	<i>Mpo</i>	↗
<i>Il1rl1</i>	↗	<i>Krt7</i>	↗	<i>Ms4a4d</i>	↗
<i>Il1rn</i>	↗	<i>Laptn5</i>	↗	<i>Mst1r</i>	↗
<i>Il21r</i>	↗	<i>Lat</i>	↗	<i>Mt3</i>	↗
<i>Il27ra</i>	↗	<i>Lat2</i>	↗	<i>Muc1</i>	↗
<i>Il2rg</i>	↗	<i>Layn</i>	↗	<i>Mxd1</i>	↗
<i>Il34</i>	↗	<i>Lck</i>	↗	<i>Myo1f</i>	↗
<i>Il4ra</i>	↗	<i>Lcp1</i>	↗	<i>Myo1g</i>	↗
<i>Il6</i>	↗	<i>Lcp2</i>	↗	<i>Naip2</i>	↗
<i>Il7r</i>	↗	<i>Lilrb3</i>	↗	<i>Napsa</i>	↗
<i>Inpp5d</i>	↗	<i>Liph</i>	↗	<i>Ncf1</i>	↗

Grooved vs. Smooth

GENE	UP/DOWN	GENE	UP/DOWN	GENE	UP/DOWN
<i>Ncf4</i>	↗	<i>Pcsk6</i>	↗	<i>Pth1r</i>	↗
<i>Nckap1l</i>	↗	<i>Pde1b</i>	↗	<i>Ptpn7</i>	↗
<i>Neurl3</i>	↗	<i>Pdzk1ip1</i>	↗	<i>Ptprc</i>	↗
<i>Nfam1</i>	↗	<i>Pf4</i>	↗	<i>Ptprcap</i>	↗
<i>Nfkb2</i>	↗	<i>Pfkfb3</i>	↗	<i>Rab20</i>	↗
<i>Nfkbie</i>	↗	<i>Pglyrp4</i>	↗	<i>Rab32</i>	↗
<i>Nfkbiz</i>	↗	<i>Pi16</i>	↗	<i>Rac2</i>	↗
<i>Ngp</i>	↗	<i>Pik3ap1</i>	↗	<i>Ramp1</i>	↗
<i>Nkg7</i>	↗	<i>Pik3cg</i>	↗	<i>Rarres1</i>	↗
<i>Nlrc5</i>	↗	<i>Pik3r5</i>	↗	<i>Rasal3</i>	↗
<i>Nlrp12</i>	↗	<i>Pilra</i>	↗	<i>Rasgrp1</i>	↗
<i>Nmb</i>	↗	<i>Pim1</i>	↗	<i>Rasgrp4</i>	↗
<i>Nnmt</i>	↗	<i>Pion</i>	↗	<i>Rbp4</i>	↗
<i>Nod2</i>	↗	<i>Pla1a</i>	↗	<i>Rel</i>	↗
<i>Nptx1</i>	↗	<i>Pla2g7</i>	↗	<i>Relb</i>	↗
<i>Npy</i>	↗	<i>Plau</i>	↗	<i>Retnlg</i>	↗
<i>Nsg2</i>	↘	<i>Plcb2</i>	↗	<i>Rimklb</i>	↗
<i>Ntn1</i>	↗	<i>Plcb4</i>	↗	<i>Rin3</i>	↗
<i>Oas2</i>	↗	<i>Plcg2</i>	↗	<i>Rinl</i>	↗
<i>Oas3</i>	↗	<i>Pmaip1</i>	↗	<i>Rnf149</i>	↗
<i>Oasl1</i>	↗	<i>Podn</i>	↗	<i>Rsad2</i>	↗
<i>Ocstamp</i>	↗	<i>Podnl1</i>	↗	<i>S100a4</i>	↗
<i>Orm1</i>	↗	<i>Pou2f2</i>	↗	<i>S100a8</i>	↗
<i>Oscar</i>	↗	<i>Ppp1r16b</i>	↗	<i>S100a9</i>	↗
<i>Otop2</i>	↗	<i>Ppp1r3d</i>	↗	<i>Samhd1</i>	↗
<i>P4ha3</i>	↗	<i>Procr</i>	↗	<i>Sash3</i>	↗
<i>Padi2</i>	↗	<i>Prss22</i>	↗	<i>Sbno2</i>	↗
<i>Padi4</i>	↗	<i>Prtn3</i>	↗	<i>Scnn1a</i>	↗
<i>Pappa2</i>	↗	<i>Psca</i>	↗	<i>Scrt1</i>	↗
<i>Parp10</i>	↗	<i>Psd4</i>	↗	<i>Sele</i>	↗
<i>Parvg</i>	↗	<i>Psmb8</i>	↗	<i>Selp</i>	↗
<i>Pax3</i>	↗	<i>Psmb9</i>	↗	<i>Selplg</i>	↗

Grooved vs. Smooth

GENE	UP/DOWN	GENE	UP/DOWN	GENE	UP/DOWN
<i>Sema4a</i>	↗	<i>Socs3</i>	↗	<i>Tnfrsf1b</i>	↗
<i>Sema6b</i>	↗	<i>Sp100</i>	↗	<i>Tnfrsf26</i>	↗
<i>37135</i>	↗	<i>Spink5</i>	↗	<i>Tnfsf11</i>	↗
<i>Serpine1</i>	↗	<i>Spn</i>	↗	<i>Tnfsf9</i>	↗
<i>Serpine2</i>	↗	<i>Spon1</i>	↗	<i>Tnip1</i>	↗
<i>Serping1</i>	↗	<i>Spp1</i>	↗	<i>Traf1</i>	↗
<i>Sfpi1</i>	↗	<i>Srpx2</i>	↗	<i>Trem12</i>	↗
<i>Sfrp2</i>	↗	<i>Sst</i>	↗	<i>Trim30a</i>	↗
<i>Sfrp4</i>	↗	<i>St6galnac5</i>	↗	<i>Trpm2</i>	↗
<i>Sgca</i>	↗	<i>Stac3</i>	↘	<i>Tyrobp</i>	↗
<i>Sgms2</i>	↗	<i>Stambpl1</i>	↗	<i>Upk1b</i>	↗
<i>Sh2b2</i>	↗	<i>Stat4</i>	↗	<i>Upp1</i>	↗
<i>Sh2d2a</i>	↗	<i>Steap4</i>	↗	<i>Ush1c</i>	↘
<i>Sh2d3c</i>	↗	<i>Stk17b</i>	↗	<i>Vegfc</i>	↗
<i>Shc2</i>	↗	<i>Susd2</i>	↗	<i>Vnn1</i>	↗
<i>Shisa3</i>	↗	<i>Svep1</i>	↗	<i>Was</i>	↗
<i>Siglece</i>	↗	<i>Syk</i>	↗	<i>Wisp2</i>	↗
<i>Six2</i>	↗	<i>Tac2</i>	↘	<i>Wnt2b</i>	↗
<i>Sla</i>	↗	<i>Tacstd2</i>	↗	<i>Xylt1</i>	↗
<i>Slamf7</i>	↗	<i>Tap1</i>	↗	<i>Zbp1</i>	↗
<i>Slamf8</i>	↗	<i>Thbs2</i>	↗	<i>Zc3h12a</i>	↗
<i>Slc12a1</i>	↘	<i>Thy1</i>	↗		
<i>Slc16a3</i>	↗	<i>Tiparp</i>	↗		
<i>Slc28a3</i>	↗	<i>Tlr2</i>	↗		
<i>Slc2a1</i>	↗	<i>Tlr4</i>	↗		
<i>Slc36a2</i>	↗	<i>Tm4sf19</i>	↗		
<i>Slc37a2</i>	↗	<i>Tmem119</i>	↗		
<i>Slc39a4</i>	↗	<i>Tmem154</i>	↗		
<i>Slc45a3</i>	↘	<i>Tmem173</i>	↗		
<i>Slc5a1</i>	↗	<i>Tmprss11bnl</i>	↗		
<i>Slfm8</i>	↗	<i>Tnfaip8l2</i>	↗		
<i>Soat2</i>	↗	<i>Tnfrsf11b</i>	↗		

Grooved vs. Smooth

GENE	UP/DOWN	GENE	UP/DOWN	GENE	UP/DOWN
<i>2610109H07Rik</i>	↗	<i>Ctsc</i>	↗	<i>Igj</i>	↗
<i>AA467197</i>	↗	<i>Ctsk</i>	↗	<i>Il10ra</i>	↗
<i>AW112010</i>	↗	<i>Ctss</i>	↗	<i>Il1f9</i>	↗
<i>Acp5</i>	↗	<i>Cxcl1</i>	↗	<i>Il1rn</i>	↗
<i>Adam12</i>	↗	<i>Cxcr4</i>	↗	<i>Il2rb</i>	↗
<i>Alox5ap</i>	↗	<i>Cybb</i>	↗	<i>Il2rg</i>	↗
<i>Antxr2</i>	↗	<i>Cyp26a1</i>	↘	<i>Il4ra</i>	↗
<i>Apod</i>	↗	<i>Cytip</i>	↗	<i>Irak3</i>	↗
<i>Arg1</i>	↗	<i>Destamp</i>	↗	<i>Irf1</i>	↗
<i>Arhgdib</i>	↗	<i>Dock2</i>	↗	<i>Itgam</i>	↗
<i>Atp6v0d2</i>	↗	<i>Dusp1</i>	↗	<i>Itgb2</i>	↗
<i>B2m</i>	↗	<i>Ecm1</i>	↗	<i>Itgb3</i>	↗
<i>Bcl3</i>	↗	<i>Egln3</i>	↗	<i>Laptm5</i>	↗
<i>C3</i>	↗	<i>F10</i>	↗	<i>Lcp2</i>	↗
<i>C5ar1</i>	↗	<i>Fcer1g</i>	↗	<i>Lilrb3</i>	↗
<i>Cass4</i>	↗	<i>Fgl2</i>	↗	<i>Litaf</i>	↗
<i>Ccl22</i>	↗	<i>Fgr</i>	↗	<i>Lrg1</i>	↗
<i>Ccr7</i>	↗	<i>Fxyd5</i>	↗	<i>Ltbp2</i>	↗
<i>Cd109</i>	↗	<i>Gjb2</i>	↗	<i>Ly6e</i>	↗
<i>Cd163l1</i>	↗	<i>Gjb3</i>	↗	<i>Lyz2</i>	↗
<i>Cd3e</i>	↗	<i>Gm11428</i>	↗	<i>Mepe</i>	↗
<i>Cd68</i>	↗	<i>Gpr35</i>	↗	<i>Mmp12</i>	↗
<i>Cebpd</i>	↗	<i>Gpx3</i>	↗	<i>Mmp13</i>	↗
<i>Chi3l1</i>	↗	<i>H2-Ab1</i>	↗	<i>Mmp3</i>	↗
<i>Coll3a1</i>	↗	<i>H2-Eb1</i>	↗	<i>Mmp9</i>	↗
<i>Col3a1</i>	↗	<i>H2-K1</i>	↗	<i>Mt3</i>	↗
<i>Col8a2</i>	↗	<i>Hvcn1</i>	↗	<i>Mxd1</i>	↗
<i>Comp</i>	↗	<i>Ibsp</i>	↗	<i>Myo1f</i>	↗
<i>Coro1a</i>	↗	<i>Icam1</i>	↗	<i>Myo1g</i>	↗
<i>Coro6</i>	↘	<i>Icos</i>	↗	<i>Ncf1</i>	↗
<i>Cp</i>	↗	<i>Ifitm5</i>	↗	<i>Ncf4</i>	↗
<i>Csf3</i>	↗	<i>Igfbp4</i>	↗	<i>Nfkbiz</i>	↗

Grooved vs. Smooth

GENE	UP/DOWN	GENE	UP/DOWN	GENE	UP/DOWN
<i>Oscar</i>	↗	<i>Selplg</i>	↗	<i>Stk17b</i>	↗
<i>Pappa2</i>	↗	<i>Serpine1</i>	↗	<i>Stx11</i>	↗
<i>Pcsk6</i>	↗	<i>Sfpi1</i>	↗	<i>Syk</i>	↗
<i>Pla2g7</i>	↗	<i>Sfrp2</i>	↗	<i>Tac2</i>	↘
<i>Prss27</i>	↗	<i>Sfrp4</i>	↗	<i>Tarm1</i>	↗
<i>Psmb8</i>	↗	<i>Sgms2</i>	↗	<i>Thy1</i>	↗
<i>Ptafr</i>	↗	<i>Sh2d2a</i>	↗	<i>Tlr2</i>	↗
<i>Ptprc</i>	↗	<i>Slc16a3</i>	↗	<i>Tmem119</i>	↗
<i>Rac2</i>	↗	<i>Slc2a6</i>	↗	<i>Tnfrsf1b</i>	↗
<i>Ramp1</i>	↗	<i>Slc37a2</i>	↗	<i>Traf1</i>	↗
<i>S100a4</i>	↗	<i>Slfn1</i>	↗	<i>Tyrobp</i>	↗
<i>S100a8</i>	↗	<i>Socs3</i>	↗	<i>Upp1</i>	↗
<i>S100a9</i>	↗	<i>Spn</i>	↗	<i>Wfdc2</i>	↗
<i>Samhd1</i>	↗	<i>Spon1</i>	↗	<i>Zap70</i>	↗
<i>Samsn1</i>	↗	<i>Spp1</i>	↗	<i>Zc3h12a</i>	↗
<i>Sash3</i>	↗	<i>Srpx2</i>	↗		↗
<i>Selp</i>	↗	<i>Stac3</i>	↘		↗

Suppl. Tab. 4. List of the genes differentially expressed in the presence or the absence of aplastic groove. All the genes listed above are differentially expressed with a $FC \geq 2$. Genes highlighted in yellow are the genes of interest to conduct further studies on the ageing of the incisor growth region. In black is the list obtained analyzing the raw data, in blue the one obtained analyzing the *Sox2*-normalized data, and in grey is the list obtained analyzing the *Fgf10*-normalized data. In bold are the genes found in at least 2 of the 3 analyses.

DISCUSSION

Our study aimed at performing a wide analysis to monitor age-related changes in gene expression profiles in the tooth growth region, and in the entire incisor, as well as gathering large-scale data on the setting of the most frequent age-related abnormality seen on the mouse upper incisors. From these wide analyses, we want to address the precise role of candidate genes we found involved

Relevance of both strategies

The analysis of the growth region transcription profile has a theoretical advantage over the one of entire incisor transcription profile because we avoid the risk of diluting the signal from the stem cell niches. However, the LCM performed to micro-dissect the growth region has two main biases. Sectioning prior to the micro-dissection has to be done on fresh tissues, without any treatment that may impact the quality of the RNAs contained in the tissue. The incisor enamel is a very hard matrix (mineralized at 96%), and even when sectioning the growth region, which is the less mineralized part of the tooth, it is difficult to ensure reproducible slicing. The second bias is that the micro-dissection has to be performed without a complete histological staining, and thus without a clear demarcation of the area of interest. The direct consequence on the biological relevance of the dataset is the risk of not having the same ratio of epithelial and mesenchymal cells sampled. Along with this risk is the possibility that we did not remove the entire structure, leading to a potentially incomplete picture of the region in terms of the represented cell types. The third bias was that given the small quantity of RNA obtained by sample, we were forced to combine different samples of the same cohort, leading to the introduction of a supplementary source of heterogeneity.

Although there is no clear strain-dependent or age-dependent relationship between the B6-6, B6-12, B6-18, CD1-6, CD1-12, and CD1-18 samples, actors involved in the

maintenance of the stem cell niches (namely *Sox2* and *Fgf10*) are not differentially expressed. The relatively small list of genes which expression profile varies along with ageing might be attributed to the small quantities extracted given the size of the biological samples. The use of two normalization methods here helped us to address part of the variability, and to remain cautious with the differentially expressed genes found.

As stated above, working with entire incisors might dilute the information from the growth region, but it also allows a better reproducibility working on replicates. Lastly, it gives us access to the transcriptomic information from the transit-amplifying and the differentiation zones, which are successively found when following the growth direction of the incisor. This explains why more differentially expressed genes were retrieved from our second analysis, but can also constitute an explanation for the non-congruence of the differentially expressed gene lists between the two experiments. Overall, the approach working on entire incisors seems to be suitable to our biological question, and especially to the molecular understanding of the groove phenotype.

What is our top 20 genes of interest?

Several groups of genes stood out during our analyses. The first one is composed of factors involved in hair development. *Fgf7*, also known as keratinocyte growth factor, as well as *Krt7* and *Krt6a*, which are coding for structural proteins that are found in hair, skin and nails make up this group (Gu and Coulombe, 2007; Sandilands *et al.*, 2013). *Fgf7* is normally expressed just around the epithelial cervical loops (Bei and Maas, 1998). Because one of the age-related defects we highlighted is the growth of hair out of the incisor dental cavity, it would be interesting to address changes in cell fate in the ageing niche. Special attention was paid during the dissection to avoid the contamination of the dissected sample and we consider such contamination by tissues outside of the studied area unlikely. All three genes might be

implicated in the differentiation of hair from the upper incisor growth region. One last gene could be added to this group because of its action in cell fate commitment: *Gfi1* (Shroyer *et al.*, 2005). Further studies on the possible link between these differentially expressed genes likely to help specify the molecular network driving cell fate.

Two genes have been associated with various mineralization defects: *Mmp20* with *amelogenesis imperfecta*, and *Dspp* with *dentinogenesis imperfecta* (Sreenath *et al.*, 2003; Wright *et al.*, 2009). Both diseases consist in the accumulation of defective traits of the enamel and the dentin, and notably in their color. Changes in color and in the enamel mineralization rate might be similar to the dysplasias seen in mice from six months on. Another metalloprotease has been found differentially expressed: *Mmp25*. It has been mainly associated with the development and the closure of the secondary palate (Brown and Nazarali, 2010), and since the incisor growth region is not in direct contact with the secondary palate, this indicates an unexpected gene detection.

Wnt signaling pathway is an actor of tooth development (Liu *et al.*, 2008). As we said earlier, the mesenchyme in-between the cervical loops is competent to Wnt signaling pathway, which help regulating the development of the correct number of incisors (Fujimori *et al.*, 2010). Although epithelial do express some Wnt genes, it has been proven that the Wnt/ β -catenin signaling pathway is not directly regulating epithelial stem cells (Suomalainen and Thesleff, 2010). Recently, the role of this pathway in tissue renewal and regeneration has also been reviewed (Clevers *et al.*, 2014). *Sost* is a member of Wnt signaling pathway, as well as *Grem1*, *Sfrp4*, *Wisp2*, and *Wnt2b* (Xu *et al.*, 2000; Semenov *et al.*, 2005; Bovolenta *et al.*, 2008; Katoh and Katoh, 2009; Katoh, 2011). Interestingly, the list of differentially expressed genes encompasses one of the rare cases where the expression level is higher in older mice (*Wnt2b*).

Among the genes highlighted in the study are also several mediators of cell migration or proliferation. This is the case of *Hand2* (specific to mesenchymal cell proliferation), *Glipr2*, *Podn*, and *Cxcr4* (Murdoch, 2000; Xiong *et al.* 2009, 2; Huang *et al.*, 2013; Hutter *et al.*, 2013). *Hrh2*, *Ibsp* and *Spp1* can also be clustered in this category because of their involvement in epithelial cell morphogenesis, and in biomineral tissue development (Kobayashi *et al.*, 2000; Vaes *et al.*, 2006). Since the continuous growth is a very dynamic process that implies a tightly regulated balance between cell proliferation and migration, the information provided by those actors could shed some light on the ageing of these cellular processes.

Lastly, our interest has also been drawn to *Cyp26a1*, which is coding for an enzyme acting notably on the retinoic acid pathway (Tahayato *et al.*, 2003). Retinoic acid pathway has been documented to act on tooth development (Jones *et al.*, 2008). *Cyp26a1* expression is promoted in the grooved incisor group, and it would be interesting to characterize its role in the development of aplastic grooves.

Correlation between the presence of a groove and a strong immune response

With 135 genes involved in immune response being up-regulated in grooved incisor group compared to similar age mice with smooth incisors, the correlation between the immune response and the development of a groove in old mice is highly marked. It is impossible right now to decipher which one causes the other, but we could imagine that the absence of any enamel within the aplastic grooves facilitates infections.

Mammalian organisms can develop a two-phase immune response (Janeway *et al.*, 2001). The first step is called innate immune response and implicates mostly members of the NF- κ B pathway (Hatada *et al.*, 2000). In our gene list, we identified many chemokines, complement genes, metalloproteases, interleukins, and histo-incompatibility complex genes.

To a lesser extent, we also identified some actors of the adaptive immune response (mainly Toll-like receptors and interferons) (Iwasaki and Medzhitov, 2004). This orientates the type of inflammation to a process that would be caused by bacterial exposure.

Interestingly, when Robins and Rowlatt described age-related abnormalities in laboratory mice (1971), they noticed a great hair impaction in the gingival tissues, and hypothesized that the accumulation of hair from grooming may be causing cyst. In their model, the cysts would be the cause of the physical disruption of the incisor growth region, leading to the formation of enamel grooves. We tend to be more cautious, firstly because no exaggerated hair impaction was detected in the mouse colony we monitored. Our transcriptomic analyses confirm the existence of an immune response, but the histological analyses we performed when characterizing the upper incisor ageing did not reveal traces of inflammation or infiltration.

CONCLUDING REMARKS

We have provided here a frame to further investigate incisor stem cell niche ageing. By addressing the questions of the experimental design and by trying to overcome the biases we encounter from sample preparation to library generation, we have tackled one key process: cellular ageing. Genes become differentially expressed as the mice grow old, and important transcriptomic changes are associated with the occurrence of age-related defects, such as an important immune response and expression of genes involved in non-dental ectodermic appendages.

ACKNOWLEDGEMENTS

We are grateful to F. Chatonnet for computing a DESeq2 function for the IGFL use. We thank M. Sémon for insightful discussions about the classical analysis workflow. We also

would like to thank C. Rey, from the ProfileXpert platform (ViroScan 3D, www.viroscan3d.com, Lyon, France), for performing the LCM experiment, as well as B. Jost and M. Phillips from the IGBMC Microarray and Sequencing platform (member of *France Génomique* program).

- Anders, S., Pyl, P. T. and Huber, W.** (2014). HTSeq—A Python framework to work with high-throughput sequencing data. *bioRxiv*.
- Arana-Chavez, V. E. and Massa, L. F.** (2004). Odontoblasts: the cells forming and maintaining dentine. *Int. J. Biochem. Cell Biol.* **36**, 1367–1373.
- Bei, M. and Maas, R.** (1998). FGFs and BMP4 induce both Msx1-independent and Msx1-dependent signaling pathways in early tooth development. *Development* **125**, 4325.
- Bovolenta, P., Esteve, P., Ruiz, J. M., Cisneros, E. and Lopez-Rios, J.** (2008). Beyond Wnt inhibition: new functions of secreted Frizzled-related proteins in development and disease. *J. Cell Sci.* **121**, 737–746.
- Brown, G. D. and Nazarali, A. J.** (2010). Matrix metalloproteinase-25 has a functional role in mouse secondary palate development and is a downstream target of TGF- β 3. *BMC Dev. Biol.* **10**, 93.
- Clevers, H., Loh, K. M. and Nusse, R.** (2014). An integral program for tissue renewal and regeneration: Wnt signaling and stem cell control. *Science* **346**, 1248012.
- Eden, E., Navon, R., Steinfeld, I., Lipson, D. and Yakhini, Z.** (2009). GOrilla: a tool for discovery and visualization of enriched GO terms in ranked gene lists. *BMC Bioinformatics* **10**, 48.
- Fujimori, S., Novak, H., Weissenböck, M., Jussila, M., Gonçalves, A., Zeller, R., Galloway, J., Thesleff, I. and Hartmann, C.** (2010). Wnt/ β -catenin signaling in the dental mesenchyme regulates incisor development by regulating Bmp4. *Dev. Biol.* **348**, 97–106.
- Goecks, J., Nekrutenko, A., Taylor, J. and others** (2010). Galaxy: a comprehensive approach for supporting accessible, reproducible, and transparent computational research in the life sciences. *Genome Biol* **11**, R86.
- Gu, L.-H. and Coulombe, P. A.** (2007). Keratin expression provides novel insight into the morphogenesis and function of the companion layer in hair follicles. *J. Invest. Dermatol.* **127**, 1061–1073.
- Harada, H., Toyono, T., Toyoshima, K., Yamasaki, M., Itoh, N., Kato, S., Sekine, K. and Ohuchi, H.** (2002a). FGF10 maintains stem cell compartment in developing mouse incisors. *Development* **129**, 1533.
- Harada, H., Toyono, T., Toyoshima, K. and Ohuchi, H.** (2002b). FGF10 maintains stem cell population during mouse incisor development. *Connect. Tissue Res.* **43**, 201–204.
- Hatada, E. N., Krappmann, D. and Scheidereit, C.** (2000). NF- κ B and the innate immune response. *Curr. Opin. Immunol.* **12**, 52–58.
- Huang, S., Liu, F., Niu, Q., Li, Y., Liu, C., Zhang, L., Ni, D. and Pu, X.** (2013). GLIPR-2 overexpression in HK-2 cells promotes cell EMT and migration through ERK1/2 activation. *PLoS One* **8**, e58574.

- Hutter, R., Huang, L., Speidl, W. S., Giannarelli, C., Trubin, P., Bauriedel, G., Klotman, M. E., Fuster, V., Badimon, J. J. and Klotman, P. E.** (2013). Novel Small Leucine-Rich Repeat Protein Podocan Is a Negative Regulator of Migration and Proliferation of Smooth Muscle Cells, Modulates Neointima Formation, and Is Expressed in Human Atheroma. *Circulation* **128**, 2351–2363.
- Iwasaki, A. and Medzhitov, R.** (2004). Toll-like receptor control of the adaptive immune responses. *Nat. Immunol.* **5**, 987–995.
- Janeway, C. A., Travers, P., Walport, M. and Shlomchik, M. J.** (2001). Immunobiology.
- Jones, D. M., Fabian, B. and Kramer, B.** (2008). The effect of retinoic acid on mouse mandibular molar development in vitro, using alkaline phosphatase as a molecular indicator of differentiation. *SADJ J. South Afr. Dent. Assoc. Tydskr. Van Suid-Afr. Tandheelkd. Ver.* **63**, 276–278.
- Jussila, M., Juuri, E. and THEsLEFF, I.** (2013). Tooth morphogenesis and renewal. *Stem Cells Craniofacial Dev. Regen.* 109–134.
- Juuri, E., Isaksson, S., Jussila, M., Heikinheimo, K. and Thesleff, I.** (2013). Expression of the stem cell marker, SOX2, in ameloblastoma and dental epithelium. *Eur. J. Oral Sci.* **121**, 509–516.
- Katoh, M.** (2011). Network of WNT and other regulatory signaling cascades in pluripotent stem cells and cancer stem cells. *Curr. Pharm. Biotechnol.* **12**, 160–170.
- Katoh, M. and Katoh, M.** (2009). Transcriptional regulation of WNT2B based on the balance of Hedgehog, Notch, BMP and WNT signals. *Int. J. Oncol.* **34**, 1411.
- Klein, O. D., Lyons, D. B., Balooch, G., Marshall, G. W., Basson, M. A., Peterka, M., Boran, T., Peterkova, R. and Martin, G. R.** (2008). An FGF signaling loop sustains the generation of differentiated progeny from stem cells in mouse incisors. *Development* **135**, 377.
- Kobayashi, T., Tonai, S., Ishihara, Y., Koga, R., Okabe, S. and Watanabe, T.** (2000). Abnormal functional and morphological regulation of the gastric mucosa in histamine H2 receptor-deficient mice. *J. Clin. Invest.* **105**, 1741–1749.
- Langmead, B. and Salzberg, S. L.** (2012). Fast gapped-read alignment with Bowtie 2. *Nat. Methods* **9**, 357–359.
- Liu, F., Chu, E. Y., Watt, B., Zhang, Y., Gallant, N. M., Andl, T., Yang, S. H., Lu, M. M., Piccolo, S., Schmidt-Ullrich, R., et al.** (2008). Wnt/[beta]-catenin signaling directs multiple stages of tooth morphogenesis. *Dev. Biol.* **313**, 210–224.
- Love, M. I., Huber, W. and Anders, S.** (2014). Moderated estimation of fold change and dispersion for RNA-Seq data with DESeq2. *bioRxiv*.
- Murdoch, C.** (2000). CXCR4: chemokine receptor extraordinaire. *Immunol. Rev.* **177**, 175–184.
- Robins, M. W. and Rowlett, C.** (1971). Dental abnormalities in aged mice. *Gerontology* **17**, 261–272.

- Rossi, D. J., Bryder, D. and Weissman, I. L.** (2007). Hematopoietic stem cell aging: mechanism and consequence. *Exp. Gerontol.* **42**, 385–390.
- Sandilands, A., Smith, F. J. D., Lunny, D. P., Campbell, L. E., Davidson, K. M., MacCallum, S. F., Corden, L. D., Christie, L., Fleming, S., Lane, E. B., et al.** (2013). Generation and characterisation of keratin 7 (K7) knockout mice. *PLoS One* **8**, e64404.
- Seidel, K., Ahn, C. P., Lyons, D., Nee, A., Ting, K., Brownell, I., Cao, T., Carano, R. A. D., Curran, T., Schober, M., et al.** (2010). Hedgehog signaling regulates the generation of ameloblast progenitors in the continuously growing mouse incisor. *Dev. Camb. Engl.* **137**, 3753–3761.
- Semënov, M., Tamai, K. and He, X.** (2005). SOST is a ligand for LRP5/LRP6 and a Wnt signaling inhibitor. *J. Biol. Chem.* **280**, 26770–26775.
- Shroyer, N. F., Wallis, D., Venken, K. J. T., Bellen, H. J. and Zoghbi, H. Y.** (2005). Gfi1 functions downstream of Math1 to control intestinal secretory cell subtype allocation and differentiation. *Genes Dev.* **19**, 2412–2417.
- Sreenath, T., Thyagarajan, T., Hall, B., Longenecker, G., D’Souza, R., Hong, S., Wright, J. T., MacDougall, M., Sauk, J. and Kulkarni, A. B.** (2003). Dentin sialophosphoprotein knockout mouse teeth display widened predentin zone and develop defective dentin mineralization similar to human dentinogenesis imperfecta type III. *J. Biol. Chem.* **278**, 24874–24880.
- Suomalainen, M. and Thesleff, I.** (2010). Patterns of Wnt pathway activity in the mouse incisor indicate absence of Wnt/ β -catenin signaling in the epithelial stem cells. *Dev. Dyn.* **239**, 364–372.
- Tahayato, A., Dollé, P. and Petkovich, M.** (2003). *Cyp26C1* encodes a novel retinoic acid-metabolizing enzyme expressed in the hindbrain, inner ear, first branchial arch and tooth buds during murine development. *Gene Expr. Patterns* **3**, 449–454.
- Vaes, B. L., Ducy, P., Sijbers, A. M., Hendriks, J., van Someren, E. P., de Jong, N. G., van den Heuvel, E. R., Olijve, W., van Zoelen, E. J. and Decherig, K. J.** (2006). Microarray analysis on Runx2-deficient mouse embryos reveals novel Runx2 functions and target genes during intramembranous and endochondral bone formation. *Bone* **39**, 724–738.
- Wright, J. T., Hart, T. C., Hart, P. S., Simmons, D., Suggs, C., Daley, B., Simmer, J., Hu, J., Bartlett, J. D., Li, Y., et al.** (2009). Human and mouse enamel phenotypes resulting from mutation or altered expression of AMEL, ENAM, MMP20 and KLK4. *Cells Tissues Organs* **189**, 224–229.
- Xiong, W., He, F., Morikawa, Y., Yu, X., Zhang, Z., Lan, Y., Jiang, R., Cserjesi, P. and Chen, Y.** (2009). Hand2 is required in the epithelium for palatogenesis in mice. *Dev. Biol.* **330**, 131–141.
- Xu, L., Corcoran, R. B., Welsh, J. W., Pennica, D. and Levine, A. J.** (2000). WISP-1 is a Wnt-1-and β -catenin-responsive oncogene. *Genes Dev.* **14**, 585–595.

B.4 CONCLUSIONS

The interest for incisors in research is multifaceted. From an evolutionary point of view, these teeth are an indicator of the level of diversity displayed in this mammalian order, and attest to the acquisition of a complex morphology. Moreover, because of their continuous growth properties, incisors are models in cell biology and genetics.

The existing variability of rodent incisors is especially visible when looking at the color and the ornamentation of their vestibular side. From this statement, I investigated changes that are set at the scale of the animal lifetime by addressing the occurrence of age-related changes in the mouse upper incisors.

As the mouse grows older than six months, its upper incisors indeed start to display mineralization defects, as well as signs of stem cell niche disruption. Among the abnormal phenotypes seen in the mineralized tissues, the occurrence of a vestibular groove is observed the most frequently. The comparative monitoring of two mouse line (CD1 “swiss” and C57Bl/6N) showed that inbred mice display more severe phenotypes, their enamel groove often becoming completely aplastic.

From the very precise growth pattern of the rodent incisors, which originates from the presence of stem cell niches fueling the organ renewal throughout the lifespan of the animal, we can deduct that abnormalities are set within the growth region. Histological analyses showed that the stem cell niches can be directly disrupted, and the defects can be traced on serial sections.

Because stem cell ageing is the major concern for the homeostasis of numerous organs, and more globally for organisms, we are eager to understand its molecular determinants. In order to further investigate the plausible age-related changes in gene expression profiles, I have set the basis for molecular studies by making use of the powerful NGS technologies. Several biological functions appear down-regulated in ageing incisor, for example cell proliferation and migration, or mineralization process. On the contrary, innate immune response appears strongly promoted in the grooved incisors when compared to the smooth ones. Dental stem cells may not be the most commonly used model in cell biology, but their morphological and molecular disruption will greatly contribute to the understanding of stem cell ageing.

CONCLUSION & PERSPECTIVES

T

he study of the FGF-activated ERK-MAPK pathway reaffirmed the crucial role of the *Rsk* gene family in craniofacial, and especially in dental development. We showed that *Rsk2^{-Y}* mice only moderately recapitulate the human Coffin-Lowry syndrome. The comparison of their dental phenotype to the one of *Spry1^{-/-}*, *Spry2^{-/-}*, and *Spry4^{-/-}* mice allowed us to specify on the potential evolutionary role of the pathway during murine rodent evolution. The atavisms found in the mutant mice studied in the course of this project confirm the importance of the whole pathway and precise the role of some of its members. Indeed, the occurrence of supernumerary teeth in three of these mutants highlights that these genes could have played a role in the reduction of the dental formula during the transition from pre-muroid to muroid rodents. This reduction is likely to have remodeled the mesial part of the 1st molars as indicated by the numerous mesial rearrangements in the mutant mice. On the distal part of the 1st molars, only the Sprouty gene family could have been an actor of the evolutionary reduction of the posterocone cusps. Bringing Tg(KRT14-Spry4)#Krum mice to the picture, we conclude that delay in forming a proper cap-staged tooth germ impacts tooth mineralization, tooth proportions and cusp arrangement, highlighting the role of FGF signaling pathway in the correct timing of tooth developmental sequence.

Results found in the study of the ERK-MAPK pathway highlight what has been stated for decades: despite an extremely reduced and specialized dentition, mice are a good model to investigate evolutionary changes in the shape and tooth number determination. The FGF-activated ERK-MAPK pathway is not the 1st pathway that has been intensively studied from

human pathology to global tooth evolution: the work of the Eda pathway reached a similar extent (Grüneberg, 1966; Miller, 1978; Charles *et al.*, 2009; Sadier *et al.*, 2014).

Of course, the evolutionary role of the FGF-activated ERK-MAPK pathway could always be further specified using gain of function or conditional mutants, but the most interesting outcome of this research is linked with the development of new tools to study gene regulatory networks. Indeed, we entered an era of data computing in which we could and should link the great amount of tooth development actors worked on so far. All the phenotypic information scientists collected in the dental evo-devo field could only help us improve the drawing of these networks.

Working on Tg(KRT14-Spry4)#Krum specimens also addressed the question of the sequential formation of mouse molar cusps. This is a more fundamental work, but it could be applied to the variations of cusp pattern seen in humans (Scott and Turner, 2000) or even linked with abnormalities observed in patients. Our understanding of the phenomenon would be greatly improved by expanding research on the formation of enamel knots. To date, enamel knots are characterized by some specific gene expression patterns and by the non-proliferating state (Vaahtokari *et al.*, 1996; Jernvall *et al.*, 1998; Laurikkala *et al.*, 2003). Focusing on the cell biology level, we could set up lineage tracing experiment at the scale of tooth development in order to understand the specification of the primary enamel knot, and of the secondary enamel knots in forming a tooth. All the rodents do not display the same molar crown shape, and a comparative approach including rodents with various dental morphologies seems adequate to address this diversity.

The review of incisor diversity in rodent has brought out the potential use of these teeth in the study of shape evolution, as well as unresolved acquisition of a grooved enamel surface and a differential coloration of the enamel layer. Interestingly, the grooved enamel surface is

found in WT mice, but only in specimens aged of at least six months. It appears that some age-related defects appear in both ageing mice and ageing sand rats. The exhaustive list of these age-related defects set in the specimens studied encompasses an increased number of enamel mineralization defects, the development of enamel grooves (one to two, aplastic or not), the growth of ectopic hair from the tooth socket, an increased occurrence of *dens in dentes* and odontomas, as well as the development of dentin grooves. The enamel grooves are the most frequent defect, being noticed in 50% of the monitored mice. The realization of an *in vivo* monitoring of mouse upper incisors ageing over approximately one year and a half not only provided an accurate list of the defects, but it also specified their timing of occurrence from six months on. Monitoring the morphometrical properties of the incisors also showed a constant increase in the mesio-distal length of the upper incisors. A further insight into the histology of the growth region in the ageing specimens revealed the occurrence of abnormal folding and proliferation events that affect the specific organization of the incisor stem cell niches. In an attempt to address the global molecular disruption of the ageing stem cell niches, we unraveled the differential expression of some genes in our region of interest, including markers of hair development, regulators of cell proliferation, differentiation and migration, as well as members of the Wnt signaling pathway. The comparison of gene expression profiles between smooth incisors and grooved incisors of the same age revealed an important immune response in the case of grooved incisors.

In performing this research, we provided a starting point for the study of the impact of ageing in the dental stem cell niches. The ultimate goal of every scientist working on the ageing of a specific stem cell niche is to be able to fully characterize and eventually counteract those mechanisms regardless of the type of niche. We should firstly focus on this very same model, and investigate the specific role of our genes of interest. The joint study of these gene expression patterns and of genetically engineered animals will help us understand

the extent of the age-related modifications. We will eventually aim at setting an *in vitro* model of dental stem cell ageing from all the *in vivo* data collected.

The question of cell fate could be addressed in trying to characterize the hair growing out of the incisor socket. Due to the difficulty of spotting this rare phenotype on ageing mice, we could start with the investigation on mutant murine lines displaying ectopic hair growth from their tooth sockets, before going back to the ageing model. Given the resemblance between the incisor stem cell niches and the hair bulge, we are confident that investigations on the differentially expressed genes belonging to the Wnt pathway will also help us understand how the fate of dental stem cells can be changed in the course of ageing.

Lastly, in order to address the link between the occurrence of aplastic enamel groove and the large innate immune response, we plan on scrutinizing the upper incisor phenotype of immunodeficient mouse models. The current availability of several lines deficient for various actors of this type of immune response will help us understanding the causality of the phenomenon and the possible predominance of some actors of the NF- κ B immune response. An interesting complementary approach would consist in performing a new RNA-seq experiment with 18-month-old mice displaying non-aplastic enamel groove, and to compare the extent of the immune response.

By addressing two levels of the rodent dentition dynamics, I have worked on classic dental evo-devo, but I have also stated the potential of the mouse incisors to become a new model of stem cell ageing. My contributions hopefully proved that we still have a lot to learn from the mouse, and that the golden age of tooth evo-devo is not over yet.

REFERENCES

- Åberg, T., Wang, X. P., Kim, J. H., Yamashiro, T., Bei, M., Rice, R., Ryoo, H. M. and Thesleff, I.** (2004). Runx2 mediates FGF signaling from epithelium to mesenchyme during tooth morphogenesis. *Dev. Biol.* **270**, 76–93.
- Ahn, Y., Sanderson, B. W., Klein, O. D. and Krumlauf, R.** (2010). Inhibition of Wnt signaling by Wise (Sostdc1) and negative feedback from Shh controls tooth number and patterning. *Development* **137**, 3221.
- Amling, M., Neff, L., Priemel, M., Schilling, A. F., Rueger, J. M. and Baron, R.** (2000). Progressive increase in bone mass and development of odontomas in aging osteopetrotic c-src-deficient mice. *Bone* **27**, 603–610.
- Anders, S., Pyl, P. T. and Huber, W.** (2014). HTSeq—A Python framework to work with high-throughput sequencing data. *bioRxiv*.
- Anderson, M. A. and Miller, B. T.** (2011). Early Iron Deposition in Teeth of the Streamside Salamander, *Ambystoma barbouri*. *J. Herpetol.* **45**, 336–338.
- Aouadi, M., Binetruy, B., Caron, L., Le Marchand-Brustel, Y. and Bost, F.** (2006). Role of MAPKs in development and differentiation: lessons from knockout mice. *Biochimie* **88**, 1091–1098.
- Arana-Chavez, V. E. and Massa, L. F.** (2004). Odontoblasts: the cells forming and maintaining dentine. *Int. J. Biochem. Cell Biol.* **36**, 1367–1373.
- Bartke, A. and Brown-Borg, H.** (2004). Life extension in the dwarf mouse. *Curr. Top. Dev. Biol.* **63**, 189–225.
- Begue-Kirn, C., Smith, A. J., Ruch, J. V., Wozney, J. M., Purchio, A., Hartmann, D. and Lesot, H.** (1992). Effects of dentin proteins, transforming growth factor beta 1 (TGF beta 1) and bone morphogenetic protein 2 (BMP2) on the differentiation of odontoblast in vitro. *Int. J. Dev. Biol.* **36**, 491.
- Bei, M. and Maas, R.** (1998). FGFs and BMP4 induce both Msx1-independent and Msx1-dependent signaling pathways in early tooth development. *Development* **125**, 4325.
- Bei, M.** (2009). Molecular genetics of tooth development. *Curr. Opin. Genet. Dev.* **19**, 504–510.
- Bittles, A. H. and Neel, J. V.** (1994). The costs of human inbreeding and their implications for variations at the DNA level. *Nat. Genet.* **8**, 117–121.
- Bland Sutton, J.** (1884). Comparative dental pathology (1). *Trans. Odontol. Soc. G. B.* **16**, 88–145.
- Bovolenta, P., Esteve, P., Ruiz, J. M., Cisneros, E. and Lopez-Rios, J.** (2008). Beyond Wnt inhibition: new functions of secreted Frizzled-related proteins in development and disease. *J. Cell Sci.* **121**, 737–746.

- Brown, G. D. and Nazarali, A. J.** (2010). Matrix metalloproteinase-25 has a functional role in mouse secondary palate development and is a downstream target of TGF- β 3. *BMC Dev. Biol.* **10**, 93.
- Cam, Y., Neumann, M. R., Oliver, L., Raulais, D., Janet, T. and Ruch, J. V.** (1992). Immunolocalization of acidic and basic fibroblast growth factors during mouse odontogenesis. *Int. J. Dev. Biol.* **36**, 381–381.
- Campos, L. S., Leone, D. P., Relvas, J. B., Brakebusch, C., Fässler, R., Suter, U. and others** (2004). β 1 integrins activate a MAPK signalling pathway in neural stem cells that contributes to their maintenance. *Development* **131**, 3433–3444.
- Carroll, S. B.** (2008). Evo-devo and an expanding evolutionary synthesis: a genetic theory of morphological evolution. *Cell* **134**, 25–36.
- Catón, J. and Tucker, A. S.** (2009). Current knowledge of tooth development: patterning and mineralization of the murine dentition. *J. Anat.* **214**, 502–515.
- Chakkalakal, J. V., Jones, K. M., Basson, M. A. and Brack, A. S.** (2012). The aged niche disrupts muscle stem cell quiescence. *Nature*.
- Chang, J. Y. F., Wang, C., Liu, J., Huang, Y., Jin, C., Yang, C., Hai, B., Liu, F., D'Souza, R. N., McKeehan, W. L., et al.** (2013). Fibroblast growth factor signaling is essential for self-renewal of dental epithelial stem cells. *J. Biol. Chem.* **288**, 28952–28961.
- Charles, C., Pantalacci, S., Tafforeau, P., Headon, D., Laudet, V. and Viriot, L.** (2009a). Distinct impacts of Eda and Edar loss of function on the mouse dentition. *PLoS One* **4**, e4985.
- Charles, C., Lazzari, V., Tafforeau, P., Schimmang, T., Tekin, M., Klein, O. and Viriot, L.** (2009b). Modulation of Fgf3 dosage in mouse and men mirrors evolution of mammalian dentition. *Proc. Natl. Acad. Sci.* **106**, 22364.
- Charles, C., Hovorakova, M., Ahn, Y., Lyons, D. B., Marangoni, P., Churava, S., Biels, B., Jheon, A., Lesot, H., Balooch, G., et al.** (2011). Regulation of tooth number by fine-tuning levels of receptor-tyrosine kinase signaling. *Development* **138**, 4063 – 4073.
- Chen, M., Choi, Y., Voytas, D. F. and Rodermeier, S.** (2000). Mutations in the Arabidopsis VAR2 locus cause leaf variegation due to the loss of a chloroplast FtsH protease. *Plant J.* **22**, 303–313.
- Chihara, T., Kato, K., Taniguchi, M., Ng, J. and Hayashi, S.** (2003). Rac promotes epithelial cell rearrangement during tracheal tubulogenesis in *Drosophila*. *Development* **130**, 1419.

- Clemen, G.** (1988). Competence and reactions of early-larval and late-larval dental laminae in original and not-original dental systems of (1) *Ambystoma mexicanum* shaw. *Arch. Biol.* **99**, 307–324.
- Clevers, H., Loh, K. M. and Nusse, R.** (2014). An integral program for tissue renewal and regeneration: Wnt signaling and stem cell control. *Science* **346**, 1248012.
- Cobourne, M. T. and Sharpe, P. T.** (2003). Tooth and jaw: molecular mechanisms of patterning in the first branchial arch. *Arch. Oral Biol.* **48**, 1–14.
- Coin, R., Lesot, H., Vonesch, J. L., Haikel, Y. and Ruch, J. V.** (1999). Aspects of cell proliferation kinetics of the inner dental epithelium during mouse molar and incisor morphogenesis: a reappraisal of the role of the enamel knot area. *Int. J. Dev. Biol.* **43**, 261–268.
- Corson, L. B., Yamanaka, Y., Lai, K.-M. V. and Rossant, J.** (2003). Spatial and temporal patterns of ERK signaling during mouse embryogenesis. *Development* **130**, 4527–4537.
- Cuvier, G.** (1812). *Recherches sur les ossements fossiles de quadrupèdes.*
- Dawson, K. H., Gruss, J. S. and Myall, R. W. .** (1997). Congenital bony syngnathia: a proposed classification. *Cleft Palate. Craniofac. J.* **34**, 141–146.
- Delaunoy, J.-P., Abidi, F., Zeniou, M., Jacquot, S., Merienne, K., Pannetier, S., Schmitt, M., Schwartz, C. E. and Hanauer, A.** (2001). Mutations in the X-linked RSK2 gene (RPS6KA3) in patients with Coffin-Lowry syndrome. *Hum. Mutat.* **17**, 103–116.
- De Maximy, A. A., Nakatake, Y., Moncada, S., Itoh, N., Thiery, J. P. and Bellusci, S.** (1999). Cloning and expression pattern of a mouse homologue of *Drosophila* sprouty in the mouse embryo. *Mech. Dev.* **81**, 213–216.
- Diez-Roux, G., Banfi, S., Sultan, M., Geffers, L., Anand, S., Rozado, D., Magen, A., Canidio, E., Pagani, M., Peluso, I., et al.** (2011). A high-resolution anatomical atlas of the transcriptome in the mouse embryo. *PLoS Biol.* **9**, e1000582.
- Downward, J.** (2003). Targeting RAS signalling pathways in cancer therapy. *Nat. Rev. Cancer* **3**, 11–22.
- Duboule, D. and Dollé, P.** (1989). The structural and functional organization of the murine HOX gene family resembles that of *Drosophila* homeotic genes. *EMBO J.* **8**, 1497–1505.
- Dumont, M., Tütken, T., Kostka, A., Duarte, M. J. and Borodin, S.** (2014). Structural and functional characterization of enamel pigmentation in shrews. *J. Struct. Biol.* **186**, 38–48.

- Eden, E., Navon, R., Steinfeld, I., Lipson, D. and Yakhini, Z.** (2009). GOrilla: a tool for discovery and visualization of enriched GO terms in ranked gene lists. *BMC Bioinformatics* **10**, 48.
- Fabre, P.-H., Hautier, L., Dimitrov, D. and Douzery, E. J.** (2012). A glimpse on the pattern of rodent diversification: a phylogenetic approach. *BMC Evol. Biol.* **12**, 88.
- Fallahi, H. R., Naeini, M., Mahmoudi, M. and Javaherforoosh, F.** (2010). Congenital zygomatico-maxillo-mandibular fusion: a brief case report and review of literature. *Int. J. Oral Maxillofac. Surg.* **39**, 930–933.
- Ferrara, N.** (2005). The role of VEGF in the regulation of physiological and pathological angiogenesis. In *Mechanisms of angiogenesis*, pp. 209–231. Springer.
- Finkel, T., Serrano, M. and Blasco, M. A.** (2007). The common biology of cancer and ageing. *Nature* **448**, 767–774.
- Fox, R. R. and Crary, D. D.** (1971). Mandibular Prognathism in the Rabbit: Genetic studies Genetic studies. *J. Hered.* **62**, 23–27.
- Frödin, M. and Gammeltoft, S.** (1999). Role and regulation of 90 kDa ribosomal S6 kinase (RSK) in signal transduction. *Mol. Cell. Endocrinol.* **151**, 65–77.
- Fujimori, S., Novak, H., Weissenböck, M., Jussila, M., Gonçalves, A., Zeller, R., Galloway, J., Thesleff, I. and Hartmann, C.** (2010). Wnt/ β -catenin signaling in the dental mesenchyme regulates incisor development by regulating Bmp4. *Dev. Biol.* **348**, 97–106.
- Ge, C., Xiao, G., Jiang, D. and Franceschi, R. T.** (2007). Critical role of the extracellular signal-regulated kinase–MAPK pathway in osteoblast differentiation and skeletal development. *J. Cell Biol.* **176**, 709–718.
- Goecks, J., Nekrutenko, A., Taylor, J. and others** (2010). Galaxy: a comprehensive approach for supporting accessible, reproducible, and transparent computational research in the life sciences. *Genome Biol* **11**, R86.
- Goldberg, M., Septier, D., Bourd, K., Hall, R., Jeanny, J.-C., Jonet, L., Colin, S., Tager, F., Chaussain-Miller, C., Garabedian, M., et al.** (2002). The dentino-enamel junction revisited. *Connect. Tissue Res.* **43**, 482–489.
- Goodwin, A. F., Oberoi, S., Landan, M., Charles, C., Groth, J., Martinez, A., Fairley, C., Weiss, L. A., Tidyman, W. E., Klein, O. D., et al.** (2013). Craniofacial and dental development in cardio-facio-cutaneous syndrome: the importance of Ras signaling homeostasis. *Clin. Genet.* **83**, 539–544.
- Gregory, W. K.** (1934). Polyisomerism and Anisomerism in Cranial and Dental Evolution among Vertebrates. *Proc. Natl. Acad. Sci. U. S. A.* **20**, 1–9.

- Grüneberg, H.** (1966). The molars of the tabby mouse, and a test of the “single-active X-chromosome” hypothesis. *J. Embryol. Exp. Morphol.* **15**, 223–244.
- Gu, L.-H. and Coulombe, P. A.** (2007). Keratin expression provides novel insight into the morphogenesis and function of the companion layer in hair follicles. *J. Invest. Dermatol.* **127**, 1061–1073.
- Hacohen, N., Kramer, S., Sutherland, D., Hiromi, Y. and Krasnow, M. A.** (1998). sprouty encodes a novel antagonist of FGF signaling that patterns apical branching of the Drosophila airways. *Cell* **92**, 253–263.
- Hanafusa, H., Torii, S., Yasunaga, T. and Nishida, E.** (2002). Sprouty1 and Sprouty2 provide a control mechanism for the Ras/MAPK signalling pathway. *Nat. Cell Biol.* **4**, 850–858.
- Hanauer, A. and Young, I. D.** (2002). Coffin-Lowry syndrome: clinical and molecular features. *J. Med. Genet.* **39**, 705–713.
- Harada, H., Kettunen, P., Jung, H. S., Mustonen, T., Wang, Y. A. and Thesleff, I.** (1999). Localization of putative stem cells in dental epithelium and their association with Notch and FGF signaling. *J. Cell Biol.* **147**, 105.
- Harada, H., Toyono, T., Toyoshima, K., Yamasaki, M., Itoh, N., Kato, S., Sekine, K. and Ohuchi, H.** (2002a). FGF10 maintains stem cell compartment in developing mouse incisors. *Development* **129**, 1533.
- Harada, H., Toyono, T., Toyoshima, K. and Ohuchi, H.** (2002b). FGF10 maintains stem cell population during mouse incisor development. *Connect. Tissue Res.* **43**, 201–204.
- Harada, H. and Ohshima, H.** (2004). New perspectives on tooth development and the dental stem cell niche. *Arch. Histol. Cytol.* **67**, 1–11.
- Hardcastle, Z., Mo, R., Hui, C. and Sharpe, P. T.** (1998). The Shh signalling pathway in tooth development: defects in Gli2 and Gli3 mutants. *Development* **125**, 2803.
- Harjunmaa, E., Seidel, K., Häkkinen, T., Renvoisé, E., Corfe, I. J., Kallonen, A., Zhang, Z.-Q., Evans, A. R., Mikkola, M. L., Salazar-Ciudad, I., et al.** (2014). Replaying evolutionary transitions from the dental fossil record. *Nature* **512**, 44–48.
- Hatada, E. N., Krappmann, D. and Scheidereit, C.** (2000). NF- κ B and the innate immune response. *Curr. Opin. Immunol.* **12**, 52–58.
- Hedrich, H.** (2004). *The laboratory mouse*. Academic Press.
- Herrera-Soto, J. A., Santiago-Cornier, A., Segal, L. S., Ramirez, N. and Tamai, J.** (2007). The musculoskeletal manifestations of the Coffin-Lowry syndrome. *J. Pediatr. Orthop.* **27**, 85–89.

- Hershkovitz, P.** (1980). *Evolution of Neotropical Cricetine Rodents (Muridae): With Special Reference to the Phyllotine Group*. University Microfilms International.
- Ho, A. D., Wagner, W. and Mahlknecht, U.** (2005). Stem cells and ageing. *EMBO Rep.* **6**, S35–S38.
- Huang, S., Liu, F., Niu, Q., Li, Y., Liu, C., Zhang, L., Ni, D. and Pu, X.** (2013). GLIPR-2 overexpression in HK-2 cells promotes cell EMT and migration through ERK1/2 activation. *PLoS One* **8**, e58574.
- Humphreys, E. R., Robins, M. W. and Stones, V. A.** (1985). Age-related and 224Ra-induced abnormalities in the teeth of male mice. *Arch. Oral Biol.* **30**, 55–64.
- Hunter, A. G.** (2002). Coffin-Lowry syndrome: A 20-year follow-up and review of long-term outcomes. *Am. J. Med. Genet.* **111**, 345–355.
- Hutter, R., Huang, L., Speidl, W. S., Giannarelli, C., Trubin, P., Bauriedel, G., Klotman, M. E., Fuster, V., Badimon, J. J. and Klotman, P. E.** (2013). Novel Small Leucine-Rich Repeat Protein Podocan Is a Negative Regulator of Migration and Proliferation of Smooth Muscle Cells, Modulates Neointima Formation, and Is Expressed in Human Atheroma. *Circulation* **128**, 2351–2363.
- Hwang, W. S. S. and Tonna, E. A.** (1965). Autoradiographic analysis of labeling indices and migration rates of cellular component of mouse incisors using tritiated thymidine (H3TDR). *J. Dent. Res.* **44**, 42–53.
- Inman, K. E., Purcell, P., Kume, T. and Trainor, P. A.** (2013). Interaction between Foxc1 and Fgf8 during Mammalian Jaw Patterning and in the Pathogenesis of Syngnathia. *PLoS Genet.* **9**, e1003949.
- Iwasaki, A. and Medzhitov, R.** (2004). Toll-like receptor control of the adaptive immune responses. *Nat. Immunol.* **5**, 987–995.
- Jacquot, S., Merienne, K., De Cesare, D., Pannetier, S., Mandel, J.-L., Sassone-Corsi, P. and Hanauer, A.** (1998). Mutation analysis of the RSK2 gene in Coffin-Lowry patients: extensive allelic heterogeneity and a high rate of de novo mutations. *Am. J. Hum. Genet.* **63**, 1631–1640.
- Janeway, C. A., Travers, P., Walport, M. and Shlomchik, M. J.** (2001). Immunobiology.
- Jernvall, J., Kettunen, P., Karavanova, I., Martin, L. B. and Thesleff, I.** (1994). Evidence for the role of the enamel knot as a control center in mammalian tooth cusp formation: non-dividing cells express growth stimulating Fgf-4 gene. *Int. J. Dev. Biol.* **38**, 463–463.
- Jernvall, J., Aberg, T., Kettunen, P., Keranen, S. and Thesleff, I.** (1998). The life history of an embryonic signaling center: BMP-4 induces p21 and is associated with apoptosis in the mouse tooth enamel knot. *Development* **125**, 161.

- Jernvall, J. and Thesleff, I.** (2000). Reiterative signaling and patterning during mammalian tooth morphogenesis. *Mech. Dev.* **92**, 19–29.
- Jernvall, J. and Thesleff, I.** (2012). Tooth shape formation and tooth renewal: evolving with the same signals. *Development* **139**, 3487–3497.
- Jheon, A. H., Li, C. Y., Wen, T., Michon, F. and Klein, O. D.** (2011). Expression of MicroRNAs in the Stem Cell Niche of the Adult Mouse Incisor. *PLoS One* **6**, e24536.
- Jones, D. M., Fabian, B. and Kramer, B.** (2008). The effect of retinoic acid on mouse mandibular molar development in vitro, using alkaline phosphatase as a molecular indicator of differentiation. *SADJ J. South Afr. Dent. Assoc. Tydskr. Van Suid-Afr. Tandheelkd. Ver.* **63**, 276–278.
- Jussila, M., Juuri, E. and Thesleff, I.** (2013). Tooth morphogenesis and renewal. *Stem Cells Craniofacial Dev. Regen.* 109–134.
- Juuri, E., Saito, K., Ahtiainen, L., Seidel, K., Tummers, M., Hochedlinger, K., Klein, O. D., Thesleff, I. and Michon, F.** (2012). *Sox2*⁺ Stem Cells Contribute to All Epithelial Lineages of the Tooth via *Sfrp5*⁺ Progenitors. *Dev. Cell* **23**, 317–328.
- Juuri, E., Isaksson, S., Jussila, M., Heikinheimo, K. and Thesleff, I.** (2013). Expression of the stem cell marker, SOX2, in ameloblastoma and dental epithelium. *Eur. J. Oral Sci.* **121**, 509–516.
- Kangas, A. T., Evans, A. R., Thesleff, I. and Jernvall, J.** (2004). Nonindependence of mammalian dental characters. *Nature* **432**, 211–214.
- Katoh, M. and Katoh, M.** (2009). Transcriptional regulation of WNT2B based on the balance of Hedgehog, Notch, BMP and WNT signals. *Int. J. Oncol.* **34**, 1411.
- Katoh, M.** (2011). Network of WNT and other regulatory signaling cascades in pluripotent stem cells and cancer stem cells. *Curr. Pharm. Biotechnol.* **12**, 160–170.
- Karavanova, I., Vainio, S. and Thesleff, I.** (1992). Transient and recurrent expression of the Egr-1 gene in epithelial and mesenchymal cells during tooth morphogenesis suggests involvement in tissue interactions and in determination of cell fate. *Mech. Dev.* **39**, 41–50.
- Kavanagh, K. D., Evans, A. R. and Jernvall, J.** (2007). Predicting evolutionary patterns of mammalian teeth from development. *Nature* **449**, 427–432.
- Kettunen, P. and Thesleff, I.** (1998). Expression and function of FGFs-4,-8, and-9 suggest functional redundancy and repetitive use as epithelial signals during tooth morphogenesis. *Dev. Dyn.* **211**, 256–268.
- Kettunen, P., Laurikkala, J., Itäranta, P., Vainio, S., Itoh, N. and Thesleff, I.** (2000). Associations of FGF-3 and FGF-10 with signaling networks regulating tooth morphogenesis. *Dev. Dyn.* **219**, 322–332.

- Klein, O. D., Minowada, G., Peterkova, R., Kangas, A., Yu, B. D., Lesot, H., Peterka, M., Jernvall, J. and Martin, G. R.** (2006). Sprouty genes control diastema tooth development via bidirectional antagonism of epithelial-mesenchymal FGF signaling. *Dev. Cell* **11**, 181–190.
- Klein, O. D., Lyons, D. B., Balooch, G., Marshall, G. W., Basson, M. A., Peterka, M., Boran, T., Peterkova, R. and Martin, G. R.** (2008). An FGF signaling loop sustains the generation of differentiated progeny from stem cells in mouse incisors. *Development* **135**, 377.
- Kim, H. J. and Bar-Sagi, D.** (2004). Modulation of signalling by Sprouty: a developing story. *Nat. Rev. Mol. Cell Biol.* **5**, 441–450.
- Kimura, Y., Jacobs, L. L. and Flynn, L. J.** (2013). Lineage-Specific Responses of Tooth Shape in Murine Rodents (Murinae, Rodentia) to Late Miocene Dietary Change in the Siwaliks of Pakistan. *PLoS ONE* **8**, e76070.
- Kobayashi, T., Tonai, S., Ishihara, Y., Koga, R., Okabe, S. and Watanabe, T.** (2000). Abnormal functional and morphological regulation of the gastric mucosa in histamine H2 receptor-deficient mice. *J. Clin. Invest.* **105**, 1741–1749.
- Kopan, R. and Ilagan, M. X. G.** (2009). The canonical Notch signaling pathway: unfolding the activation mechanism. *Cell* **137**, 216–233.
- Kraatz, B. P., Badamgarav, D. and Bibi, F.** (2009). Gomphos ellae, a new mimotomid from the Middle Eocene of Mongolia and its implications for the origin of Lagomorpha. *J. Vertebr. Paleontol.* **29**, 576–583.
- Kuhn, H. G., Dickinson-Anson, H. and Gage, F. H.** (1996). Neurogenesis in the dentate gyrus of the adult rat: age-related decrease of neuronal progenitor proliferation. *J. Neurosci.* **16**, 2027–2033.
- Lagronova-Churava, S., Spoutil, F., Vojtechova, S., Lesot, H., Peterká, M., Klein, O. D. and Peterková, R.** (2013). The Dynamics of Supernumerary Tooth Development Are Differentially Regulated by Sprouty Genes. *J. Exp. Zool. B Mol. Dev. Evol.*
- Langmead, B. and Salzberg, S. L.** (2012). Fast gapped-read alignment with Bowtie 2. *Nat. Methods* **9**, 357–359.
- Laugel-Haushalter, V., Paschaki, M., Marangoni, P., Pilgram, C., Langer, A., Kuntz, T., Demassue, J., Morkmued, S., Choquet, P., Constantinesco, A., et al.** (2014). RSK2 Is a Modulator of Craniofacial Development. *PloS One* **9**, e84343.
- Laurikkala, J., Kassai, Y., Pakkasjärvi, L., Thesleff, I. and Itoh, N.** (2003). Identification of a secreted BMP antagonist, ectodin, integrating BMP, FGF, and SHH signals from the tooth enamel knot. *Dev. Biol.* **264**, 91–105.

- Li, C.-Y., Cha, W., Luder, H.-U., Charles, R.-P., McMahon, M., Mitsiadis, T. A. and Klein, O. D.** (2012). E-cadherin regulates the behavior and fate of epithelial stem cells and their progeny in the mouse incisor. *Dev. Biol.* **366**, 357–366.
- Li, C.-Y., Prochazka, J., Goodwin, A. F. and Klein, O. D.** (2014). Fibroblast growth factor signaling in mammalian tooth development. *Odontol. Soc. Nippon Dent. Univ.* **102**, 1–13.
- Li, Y.-X., Yun-Xiang, Z. and Xiang-Xu, X.** (2012). The composition of three mammal faunas and environmental evolution in the last glacial maximum, Guanzhong area, Shaanxi Province, China. *Quat. Int.* **248**, 86–91.
- Lin, G. H.** (2010). Morphological adaptations of digging apparatus and population genetics of the subterranean rodent *Myospalax cansus*.
- Liu, F., Chu, E. Y., Watt, B., Zhang, Y., Gallant, N. M., Andl, T., Yang, S. H., Lu, M. M., Piccolo, S., Schmidt-Ullrich, R., et al.** (2008). Wnt/ β -catenin signaling directs multiple stages of tooth morphogenesis. *Dev. Biol.* **313**, 210–224.
- Liu, L. and Rando, T. A.** (2011). Manifestations and mechanisms of stem cell aging. *J. Cell Biol.* **193**, 257–266.
- Love, M. I., Huber, W. and Anders, S.** (2014). Moderated estimation of fold change and dispersion for RNA-Seq data with DESeq2. *bioRxiv*.
- Luckett, W. P.** (1985). Superordinal and intraordinal affinities of rodents: developmental evidence from the dentition and placentation. In *Evolutionary relationships among rodents*, pp. 227–276. Springer.
- Luo, Z.-X., Kielan-Jaworowska, Z. and Cifelli, R. L.** (2004). Evolution of dental replacement in mammals. *Bull. Carnegie Mus. Nat. Hist.* 159–175.
- Luo, J., Solimini, N. L. and Elledge, S. J.** (2009). Principles of cancer therapy: oncogene and non-oncogene addiction. *Cell* **136**, 823–837.
- Maas, R. and Bei, M.** (1997). The genetic control of early tooth development. *Crit. Rev. Oral Biol. Med.* **8**, 4.
- Mason, J. M., Morrison, D. J., Albert Basson, M. and Licht, J. D.** (2006). Sprouty proteins: multifaceted negative-feedback regulators of receptor tyrosine kinase signaling. *Trends Cell Biol.* **16**, 45–54.
- Massague, J.** (2003). Integration of Smad and MAPK pathways: a link and a linker revisited. *Genes Dev.* **17**, 2993–2997.
- McKenna, M. C.** (1975). Toward a phylogenetic classification of the Mammalia. In *Phylogeny of the Primates*, pp. 21–46. Springer.

- McKenna, M. C. and Bell, S. K.** (1997). *Classification of mammals above the species level*. Columbia University Press.
- Meng, J., Bowen, G. J., Jie, Y., Koch, P. L., Ting, S., Qian, L. and Jin, X.** (2004). Gomphos elkema (Glires, Mammalia) from the Erlian Basin: Evidence for the Early Tertiary Bumbanian Land Mammal Age in Nei-Mongol, China. *Am. Mus. Novit.* 1–24.
- Michon, F., Tummers, M., Kyyrönen, M., Frilander, M. J. and Thesleff, I.** (2010). Tooth morphogenesis and ameloblast differentiation are regulated by micro-RNAs. *Dev. Biol.* **340**, 355–368.
- Miller, W. A.** (1978). The dentitions of tabby and crinkled mice. *Dev. Funct. Evol. Teeth Butl. PM Joysey KA Ed. Lond. Acad. Press* 99–109.
- Miller, R. A., Harper, J. M., Dysko, R. C., Durkee, S. J. and Austad, S. N.** (2002). Longer life spans and delayed maturation in wild-derived mice. *Exp. Biol. Med. Maywood NJ* **227**, 500–508.
- Mitsiadis, T. A., Regaudiat, L. and Gridley, T.** (2005). Role of the Notch signalling pathway in tooth morphogenesis. *Arch. Oral Biol.* **50**, 137–140.
- Moon, B.-S., Jeong, W.-J., Park, J., Kim, T. I., Choi, K.-Y. and others** (2014). Role of Oncogenic K-Ras in Cancer Stem Cell Activation by Aberrant Wnt/ β -Catenin Signaling. *J. Natl. Cancer Inst.* **106**, djt373.
- Motta, P. J.** (1987). A quantitative analysis of ferric iron in butterflyfish teeth (Chaetodontidae, Perciformes) and the relationship to feeding ecology. *Can. J. Zool.* **65**, 106–112.
- Muller, H. J.** (1930). Types of visible variations induced by X-rays in *Drosophila*. *J. Genet.* **22**, 299–334.
- Müller, G. B.** (2007). Evo–devo: extending the evolutionary synthesis. *Nat. Rev. Genet.* **8**, 943–949.
- Murdoch, C.** (2000). CXCR4: chemokine receptor extraordinaire. *Immunol. Rev.* **177**, 175–184.
- Nanci, A.** (2007). *Ten Cate's Oral Histology-Pageburst on VitalSource: Development, Structure, and Function*. Elsevier Health Sciences.
- Naveau, A., Seidel, K. and Klein, O. D.** (2014). Tooth, hair and claw: Comparing epithelial stem cell niches of ectodermal appendages. *Exp. Cell Res.*
- Neubüser, A., Peters, H., Balling, R. and Martin, G. R.** (1997). Antagonistic interactions between FGF and BMP signaling pathways: a mechanism for positioning the sites of tooth formation. *Cell* **90**, 247–255.

- Nie, X., Luukko, K. and Kettunen, P.** (2006). FGF signalling in craniofacial development and developmental disorders. *Oral Dis.* **12**, 102–111.
- Nishimura, E. K., Granter, S. R. and Fisher, D. E.** (2005). Mechanisms of hair graying: incomplete melanocyte stem cell maintenance in the niche. *Science* **307**, 720–724.
- Nowak, R. M.** (1999). *Walker's Mammals of the World*. JHU Press.
- Ohazama, A., Haycraft, C. J., Seppala, M., Blackburn, J., Ghafoor, S., Cobourne, M., Martinelli, D. C., Fan, C.-M., Peterkova, R. and Lesot, H.** (2009). Primary cilia regulate Shh activity in the control of molar tooth number. *Development* **136**, 897–903.
- Ohazama, A., Blackburn, J., Porntaveetus, T., Ota, M. S., Choi, H. Y., Johnson, E. B., Myers, P., Oommen, S., Eto, K., Kessler, J. A., et al.** (2010). A role for suppressed incisor cuspal morphogenesis in the evolution of mammalian heterodont dentition. *Proc. Natl. Acad. Sci.* **107**, 92.
- Ooë, T.** (1980). Développement embryonnaire des incisives chez le lapin (*Oryctolagus cuniculus* L.). Interprétation de la formule dentaire. *Mammalia* **44**, 259–270.
- Orr-Urtreger, A., Bedford, M. T., Burakova, T., Arman, E., Zimmer, Y., Yayon, A., Givol, D. and Lonai, P.** (1993). Developmental localization of the splicing alternatives of fibroblast growth factor receptor-2 (FGFR2). *Dev. Biol.* **158**, 475–486
- Pelton, R. W., Saxena, B., Jones, M., Moses, H. L. and Gold, L. I.** (1991). Immunohistochemical localization of TGF beta 1, TGF beta 2, and TGF beta 3 in the mouse embryo: expression patterns suggest multiple roles during embryonic development. *J. Cell Biol.* **115**, 1091–1105.
- Peterka, M., Vonesch, J. L., Ruch, J. V., Cam, Y., Peterková, R. and Lesot, H.** (2000). Position and growth of upper and lower tooth primordia in prenatal mouse--3D study. *J. Craniofac. Genet. Dev. Biol.* **20**, 35–43.
- Peterková, R., Lesot, H., Vonesch, J. L., Peterka, M. and Ruch, J. V.** (1996). Mouse molar morphogenesis revisited by three dimensional reconstruction. I. Analysis of initial stages of the first upper molar development revealed two transient buds. *Int. J. Dev. Biol.* **40**, 1009–1016.
- Peterková, R., Peterka, M., Vonesch, J. L., Turecková, J., Viriot, L., Ruch, J. V. and Lesot, H.** (1998). Correlation between apoptosis distribution and BMP-2 and BMP-4 expression in vestigial tooth primordia in mice. *Eur. J. Oral Sci.* **106**, 667–670.
- Peterková, R., Peterka, M. and Lesot, H.** (2003). The developing mouse dentition: a new tool for apoptosis study. *Ann. N. Y. Acad. Sci.* **1010**, 453–466.

- Peters, K. G., Werner, S., Chen, G. and Williams, L. T.** (1992). Two FGF receptor genes are differentially expressed in epithelial and mesenchymal tissues during limb formation and organogenesis in the mouse. *Development* **114**, 233–243.
- Peters, H. and Balling, R.** (1999). Teeth: where and how to make them. *Trends Genet.* **15**, 59–65.
- Petznek, H., Kappler, R., Scherthan, H., Müller, M., Brem, G. and Aigner, B.** (2002). Reduced body growth and excessive incisor length in insertional mutants mapping to mouse Chromosome 13. *Mamm. Genome* **13**, 504–509.
- Pispa, J., Jung, H. S., Jernvall, J., Kettunen, P., Mustonen, T., Tabata, M. J., Kere, J. and Thesleff, I.** (1999). Cusp patterning defect in Tabby mouse teeth and its partial rescue by FGF. *Dev. Biol.* **216**, 521–534.
- Pispa, J. and Thesleff, I.** (2003). Mechanisms of ectodermal organogenesis. *Dev. Biol.* **262**, 195–205.
- Porntaveetus, T., Otsuka-Tanaka, Y., Basson, M. A., Moon, A. M., Sharpe, P. T. and Ohazama, A.** (2011). Expression of fibroblast growth factors (Fgfs) in murine tooth development. *J. Anat.* **218**, 534–543.
- Pough, F. H., Janis, C. M. and Heiser, J. B.** (2005). *Vertebrate life*. Pearson/Prentice Hall.
- Pucek, Z., Niethammer, J. and Krapp, F.** (1982). *Sicista betulina* (Pallas, 1778)-Waldbirkenmaus. *Handb. Säugetiere Eur. Bd 2*, 516–538.
- Reich, A., Sapir, A. and Shilo, B.** (1999). Sprouty is a general inhibitor of receptor tyrosine kinase signaling. *Development* **126**, 4139.
- Renvoisé, E. and Michon, F.** (2014). An Evo-Devo perspective on ever-growing teeth in mammals and dental stem cell maintenance. *Front. Physiol.* **5**,
- Robins, M. W. and Rowlatt, C.** (1971). Dental abnormalities in aged mice. *Gerontology* **17**, 261–272.
- Rodrigues, H. G., Marangoni, P., Sumbera, R., Tafforeau, P., Wendelen, W. and Viriot, L.** (2011). Continuous dental replacement in a hyper-chisel tooth digging rodent. *Proc. Natl. Acad. Sci.* **108**, 17355–17359.
- Romeo, Y., Moreau, J., Zindy, P. J., Saba-El-Leil, M., Lavoie, G., Dandachi, F., Baptissart, M., Borden, K. L. B., Meloche, S. and Roux, P. P.** (2012). RSK regulates activated BRAF signalling to mTORC1 and promotes melanoma growth. *Oncogene* **32**, 2917–2926.
- Rossi, D. J., Bryder, D. and Weissman, I. L.** (2007). Hematopoietic stem cell aging: mechanism and consequence. *Exp. Gerontol.* **42**, 385–390.

- Ruch, J. V., Lesot, H. and Begue-Kirn, C.** (1995). Odontoblast differentiation. *Int. J. Dev. Biol.* **39**, 51.
- Sashima, M., Satoh, M. and Suzuki, A.** (1987). Incisor Abnormality of Senescence Accelerated Mouse (SAM) 1. *Gerodontology* **6**, 145–148.
- Sadier, A., Viriot, L., Pantalacci, S. and Laudet, V.** (2014). The ectodysplasin pathway: from diseases to adaptations. *Trends Genet.* **30**, 24–31.
- Salazar-Ciudad, I. and Jernvall, J.** (2010). A computational model of teeth and the developmental origins of morphological variation. *Nature* **464**, 583–586.
- Sandilands, A., Smith, F. J. D., Lunny, D. P., Campbell, L. E., Davidson, K. M., MacCallum, S. F., Corden, L. D., Christie, L., Fleming, S., Lane, E. B., et al.** (2013). Generation and characterisation of keratin 7 (K7) knockout mice. *PloS One* **8**, e64404.
- Scott, G. R. and Turner, C. G.** (2000). *The anthropology of modern human teeth: dental morphology and its variation in recent human populations*. Cambridge University Press.
- Sebolt-Leopold, J. S. and Herrera, R.** (2004). Targeting the mitogen-activated protein kinase cascade to treat cancer. *Nat. Rev. Cancer* **4**, 937–947.
- Seidel, K., Ahn, C. P., Lyons, D., Nee, A., Ting, K., Brownell, I., Cao, T., Carano, R. A. D., Curran, T., Schober, M., et al.** (2010). Hedgehog signaling regulates the generation of ameloblast progenitors in the continuously growing mouse incisor. *Dev. Camb. Engl.* **137**, 3753–3761.
- Semënov, M., Tamai, K. and He, X.** (2005). SOST is a ligand for LRP5/LRP6 and a Wnt signaling inhibitor. *J. Biol. Chem.* **280**, 26770–26775.
- Shadle, A. R., Ploss, W. R. and Marks, E. M.** (1944). The extrusive growth and attrition of the incisor teeth of *Erethizon dorsatum*. *Anat. Rec.* **90**, 337–341.
- Sharpless, N. E. and DePinho, R. A.** (2007). How stem cells age and why this makes us grow old. *Nat. Rev. Mol. Cell Biol.* **8**, 703–713.
- Shroyer, N. F., Wallis, D., Venken, K. J. T., Bellen, H. J. and Zoghbi, H. Y.** (2005). Gfi1 functions downstream of Math1 to control intestinal secretory cell subtype allocation and differentiation. *Genes Dev.* **19**, 2412–2417.
- Signer, R. A. J. and Morrison, S. J.** (2013). Mechanisms that Regulate Stem Cell Aging and Life Span. *Cell Stem Cell* **12**, 152–165.
- Snead, M. L., Luo, W., Oliver, P., Nakamura, M., Don-Wheeler, G., Bessem, C., Bell, G. I., Rall, L. B. and Slavkin, H. C.** (1989). Localization of epidermal growth factor precursor in tooth and lung during embryonic mouse development. *Dev. Biol.* **134**, 420–429

- Sparks, N. H., Motta, P. J., Shellis, R. P., Wade, V. J. and Mann, S.** (1990). An analytical electron microscopy study of iron-rich teeth from the butterflyfish (*Chaetodon ornatissimus*). *J. Exp. Biol.* **151**, 371–385.
- Sreenath, T., Thyagarajan, T., Hall, B., Longenecker, G., D'Souza, R., Hong, S., Wright, J. T., MacDougall, M., Sauk, J. and Kulkarni, A. B.** (2003). Dentin sialophosphoprotein knockout mouse teeth display widened predentin zone and develop defective dentin mineralization similar to human dentinogenesis imperfecta type III. *J. Biol. Chem.* **278**, 24874–24880.
- Suga, S., Taki, Y. and Ogawa, M.** (1992). Iron in the enameloid of perciform fish. *J. Dent. Res.* **71**, 1316–1325.
- Suomalainen, M. and Thesleff, I.** (2010). Patterns of Wnt pathway activity in the mouse incisor indicate absence of Wnt/ β -catenin signaling in the epithelial stem cells. *Dev. Dyn.* **239**, 364–372.
- Tahayato, A., Dollé, P. and Petkovich, M.** (2003). *Cyp26C1* encodes a novel retinoic acid-metabolizing enzyme expressed in the hindbrain, inner ear, first branchial arch and tooth buds during murine development. *Gene Expr. Patterns* **3**, 449–454.
- Temtamy, S. A., Miller, J. D., Dorst, J. P., Hussels-Maumenee, I., Salinas, C., Lacassie, Y. and Kenyon, K. R.** (1974). The Coffin-Lowry syndrome: a simply inherited trait comprising mental retardation, faciodigital anomalies and skeletal involvement. *Birth Defects Orig. Artic. Ser.* **11**, 133–152.
- Temtamy, S. A., Miller, J. D. and Hussels-Maumenee, I.** (1975). The Coffin-Lowry syndrome: an inherited faciodigital mental retardation syndrome. *J. Pediatr.* **86**, 724–731.
- Thesleff, I., Keranen, S. and Jernvall, J.** (2001). Enamel knots as signaling centers linking tooth morphogenesis and odontoblast differentiation. *Adv. Dent. Res.* **15**, 14.
- Thesleff, I. and Mikkola, M.** (2002). The role of growth factors in tooth development. *Int. Rev. Cytol.* **217**, 93–135.
- Thesleff, I.** (2003). Epithelial-mesenchymal signalling regulating tooth morphogenesis. *J. Cell Sci.* **116**, 1647.
- Thesleff, I., Wang, X.-P. and Suomalainen, M.** (2007). Regulation of epithelial stem cells in tooth regeneration. *C. R. Biol.* **330**, 561–564.
- Tompkins, K.** (2006). Molecular mechanisms of cytodifferentiation in mammalian tooth development. *Connect. Tissue Res.* **47**, 111–118.
- Tong, Y. S.** (1992). Pappocricetodon, a pre-Oligocene cricetid genus (Rodentia) from central China. *Vertebr. Palasiat.* **30**, 1–16.

- Trivier, E., De Cesare, D., Jacquot, S., Pannetier, S., Zackai, E., Young, I., Mandel, J.-L., Sassone-Corsi, P. and Hanauer, A.** (1996). Mutations in the kinase Rsk-2 associated with Coffin-Lowry syndrome.
- Tsuboi, T., Mizutani, S., Nakano, M., Hirukawa, K. and Togari, A.** (2003). Fgf-2 regulates enamel and dentine formation in mouse tooth germ. *Calcif. Tissue Int.* **73**, 496–501.
- Tucker, A. S., Matthews, K. L. and Sharpe, P. T.** (1998). Transformation of tooth type induced by inhibition of BMP signaling. *Science* **282**, 1136.
- Tucker, A. S. and Sharpe, P. T.** (1999). Molecular genetics of tooth morphogenesis and patterning: the right shape in the right place. *J. Dent. Res.* **78**, 826.
- Tucker, A. and Sharpe, P.** (2004). The cutting-edge of mammalian development; how the embryo makes teeth. *Nat. Rev. Genet.* **5**, 499–508.
- Tummers, M. and Thesleff, I.** (2003). Root or crown: a developmental choice orchestrated by the differential regulation of the epithelial stem cell niche in the tooth of two rodent species. *Development* **130**, 1049.
- Ulmansky, M., Ungar, H. and Adlhr, J. H.** (1984). Dental abnormalities in aging sand rats (*Psammomys obesus*). *J. Oral Pathol. Med.* **13**, 366–372.
- Ungar, P. S.** (2010). *Mammal teeth: origin, evolution, and diversity*. JHU Press.
- Vahtokari, A., Vainio, S. and Thesleff, I.** (1991). Associations between transforming growth factor beta 1 RNA expression and epithelial-mesenchymal interactions during tooth morphogenesis. *Development* **113**, 985–994.
- Vahtokari, A., Åberg, T., Jernvall, J., Keränen, S. and Thesleff, I.** (1996a). The enamel knot as a signaling center in the developing mouse tooth. *Mech. Dev.* **54**, 39–43.
- Vahtokari, A., Åberg, T. and Thesleff, I.** (1996b). Apoptosis in the developing tooth: association with an embryonic signaling center and suppression by EGF and FGF-4. *Development* **122**, 121.
- Vaes, B. L., Ducy, P., Sijbers, A. M., Hendriks, J., van Someren, E. P., de Jong, N. G., van den Heuvel, E. R., Olijve, W., van Zoelen, E. J. and Dechering, K. J.** (2006). Microarray analysis on Runx2-deficient mouse embryos reveals novel Runx2 functions and target genes during intramembranous and endochondral bone formation. *Bone* **39**, 724–738.
- Van Rijssel, T. G. and Mühlbock, O.** (1955). Intramandibular tumors in mice. *J. Natl. Cancer Inst.* **16**, 659–689.
- Viriot, L., Lesot, H., Vonesch, J. L., Ruch, J. V., Peterka, M. and Peterková, R.** (2000). The presence of rudimentary odontogenic structures in the mouse embryonic mandible

requires reinterpretation of developmental control of first lower molar histomorphogenesis. *Int. J. Dev. Biol.* **44**, 233–240.

- Viriot, L., Peterková, R., Peterka, M. and Lesot, H.** (2002). Evolutionary implications of the occurrence of two vestigial tooth germs during early odontogenesis in the mouse lower jaw. *Connect. Tissue Res.* **43**, 129–133.
- Wang, X. P., Suomalainen, M., Jorgez, C. J., Matzuk, M. M., Werner, S. and Thesleff, I.** (2004). Follistatin regulates enamel patterning in mouse incisors by asymmetrically inhibiting BMP signaling and ameloblast differentiation. *Dev. Cell* **7**, 719–730.
- Wang, X. P., Åberg, T., James, M., Levanon, D., Groner, Y. and Thesleff, I.** (2005). Runx2 (Cbfa1) inhibits Shh signaling in the lower but not upper molars of mouse embryos and prevents the budding of putative successional teeth. *J. Dent. Res.* **84**, 138.
- Wang, X. P., Suomalainen, M., Felszeghy, S., Zelarayan, L. C., Alonso, M. T., Plikus, M. V., Maas, R. L., Chuong, C. M., Schimmang, T. and Thesleff, I.** (2007). An integrated gene regulatory network controls stem cell proliferation in teeth. *PLoS Biol.* **5**, e159.
- Wang, X. P., O’Connell, D. J., Lund, J. J., Saadi, I., Kuraguchi, M., Turbe-Doan, A., Cavalleco, R., Kim, H., Park, P. J., Harada, H., et al.** (2009). Apc inhibition of Wnt signaling regulates supernumerary tooth formation during embryogenesis and throughout adulthood. *Development* **136**, 1939.
- Weijs, W. A.** (1994). Evolutionary Approach of Masticatory Motor Patterns in Mammals. In *Biomechanics of Feeding in Vertebrates* (ed. Bels, V. L., Chardon, M., and Vandewalle, P.), pp. 281–320. Springer Berlin Heidelberg.
- Wen, X. and Paine, M. L.** (2013). Iron Deposition and Ferritin Heavy Chain (Fth) Localization in Rodent Teeth. *BMC Res. Notes* **6**, 1.
- Wheelock, M. J. and Johnson, K. R.** (2003). Cadherins as modulators of cellular phenotype. *Annu. Rev. Cell Dev. Biol.* **19**, 207–235.
- WHO | WHO Global Forum on Innovations for Ageing Populations** *WHO*.
- Wilkie, A. O. and Morriss-Kay, G. M.** (2001). Genetics of craniofacial development and malformation. *Nat. Rev. Genet.* **2**, 458–468.
- Wilson, D. E. and Reeder, D. M.** (2005). *Mammal species of the world: a taxonomic and geographic reference*. JHU Press.
- Wright, J. T., Hart, T. C., Hart, P. S., Simmons, D., Suggs, C., Daley, B., Simmer, J., Hu, J., Bartlett, J. D., Li, Y., et al.** (2009). Human and mouse enamel phenotypes

- resulting from mutation or altered expression of AMEL, ENAM, MMP20 and KLK4. *Cells Tissues Organs* **189**, 224–229.
- Xiong, W., He, F., Morikawa, Y., Yu, X., Zhang, Z., Lan, Y., Jiang, R., Cserjesi, P. and Chen, Y.** (2009). Hand2 is required in the epithelium for palatogenesis in mice. *Dev. Biol.* **330**, 131–141.
- Xu, L., Corcoran, R. B., Welsh, J. W., Pennica, D. and Levine, A. J.** (2000). WISP-1 is a Wnt-1-and β -catenin-responsive oncogene. *Genes Dev.* **14**, 585–595.
- Xu, X., Han, J., Ito, Y., Bringas Jr, P., Deng, C. and Chai, Y.** (2008). Ectodermal Smad4 and p38 MAPK are functionally redundant in mediating TGF- β /BMP signaling during tooth and palate development. *Dev. Cell* **15**, 322–329.
- Yamashiro, T., Tummers, M. and Thesleff, I.** (2003). Expression of Bone Morphogenetic Proteins and Msx Genes during Root Formation. *J. Dent. Res.* **82**, 172–176.
- Yang, X., Matsuda, K., Bialek, P., Jacquot, S., Masuoka, H. C., Schinke, T., Li, L., Brancorsini, S., Sassone-Corsi, P., Townes, T. M., et al.** (2004). ATF4 is a substrate of RSK2 and an essential regulator of osteoblast biology: implication for Coffin-Lowry syndrome. *Cell* **117**, 387–398.
- Young, I. D.** (1988). The Coffin-Lowry syndrome. *J. Med. Genet.* **25**, 344.
- Zeichner-David, M., Diekwisch, T., Fincham, A., Lau, E., MacDougall, M., Moradian-Oldak, J., Simmer, J., Snead, M. and Slavkin, H. C.** (1995). Control of ameloblast differentiation. *Int. J. Dev. Biol.* **39**, 69–92.
- Zeniou, M., Ding, T., Trivier, E. and Hanauer, A.** (2002). Expression analysis of RSK gene family members: the RSK2 gene, mutated in Coffin–Lowry syndrome, is prominently expressed in brain structures essential for cognitive function and learning. *Hum. Mol. Genet.* **11**, 2929–2940.
- Zhang, S., Lin, Y., Itaranta, P., Yagi, A. and Vainio, S.** (2001). Expression of Sprouty genes 1, 2 and 4 during mouse organogenesis. *Mech. Dev.* **109**, 367–370.
- Zhao, H., Feng, J., Seidel, K., Shi, S., Klein, O., Sharpe, P. and Chai, Y.** (2014). Secretion of Shh by a Neurovascular Bundle Niche Supports Mesenchymal Stem Cell Homeostasis in the Adult Mouse Incisor. *Cell Stem Cell* **14**, 160–173.

ANNEXES

Annex 1

Continuous dental replacement in mammals

Continuous dental replacement in a hyper-chisel tooth digging rodent

Helder Gomes Rodrigues^{a,1}, Pauline Marangoni^a, Radim Šumbera^b, Paul Tafforeau^c, Wim Wendelen^d, and Laurent Viriot^{a,1}

^aTeam "Evo-Devo of Vertebrate Dentition," Institut de Génétique Fonctionnelle de Lyon, Université de Lyon, Unité Mixte de Recherche 5242, Centre National de la Recherche Scientifique, Université Claude Bernard de Lyon 1, Ecole Normale Supérieure de Lyon, 69364 Lyon Cedex 07, France; ^bDepartment of Zoology, Faculty of Science, University of South Bohemia, České Budějovice 37005, Czech Republic; ^cEuropean Synchrotron Radiation Facility, 38043 Grenoble Cedex, France; and ^dVertebrate Section, Zoology Department, Royal Museum for Central Africa, B-3080 Tervuren, Belgium

Edited by David B. Wake, University of California, Berkeley, CA, and approved September 8, 2011 (received for review June 15, 2011)

Contrary to their reptilian ancestors, which had numerous dental generations, mammals are known to usually develop only two generations of teeth. However, a few mammal species have acquired the ability to continuously replace their dentition by the constant addition of supernumerary teeth moving secondarily toward the front of the jaw. The resulting treadmill-like replacement is thus horizontal, and differs completely from the vertical dental succession of other mammals and their extinct relatives. Despite the developmental implications and prospects regarding the origin of supernumerary teeth, this striking innovation remains poorly documented. Here we report another case of continuous dental replacement in an African rodent, *Heliophobius argenteocinereus*, which combines this dental system with the progressive eruption of high-crowned teeth. The escalator-like mechanism of *Heliophobius* constitutes an original adaptation to hyper-chisel tooth digging involving high dental wear. Comparisons between *Heliophobius* and the few mammals that convergently acquired continuous dental replacement reveal that shared inherited traits, including dental mesial drift, delayed eruption, and supernumerary molars, comprise essential prerequisites to setting up this dental mechanism. Interestingly, these dental traits are present to a lesser extent in humans but are absent in mouse, the usual biological model. Consequently, *Heliophobius* represents a suitable model to investigate the molecular processes leading to the development of supernumerary teeth in mammals, and the accurate description of these processes could be a significant advance for further applications in humans, such as the regeneration of dental tissues.

mole-rats | intensive burrowing activity | hypsodonty | abrasion | attrition

Most nonmammalian vertebrates continuously replace their dentition, entailing many generations of identical teeth. In contrast, mammals develop a limited dentition composed at most of two generations of heteromorphous teeth, decreasing in number but generally increasing in shape complexity during evolution (1, 2). This has contributed to the acquisition of a more efficient masticatory apparatus than reptile jaws (3) that allowed mammals to diversify their feeding habits (4) and to include tough and abrasive plants in their diets. To withstand abrasive intakes, many mammals acquired a more durable dentition by way of diverse evolutionary trends (5). The most frequently observed is the increase in tooth height (i.e., hypsodonty), which leads in extreme cases to ever-growing teeth. Another trend to improve durability is continuous dental replacement (CDR), an extremely rare phenomenon in mammals. CDR corresponds to a progressive replacement of the dentition by regular development of additional teeth, which move from the rear to the front of the jaw throughout the animal's life. Among the ca. 5,500 species of mammals, only the three manatee species (*Trichechus*, *Sirenia*) and the pygmy-rock wallaby (*Petrogale concinna*, *Macropodiformes*) are known to display this striking innovation (6, 7). To date, this mechanism appears poorly documented. Furthermore, the genetic etiology and the developmental and molecular

mechanisms leading to CDR, notably the occurrence of supernumerary teeth in mammals (8, 9), remain to be determined.

Here we report a case of CDR in a subterranean rodent, the silvery mole-rat *Heliophobius argenteocinereus*, belonging to African mole-rats (Bathyergidae, Rodentia), which could significantly contribute to the understanding of this rare phenomenon. The dental peculiarities of this species further underscore the interest of African mole-rats as models for examining topical issues, such as "eusociality" (10, 11), extreme longevity (12), and cancer resistance (13). We investigated *Heliophobius* dentition compared with *Trichechus*, *P. concinna*, and another African mole-rat (the Cape mole-rat, *Georychus capensis*) to appraise the main dental characteristics of this rodent on the one hand and to identify the specific traits relevant to improved knowledge of the CDR mechanism on the other.

Results and Discussion

Original System of Dental Replacement Among Mammals Combining Hypsodonty and Continuous Dental Replacement. *Heliophobius* displays four to seven cheek teeth (Fig. 1 A–C and Tables S1 and S2), whereas the maximum cheek tooth number per dental quadrant does not usually exceed five in rodents and four in African mole-rats. It is thus the only known rodent displaying so many supernumerary cheek teeth. Although its abnormal tooth number has previously been reported (14), the underlying dental mechanism has never been properly interpreted. *Heliophobius* has single-rooted and bilophate hypsodont teeth. Tooth occlusal surfaces rapidly become flat and undergo a series of shape transformations, finally resulting in upper heart-shaped and lower pear-shaped teeth (Fig. 1 A–C) that lack enamel to varying degrees and are covered by cementum. Morphometric comparisons between occlusal crown shapes observed from rear to front and virtual transverse slices of an erupting tooth belonging to the same row lead to the conclusion that the various crown shapes result from an increasing degree of dental wear (Fig. 1D). All teeth have an overall identical cone-like shape and only their relative size is susceptible to change during life. We cannot say whether the first erupting tooth is a premolar (Fig. S1), as in most African mole-rats, but all subsequent teeth are molars.

Most specimens of *Heliophobius* show either one erupting or freshly erupted molar behind the functional tooth row. After eruption, each tooth drifts from rear to front. Evidence of horizontal movements is demonstrated by continual remodeling of

Author contributions: W.W. and L.V. designed research; H.G.R., P.M., and P.T. performed research; H.G.R. and P.M. analyzed data; and H.G.R., P.M., R.S., P.T., W.W., and L.V. wrote the paper.

The authors declare no conflict of interest.

This article is a PNAS Direct Submission.

¹To whom correspondence may be addressed. E-mail: helder.gomes.rodrigues@ens-lyon.fr or laurent.viriot@ens-lyon.fr.

This article contains supporting information online at www.pnas.org/lookup/suppl/doi:10.1073/pnas.1109615108/-DCSupplemental.

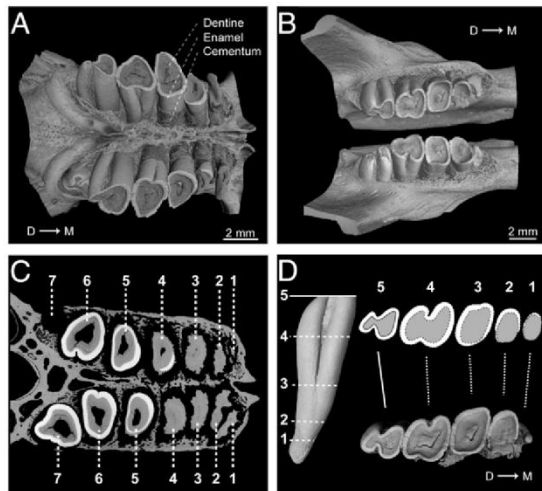


Fig. 1. Dental characteristics of *H. argenteocinereus* (RMCA96.036-M-5467). (A) X-ray synchrotron microtomographic 3D rendering of upper jugal tooth rows. (B) X-ray synchrotron microtomographic 3D rendering of lower jugal tooth rows. (C) Virtual cross-section of upper jugal tooth rows from synchrotron microtomographic data. (D) Morphological correspondences between virtual transverse slices of erupting lower molar and dental wear stages observed from the rear to front of the lower tooth row. D → M, distal-to-mesial point.

interalveolar bone septa (Fig. S24). The stress is particularly intense along the mesiodistal axis, inducing extremely thin interalveolar bone and dental resorption (Fig. 1C). All teeth display more intense resorption on the distal root side because of the compressive stress of subsequent teeth (15) (Fig. 2A and B). Teeth that have drifted to the mesial extremity of the row display crowns entirely worn by the combined action of wear and resorption (Fig. 2C). These molars, which are no longer occluding, have the highest rate of root resorption, which is probably induced by a hypofunctional periodontium coupled with a continuous dental drift (16). They are not truly shed, but their remains

are pushed out from the row alignment before being completely resorbed inside the bone (Figs. 1C and 2C). Because the molar progression is not synchronized between each quadrant, asymmetric dental rows occur (Fig. 1A and B), as do rare cases of misalignment (Fig. S2B). Teeth also continue to grow and erupt vertically while moving to the front (Fig. 2A and D). The originality of the *Heliophobius* dental system relies on the superimposition of CDR over preexisting hypsodonty resulting in an escalator-like movement of teeth, constantly compensating for intensive dental wear. This dental replacement is not observed in other bathyergid rodents. Among other mammals, elephants present an analogous dental replacement, but their regular dentition develops sequentially, without the occurrence of any supplementary teeth.

Unlike *Heliophobius*, *Trichechus* and *P. concinna* have low-crowned and bi- or trirooted cheek teeth but are bilophodont as well (Fig. 3A and B). The replacement of their jugal dentition works like a simple treadmill in which each freshly developed molar erupts vertically at the rear of the row and then migrates horizontally toward the front (Fig. 3C–F). A part of the regular dentition, including premolars (Fig. 3D), clearly develops before the system changes course, such that a single molar could become regularly ever-duplicated. Such an assumption relies on the fact that additional molars are identical to the second molars in manatees (6). The distal root is first intensively resorbed, and the crown breaks away from the mesial root when the tooth reaches the front of the row (Fig. 3C–F). Even if the crown is severely eroded during the drift, it is not resorbed and vertical readjustments are not significant, contrary to what happens in *Heliophobius*.

Dental Mechanism Adapted to High Dental Wear. Manatees and the pygmy-rock wallaby consume, respectively, floating meadow grasses and specific ferns, which contain highly abrasive hard silica phytoliths (17, 18). *Heliophobius* feeds on underground parts of plants such as tubers and bulbs, which are by far less abrasive. At present, it is not clear why this dentition evolved in *Heliophobius* and not in other African mole-rats. Nonetheless, *Heliophobius* is the only solitary mole-rat living in mesic Afro-tropics, where the soil is very hard and difficult to work during the dry season (19) and, contrary to social bathyergids, this

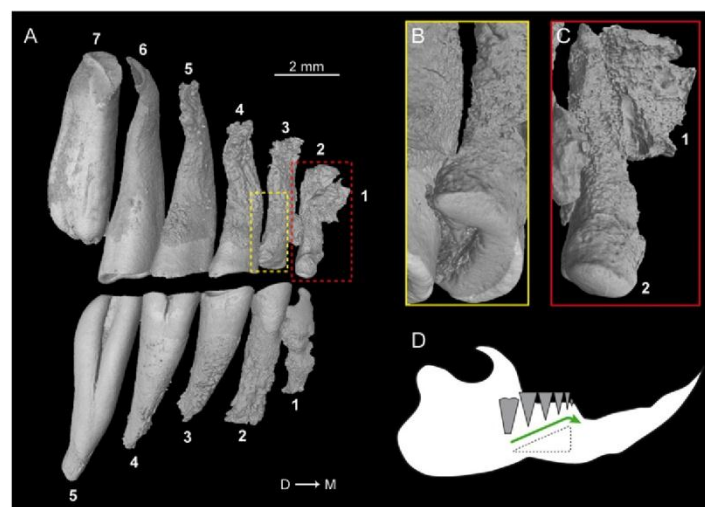


Fig. 2. Dental resorption and replacement in the silvery mole-rat. (A) Lateral view of X-ray synchrotron microtomographic 3D rendering of right upper and lower jugal tooth rows of *Heliophobius* (RMCA96.036-M-5467). (B and C) Focus on slightly and highly resorbed mesial upper teeth. (D) Dental replacement system in *Heliophobius*. The green arrow indicates dental drift.

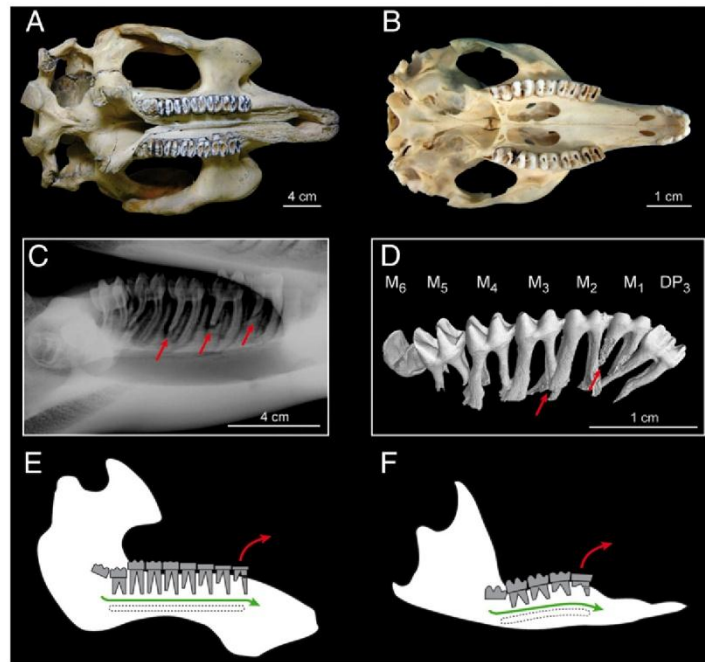


Fig. 3. Characteristics of the dental dynamics of manatees and the pygmy-rock wallaby. (A and B) Palatal view of skulls of *T. manatus* (NHM1985.6.30.2) and *P. concinna* (WAM-M4169). (C) Lateral X-ray radiograph of a left lower tooth row of *T. senegalensis* (Poulard's Coll. M201). (D) Lateral view of X-ray synchrotron microtomographic 3D rendering of the left lower tooth row of a juvenile specimen of *P. concinna* (WAM-M9346). DP, deciduous premolar; M, molar. Red arrows indicate root resorption. (E and F) Dental replacement systems of *Trichechus* and *P. concinna*. Green arrows indicate dental drift; red arrows indicate molar loss.

chisel-tooth digger builds extended burrow systems alone to find food resources (20, 21). Such extensive burrowing activity could induce important attrition on its dentition and an ingestion of higher amounts of abrasive dust compared with other bathyergids. We therefore suppose that the dental system of *Heliophobius* might be a striking adaptation to hyper-chisel tooth digging, necessary to counterbalance the effects of severe friction (both attrition and abrasion) and to maintain the dentition functional throughout its life.

In manatees, tooth movement rate is correlated to food intake (6). Whereas growing tooth germs at the rear of the jaw principally generate the forward pressure, the dental movement is controlled by the quality and amount of ingested food, which impact on mechanical stress during mastication. As it mainly affects tooth wear, one can say that abrasion plays a major role in mechanical stress. In fact, the tough component of fibrous grasses mainly regulates the rate of displacement. For instance, a high exogenous grit intake, such as sand, can lead to severe wear and high loss of teeth coupled with a low tooth-movement rate in manatees. In the case of *Heliophobius*, where the ingestion of exogenous abrasive matter is inevitable during digging, and notably foraging, hypsodonty limits the effect of severe wear. This dental characteristic might comprise one of the components that regulate, even indirectly, the rate of dental regeneration of this mole-rat.

Three Dental Traits Are Essential for Continuous Dental Replacements in Mammals. *Trichechus*, *P. concinna*, and *Heliophobius* have highly different ecological traits, and are very distant phylogenetically. CDR is clearly a convergent mechanism resulting in similar strategies closely related to high rates of dental wear. However, these mammals share three dental traits that we assume to be crucial prerequisites to setting up CDR: dental mesial

drift, delayed eruption, and the occurrence of supernumerary molars. Interestingly, these dental characteristics have been identified in some of their extant or extinct relatives (Fig. 4).

Mesial drift corresponds to a forward movement of teeth as a result of distal pressure. It is well-known in elephants and exists in dugongs (22), the sister group of manatees. It also occurs in macropods, especially in grazing forms (e.g., kangaroos), including other *Petrogale* species (23). To date, mesial drift has never been described in African mole-rats. However, our analysis of some specimens of the bathyergid species *G. capensis* revealed that mesial drift, even slight, is not only confined to *Heliophobius*. The Cape mole-rat displays root resorption of the mesial teeth (notably the fourth premolars) as well as remodeling of inter-alveolar septa, as does the silvery mole-rat (Fig. S3 A–C). These features are due to both subsequent eruption and forward pressure of the last molars. The presence of large mesial diastemata in these rodents, as in other mammals showing mesial drift (e.g., elephants, sirenians, and macropods), is also essential to prevent orthodontic problems that sometimes occur in humans, inasmuch as diastemata can act as a buffer between jugal and frontal teeth.

The delayed dental eruption extends dentition longevity and corresponds to the acquisition of a definitive dentition during adulthood; this means that the last tooth erupts after the age of sexual maturity is reached. Three stages of eruption can be defined. As most mammals acquire a definitive dentition by sexual maturity, this stage is defined as “normal eruption.” A “slightly delayed eruption” corresponds to the completion of dentition before twice the age of sexual maturity is reached, as in humans (~20 y for a permanent dentition and ~13 y for sexual maturity) and many primates (24). After this limit, mammals can be considered as having a true “delayed eruption,” and this is the case for most of the afrotherian species, which spend the majority of their lifespan without a complete dentition (24). Such delayed

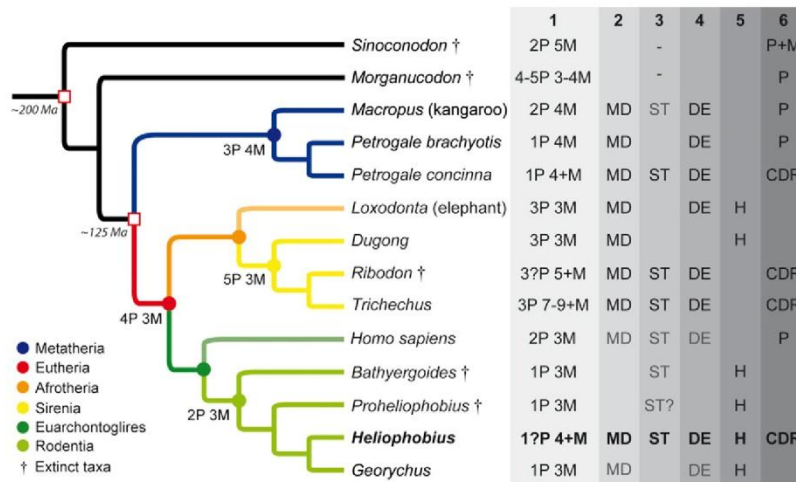


Fig. 4. Phylogenetic relationships and main dental characteristics of mammals developing CDR and some of their closest extant and extinct relatives. (1 and nodes) Jugal dental formula. (2) Presence of dental mesial drift (MD). (3) Presence of supernumerary teeth (ST). (4) Presence of delayed dental eruption (DE). (5) Presence of hypsodonty (H). (6) Jugal tooth replacement: premolar (P), molar (M), continuous dental replacement (CDR). In gray: occasional characteristic (for ST) or slightly manifested characteristic (for MD and DE).

eruption also occurs in macropods (23). Mammals with CDR can be considered as having a delayed eruption because their dentition is apparently endless. As with some subterranean rodents, *Georychus* displays a slightly delayed eruption of its dentition according to its pronounced dental wear gradient (Fig. S3 D and E) compared with other rodents. For instance, the last permanent teeth of *Georychus* generally erupt after its sexual maturity [~ 15 mo for a permanent dentition and ~ 10 mo for sexual maturity (25)], whereas the whole adult dentition of the mouse becomes functional well before sexual maturity (~ 4 wk for a permanent dentition and ~ 6 wk for sexual maturity), as in most of rodents (24).

Supernumerary teeth are rare in mammals because they generally cause functional pathologies. For instance, they are frequently associated with diseases caused by gene mutations in humans (9), but they can sometimes be related to nonsyndromic cases transmitted between generations (26). More generally, permanent supernumerary teeth are often associated with a lengthening of the jaws, as with simplified and nonreplaced teeth observed in odontocete cetaceans. The earliest true manatee, the Miocene *Potamosiren*, did not have supernumerary molars, whereas the Pliocene form, *Ribodon*, already had CDR (17). Additional molars frequently occur in kangaroos (23), even if these molars appear later in life history. A fourth molar probably occurred in the earliest known bathyergid *Proheliophobius* as in their extinct sister *Batherygoides* (27), but actually cases of supernumerary molars remain scarce in bathyergid rodents.

Developmental Implications and Prospects Concerning Supernumerary Teeth in Mammals. Such shared biological traits suggest that analogous molecular processes probably control CDR and were independently activated at least three times in recent mammalian history. The fossil record indicates the capacities to vertically replace molars and to possess more than three or four molars were lost since nearly 200 Mya in mammals [e.g., *Sinoconodon* (1)]. CDR could not involve the same developmental pathways, given that the pathways concerned were probably lost well over the time lapse generally assumed to coincide with irreversible losses of gene function [i.e., from 16 to 24 Mya (28)]. Although the developmental mechanisms remain unknown, it is likely that epithelial odontogenic tissues contain a permanent dental lamina permitting continual replacement of the previously erupted

teeth, as documented in dental families of nonmammalian vertebrates (29, 30). Dental lamina and associated stem cells could indeed play a major role in CDR because of their deep involvement in vertebrate tooth renewal (31), notably in mammals (32). Considering that supernumerary molars are the result of a putative duplication of one molar (6), they probably derive from an extension of the dental lamina arising from first molars. This assumption needs further investigation, particularly focusing on the potential genes that have a bearing on such an extension.

A complex network of signaling pathways drives tooth development. Among all these actors, *Runx2*, *Il11*, *Apc*, and some master genes from the Wnt/ β -catenin signaling pathway appear to be suitable candidates to explain the origin of supernumerary teeth (9). Indeed, they have been demonstrated to be involved in the development of such abnormalities in humans and, sometimes, mutant mice (33–36). However, when their expression is affected, the occurrence of supernumerary teeth is generally accompanied by disorders or diseases: Cleidocranial dysplasia (CCD) is related to heterozygous mutations (haploinsufficiency) in *Runx2* (33); craniosynostosis is linked to *Il11* loss of function (34); and adenomatous polyposis, tumors, and odontomes can be related to *Apc* loss of function (35) or activation of Wnt/ β -catenin signaling (35, 36). *Runx2* seems to be the best candidate given that delayed eruption is also one of the symptoms of CCD, in addition to supernumerary teeth. Even if a comparison has already been drawn between some afrotherian anatomical traits and CCD symptoms (24), the presence of addition molars in manatees has not been discussed in relation to *Runx2*. To the extent that mutations in *Runx2* are extremely variable and sporadically induce isolated dental anomalies (9), implications of this gene in CDR are likely for the three concerned mammalian genera, even if its accurate role remains to be tested. *Il11* could also be involved in CDR, because delayed eruption is also associated with *Il11* loss of function. However, additional molars were never noticed among supernumerary teeth, and dental anomalies cannot be dissociated from bone disorders (34), contrary to some cases of haploinsufficiency for *Runx2*.

Our study demonstrates that *Heliophobius* presents striking dental characteristics related to CDR, including supernumerary molars. These characteristics are partially present in humans, but are absent in mice. *Heliophobius* therefore represents a model

more appropriate than mice to explore the genetic etiology of supernumerary teeth in mammals. Maintaining a perennial dentition in a context of hyperabrasive intakes mainly involves two radically different adaptations in mammals. Although hypsodonty is inappropriate for the human dental system, the understanding of both CDR and the molecular processes leading to supernumerary molars could constitute a basis for further studies on regeneration of dental tissues and their applications in tooth engineering (37).

Materials and Methods

Skulls. Fifty-five skulls of *H. argenteocinereus* were investigated. These specimens are mainly housed in the Royal Museum for Central Africa (RMCA) of Tervuren (Belgium), and others come from the Museum National d'Histoire Naturelle (MNHN) of Paris. The skulls of *T. senegalensis* from Poulard's Collection (Poulard's Coll. M201) of Lyon (France), *T. manatus* (NHM1985.6.30.2) from the National History Museum (NHM) of London, and *P. concinna* (WAM-M4169 and WAM-M9346) from the Western Australian Museum (WAM) of Perth (Australia) were also used here for comparison and illustrations. Fifteen skulls of *G. capensis* from the NHM and MNHN were studied to draw comparisons. The main interest of this bathyergid species concerns its dental eruption sequence, which is already known and accurately detailed (25).

Two- and Three-Dimensional Data Acquisition of Dentitions. Dentitions of *H. argenteocinereus* were digitized using a stereomicroscope (Leica; M165C) connected to a spot CCD camera (Leica; DFC420) at 7.3 \times magnification. Different X-ray methods were performed to more accurately depict and analyze tooth morphologies, including roots and osteological characteristics. X-ray radiography from the Ecole Nationale Vétérinaire de Lyon was used to image a skull of *Trichechus*. High-quality images of two skulls of *Heliophobius*, including a young specimen (Fig. S2), were obtained using X-ray synchrotron microtomography at the European Synchrotron Radiation Facility (ESRF; Grenoble, France), beamlines ID19 and BM5, with a monochromatic beam at an energy of 25 keV and using a cubic voxel of 5.06 μm . A pink beam at an energy of 60 keV, using a cubic voxel of 7.46 μm (beamline ID19; ESRF), was also used to scan the skull of *P. concinna*. This method has been proven to be very useful for accurate imaging of small elements (38, 39) such as teeth (40). Noninvasive virtual extraction of entire teeth (i.e., crown and roots) is also permitted (41). Three-dimensional renderings and virtual slices were then performed using VGStudio Max 2.0 software (Volume Graphics).

Statistics. Dentitions of *Heliophobius* are described according to the number of erupting teeth, functional teeth, and worn-out teeth; skull lengths were also measured (Table S1). Percentages were then calculated for the whole sample (Table S2). Similar descriptions were realized on *Georchys* specimens (Table S3).

ACKNOWLEDGMENTS. We acknowledge the curators J. Cuisin (MNHN, Paris), R. How and C. Stevenson (WAM, Perth), and R. Portela Miguez (NHM, London), who allowed access to their mammal collections. We are grateful to the ESRF (Grenoble) and the team of beamlines ID19 and BM5 for support of this research project by giving access to their experimental stations. Thanks to all the members of Team "Evo-Devo of Vertebrate Dentition," and to V. Laudet, H. Magloire, M.-L. Couble, and J. Burden (Institut de Génétique Fonctionnelle de Lyon), for both technical assistance and comments on the manuscript. We also thank two anonymous reviewers for manuscript improvements. This work was supported by the ANR "Quenottes" Program (L.V.), National Science Foundation/Revealing Hominid Origins Initiative "Small Mammals" Award BCS-0321893 (to L.V.), a Centre National de la Recherche Scientifique postdoctoral grant (to H.G.R.), and Project Ministerstvo Školství, Mládeže a Tělovýchovy 600766580 (to R.S.).

REFERENCES. 1. Luo Z-X, Kielan-Jaworowska Z, Cifelli RL (2004) Evolution of dental replacement in mammals. *Bull Carnegie Mus Nat Hist* 36:159–175.
2. Koussoulakou DS, Margaritis LH, Koussoulakos SL (2009) A curriculum vitae of teeth: Evolution, generation, regeneration. *Int J Biol Sci* 5:226–243.
3. Ross CF, et al. (2007) Modulation of intra-oral processing in mammals and lepidosaurs. *Integr Comp Biol* 47:118–136.
4. Luo Z-X (2007) Transformation and diversification in early mammal evolution. *Nature* 450:1011–1019.
5. Janis CM, Fortelius M (1988) On the means whereby mammals achieve increased functional durability of their dentitions, with special reference to limiting factors. *Biol Rev Camb Philos Soc* 63:197–230.
6. Domning DP, Hayek L-AC (1984) Horizontal tooth replacement in the Amazonian manatee (*Trichechus inunguis*). *Mammalia* 48:105–127.
7. Sanson GD (1989) Morphological adaptations of teeth to diets and feeding in the Macropodoidea. *Kangaroos, Wallabies and Rat-Kangaroos*, eds Grigg G, Jarman P, Hume I (Surrey Beatty & Sons, Sydney), pp 151–168.
8. D'Souza RN, Klein OD (2007) Unraveling the molecular mechanisms that lead to supernumerary teeth in mice and men: Current concepts and novel approaches. *Cells Tissues Organs* 186:60–69.
9. Wang X-P, Fan J (2011) Molecular genetics of supernumerary tooth formation. *Genesis* 49:261–277.
10. Jarvis JUM (1981) Eusociality in a mammal: Cooperative breeding in naked mole-rat colonies. *Science* 212:571–573.
11. Jarvis JUM, O'Riain MJ, Bennett NC, Sherman PW (1994) Mammalian eusociality: A family affair. *Trends Ecol Evol* 9:47–51.
12. Pérez VI, et al. (2009) Protein stability and resistance to oxidative stress are determinants of longevity in the longest-living rodent, the naked mole-rat. *Proc Natl Acad Sci USA* 106:3059–3064.
13. Seluanov A, et al. (2009) Hypersensitivity to contact inhibition provides a clue to cancer resistance of naked mole-rat. *Proc Natl Acad Sci USA* 106:19352–19357.
14. Landry SC (1957) The interrelationships of the New and Old World hystricomorph rodents. *Univ Calif Publ Zool* 56:1–118.
15. Wise GE, King GJ (2008) Mechanisms of tooth eruption and orthodontic tooth movement. *J Dent Res* 87:414–434.
16. Sringkarnboriboon S, Matsumoto Y, Soma K (2003) Root resorption related to hypofunctional periodontium in experimental tooth movement. *J Dent Res* 82:486–490.
17. Domning DP (1982) Evolution of manatees; a speculative history. *J Paleontol* 56:599–619.
18. Sanson GD, Nelson JE, Fell P (1985) Ecology of *Peradorcas concinna* in Arnhem land in the wet and dry season. *Proc Ecol Soc Aust* 13:69–72.
19. Škliba J, Šumbera R, Chitaukali WN, Burda H (2009) Home-range dynamics in a solitary subterranean rodent. *Ethology* 115:217–226.
20. Šumbera R, Burda H, Chitaukali WN, Kubová J (2003) Silvery mole-rats (*Heliophobius argenteocinereus*, Bathyergidae) change their burrow architecture seasonally. *Naturwissenschaften* 90:370–373.

21. Škliba J, Šumbera R, Vitámvás M (2011) Resource characteristics and foraging adaptations in the silvery mole-rat (*Heliophobius argenteocinereus*), a solitary Afrotropical bathyergid. *Ecol Res*, 10.1007/s11284-011-0860-1.
22. Lanyon JM, Sanson GD (2006) Degenerate dentition of the dugong (*Dugong dugon*), or why a grazer does not need teeth: Morphology, occlusion and wear of mouthparts. *J Zool (Lond)* 268:133–152.
23. Jackson SM (2003) *Australian Mammals: Biology and Captive Management* (CSIRO, Melbourne).
24. Asher RJ, Lehmann T (2008) Dental eruption in afrotherian mammals. *BMC Biol* 6:14.
25. Taylor PJ, Jarvis JUM, Crowe TM (1985) Age determination in the Cape mole rat *Georchys capensis*. *S Afr J Zool* 20:261–267.
26. Batra P, Duggal R, Parkash H (2005) Non-syndromic multiple supernumerary teeth transmitted as an autosomal dominant trait. *J Oral Pathol Med* 34:621–625.
27. Lavocat R (1973) [East African Miocene rodents I. Early Miocene.] *Mém Trav EPHE Inst Montpellier*, 1:1–284. French.
28. Collin R, Miglietta MP (2008) Reversing opinions on Dollo's Law. *Trends Ecol Evol* 23:602–609.
29. Smith MM, Fraser GJ, Mitsiadis TA (2009) Dental lamina as source of odontogenic stem cells: Evolutionary origins and developmental control of tooth generation in gnathostomes. *J Exp Zool B Mol Dev Evol* 312B:260–280.
30. Moriyama K, Watanabe S, Iida M, Sahara N (2010) Plate-like permanent dental laminae of upper jaw dentition in adult gobioid fish, *Sicyopterus japonicus*. *Cell Tissue Res* 340:189–200.
31. Huyseune A, Thesleff I (2004) Continuous tooth replacement: The possible involvement of epithelial stem cells. *Bioessays* 26:665–671.
32. Järvinen E, Tummers M, Thesleff I (2009) The role of the dental lamina in mammalian tooth replacement. *J Exp Zool B Mol Dev Evol* 312B:281–291.
33. Wang X-P, et al. (2005) Runx2 (Cbfa1) inhibits Shh signaling in the lower but not upper molars of mouse embryos and prevents the budding of putative successional teeth. *J Dent Res* 84:138–143.
34. Nieminen P, et al. (2011) Inactivation of IL11 signaling causes craniosynostosis, delayed tooth eruption, and supernumerary teeth. *Am J Hum Genet* 89:67–81.
35. Wang X-P, et al. (2009) Apc inhibition of Wnt signaling regulates supernumerary tooth formation during embryogenesis and throughout adulthood. *Development* 136:1939–1949.
36. Järvinen E, et al. (2006) Continuous tooth generation in mouse is induced by activated epithelial Wnt/ β -catenin signaling. *Proc Natl Acad Sci USA* 103:18627–18632.
37. Bluteau G, Luder H-U, De Bari C, Mitsiadis TA (2008) Stem cells for tooth engineering. *Eur Cell Mater* 16:1–9.
38. Tafforeau P, et al. (2006) Applications of X-ray synchrotron microtomography for non-destructive 3D studies of paleontological specimens. *Appl Phys A-Mater* 83:195–202.
39. Kruta I, Landman N, Rouget I, Cecca F, Tafforeau P (2011) The role of ammonites in the Mesozoic marine food web revealed by jaw preservation. *Science* 331:70–72.
40. Charles C, et al. (2009) Modulation of *Fgf3* dosage in mouse and men mirrors evolution of mammalian dentition. *Proc Natl Acad Sci USA* 106:22364–22368.
41. Tabuce R, et al. (2009) Anthropoid versus strepsirrhine status of the African Eocene primates *Algeripithecus* and *Azibius*: Craniodental evidence. *Proc Biol Sci* 276:4087–4094.

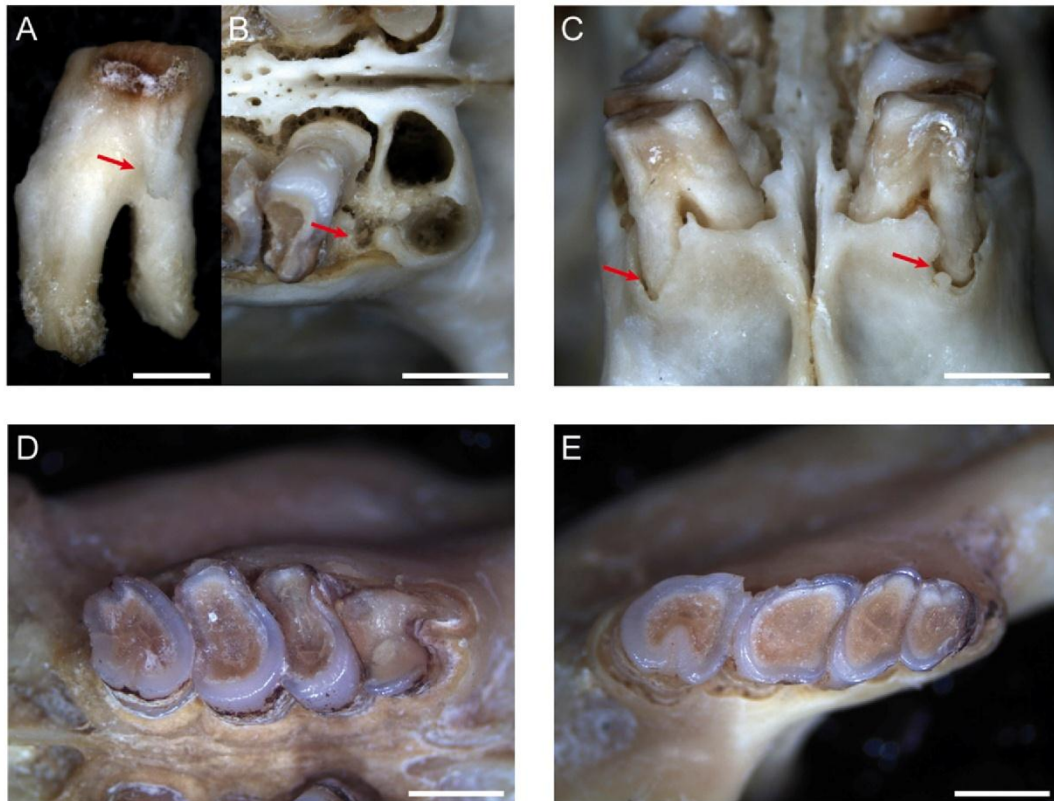


Fig. 53. Photographs showing consequences of a slight mesial drift and dental wear gradient in *Georychus*. (A) Upper fourth premolar showing the distal root partially resorbed as in manatees (MNHN-CG1988-111). (Scale bar, 1 mm.) MNHN, Museum National d'Histoire Naturelle, Paris. (B) Upper dentitions showing the bone socket of a distal root of a fourth premolar partially resorbed (MNHN-CG1988-111). (Scale bar, 2 mm.) (C) Upper dentition from a mesial view showing bone resorption (MNHN-CG1988-111). (Scale bar, 2 mm.) (D and E) Dental wear gradient on upper and lower dentitions (NHM66.6.16.2). NHM, National History Museum, London (Scale bars, 2 mm.) Red arrows indicate resorption.

Table S1. Data concerning the jugal dentition of each *Heliophobius* specimen

Institution	Specimen	Left lower teeth			Right lower teeth			Left upper teeth			Right upper teeth			Skull length, mm
		Erupting	Functional	Worn out	Erupting	Functional	Worn out	Erupting	Functional	Worn out	Erupting	Functional	Worn out	
RMCA	a4.036-M-0077	1	3	1	1	3	1	1	4	0	1	4	0	40.7
RMCA	96.036-M-5432	1	3	1	0	4	1	1	4	1	1	4	0	35.4
RMCA	96.036-M-5433	1	4	0	1	3	1	1	4	0	0	4	1	38.2
RMCA	96.036-M-5439	1	4	0	1	4	0	1	4	0	1	4	0	34.0
RMCA	96.036-M-5441	1	4	1	1	4	1	1	4	1	1	4	1	34.8
RMCA	96.036-M-5443	0	4	1	1	4	0	0	5	0	0	4	1	35.5
RMCA	96.036-M-5449	0	3	1	0	4	0	1	4	0	1	3	1	36.5
RMCA	96.036-M-5453	0	5	0	0	5	0	0	5	0	0	5	0	34.9
RMCA	96.036-M-5454	1	4	0	0	4	1	0	5	0	0	4	1	32.7
RMCA	96.036-M-5459	1	5	0	1	5	0	1	5	0	1	5	0	36.5
RMCA	96.036-M-5460	1	3	1	1	3	1	0	4	0	0	4	0	32.2
RMCA	96.036-M-5462	1	2	0	1	2	0	1	2	0	1	2	0	26.8
RMCA	96.036-M-5467	0	5	1	0	5	1	1	5	1	1	5	1	45.6
RMCA	96.036-M-5472	0	4	0	0	4	0	1	4	1	1	4	1	33.4
RMCA	96.036-M-5473	1	3	0	0	4	0	1	4	0	1	3	1	37.8
RMCA	96.036-M-5474	0	4	1	0	4	0	1	4	1	1	4	1	38.4
RMCA	96.036-M-5537	1	3	1	1	3	1	1	4	1	0	5	0	42.4
RMCA	96.037-M-5591	1	3	0	1	3	0	1	3	0	1	3	0	30.7
RMCA	96.037-M-5596	1	4	1	1	4	0	1	5	0	1	5	0	34.6
RMCA	96.037-M-5599	1	3	0	1	3	0	1	3	0	1	3	0	28.1
RMCA	96.037-M-5601	1	3	1	0	4	0	1	5	0	1	5	0	35.4
RMCA	96.037-M-5607	1	3	0	1	3	0	1	3	1	1	3	1	33.4
RMCA	96.037-M-5616	1	3	0	1	3	0	1	2	1	1	3	0	30.0
RMCA	96.037-M-5617	0	3	1	0	3	1	0	3	1	0	3	1	36.1
RMCA	96.037-M-5620	1	3	1	1	4	0	1	4	0	1	4	0	34.4
RMCA	96.037-M-5622	1	3	0	1	3	0	1	3	0	1	3	0	33.2
RMCA	96.037-M-5627	1	3	0	1	3	0	1	3	0	1	3	0	29.6
RMCA	96.037-M-5628	1	4	0	1	4	0	1	4	1	1	4	1	34.0
RMCA	96.037-M-5630	0	5	0	0	4	1	0	5	0	1	4	1	37.1

Table S2. Statistics on *Heliophobius* dentitions

Statistics	Left lower teeth			Right lower teeth			Left upper teeth			Right upper teeth		
	Erupting	Functional	Worn out	Erupting	Functional	Worn out	Erupting	Functional	Worn out	Erupting	Functional	Worn out
Percentages	70.9		45.5	60.0		36.4	69.1		41.8	67.3		41.8
Two functional teeth		1.8			1.8			3.6			1.8	
Three functional teeth		30.9			25.5			14.5			21.8	
Four functional teeth		58.2			61.8			58.2			49.1	
Five functional teeth		9.1			10.9			23.6			27.3	

Table S3. Data concerning the jugal dentition of each *Georychus* specimen

Institution	Specimen	Functional teeth	Erupting teeth	Skull length, mm
NHM	37.9.26.111	P4		20
MNHN	1988-111	P4	M1	22
NHM	43.2.28.5	P4-M1		27.9
NHM	95.9.3.18	P4-M1	M2	32.3
NHM	859b	P4-M1-M2		33.9
NHM	859e	P4-M1-M2		36.7
NHM	95.9.3.15	P4-M1-M2		34.3
NHM	95.9.3.14	P4-M1-M2		33.7
MNHN	1988-112	P4-M1-M2		38.3
NHM	46.11.18.46	P4-M1-M2	M3	39.4
NHM	43.2.28.4	P4-M1-M2	M3	33.7
NHM	859c	P4-M1-M2	M3	39
NHM	95.9.3.16	P4-M1-M2-M3		39.4
NHM	66.6.16.2	P4-M1-M2-M3		—
MNHN	1988-113	P4-M1-M2-M3		49.1

Annex 2

Rsk2 and the mouse craniofacial development

RSK2 Is a Modulator of Craniofacial Development

Virginie Laugel-Haushalter¹, Marie Paschaki¹, Pauline Marangoni², Coralie Pilgram³, Arnaud Langer³, Thibaut Kuntz³, Julie Demassue³, Supawich Morkmued^{1,3,7}, Philippe Choquet⁴, André Constantinesco⁴, Fabien Bornert^{3,6}, Matthieu Schmittbuhl^{3,5,6}, Solange Pannetier¹, Laurent Viriot², André Hanauer¹, Pascal Dollé¹, Agnès Bloch-Zupan^{1,3,5*}

1 Institute of Genetics and Molecular and Cellular Biology (IGBMC), Centre National de la Recherche Scientifique (UMR 7104), Institut National de la Santé et de la Recherche Médicale (U 964), University of Strasbourg, Illkirch, France, **2** Team «Evo-Devo of Vertebrate Dentition», Institut de Génétique Fonctionnelle de Lyon, Unité Mixte de Recherche 5242 Centre National de la Recherche Scientifique, Ecole Normale Supérieure de Lyon, Claude Bernard Lyon 1 University, Lyon, France, **3** Faculty of Dentistry, University of Strasbourg, Strasbourg France, **4** UF6237 Preclinical Imaging Lab, Biophysics and Nuclear Medicine, Hôpitaux Universitaires de Strasbourg (HUS), Strasbourg, France; ICube, CNRS, University of Strasbourg, Strasbourg, France, **5** Reference Centre for Orofacial Manifestations of Rare Diseases, Pôle de Médecine et Chirurgie Bucco-dentaires, Hôpitaux Universitaires de Strasbourg (HUS), Strasbourg, France, **6** INSERM U1121, "Biomaterials and Bioengineering", University of Strasbourg, Strasbourg, France, **7** Faculty of Dentistry, Khon Kaen University, Khon Kaen, Thailand

Abstract

Background: The *RSK2* gene is responsible for Coffin-Lowry syndrome, an X-linked dominant genetic disorder causing mental retardation, skeletal growth delays, with craniofacial and digital abnormalities typically associated with this syndrome. Craniofacial and dental anomalies encountered in this rare disease have been poorly characterized.

Methodology/Principal Findings: We examined, using X-Ray microtomographic analysis, the variable craniofacial dysmorphism and dental anomalies present in *Rsk2* knockout mice, a model of Coffin-Lowry syndrome, as well as in triple *Rsk1,2,3* knockout mutants. We report *Rsk* mutation produces supernumerary teeth midline/mesial to the first molar. This highly penetrant phenotype recapitulates more ancestral tooth structures lost with evolution. Most likely this leads to a reduction of the maxillary diastema. Abnormalities of molar shape were generally restricted to the mesial part of both upper and lower first molars (M1). Expression analysis of the four *Rsk* genes (*Rsk1*, 2, 3 and 4) was performed at various stages of odontogenesis in wild-type (WT) mice. *Rsk2* is expressed in the mesenchymal, neural crest-derived compartment, correlating with proliferative areas of the developing teeth. This is consistent with RSK2 functioning in cell cycle control and growth regulation, functions potentially responsible for severe dental phenotypes. To uncover molecular pathways involved in the etiology of these defects, we performed a comparative transcriptomic (DNA microarray) analysis of mandibular wild-type versus *Rsk2*-Y molars. We further demonstrated a misregulation of several critical genes, using a *Rsk2* shRNA knock-down strategy in molar tooth germs cultured *in vitro*.

Conclusions: This study reveals RSK2 regulates craniofacial development including tooth development and patterning via novel transcriptional targets.

Citation: Laugel-Haushalter V, Paschaki M, Marangoni P, Pilgram C, Langer A, et al. (2014) RSK2 Is a Modulator of Craniofacial Development. PLoS ONE 9(1): e84343. doi:10.1371/journal.pone.0084343

Editor: Yann Gibert, Deakin School of Medicine, Australia

Received: May 21, 2013; **Accepted:** November 21, 2013; **Published:** January 8, 2014

Copyright: © 2014 Laugel-Haushalter et al. This is an open-access article distributed under the terms of the Creative Commons Attribution License, which permits unrestricted use, distribution, and reproduction in any medium, provided the original author and source are credited.

Funding: This work was supported by grants (to AB-Z) from the University of Strasbourg, the Hôpitaux Universitaires de Strasbourg (API, 2009-2012, "Development of the oral cavity: from gene to clinical phenotype in Human"), IFRO (Institut Français pour la Recherche Odontologique), by institutional funds from the Centre National de la Recherche Scientifique (CNRS) and Institut National de la Santé et de la Recherche Médicale (INSERM). This project, A27 "Orofacial manifestations of rare diseases", selected by the Offensive Sciences of the Trinational Metropolitan Area Upper Rhine (TMR), is co-financed by the European Regional Development Fund (ERDF) of the European Union, in the framework of the INTERREG IV Upper Rhine programme. VL-H was the recipient of a PhD fellowship from the Ministère Français de la Recherche. MP was supported by a grant from the Agence Nationale de la Recherche (to PD). The funders had no role in study design, data collection and analysis, decision to publish, or preparation of the manuscript.

Competing Interests: The authors have declared that no competing interests exist.

* E-mail: agnes.bloch-zupan@unistra.fr

Introduction

The ribosomal S6 family of serine/threonine kinases is composed of 4 highly related members in mammals: RSK1 (human chromosome 3), RSK2 (*RPS6KA3*, Xp22.2-p22.1), RSK3 (chromosome 6) and RSK4 (Xq21), which are 75% homologous and are implicated in several important cellular events including proliferation, differentiation, cellular stress response and apoptosis. Mutations in *RSK2* cause X-linked Coffin-Lowry syndrome (OMIM #303600) characterized by psychomotor and growth

retardation, with typical facial and digital abnormalities and progressive skeletal malformations like delayed bone development, spinal kyphosis/scoliosis, and sternum/rib protrusions (pectus carinatum) or depression (excavatum) [1,2,3]. Orofacial findings include a high narrow palate, a midline lingual furrow, malocclusion, hypodontia, and peg shaped incisors (Fig. 1). Premature loss of the primary dentition was also observed, and wide spaced teeth and large medial incisors were reported [1,4,5].

RSKs are Ser/Thr protein kinases that act at the distal end of the Mitogen-Activated Protein Kinase/Extracellular signal-Regu-

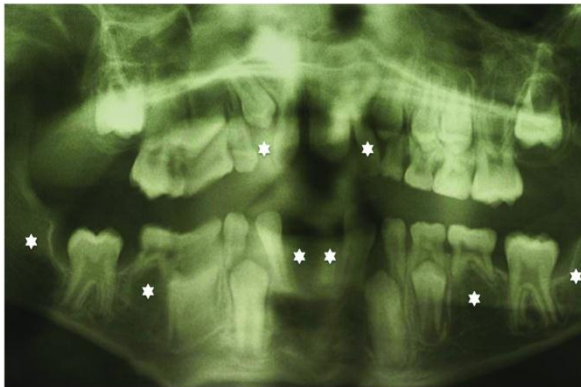


Figure 1. Dental anomalies encountered in Coffin-Lowry syndrome. This panoramic radiograph shows oligodontia (more than six permanent missing teeth (white stars: 12, 22, 41, 31, 45, 35, 47, 37). The deformations observed on this panoramic radiograph are linked to movements during the X-Ray acquisition process and difficulties for handicapped patient to remain still during the procedure.
doi:10.1371/journal.pone.0084343.g001

lated Kinase (MAPK/ERK) signalling pathway. The various RSK proteins are widely expressed, with many cell types expressing several members. RSKs are directly phosphorylated and activated by ERK1/2 in response to several growth factors [6]. In the cytosol, RSK proteins have been shown to phosphorylate substrates including GSK3, LICAM, the Ras GEF-Sos, I κ B, the p34cdc2-inhibitory kinase Myt1, the translation factors eEF2 and eIF4B, and the pro-apoptotic protein BAD [7,8]. Moreover, upon activation a fraction of the cytosolic RSKs translocate to the nucleus where they are thought to regulate gene expression through phosphorylation of transcription factors such as CREB1, ER α , Nurr77 and SRF, as well as histones [7]. The contribution of each RSK family member to the *in vivo* activation of most of these substrates is currently not well defined.

RSK orthologues have been identified in mouse, rat, chicken, *Xenopus* and *Drosophila* [9]. *Rsk2* knockout mice display spatial learning and memory impairment [10] and develop a progressive osteopenia due to impaired osteoblast function [11]. Lack of phosphorylation of the transcription factor ATF4 is responsible for the skeletal abnormalities in *Rsk2* knockout mice [10]. Murine *Rsk2* is highly expressed during somitogenesis, suggesting skeletal and muscle growth and/or patterning roles, potentially leading to the numerous skeletal abnormalities encountered in the human syndrome [12]. It is interesting to note that *Rsk2* shows specific developmental patterns of expression in the maxillary and the mandibular components of the first branchial arch [12], and that craniofacial and dental anomalies are present in the clinical synopsis of Coffin-Lowry syndrome.

The mouse dentition is a powerful and useful model to study the mechanisms leading to human dental anomalies, despite some intrinsic differences. The mouse has a monophyodont dentition that encompasses only four permanently growing incisors and 12 molars separated by a diastema [13]. Most mutant mouse models for human syndromic and non-syndromic genetic disorders displaying dental defects mimicking human pathologic phenotypes [14], although some discrepancies have been reported [15]. In this study, we describe the craniofacial and orodontal phenotype of *Rsk2*-*Y* knockout mice, as well as triple *Rsk1,2,3*-/- mutants. By employing several additional approaches (expression analysis by *in situ* hybridization, comparative transcriptomic analysis, shRNA

knock-down in tooth germ explants) we establish RSK2 regulates defined processes in odontogenesis and craniofacial growth.

Results

Rsk2-*Y* craniofacial phenotype

The craniofacial phenotype was assessed by X-Ray microtomographic imaging and analyzed through euclidean distances measurement and comparison. This phenotype was variable, ranging from normality (mutant mice 702, 731) to obvious craniofacial dysmorphology (mutant mice 150, 700) (Fig. 2). Some mutant mice show an intermediate phenotype, with skulls smaller in length but not in width.

An overall skull length reduction from the nasal to the occipital bone was a collective measure of the sum defects in the nasal, frontal, parietal, interparietal/occipital bones. The frontal bone always exhibited the greatest reductions in length of all skull bones. The interparietal/occipital bones were the least affected (distances 1-4, 1-5, 2-3, 2-4, 2-5 being more reduced than 1-2 or 1-3; see Table 1; measurements were performed according to anatomical landmarks detailed in Fig. S1). A nasal deviation was observed in some mutant mice (Fig. 2B,C,E; Table 1). Craniofacial microtomographic analysis of *Rsk1,2,3*-/- mice was not performed, due to rare availability of these triple mutants. Analysis thus focused on *Rsk2*-*Y* mice, a defined genetic model of human Coffin-Lowry syndrome.

Rsk2-*Y* and *Rsk1,2,3*-/- dental phenotype

Phenotype of molar tooth rows. We analyzed 15 *Rsk2*-*Y* mice and 9 *Rsk1,2,3*-/- mutant mice (see Table 2 and Fig. 3). Supernumerary teeth (ST) occurred in all specimens except for two *Rsk2*-*Y* mice (702, 731). ST were aligned with the molar tooth row and located just in front and at the contact of the first molars (M1).

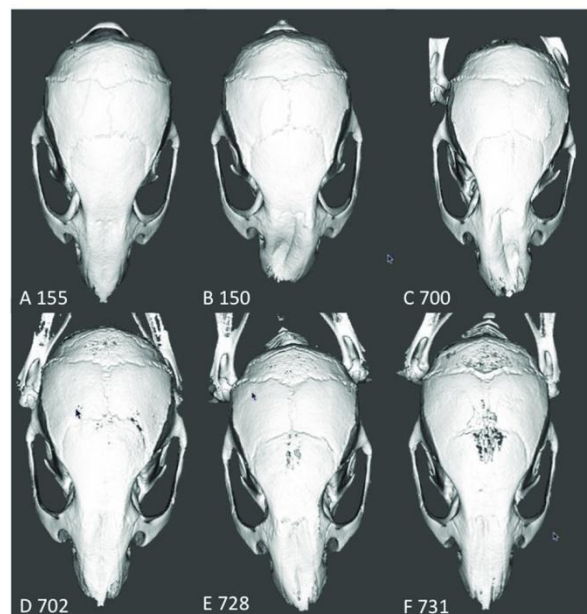


Figure 2. Craniofacial phenotype of *Rsk2*-*Y* mice assessed by X-Ray microtomography. The craniofacial phenotype is highly variable, ranging from an almost normal-shaped cranium (mutant 155), although smaller in length, to a very dysmorphic appearance with a lateral nasal deviation. For mutant identification see Table 1.
doi:10.1371/journal.pone.0084343.g002

Table 1. Distances between skull landmarks on wild-type and *Rsk2*-*Y* mutant mice.

Distances	Mean WT	STD WT	Mean <i>Rsk2</i> mutants	STD <i>Rsk2</i> mutants	p-value
Between 1 and 2	7.10	0.59	6.84	0.35	0.03
Between 1 and 3	15.05	0.46	13.92	0.59	0.01
Between 1 and 4	18.59	0.41	17.24	0.57	0.005
Between 1 and 5	21.87	0.49	20.48	0.48	0.005
Between 2 and 3	8.07	0.45	7.25	0.47	0.005
Between 2 and 4	11.72	0.38	10.69	0.45	0.005
Between 2 and 5	15.21	0.35	14.13	0.31	0.005
Between L and R 6	12.08	0.17	12.16	0.13	0.47
Between L and R 7	6.42	0.21	6.45	0.27	0.68
Between L and R 8	4.77	0.11	4.79	0.73	0.22
Between L and R 9	6.27	0.25	6.13	0.12	0.06
Between L and R 10	0.74	0.06	0.71	0.08	0.47
Between L and R 11	1.05	0.05	1.13	0.11	0.29
Between L and R 12	10.08	0.37	10.22	0.28	0.29
Between L and R 15	4.53	0.19	4.72	0.51	0.37
Between L and R 16	2.29	0.22	2.23	0.23	0.57
Between 1 and 6R	15.24	0.34	14.39	0.52	0.008
Between 1 and 6L	15.20	0.32	14.47	0.31	0.008
Between 1 and 7R	7.92	0.28	7.18	0.58	0.008
Between 1 and 7L	7.89	0.22	7.24	0.34	0.005
Between 1 and 8R	6.90	0.24	6.29	0.46	0.88
Between 1 and 8L	6.90	0.25	6.35	0.29	0.68
Between 1 and 9R	20.65	0.47	19.55	0.46	0.008
Between 1 and 9L	20.62	0.48	19.56	0.32	0.008

In bold are distances significantly different between wild-type (WT) and mutants (all these distances were shorter in mutants). Anatomical landmarks are explained in Fig. S1 (supplementary information). All distances are in millimeters. STD: standard deviation; L: left; R: right.
doi:10.1371/journal.pone.0084343.t001

The phenotype penetrance was higher in the upper dentition (65% in *Rsk2*-*Y* mice, 83% in *Rsk1,2,3*-/- mice) than in the lower dentition (31% and 11%, respectively). Shape and size of the supernumerary teeth were variable and ranged from a monocuspid tooth to a well-shaped molar-like tooth. ST were always smaller in size than the adjacent first molars, and they were sometimes, especially in the *Rsk1,2,3*-/- upper rows, as big as the M2. Inactivation of *Rsk2* alone was sufficient to generate the phenotype. When a ST was present, the mesial part of the first molar displayed altered crown morphology (Fig. 3). Even when the phenotype looked almost normal, a significant reduction in M1-M3 length was observed (Table 3). When ST occurred, the length mean value was always reduced for both M1 and M2 (Table 3). ST were always longer than M3. Molar width remained stable for M1, but was reduced for M2 and M3, except when only 3 molars were present in the mandible (Table 4). Shape abnormalities mainly occurred in mesial parts of the first lower (M1) and first upper (M1) molars in *Rsk2*-*Y* mice. In upper M1, the central cusp of the mesial crest tended to be reduced, and the crest itself was more flattened (see red dotted circles in Fig. 3). Accordingly the mesial crest of the lower M1 also had an abnormal shape, because this crest tended to be strongly reduced when a ST occurred (see yellow dotted circles in Fig. 3). In triple mutants without ST (e.g. 789), the lower M1 displayed a mesial crest with vestibular cusp bigger than in WT.

The length of the molar row was significantly reduced in both the lower and upper jaws when no ST was present. When a ST

occurred, the length of the molar row was almost normal in the mandible, but was significantly higher in the maxilla when compared to WT (Table 3). Some *Rsk1,2,3*-/- mouse specimens displayed 3 upper postcanine teeth, as in the WT, but the dental row encompassed maxillary ST-M1-M2, and lacked the M3. Consequently, the second tooth (M1) was bigger than neighbouring teeth ST and M2 (Fig. 3, specimen 1283).

Incisor phenotype. No statistically significant differences were revealed between right and left incisors in both groups ($p > 0.05$). As a consequence, results from right and left incisors were merged (Table 5). No statistical difference was observed between WT and *Rsk2*-*Y* ($p > 0.05$). No obvious incisor anomaly was detected. Analysis of the incisor phenotype in *Rsk1,2,3*-/- mice was not performed due to a reduced number of available animals, visual inspection however did not reveal any incisor dental defects. The existence of incisor anomalies in *Rsk1,2,3*-/- cannot be ruled out.

Abnormal molar root development in *Rsk2*-*Y* mice. Both the number and shape of molar roots also reflect the tooth identity. In WT mice the mandibular molars M1 and M2 have 2 roots, whereas M3 has only one root. The maxillary molars M1 and M2 have 3 roots. Variations in the root number of M3 occur both within and among various WT strains. The upper M3 molar usually has 2 or 3 roots, although sometimes it has only 1 root. Thus, the total number of molar roots is 5 per hemi-mandible, whereas it can vary from 7 to 9 per hemi-maxillary. In *Rsk2*-*Y* mice, hemi-mandibles harbouring a ST had a total root number of 6, with the ST always having a single root. In the

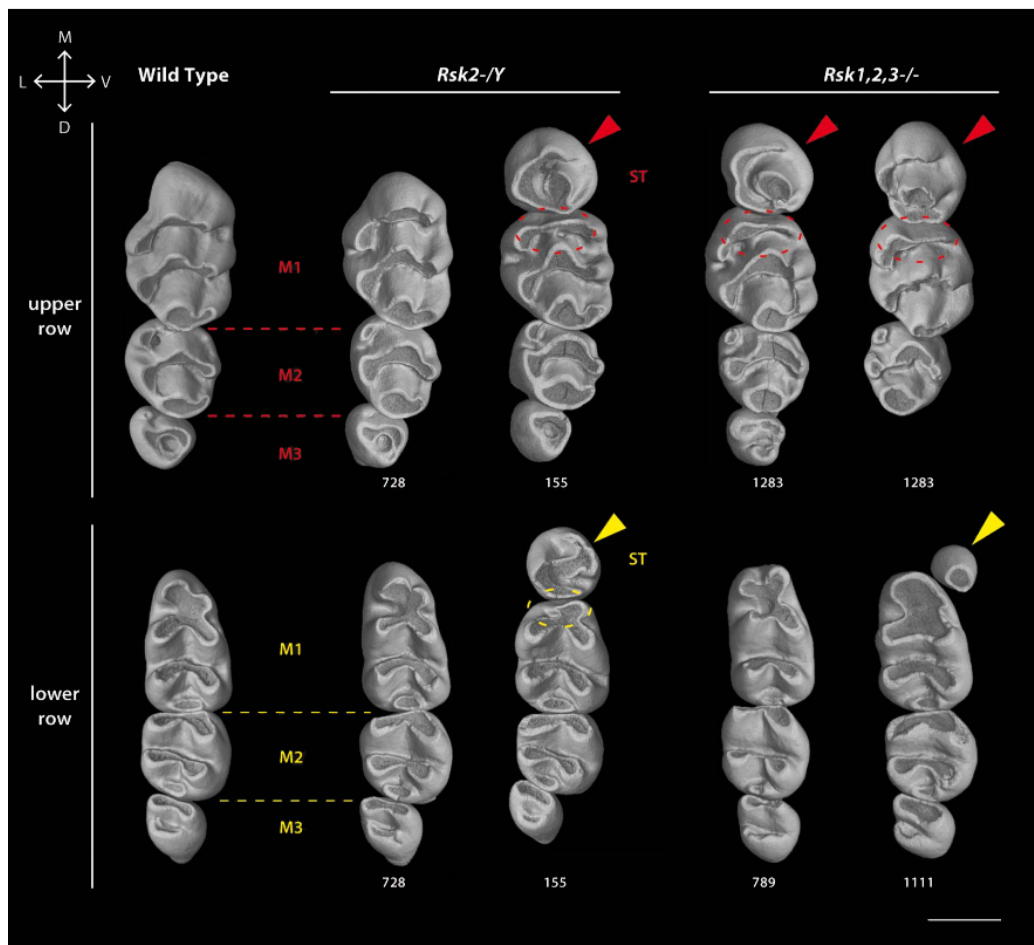


Figure 3. Variation of molar shape, size and number in *Rsk2*^{-/Y} and *Rsk1,2,3*^{-/-} mice analyzed by X-Ray microtomography. All molar rows are oriented in the same manner (top corresponds to mesial and left to lingual side). At the left are wild-type molars, other rows are mutants as indicated. Arrowheads point to the supernumerary teeth ST; dotted ellipses show the reduction of the mesial-most affected cusp. Scale bar: 0.7 mm. doi:10.1371/journal.pone.0084343.g003

maxillary quadrant, the total root number varied from 8 to 9 when a ST was present. ST could have 1 or 2 roots, M1 had 2 roots, but the M2 root number remained stable with 3 roots (Table S1 in File S1). The presence of maxillary M1 with only 2 roots probably correlates with the occurrence of ST, often associated to a compression and a reduction of the mesial part of M1.

Rsk2^{-/Y} and the diastema. The maxillary diastema was significantly reduced in *Rsk2*^{-/Y} mice harbouring ST (Table 6). This was not the case for the mandibular diastema, whatever the number of teeth.

Expression patterns of *Rsk* genes during mouse odontogenesis

To investigate whether the dental anomalies observed in the *Rsk*-deficient mice may correlate with distinct patterns of expression of *Rsk* genes during odontogenesis, we performed an in situ hybridization analysis of *Rsk1*, *Rsk2*, *Rsk3* and *Rsk4* mRNA transcripts at various stages of tooth development. All four genes were found to be expressed in specific areas of the tooth anlagen, as illustrated in Fig. 4

for the developing first molars, and Fig. 5 for the mandibular incisors. Their expression features are summarized in Table 7.

Rsk2 transcripts were mainly localized in the mesenchymal compartment or dental papilla from E12.5 (dental lamina stage) to E19.5 (late bell stage). At E16.5 (bell stage), the transcripts were scattered in the area facing the epithelial loops or at the base of the cusps; the second molar dental mesenchyme was uniformly labelled. In the incisors the transcripts were also located in the mesenchyme, and the signal was more intense in the labial area and posterior area.

The expression of *Rsk1* and *Rsk4* was mainly epithelial, marking the inner dental epithelium and especially the epithelial loop areas. A faint signal was also observed for *Rsk4* in the posterior mesenchymal area facing the epithelial loops especially the labial loop for incisors (E16.5 and 19.5).

Rsk3 transcripts were mainly visible in the dental papilla at E14.5 (cap stage), E16.5 (bell stage) and E19.5 (Figs. 4, 5 and Table 7). At E19.5 the transcripts were concentrated in the cervical part of the papilla for the first molar and had a wider distribution in the second molar mesenchyme.

Table 2. Presence (+) of a supernumerary tooth (mesial to the first molar) in *Rsk* mutant mice.

Mouse	Genotype	Upper Right	Upper Left	Lower Right	Lower Left
11	<i>Rsk2</i> ^{-Y}	+ (4)	+ (4)	+ (4)	N
25	<i>Rsk2</i> ^{-Y}	+ (4)	+ (4)	N	+ (4)
37	<i>Rsk2</i> ^{-Y}	+ (4)	+ (4)	+ (4)	N
39	<i>Rsk2</i> ^{-Y}	+ (4)	+ (4)	N	N
46	<i>Rsk2</i> ^{-Y}	+ (4)	N	N	N
61	<i>Rsk2</i> ^{-Y}	+ (4)	+ (4)	N	N
62	<i>Rsk2</i> ^{-Y}	N	+ (4)	N	N
150	<i>Rsk2</i> ^{-Y}	+ (4)	+ (4)	+ (4)	+ (4)
155	<i>Rsk2</i> ^{-Y}	+ (4)	+ (4)	+ (4)	+ (4)
184	<i>Rsk2</i> ^{-Y}	+ (4)	+ (4)	+ (4)	+ (4)
185	<i>Rsk2</i> ^{-Y}	+ (4)	+ (4)	N	N
700	<i>Rsk2</i> ^{-Y}	N	N	N	+ (4)
702	<i>Rsk2</i> ^{-Y}	N	N	N	N
728	<i>Rsk2</i> ^{-Y}	+ (4)	N	N	N
731	<i>Rsk2</i> ^{-Y}	N	N	N	N
789	<i>Rsk1,2,3</i> ^{-/-}	+ (4)	+ (4)	N	N
793	<i>Rsk1,2,3</i> ^{-/-}	+ (4)	N	N	N
860	<i>Rsk1,2,3</i> ^{-/-}	+ (4)	N	+ (4)	N
883	<i>Rsk1,2,3</i> ^{-/-}	+ (4)	+ (3)	N	N
1105	<i>Rsk1,2,3</i> ^{-/-}	+ (4)	N	N	N
1111	<i>Rsk1,2,3</i> ^{-/-}	+ (3)	+ (3)	+ (4)	N
1283	<i>Rsk1,2,3</i> ^{-/-}	+ (3)	+ (4)	N	N
1139	<i>Rsk1,2,3</i> ^{-/-}	+ (3)	+ (4)	N	N
1159	<i>Rsk1,2,3</i> ^{-/-}	+ (4)	+ (3)	N	N

N: normal pattern of 3 molars M1, M2, M3. (3) means the presence of only 3 molars but the size of the second one is bigger (most probably there is a supernumerary tooth ST in front of M1, and M3 is missing).
doi:10.1371/journal.pone.0084343.t002

Rsk2^{-Y} supernumerary tooth is associated with an extra mesial placode

An extra tooth placode, and subsequent enamel knot labelled with *Sonic hedgehog* (*Shh*) as a marker, was clearly visible at E14.5, mesially to M1 in *Rsk2*^{-Y} mice when compared to WT littermates (Fig. 6). The presence of this extra placode was seen in nearly 30% of the analysed embryo and was not always simultaneously present on right and left sides of the jaw. During WT development the three molars (M1, M2 and M3) are forming from a unique molar placode. The presence of an additional dental placode mesially to the M1 placode likely corresponds to the primordium of ST developing in *Rsk2*^{-Y} mutants.

Rsk2^{-Y} transcriptome analysis

We performed a comparative transcriptomic analysis (Affymetrix GeneChips) of wild-type and *Rsk2*^{-Y} mice, analyzing RNA isolated from dissected E14.5 mandibular molar tooth germs. By using a principal component analysis (PCA), it was possible to discriminate between the molar samples according to their genotype (wild-type versus *Rsk2*^{-Y}) (Fig. 7). 504 genes were retrieved as being differentially expressed, with fold changes exceeding ± 1.2 and a false discovery rate below 0.1. The fold changes were however rather low, ranking between +2.044 and

-1.98, suggesting that rather minimal molecular changes, at the transcriptome level, were taking place. These changes could be also minimized by a heterogeneous sampling for *Rsk2*^{-Y} molars, with putative phenotypes ranking as previously described between normality and a 3 molars with a supernumerary tooth phenotype; this phenotype was not known at the E14.5 cap stage, when molar germs were pooled for transcriptomic analysis. The most affected (“top ten”) genes, and a selection of additional genes being up- or down-regulated, are listed in Table 8 and Table 9.

The *Rdh1* gene encoding retinol dehydrogenase (RDH) 1 was found to be the most up-regulated gene in *Rsk2*^{-Y} mutant mice. In addition to retinol dehydrogenase activity, this enzyme has strong 3 α -hydroxy steroid dehydrogenase- and weak 17 β -hydroxy steroid dehydrogenase- activities. *Rdh1* exhibits widespread and intense mRNA expression in many embryonic tissues including the neural tube, gut, and neural crest, as well as in adult mice [16]. Interestingly, retinoic acid (the end product of retinol oxidation initiated by RDH enzymes) is involved in tooth morphogenesis and differentiation, and abnormal retinoic acid levels can lead to dental anomalies [17,18,19,20].

Sectm1b, encoding secreted and transmembrane protein 1B, was the most down-regulated gene in *Rsk2*^{-Y} mutant mice. This gene and protein had never been described previously as potentially involved in odontogenesis.

Among the differentially expressed genes selected (Table 9) as belonging to signalling pathways acting during tooth development (TGF- β , FGF, Wnt, NF- κ B) and/or cell cycle progression, *Egf2* is a proto-oncogene acting together with Wnt4 in an autoregulatory feedback loop [21]. Inactivation of this gene causes numerous tumours in mice [22]. *Egf2* was down-regulated in *Rsk2*^{-Y} mutants.

We tried unsuccessfully to confirm those results on a selection of genes by qRT-PCR, comparing three *Rsk2*^{-Y} and three WT molar RNA samples. This negative result might be explained by the heterogeneous nature of the *Rsk2*^{-Y} phenotype (as described above), the relative low level of expression changes, and may not invalidate the microarray data.

Rsk2 inactivation *in vitro*

In order to overcome the potential problem of *Rsk2*^{-Y} molar samples heterogeneity we decided to use an *in vitro* system, and inactivated *Rsk2* by microinjection and electroporation of shRNA in E14.5 molar tooth germs. *In vivo* electroporation in the mandible, as previously described by [23] was not suitable for our study, because of the lack of precision on the targeted zone and our aim to inactivate the gene directly within the tooth anlagen.

We optimized the experimental settings to inject and electroporate *Rsk2* shRNA in cap stage molars explanted and cultured *ex vivo*. Control explants were electroporated with a random shRNA construct. After electroporation the explants were placed into collagen drop culture to maintain their morphology [24] and kept in a defined culture medium for 24 h, before being processed for qRT-PCR analysis. Tooth morphology was preserved and neither apoptosis nor cell death were induced, as shown by activated caspase3 and TUNEL assays (data not shown).

Rsk2 shRNA electroporation efficiently diminished *Rsk2* expression by 75% (Fig. 8A). We then analyzed *Egf2* and *Rdh1* expression, and found that *Egf2* expression was down-regulated (75% decrease) (Fig. 8B), while *Rdh1* expression was up-regulated (50% increase) (Fig. 8C). These results were in accordance with the microarray data. The new combined technique allowed us not only to optimize a protocol for studying the molecular mechanisms of early tooth development, but also to set up a new approach for microarray validation.

Table 3. Comparison of each molar length, of the total molar field length, and the total length of M1+ M2, between wild-type (WT) mice and *Rsk2*-Y mutant mice with 3 or 4 molars.

	Mandibular molars WT	Mandibular molars Mutant 3M	Mandibular molars Mutant 4M	Maxillary molars WT	Maxillary molars Mutant 3M	Maxillary molars Mutant 4M
Mean ST			0.60			0.74
STD			0.01			0.02
Mean M1	1.44	1.37	1.14	1.56	1.38	1.14
STD	0.03	0.11	0.05	0.07	0.10	0.09
p-value		0.23	0.0004		0.01	0.001
Mean M2	0.89	0.85	0.79	0.92	0.85	0.82
STD	0.03	0.02	0.03	0.02	0.04	0.05
p-value		0.003	0.004		0.02	0.01
Mean M3	0.59	0.53	0.49	0.60	0.63	0.63
STD	0.02	0.03	0.04	0.03	0.03	0.05
p-value		0.0002	0.0004		0.96	0.15
Total	2.93	2.75	2.88	3.08	2.85	3.31
STD	0.04	0.15	0.28	0.10	0.13	0.06
p-value		0.0008	0.36		0.01	0.001
M1+ M2	2.33	2.10	2.15	2.48	2.30	1.96
STD	0.04	0.16	0.21	0.08	0.14	0.13
p-value		0.03	0.004		0.002	0.001

M1 size is reduced in mutants with 4 molars both in mandible and maxilla, but only in the maxilla of mutants showing 3 molars. M2 is reduced both in maxilla and mandible whatever the molar mutant phenotype. M3 mesiodistal dimension is reduced only in the mandible, irrespective of the presence of 3 or 4 molars. The total size of the molar field is reduced in the mandible and maxilla in mutant with 3 molars. The total size of the molar field is significantly increased in the maxilla in mutants with 4 molars. The total size of M1+M2 was always reduced when compared to the wild type value. All distances are in millimeters. Significant p-values are shown in bold. M1 : molar 1; M2 : molar 2; M3 : molar 3; ST : supplementary tooth in front of M1; STD : standard deviation; Mutant 3M : mutant with 3 molars; Mutant 4M : mutant with 4 molars; Total : total length of all molars in the molar field.
doi:10.1371/journal.pone.0084343.t003

Discussion

A peculiar dental phenotype

Mice are commonly studied mammals for investigating the mechanisms of tooth development and evolution. The orodental

phenotype of mouse models of human genetic disorders also often mimics dental anomalies encountered in human rare diseases [14]. Basal placental mammals had a dental formula including three incisors, one canine, four premolars, and three molars per dentition quadrant [13,25]. Through evolution, almost all

Table 4. Comparison of each molar width (vestibulolingual dimension) between wild-type and *Rsk2*-Y mutant mice with 3 or 4 molars.

	Mandibular molars WT	Mandibular molars Mutants 3M	Mandibular molars Mutants 4M	Maxillary molars WT	Maxillary molars Mutants 3M	Maxillary molars Mutants 4M
Mean ST			0.59			0.76
STD			0.09			0.04
Mean M1	0.79	0.77	0.82	1.04	1.01	1.06
STD	0.02	0.04	0.03	0.05	0.05	0.02
p-value		0.19	0.12		0.19	0.56
Mean M2	0.85	0.85	0.81	0.90	0.86	0.86
STD	0.02	0.02	0.03	0.02	0.05	0.03
p-value		0.89	0.02		0.03	0.02
Mean M3	0.60	0.57	0.58	0.61	0.58	0.54
STD	0.02	0.02	0.05	0.03	0.02	0.04
p-value		0.006	0.06		0.02	0.01

In mutants the width of M1 was not modified. The width of the maxillary M2 and M3 was reduced. In the mandible the width of M2 was lower only when 4 molars were present, and the width of M3 was lower only in mutants with 3 molars (all distances in millimeters; significant p-values in bold).

M1 : molar 1; M2 : molar 2; M3 : molar 3; ST : supplementary tooth in front of M1; STD : standard deviation; Mutant 3M : mutant with 3 molars; Mutant 4M : mutant with 4 molars.

doi:10.1371/journal.pone.0084343.t004

Table 5. Morphological analysis of mandibular incisors in WT and *Rsk2*-*Y* mice.

		Li (mm)	hi (mm)	Hi (mm)	li (mm)	ti (mm)	lpa (mm ²)
WT	Mean	11.33	1.11	2.96	9.38	0.65	10.36
	STD	2.34	0.07	0.20	1.56	0.02	1.07
<i>Rsk2</i> - <i>Y</i>	Mean	11.29	1.14	2.97	9.05	0.65	10.18
	STD	1.66	0.05	0.21	1.65	0.03	1.33

No statistically significant differences were revealed between right and left incisors in both groups ($p > 0.05$). As a consequence, results from right and left incisors were merged. No statistical difference was observed between WT and *Rsk2*-*Y* ($p > 0.05$).

(Li) length of the longest and external bow, (hi) height of median part of the incisor, (Hi) total height of the incisor, (li) horizontal length of the incisor joining the tip to the distal extremity of the root, (lpa) projected area in lateral view of the incisor, (ti) thickness the median part of the incisor. For more explanations on the measured distances, see Figure S3. STD : standard deviation.
doi:10.1371/journal.pone.0084343.t005

mammals reduced their dental formulas, but lost functional teeth sometimes remaining as rudiments that begin to develop and then abort. The dentition of the mouse comprises 4 functional teeth in each quadrant (1 incisor and 3 molars separated by a toothless space called diastema). Rudimentary tooth primordia have been reported to develop in the distal part of the diastema through the initial stages of odontogenesis of WT mice. However their development ceases before the cap stage and they regress by apoptosis [26,27,28]. The tooth phenotype encountered in the *Rsk2*-*Y* mutant mouse is remarkable by the occurrence of supernumerary teeth at the positions of the fourth premolars. Fourth premolars are still present in certain rodent groups such as squirrels, and have been lost through muroid rodent evolution [13].

Rsk2 phenotype is similar to the tabby phenotype

Supernumerary teeth within the diastema were described in other mouse mutants for *ectodin*, *Lrp4*, *Sprouty2/4*, *Wise*, *Polaris*, and *Gas1* [29,30,31,32,33,34,35,36]. Dysfunctions of the FGF, Shh, Wnt, and/or NF-kappaB signalling pathways are thought to induce formation of these supernumerary teeth within the diastema, indicating that the mouse maintains genetic potentialities that could be stimulated and induce the formation of supernumerary teeth [37,38].

Ectopic teeth in the diastema are also observed in mice misexpressing *Eda* (ectodysplasin A; also known as Ta; Ed1; EDA1; XLHED; tabby) and *EdaA* receptor (Edar) [39,40,41,42].

The dental phenotype of the *Rsk2*-*Y* mouse resembles that encountered in the *tabby* mouse (a model for X-linked hypohidrotic ectodermal dysplasia- an ectodermal dysplasia characterized by an absence or dystrophic development of hair, nail, sweat- lacrymal-mammary- glands and tooth; OMIM #305100). Mutations in the human X-linked gene *ED1* (the *Eda* orthologue) are responsible for this disorder [43,44,45,46]. Ontogenetic and phylogenetic data together suggest that the occurrence of functional supernumerary teeth in *tabby* mice diastema is caused by the persistence of the premolar rudiments that usually regress in WT mice. It has thus been proposed that this phenotype may represent an evolutionary throwback or atavism [43,44,45,46].

Recently it has been shown that the number of teeth is regulated by fine-tuning of the level of receptor-tyrosine kinase signalling [32]. Known cytosolic RSK substrates include I-kappaB alpha [7,47,48], a member of the NF-kappaB pathway. This pathway is involved in development and in some human disorders including ectodermal dysplasias that affect ectodermal derivatives like the teeth, hair, salivary, mammary glands and skin. I-kappaB alpha has specifically been associated with an autosomal dominant form of anhidrotic ectodermal dysplasia and with T cell immunodeficiency [49]. The fact that I-kappaB alpha can be phosphorylated by RSKs, leading to increase of NF-kappaB activity, may therefore explain some of the dental anomalies encountered in the *Rsk2*-*Y* transgenic mice and in Coffin-Lowry syndrome patients. However, the downstream signalling pathway(s) of *Eda*/*Edar* involved in tooth formation in the diastema are not yet known.

The phenotype in the light of Coffin-Lowry syndrome

The mouse model for Coffin-Lowry syndrome, obtained by inactivation of the *Rsk2* gene and used in this study, was previously described by [11]. Mutant mice weigh 10% less and are 14% shorter than their wild-type littermates. This is in agreement with a role of RSK2 in organismal growth. These mice exhibit impaired learning and poor coordination, providing evidence that RSK2 plays similar roles at least for cognitive functions, in mouse and human. No previous description of the craniofacial or dental phenotype was so far reported. The craniofacial features described in Coffin-Lowry syndrome include a thick calvarium, hyperplastic supra-orbital ridges, hypertelorism, a flat malar region, and a prominent mandible. Clearly it is difficult in the light of our present observations, to relate the *Rsk*-knockout craniofacial phenotype to the anomalies encountered in patients. The small size of the skull could be associated to the general growth defect. However it is interesting to notice that in Coffin-Lowry patients, teeth agenesis and/or hypodontia is described. An apparent opposite phenotype between human patients and a mouse model has already been described in another rare disease, the cleidocranial dysplasia syndrome, which is characterized by skeletal

Table 6. Upper and lower diastema size in wild-type and *Rsk2*-*Y* mutant mice with 3 or 4 molars.

	Mean size (mm)	STD	p-value
Mandibular diastema Wild-type	2.99	0.09	
Mandibular diastema Mutants with 3 molars	2.83	0.21	0.22
Mandibular diastema Mutants with 4 molars	2.71	0.1	0.26
Maxillary diastema Wild-type	5.45	0.18	
Maxillary diastema Mutants with 3 molars	5.33	0.21	0.49
Maxillary diastema Mutants with 4 molars	5.01	0.21	0.0019

Only the upper (maxillary) diastema from mutants with 4 molars was significantly smaller compared to wild-type (bold). STD : standard deviation.
doi:10.1371/journal.pone.0084343.t006

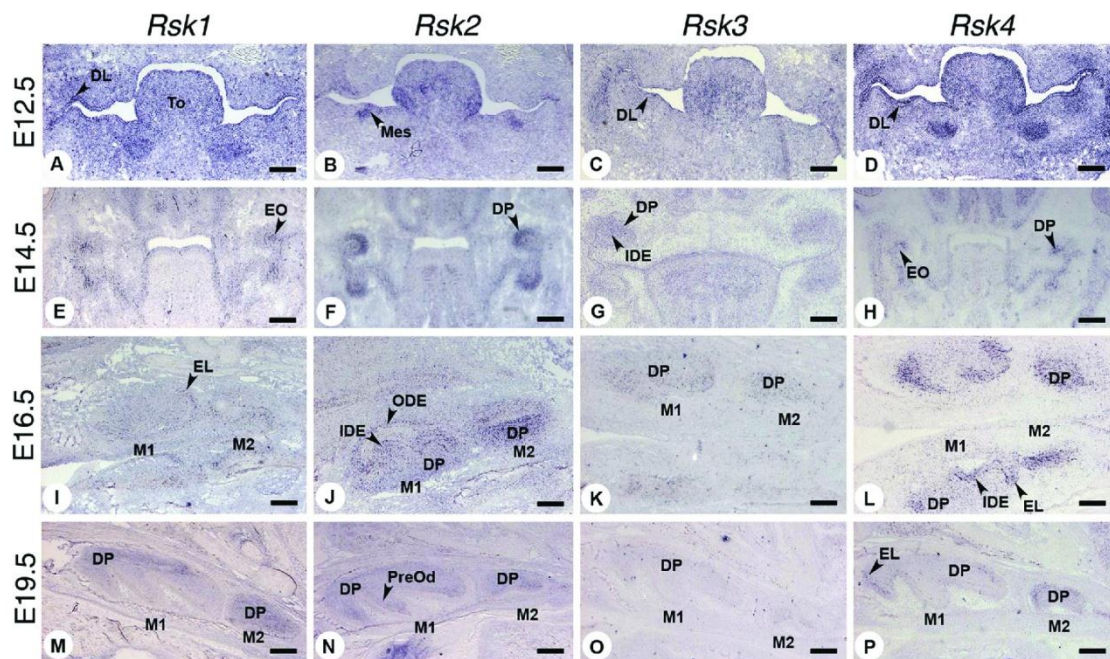


Figure 4. Expression patterns of *Rsk* genes during mouse molar odontogenesis at E12.5 (dental lamina), E14.5 (cap), E16.5 (bell) and E19.5 (late bell) stages, analyzed by *in situ* hybridization. Abbreviations: DL dental lamina, DP dental papilla, EL epithelial loop, EO enamel organ, IDE inner dental epithelium, M1 first molar, M2 second molar, Mes ectomesenchyme, ODE outer dental epithelium, PreOd preodontoblasts, To tongue. Scale bars 140 μm (A,B,C,D,I,J,K and L) and 250 μm (E,F,G,H,M,N,O and P). doi:10.1371/journal.pone.0084343.g004

defects, numerous supernumerary teeth, and delayed tooth eruption. The mouse model of this disease (*Chfa1-KO*) exhibits arrested tooth development [15]. Mostly loss of function mutations

in *RSK2* both in human and mouse are responsible for the phenotype. Despite striking similarities mouse and human tooth development, cross-species comparison of mouse/human denti-

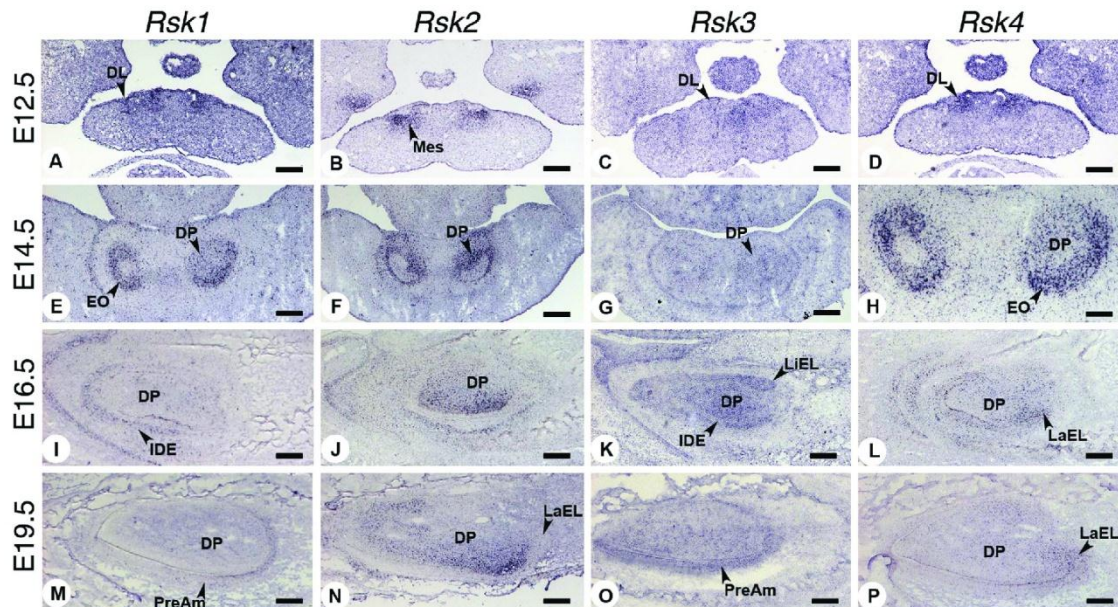


Figure 5. Expression patterns of *Rsk* genes during incisor odontogenesis at E12.5 (dental lamina), E14.5 (cap), E16.5 (bell) and E19.5 (late bell) stages analyzed by *in situ* hybridization. Abbreviations: DL dental lamina, DP dental papilla, EL epithelial loop, EO enamel organ, IDE inner dental epithelium, LaEL labial epithelial loop, LiEL lingual epithelial loop, Mes ectomesenchyme, PreAm preameloblasts. Scale bars 140 μm (A,B and C), 200 μm (D,E, F,G,I, J, K and L), 250 μm (M,N,O and P) and 50 μm (H). doi:10.1371/journal.pone.0084343.g005

Table 7. *Rsk*s expression patterns during odontogenesis.

	<i>Rsk1</i>			<i>Rsk2</i>			<i>Rsk3</i>			<i>Rsk4</i>		
	Inc	M1	M2	M3	Inc	M1	M2	M3	Inc	M1	M2	M3
E12.5												
Oral epithelium	+	+								+		+
Dental lamina	+	+						+ faint	+	+		+
Mesenchyme					+	+			+	+		
E14.5												
Enamel organ	+	+								+		+
IDE	+					+			+	+		
Enamel knot												
Dental Papilla	+ π faint				+	+		+	+	+		+
Dental sac					+							
E16.5												
ODE	+					+	+					
IDE	+	+	+				+	+		+		+
Epithelial loop	+	+	+					+		+		+
Dental Papilla	+ lab				+	+		+ π	+	+	+	+
E19.5												
ODE												
SR												
SI												
IDE								+		+		+
PreAm	+							+				
Am												
Epithelial loop	+	+						+		+	lab	+
Od												
PreOd							+					
Dental papilla	+	+	+		+	+		+	+	+	lab	+
Dental sac					+							

+ : positive signal; lab: labial; π posterior area

IDE: inner dental epithelium; ODE: outer dental epithelium; SR: stellate reticulum; SI: stratum intermedium; PreAm: preameloblasts; Am: ameloblasts; Od: odontoblasts, PreOd: Preodontoblasts

doi:10.1371/journal.pone.0084343.t007

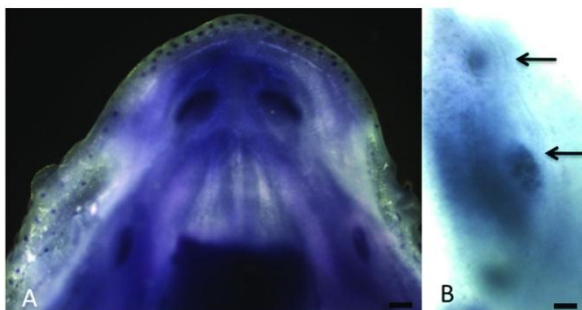


Figure 6. Whole mount in situ hybridization showing the molar and incisor placodes within the mandible at E14.5 in a wild-type mouse (A) and *Rsk2*^{-/-} mouse (B: detail of the right-side mandible) labelled with a *Shh* riboprobe. Two molar placodes are clearly visible in B (arrows) Scale bars 200 μm (A), 100 μm (B). doi:10.1371/journal.pone.0084343.g006

tions show they are clearly not alike. This suggests differential output and involvement of identical or superimposed pathways. These differences may account for this apparently opposite in nature dental phenotype i.e. hypodontia in human versus supernumerary teeth in mouse.

Cell cycle progression and cell proliferation

It has been shown that tooth number, size, and shape are linked to cell proliferation and apoptosis events [50,51,52,53]. It is interesting to note that *Rsk*s genes are expressed throughout tooth development, especially in proliferating areas (this study, Figs. 4 and 5), either in the mesenchyme (*Rsk2*, *Rsk3*) or in the epithelial loops (*Rsk1*, *Rsk4*). The expression patterns described for the *Rsk* genes in other embryonic regions [12,54,55] also indicate a correlation with proliferative areas. *Rsk1* is highly expressed in tissues harbouring highly proliferating cells like liver, lung, thymus, and olfactory and respiratory epithelia. Particularly intense *Rsk1* expression is observed in the gut epithelium. *Rsk2* is expressed at very low levels throughout mouse development in dorsal root ganglia, thyroid gland, kidney, lung, liver and skeletal muscles. *Rsk3* is mainly expressed in the nervous system, but also in the

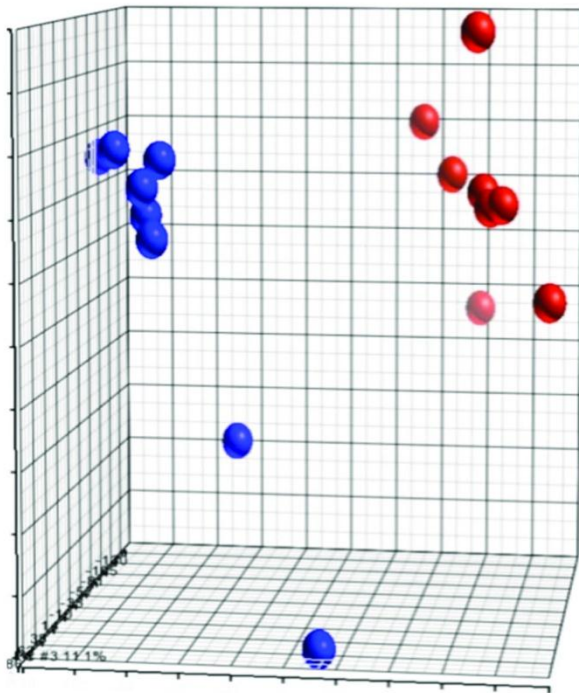


Figure 7. Principal component analysis (PCA) of transcriptomic data of wild-type versus *Rsk2*^{-/-} mandibular molars samples. Wild-type samples are represented as red balls, whereas mutant samples are represented in blue (X, Y and Z units are arbitrary units created by the software). The units are data-dependent and are generated by the software, which gives coordinates to each sample according to three axes that relate to the weight (inertia) of the decomposition into 3 principal components. For this analysis, samples segregate in two distinct groups, showing relevant transcriptional differences between WT and *Rsk2*^{-/-} samples.
doi:10.1371/journal.pone.0084343.g007

thyroid gland and testis cords. RSK3 may regulate proliferation and seems linked to cellular differentiation of neuroepithelial cells during development [55]. *Rsk4* ubiquitous low expression was observed throughout development. In teeth *Rsk4* expression was rather specifically marking the epithelial loops.

It is well established that RSKs control cell proliferation through the regulation of mediators of the cell cycle [7]. RSK2 for example promotes cell cycle progression by phosphorylating c-Fos, a transcription factor regulating the expression of cyclin D1 during G1/S transition. RSK2 activates and phosphorylates p53 *in vitro* and *in vivo* and colocalizes with p53 in the nucleus. The RSK2-p53-histone H3 complex may likely contribute to chromatin remodelling and cell cycle regulation [56]. A list of phosphorylation substrates of the RSK isoforms was reported by [7] including c-Fos, NHE-1, Er α , p27^{kip1}, Sos1, RanBP13, YB-1, Erp1, eIF4B, rpS6, Bad, DAPK, Nur77, NFAT3, TIF-1A, ATF4, ATF1, MEF2c, Filamin A, Raptor, CCT β , CRHSP24, Shank. Interestingly, alterations in the expression of a number of genes involved in cell cycle control (*Ccn1*, *Hmgb1*, *Mdm2*, *Tpd52*) or in cell growth (*Ngf*, *Bdkrb1*, *Amhr2*) is shown in our microarray analysis.

Increased proliferation and decreased apoptosis are necessary to develop supernumerary teeth, as seen by differential regulation of *Sprouty* genes [57]. The localisation of *Rsk*s genes in proliferative

areas, their role in the regulation of proliferation and apoptosis [58] as well as the interconnection of the involved pathways could explain that the deletion of *Rsk2* gene could induce the formation of supernumerary teeth and therefore reveal ancestral stages of murine dental evolution.

RSK and the Ras/MAPK pathway

Altered ERK/MAPK signalling (with abnormally increased phosphorylation of ERK1/2) was recently reported in the hippocampus of the *Rsk2*^{-/-} mice [59]. RSK2 was also proven to exert a feedback inhibitory effect on the ERK1/2 pathway. Our microarray data did not indicate a similar trend at the level of the developing molar. *Ngf* was the only gene detected by our microarray analysis, known to be regulated at the transcriptional level by ERK1/2 and involved in tooth development [60].

Unravelling target genes and involved pathways

The heterogeneity of the molar samples and the variability of the *Rsk2*^{-/-} molar phenotype has certainly interfered with the analysis of the microarray data and may have prevented the confirmation of target gene expression by qRT-PCR. However, genes involved in TGF-beta receptor signalling (*Amhr2*), or in the FGF (*Fgfbp3*) and Wnt (*Sfrp5*) pathways, were shown to be affected by the inactivation of *Rsk2*. These pathways are known to be involved in tooth development [61] and, when affected, are responsible for dental anomalies both in mouse models and human [62]. The *in vitro* assay we have developed, involving micro-injection and electroporation of a *Rsk2* shRNA in explanted molar tooth germs, proved to be a valuable system to assess quantitative changes in target gene expression.

Conclusions

Analysis of *Rsk2*^{-/-} mutant mice revealed an important role of *Rsk2* in craniofacial development, especially in dentition development and patterning. The loss of function of *Rsk2* allows the reappearance of supernumerary diastemal teeth considered as remnants of teeth lost over evolution. Our *in situ* hybridization analysis indicated that *Rsk2* expression pattern may correlate with proliferative areas of the developing teeth, consistent with a biological function of RSK2 in cell-cycle control and cell growth. Transcriptome profiling analysis was difficult because of the heterogeneity and variability of the *Rsk2*^{-/-} dental phenotype, however it provided candidate genes and pathways potentially involved in this phenotype. *In vitro* inactivation of *Rsk2* using shRNA was found to be a promising approach to address target genes and showed, in particular, an interference with an enzyme involved in the retinoid/steroid biosynthesis pathway. The fact that the regression of the fourth premolar seen in mouse is not found in all mammals, and is never observed in humans, may provide an explanation for the divergent phenotypes in *Rsk2*^{-/-} and human patients.

Materials and Methods

Patients and Ethics Statement

Patients attending the Reference centre for orodental manifestations of rare diseases, Pôle de médecine et chirurgie bucco-dentaire, Hôpitaux Universitaires de Strasbourg, or their legal representatives (parents, next of kin, caretakers or guardians) if minor and/or not in capacity to provide his or her own consent, give written informed consent for the use and publication of medical data. The picture proposed as figure 1 was uploaded in D4/phenodent database (CCTIRS positive report 11/09/2008, CNIL authorization 18/05/

Table 8. Overview of top ten genes differentially expressed in *Rsk2*^{-Y} and wild-type developing mandibular molars.

Top ten up-regulated genes	Fold change	P-value	Name
<i>Rdh1</i>	2.04458	5.22E-11	retinol dehydrogenase 1 (all trans)
<i>Dip2c</i>	1.82248	4.50E-11	DIP2 disco-interacting protein 2 homolog C (<i>Drosophila</i>)
<i>1700001J11Rik</i>	1.6761	2.92E-08	-
<i>Olf319</i>	1.66441	1.56E-08	olfactory receptor 319
<i>Myh1</i>	1.64957	1.91E-06	myosin, heavy polypeptide 1 skeletal muscle
<i>Acaa1b</i>	1.62775	1.64E-07	acetyl-Coenzyme A acyltransferase 1B
<i>6430550D23Rik</i>	1.62394	3.80E-08	-
<i>Hmgb1</i>	1.61691	4.11E-10	high mobility group box 1
<i>4930555K19Rik</i>	1.58002	2.16E-09	-
<i>9630041A04Rik</i>	1.57948	3.38E-09	-
<i>BC022713</i>	1.57732	2.80E-07	cDNA sequence
<i>Gm9968</i>	1.56689	4.24E-12	predicted gene 9968
<i>Gm6718</i>	1.56677	4.74E-07	predicted gene 6718
<i>Naip2</i>	1.56543	3.72E-09	NLR family, apoptosis inhibitory protein 2
Top ten down-regulated genes	Fold change	P-value	Name
<i>Glycam1</i>	-1.55694	1.83E-10	glycosylation dependent cell adhesion molecule 1
<i>Sfrp5</i>	-1.5577	2.67E-06	secreted frizzled-related sequence protein 5
<i>Olf459</i>	-1.56115	8.07E-10	olfactory receptor 459
<i>Fgl2</i>	-1.59412	7.32E-08	fibrinogen-like protein 2
<i>Ttc29</i>	-1.59842	6.35E-10	tetratricopeptide repeat domain 29
<i>2510003E04Rik</i>	-1.61995	2.51E-10	-
<i>Tas2r117</i>	-1.63064	9.61E-12	taste receptor, type 2, member 117
<i>4930529M08Rik</i>	-1.65052	1.67E-07	-
<i>4930529M08Rik</i>	-1.65555	3.89E-11	-
<i>Rnf39</i>	-1.6586	7.87E-09	ring finger protein 39
<i>LOC100134990</i>	-1.67412	2.18E-09	selenoprotein K pseudogene
<i>Muc19</i>	-1.68802	5.59E-07	mucin 19
<i>Tpd52</i>	-1.74912	1.10E-10	tumor protein D52
<i>Sectm1b</i>	-1.9796	2.54E-06	secreted and transmembrane 1B

The table is highlighting genes showing the highest degree of enrichment (positive values) or down-regulation (negative values).
doi:10.1371/journal.pone.0084343.t008

2009 (N°908416). A copy of the consent form can be downloaded at <http://www.phenodent.org/consentement.php>

Animals and Ethics Statement

Rsk2 gene targeting was previously described [11]. As in human, the mouse *Rsk2* gene is located on the X chromosome. Analyses were performed on *Rsk2*^{-Y} ("knockout") male mice, with littermate wild-type (*Rsk2*^{+Y}) males used as control animals. Triple *Rsk1,2,3*^{-/-} mutant mice were obtained by breeding of single knockout mice, themselves obtained by excision of exons three and four (*RSK1* knockout) or exon two (*RSK2* and *RSK3* knockouts) of the corresponding genes, leading to frameshift mutations [11]. The experiments were performed in accordance with the French national and European Laws and Directives Concerning Laboratory Animal Housing, Welfare and Experimentation and after approval from the CERBM-GIE: ICS/IGBMC Ethical Research Board.

X-Ray microtomography

A cohort of 6 mutant *Rsk2*^{-Y} male mice (#150, 155, 700, 702, 728, 731) and 6 wild-type (WT) littermates (#149, 154, 699, 727,

729, 730), as well as 7 *Rsk1,2,3* compound mutant male mice (#789, 860, 883, 1105, 1111, 1139, 1283), were analyzed through X-ray micro-computed tomography (micro-CT) (GE eXplore Vision CT120 (General Electric, Waukesha, USA) for craniofacial exploration and Phoenix Nanotom (General Electric measurement and control, Billerica, USA) for tooth analysis). For craniofacial exploration the micro-CT was performed using 220 projections with an angle increment of 0.877 degrees (Parker mode) and one average frame per projection (70.0 kV, 32 mA, and exposition time of 16 milliseconds). 3D-reconstructions were done using a Feldkamp algorithm giving voxels of 100×100×100 μm³. For teeth a second micro-CT acquisition was performed with a smaller reconstructed voxel size (3×3×3 μm³) using 2 000 projections and three average frames per projection (100.0 kV, 70 μA, and exposure time of 500 ms). 3D-reconstructions were done using datos|x software and algorithm including beam hardening correction and ring artefact reduction.

Anatomical landmarks were identified as remarkable points (for instance cranial sutures) that could be easily recognized on each specimen. Fig. S1 (supplementary material) illustrates this step, showing on a 3D isosurface rendering the landmarks (red points)

Table 9. Overview of other genes differentially expressed in *Rsk2*-Y and wild-type developing mandibular molars.

Up-regulated genes	Fold change	P-value	Name
<i>Mdm2</i>	1.42143	6.43E-07	p53 E3 ubiquitin protein ligase homolog oncoprotein
<i>Neurog3</i>	1.39695	4.46E-08	neurogenin 3
<i>Pou6f2</i>	1.38695	2.35E-07	POU domain class 6 transcription factor 2
<i>Dffa</i>	1.38653	4.93E-10	DNA fragmentation factor alpha subunit
<i>Bdkrb1</i>	1.38509	4.15E-08	bradykinin receptor beta 1
<i>Ofd1</i>	1.37103	4.33E-08	oral-facial-digital syndrome 1 gene homolog; ciliogenic protein
<i>Zfp759</i>	1.35236	5.23E-07	zinc finger protein 759
<i>Cflar</i>	1.32394	7.32E-07	CASP8 and FADD-like apoptosis regulator
<i>Aak1</i>	1.23472	3.15E-06	AP2 associated kinase 1 positive regulation of Notch signaling pathway
Down-regulated genes	Fold change	P-value	Name
<i>Pde4a</i>	-1.20556	1.57E-07	phosphodiesterase 4A cAMP specific
<i>Eaf2/U19</i>	-1.23309	1.52E-06	ELL associated factor 2, ehrlieh S-II transcriptional activator factor testosterone regulated apoptosis inducer and tumor suppressor
<i>Sp3</i>	-1.24825	9.34E-08	trans-acting transcription factor 3
<i>Ndutf4</i>	-1.26049	5.41E-08	NADH dehydrogenase (ubiquinone) 1 alpha subcomplex. assembly factor 4
<i>Wnt11</i>	-1.28904	3.63E-08	wingless-related MMTV integration site 11
<i>Fgfbp3</i>	-1.30479	5.46E-07	fibroblast growth factor binding protein 3
<i>Ccna1</i>	-1.31914	9.33E-09	cyclin A1
<i>Trim69</i>	-1.35725	5.04E-08	tripartite motif-containing 69
<i>Npy5r</i>	-1.37768	5.33E-10	neuropeptide Y receptor Y5
<i>Zfp78</i>	-1.38882	1.95E-09	zinc finger protein 78
<i>Amhr2</i>	-1.46255	5.42E-09	anti-Mullerian hormone type 2 receptor transforming growth factor beta receptor signalling pathway
<i>L3mbtl4</i>	-1.48069	4.21E-08	l(3)mbt-like 4
<i>Zkscan17</i>	-1.48573	4.10E-08	zinc finger with KRAB and SCAN domains 17
<i>Ngf</i>	-1.49018	1.63E-08	nerve growth factor
<i>Nlrc5</i>	-1.53839	1.64E-08	NLR family, CARD domain containing 5 negative regulation of NF-kappaB transcription factor activity

The table is highlighting genes selected on the basis of their known involvement in pathways regulating odontogenesis.
doi:10.1371/journal.pone.0084343.t009

and their anatomical definitions. A similar approach was used for molar analysis (Fig. S2).

Calculation involved euclidean distances between selected pairs of points that could be compared to identify statistical significant

differences between WT and mutant mice. The methodology is based upon previously described work [63,64]. To avoid any bias in landmarks position, landmarks were placed two times by one investigator (intra-investigator reproducibility) and one time by

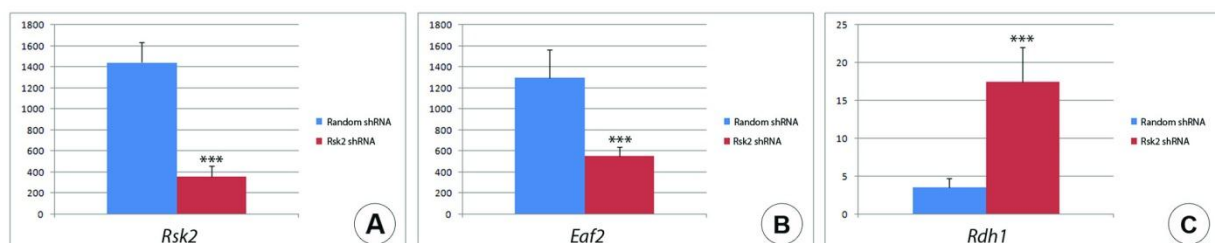


Figure 8. Summary of experiments involving *in vitro* inactivation of *Rsk2* and its consequences on target gene expression, as observed after microinjection in E14.5 mandibular molar explants of a *Rsk2* shRNA, followed by qRT-PCR analysis 24 h after injection. A: *Rsk2* was down regulated 4.01 fold after electroporation. B: *Eaf2* was significantly down-regulated, and C: *Rdh1* was up-regulated after electroporation. Histograms show expression levels in molars electroporated with the random shRNA (blue) and microinjected-electroporated explants with the *Rsk2* shRNA (red), with values normalized with respect to *Gapdh* expression. Data (mean \pm SEM) were analyzed with Student t-test; *** $p < 0.001$; ** $p < 0.01$; * $p < 0.05$.
doi:10.1371/journal.pone.0084343.g008

another (inter-investigator reproducibility). As no statistical differences were observed between distances measured within or in between investigators, we decided to base our study on the average of the three measured distances. Statistical analysis comparing WT and mutant mice was performed using Mann-Whitney non parametric test. P-values lower than 0.05 were considered as significant.

Analysis of incisor morphology

All image processing tasks were done using MicroView (GE Healthcare, Waukesha, USA). Right and left mandibular incisors were isolated by manual segmentation from mandible micro-CT acquisitions of the two mouse groups (6 *Rsk2*^{-/-} and 6 WT mice). Several measurements were achieved for morphology description, on the lateral and dorsal views of a 3D isosurface rendering of incisors (threshold value = 700 Hounsfield units): the length of the longest and external bow (Li), the height of median part of the incisor (hi), the total height (Hi), the horizontal length joining the tip of the incisor and the distal extremity of the root (li), projected area in lateral view of the incisor (lpa) and the thickness of the median part of the incisor (ti) (Fig. S3). A Wilcoxon-Mann Whitney test was used to compare both groups.

In situ hybridization on cryosections

In situ hybridizations were performed according to an automated procedure described in [65], using cDNA plasmids described in Table S2 in File S1. Mouse embryos/fetuses (C57BL6) were collected at E12.5, E14.5, E16.5, and at the day of birth (referred to as E19.5). For E14.5 and older samples, the whole head was embedded in OCT 4583 medium (Tissue-TEK, Sakura) and frozen on the surface of dry ice. E12.5 embryos were fixed overnight in 4% paraformaldehyde (pH 7.5, w/v) in phosphate-buffered saline (PBS), cryo-protected by overnight incubation in 20% sucrose (w/v) in PBS, and cryo-embedded as described above. Cryosections (Leica CM3050S cryostat) at 10 μ m were collected on Superfrost plus slides and stored at -80°C until hybridization. E12.5 and E14.5 samples were sectioned in a frontal plane, whereas other stages were sectioned sagittally.

Whole mount in situ hybridization

Whole mount in situ hybridization of mandibles collected at E14.5 was performed with a digoxigenin-labeled *Shh* riboprobe as described [66], using an Intavis InSituPro robot (for details, see <http://www.empress.har.mrc.ac.uk/browser/>, Gene Expression section). The *Shh* template plasmid was kindly provided by A. McMahon (Harvard University).

DNA microarray analysis

Tissue preparation. Embryos at E14.5 were dissected and mandibular molars were isolated. The tail was used for embryo genotyping. Individual tissue samples were frozen in liquid nitrogen and kept at -80°C until genotyping results were available and further used.

Microarray hybridization. To obtain enough RNA for hybridization on DNA microarrays, total RNA was extracted from molar tooth germs dissected manually (pooling samples from two independent wild-type or *Rsk2*^{-/-} embryos). Total RNA was extracted with the RNeasy micro Kit (Qiagen). RNA quality was verified by analysis on the 2100 Bioanalyzer (Agilent). All samples displayed a RNA Integrity Number greater than 9.8. Eight *Rsk2*^{-/-} and 8 WT samples were hybridized and compared.

Biotinylated single strand cDNA targets were prepared, starting from 300 ng of total RNA, using the Ambion WT Expression Kit (Cat #4411974) and the Affymetrix GeneChip WT Terminal Labeling Kit (Cat #900671), according to Affymetrix recommendations. Following fragmentation and end-labeling, 1.9 μ g of cDNAs were hybridized for 16 h at 45°C on GeneChip Mouse Gene 1.0 ST arrays (Affymetrix) interrogating 28,853 genes represented by approximately 27 probes spread across the full length of the gene. The chips were washed and stained in the GeneChip Fluidics Station 450 (Affymetrix) and scanned with the GeneChip Scanner 3000 7G (Affymetrix). Finally, raw data (.CEL Intensity files) were extracted from the scanned images using the Affymetrix GeneChip Command Console (AGCC) version 3.1. See also [67].

The data discussed in this publication have been deposited in NCBI's Gene Expression Omnibus (GEO) [68] and are accessible through GEO Series accession number GSE51034. (<http://www.ncbi.nlm.nih.gov/geo/query/acc.cgi?acc=GSE51034>)

Microarray analysis. CEL files were further processed with the Partek software to obtain principal component analysis (PCA) and to select and consider only genes with a signal value above 5 (20th percentile of all expression values) in at least one sample. Genes were considered as differentially expressed if the false discovery rate from Benjamini and Hochberg test was under 0.1 and if the fold change was greater than 1.2 or lower than -1.2.

In vitro culture and shRNA inactivation

E14.5 tooth germs were dissected and cultured in chemically defined culture medium as previously described [19]. The tooth explant consisted of both the enamel organ (epithelial component) and the attached dental mesenchyme. A DNA solution containing 1 μ g of *Rsk2* shRNA (SABiosciences SureSilencing shRNA Plasmid for Mouse Rps6ka3 clone ID1—linearized pGeneclip Neomycin vector, insert sequence TGATGACTCCAGAG-GAAT) or a random shRNA (insert sequence GGAATCT-CATTGATGCATAC), 0.5% sucrose, and Fast Green (Sigma; 1/10,000) was injected into the developing molars with a Femtojet Eppendorf device ($t=0.2$ s, $P=61$ hPa). Two platinum needle electrodes (0.1 mm tip, Sonidel) were inserted into the tissue lying in a cover round platinum flat electrode (Sonidel). DNA was then transferred into the cells using an ECM 830 Electroporation System (BTX Harvard Apparatus), applying 1 set of 5 pulses. Electroporation settings were set to 5 V for 50 ms, spaced by 50 ms intervals. As negative control, explants were electroporated with a random shRNA sequence.

After electroporation, the explants were embedded into 14 μ l rat collagen drops (BD Biosciences) containing 0.2 ng laminin (BD Biosciences), 50 μ l DMEM 10x concentrated, 5 μ l HEPES (1 mM), 60 μ l 7.5% NaHCO_3 (adapted from [24]). The collagen drops were kept on ice to prevent them from polymerizing. The collagen was then polymerized at 37°C for 10–15 min before addition of the culture medium.

All explants were subsequently cultured for 24 hours in a DMEM-HAM F12 medium supplemented with Vitamin C (18 mg/ml); L-Glutamine (200 mM); Streptomycin (1000 U/ml) and 20% fetal calf serum for optimal tooth growth. Explants were then processed for RT-qPCR analysis.

Real-time quantitative RT-PCR

RT-PCR assays were performed in duplicate, comparing 3 wild-type and 3 *Rsk2*^{-/-} RNA samples (4 teeth were used in each sample for validation of microarray data), or 6 molar samples electroporated with *Rsk2* shRNA and 6 control samples (for shRNA experiments). RNA extractions were performed as previously described (ref. [67]). Oligo-dT primed cDNAs were generated

using the Superscript II kit (Invitrogen) according to the manufacturer's protocol. Quantitative real-time PCR was achieved using SybrGreen and LightCycler 480 (Roche). The sequences of primers used for the various tested genes are given in Table S3 in File S1. A probe set for detection of mouse *Gapdh* mRNA (encoded by a housekeeping gene) was used for normalization. For each sample the ratio between signals for the gene of interest and *Gapdh* was calculated to normalize concentration values. To verify if genes were differentially expressed between electroporated and control samples, the average of ratios were then compared.

Statistical tests

Data, presented as means \pm SEM, were compared using Student t-test (for 2 groups comparison). P-values below 0.05 were considered as significant.

Supporting Information

Figure S1 Description of the craniofacial anatomical landmarks used for X-Ray microtomographic analysis of *Rsk* mutant mice.

(TIF)

Figure S2 Molar landmarks used for the analysis of X-Ray tomography images.

(TIF)

Figure S3 Three-dimensional isosurface rendering of a right mandibular incisor from a wild-type mouse, in lateral

(A) and dorsal (B) views, depicting the distances measured for the morphometric analysis.

(TIF)

File S1 Supporting Information file containing Tables S1–S3. Table S1 in file S1. Molar root numbers in WT and *Rsk2*^{-/-} mice. UR: upper right. UL: upper left. LR: lower right. LL: lower left. M1: first molar. M2: second molar. M3: third molar. ST: supernumerary tooth. Table S2 in file S1. Template plasmids used for *in situ* hybridization. Table S3 in file S1. Sequences of primers used for quantitative RT-PCR experiments. (DOCX)

Acknowledgments

The authors are grateful to the patients and families attending the Reference centre for orodental manifestations of rare diseases, HUS, Strasbourg, France, and to Dr. Karen Niederreither for proofreading of the manuscript. They also wish to thank Cathy Herouard-Molina, Doulaye Dembele, and Christelle Thibault from the IGBMC Microarray and sequencing platform.

Author Contributions

Conceived and designed the experiments: VH-L MP PC AC LV AH PD AB-Z. Performed the experiments: VL-H MP PM AL TK JD SM FB SP. Analyzed the data: VL-H LV PD AB-Z. Contributed reagents/materials/analysis tools: CP AL TK JD MS FB SP. Wrote the paper: VL-H MP LV AH PD AB-Z.

References

- Hanauer A, Young ID (2002) Coffin-Lowry syndrome: clinical and molecular features. *J Med Genet* 39: 705–713.
- Temtamy SA, Miller JD, Hussels-Maumenee I (1975) The Coffin-Lowry syndrome: an inherited facioidigital mental retardation syndrome. *J Pediatr* 86: 724–731.
- Temtamy SA, Miller JD, Dorst JP, Hussels-Maumenee I, Salinas C, et al. (1975) The Coffin-Lowry syndrome: a simply inherited trait comprising mental retardation, facioidigital anomalies and skeletal involvement. *Birth Defects Orig Artic Ser* 11: 133–152.
- Igari K, Hozumi Y, Monma Y, Mayanagi H (2006) A case of Coffin-Lowry syndrome with premature exfoliation of primary teeth. *Int J Paediatr Dent* 16: 213–217.
- Day P, Cole B, Welbury R (2000) Coffin-Lowry syndrome and premature tooth loss: a case report. *ASDC J Dent Child* 67: 148–150.
- Frodin M, Gammeltoft S (1999) Role and regulation of 90 kDa ribosomal S6 kinase (RSK) in signal transduction. *Mol Cell Endocrinol* 151: 65–77.
- Romeo Y, Zhang X, Roux PP (2012) Regulation and function of the RSK family of protein kinases. *Biochem J* 441: 553–569.
- Tan Y, Ruan H, Demeter MR, Comb MJ (1999) p90(RSK) blocks bad-mediated cell death via a protein kinase C-dependent pathway. *J Biol Chem* 274: 34859–34867.
- Hauge C, Frodin M (2006) RSK and MSK in MAP kinase signalling. *J Cell Sci* 119: 3021–3023.
- Poirier L, Jacquot S, Vaillend C, Southiphong AA, Libbey M, et al. (2007) Deletion of the Coffin-Lowry Syndrome Gene *Rsk2* in Mice is Associated With Impaired Spatial Learning and Reduced Control of Exploratory Behavior. *Behav Genet* 37: 31–50.
- Yang X, Matsuda K, Bialek P, Jacquot S, Masuoka HC, et al. (2004) ATF4 is a substrate of RSK2 and an essential regulator of osteoblast biology; implication for Coffin-Lowry Syndrome. *Cell* 117: 387–398.
- Kohn M, Hameister H, Vogel M, Kehrer-Sawatzki H (2003) Expression pattern of the *Rsk2*, *Rsk4* and *Pdk1* genes during murine embryogenesis. *Gene Expr Patterns* 3: 173–177.
- Viriot L, Peterkova R, Peterka M, Lesot H (2002) Evolutionary implications of the occurrence of two vestigial tooth germs during early odontogenesis in the mouse lower jaw. *Connect Tissue Res* 43: 129–133.
- Fleischmannova J, Matalova E, Tucker AS, Sharpe PT (2008) Mouse models of tooth abnormalities. *Eur J Oral Sci* 116: 1–10.
- Aberg T, Cavender A, Gaikwad JS, Bronckers AL, Wang X, et al. (2004) Phenotypic Changes in Dentition of *Runx2* Homozygote-null Mutant Mice. *J Histochem Cytochem* 52: 131–140.
- Zhang M, Chen W, Smith SM, Napoli JL (2001) Molecular characterization of a mouse short chain dehydrogenase/reductase active with all-trans-retinol in intact cells, mRDH1. *J Biol Chem* 276: 44083–44090.
- Bloch-Zupan A, Decimo D, Lorient M, Mark MP, Ruch JV (1994) Expression of nuclear retinoic acid receptors during mouse odontogenesis. *Differentiation* 57: 195–203.
- Bloch-Zupan A, Mark MP, Weber B, Ruch JV (1994) In vitro effects of retinoic acid on mouse incisor development. *Arch Oral Biol* 39: 891–900.
- Mark MP, Bloch-Zupan A, Ruch JV (1992) Effects of retinoids on tooth morphogenesis and cytodifferentiations, in vitro. *Int J Dev Biol* 36: 517–526.
- Mark MP, Bloch-Zupan A, Wolf C, Ruberte E, Ruch JV (1991) Involvement of cellular retinoic acid-binding proteins I and II (CRABPI and CRABPII) and of the cellular retinol-binding protein I (CRBPI) in odontogenesis in the mouse. *Differentiation* 48: 89–98.
- Wan X, Ji W, Mei X, Zhou J, Liu JX, et al. (2010) Negative feedback regulation of Wnt4 signaling by EAF1 and EAF2/U19. *PLoS One* 5: e9118.
- Xiao W, Zhang Q, Habermacher G, Yang X, Zhang AY, et al. (2008) U19/Eaf2 knockout causes lung adenocarcinoma, B-cell lymphoma, hepatocellular carcinoma and prostatic intraepithelial neoplasia. *Oncogene* 27: 1536–1544.
- Wise GE, He H, Gutierrez DL, Ring S, Yao S (2011) Requirement of alveolar bone formation for eruption of rat molars. *Eur J Oral Sci* 119: 333–338.
- Wright TJ, Ladher R, McWhirter J, Murre C, Schoenwolf GC, et al. (2004) Mouse FGF15 is the ortholog of human and chick FGF19, but is not uniquely required for otic induction. *Dev Biol* 269: 264–275.
- Ji Q, Luo ZX, Yuan CX, Wible JR, Zhang JP, et al. (2002) The earliest known eutherian mammal. *Nature* 416: 816–822.
- Peterka M, Vonesch JL, Ruch JV, Cam Y, Peterkova R, et al. (2000) Position and growth of upper and lower tooth primordia in prenatal mouse—3D study. *J Craniofac Genet Dev Biol* 20: 35–43.
- Viriot L, Lesot H, Vonesch JL, Ruch JV, Peterka M, et al. (2000) The presence of rudimentary odontogenic structures in the mouse embryonic mandible requires reinterpretation of developmental control of first lower molar histomorphogenesis. *Int J Dev Biol* 44: 233–240.
- Peterkova R, Peterka M, Lesot H (2003) The developing mouse dentition: a new tool for apoptosis study. *Ann N Y Acad Sci* 1010: 453–466.
- Porntaveetus T, Ohazama A, Choi HY, Herz J, Sharpe PT (2011) Wnt signaling in the murine diastema. *Eur J Orthod*.
- Ohazama A, Blackburn J, Porntaveetus T, Ota MS, Choi HY, et al. (2010) A role for suppressed incisor cuspal morphogenesis in the evolution of mammalian heterodont dentition. *Proc Natl Acad Sci U S A* 107: 92–97.
- Klein OD, Minowada G, Peterkova R, Kangas A, Yu BD, et al. (2006) Sprouty genes control diastema tooth development via bidirectional antagonism of epithelial-mesenchymal FGF signaling. *Dev Cell* 11: 181–190.
- Charles C, Hovorakova M, Ahn Y, Lyons DB, Marangoni P, et al. (2011) Regulation of tooth number by fine-tuning levels of receptor-tyrosine kinase signaling. *Development* 138: 4063–4073.

33. Ohazama A, Haycraft CJ, Seppala M, Blackburn J, Ghafoor S, et al. (2009) Primary cilia regulate Shh activity in the control of molar tooth number. *Development* 136: 897–903.
34. Kassai Y, Munne P, Hotta Y, Penttila E, Kavanagh K, et al. (2005) Regulation of mammalian tooth cusp patterning by ectodin. *Science* 309: 2067–2070.
35. Murashima-Suginami A, Takahashi K, Sakata T, Tsukamoto H, Sugai M, et al. (2008) Enhanced BMP signaling results in supernumerary tooth formation in USAG-1 deficient mouse. *Biochem Biophys Res Commun* 369: 1012–1016.
36. Ohazama A, Johnson EB, Ota MS, Choi HY, Pomtaveetus T, et al. (2008) Lrp4 modulates extracellular integration of cell signaling pathways in development. *PLoS One* 3: e4092.
37. Hacohen N, Kramer S, Sutherland D, Hiromi Y, Krasnow MA (1998) sprouty encodes a novel antagonist of FGF signaling that patterns apical branching of the *Drosophila* airways. *Cell* 92: 253–263.
38. Kim HJ, Bar-Sagi D (2004) Modulation of signalling by Sprouty: a developing story. *Nat Rev Mol Cell Biol* 5: 441–450.
39. Tucker AS, Headon DJ, Courtney JM, Overbeek P, Sharpe PT (2004) The activation level of the TNF family receptor, Edar, determines cusp number and tooth number during tooth development. *Dev Biol* 268: 185–194.
40. Pispá J, Mikkola ML, Mustonen T, Thesleff I (2003) Ectodysplasin, Edar and TNFRSF19 are expressed in complementary and overlapping patterns during mouse embryogenesis. *Gene Expr Patterns* 3: 675–679.
41. Mustonen T, Pispá J, Mikkola ML, Pummila M, Kangas AT, et al. (2003) Stimulation of ectodermal organ development by Ectodysplasin-A1. *Dev Biol* 259: 123–136.
42. Peterkova R, Lesot H, Viriot L, Peterka M (2005) The supernumerary cheek tooth in tabby/EDA mice—a reminiscence of the premolar in mouse ancestors. *Arch Oral Biol* 50: 219–225.
43. Peterkova R, Kristenova P, Lesot H, Lisi S, Vonesch JL, et al. (2002) Different morphotypes of the tabby (EDA) dentition in the mouse mandible result from a defect in the mesio-distal segmentation of dental epithelium. *Orthod Craniofac Res* 5: 215–226.
44. Lesot H, Peterkova R, Kristenova P, Lisi S, Peterka M (2003) [Effect of the Tabby mutation on the dentition of mice]. *Bull Group Int Rech Sci Stomatol Odontol* 45: 1–11.
45. Charles C, Pantalacci S, Peterkova R, Tafforeau P, Laudet V, et al. (2009) Effect of eda loss of function on upper jugal tooth morphology. *Anat Rec (Hoboken)* 292: 299–308.
46. Kristenova P, Peterka M, Lisi S, Gendrault JL, Lesot H, et al. (2002) Different morphotypes of functional dentition in the lower molar region of tabby (EDA) mice. *Orthod Craniofac Res* 5: 205–214.
47. Ghoda L, Lin X, Greene WC (1997) The 90-kDa ribosomal S6 kinase (pp90rsk) phosphorylates the N-terminal regulatory domain of I κ B α and stimulates its degradation in vitro. *J Biol Chem* 272: 21281–21288.
48. Schouten GJ, Vertegaal AC, Whiteside ST, Israel A, Toebes M, et al. (1997) I κ B α is a target for the mitogen-activated 90 kDa ribosomal S6 kinase. *Embo J* 16: 3133–3144.
49. Courtois G, Smahi A, Reichenbach J, Doffinger R, Cancrini C, et al. (2003) A hypermorphic I κ B α mutation is associated with autosomal dominant anhidrotic ectodermal dysplasia and T cell immunodeficiency. *J Clin Invest* 112: 1108–1115.
50. Boran T, Lesot H, Peterka M, Peterkova R (2005) Increased apoptosis during morphogenesis of the lower cheek teeth in tabby/EDA mice. *J Dent Res* 84: 228–233.
51. Coin R, Lesot H, Vonesch JL, Haikel Y, Ruch JV (1999) Aspects of cell proliferation kinetics of the inner dental epithelium during mouse molar and incisor morphogenesis: a reappraisal of the role of the enamel knot area. *Int J Dev Biol* 43: 261–267.
52. Lesot H, Peterkova R, Viriot L, Vonesch JL, Tureckova J, et al. (1998) Early stages of tooth morphogenesis in mouse analyzed by 3D reconstructions. *Eur J Oral Sci* 106 Suppl 1: 64–70.
53. Viriot L, Peterkova R, Vonesch JL, Peterka M, Ruch JV, et al. (1997) Mouse molar morphogenesis revisited by three-dimensional reconstruction. III. Spatial distribution of mitoses and apoptoses up to bell-staged first lower molar teeth. *Int J Dev Biol* 41: 679–690.
54. Guimiot F, Delezoide AL, Hanauer A, Simonneau M (2004) Expression of the RSK2 gene during early human development. *Gene Expr Patterns* 4: 111–114.
55. Zeniou M, Ding T, Trivier E, Hanauer A (2002) Expression analysis of RSK gene family members: the RSK2 gene, mutated in Coffin-Lowry syndrome, is prominently expressed in brain structures essential for cognitive function and learning. *Hum Mol Genet* 11: 2929–2940.
56. Cho YY, He Z, Zhang Y, Choi HS, Zhu F, et al. (2005) The p53 protein is a novel substrate of ribosomal S6 kinase 2 and a critical intermediary for ribosomal S6 kinase 2 and histone H3 interaction. *Cancer Res* 65: 3596–3603.
57. Lagronova-Churava S, Spoutil F, Vojtechova S, Lesot H, Peterka M, et al. (2013) The dynamics of supernumerary tooth development are differentially regulated by Sprouty genes. *J Exp Zool B Mol Dev Evol* 320: 307–320.
58. Liu Z, Li T, Reinhold MI, Naski MC (2012) MEK1-RSK2 contributes to hedgehog signaling by stabilizing Gli2 transcription factor and inhibiting ubiquitination. *Oncogene*.
59. Schneider A, Mehmood T, Pannetier S, Hanauer A (2011) Altered ERK/ MAPK signaling in the hippocampus of the *mrsk2_KO* mouse model of Coffin-Lowry syndrome. *J Neurochem* 119: 447–459.
60. Mitsiadis TA, Luukko K (1995) Neurotrophins in odontogenesis. *Int J Dev Biol* 39: 195–202.
61. Tummers M, Thesleff I (2009) The importance of signal pathway modulation in all aspects of tooth development. *J Exp Zool B Mol Dev Evol* 312B: 309–319.
62. Bloch-Zupan A, Sedano H, Scully C (2012) *Dento/Oro/Craniofacial Anomalies and Genetics*. London: Elsevier Inc.
63. Richtsmeier JT, Paik CH, Elfert PC, Cole TM 3rd, Dahlman HR (1995) Precision, repeatability, and validation of the localization of cranial landmarks using computed tomography scans. *Cleft Palate Craniofac J* 32: 217–227.
64. Richtsmeier JT, Baxter LL, Reeves RH (2000) Parallels of craniofacial maldevelopment in Down syndrome and Ts65Dn mice. *Dev Dyn* 217: 137–145.
65. Diez-Roux G, Banfi S, Sultan M, Geffers L, Anand S, et al. (2011) A high-resolution anatomical atlas of the transcriptome in the mouse embryo. *PLoS Biol* 9: e1000582.
66. Chotteau-Lelievre A, Dolle P, Gofflot F (2006) Expression analysis of murine genes using in situ hybridization with radioactive and nonradioactively labeled RNA probes. *Methods Mol Biol* 326: 61–87.
67. Laugel-Haushalter V, Paschaki M, Thibault-Carpentier C, Dembele D, Dolle P, et al. (2013) Molars and incisors: show your microarray IDs. *BMC Res Notes* 6: 113.
68. Edgar R, Domrachev M, Lash AE (2002) Gene Expression Omnibus: NCBI gene expression and hybridization array data repository. *Nucleic Acids Res* 30: 207–210.

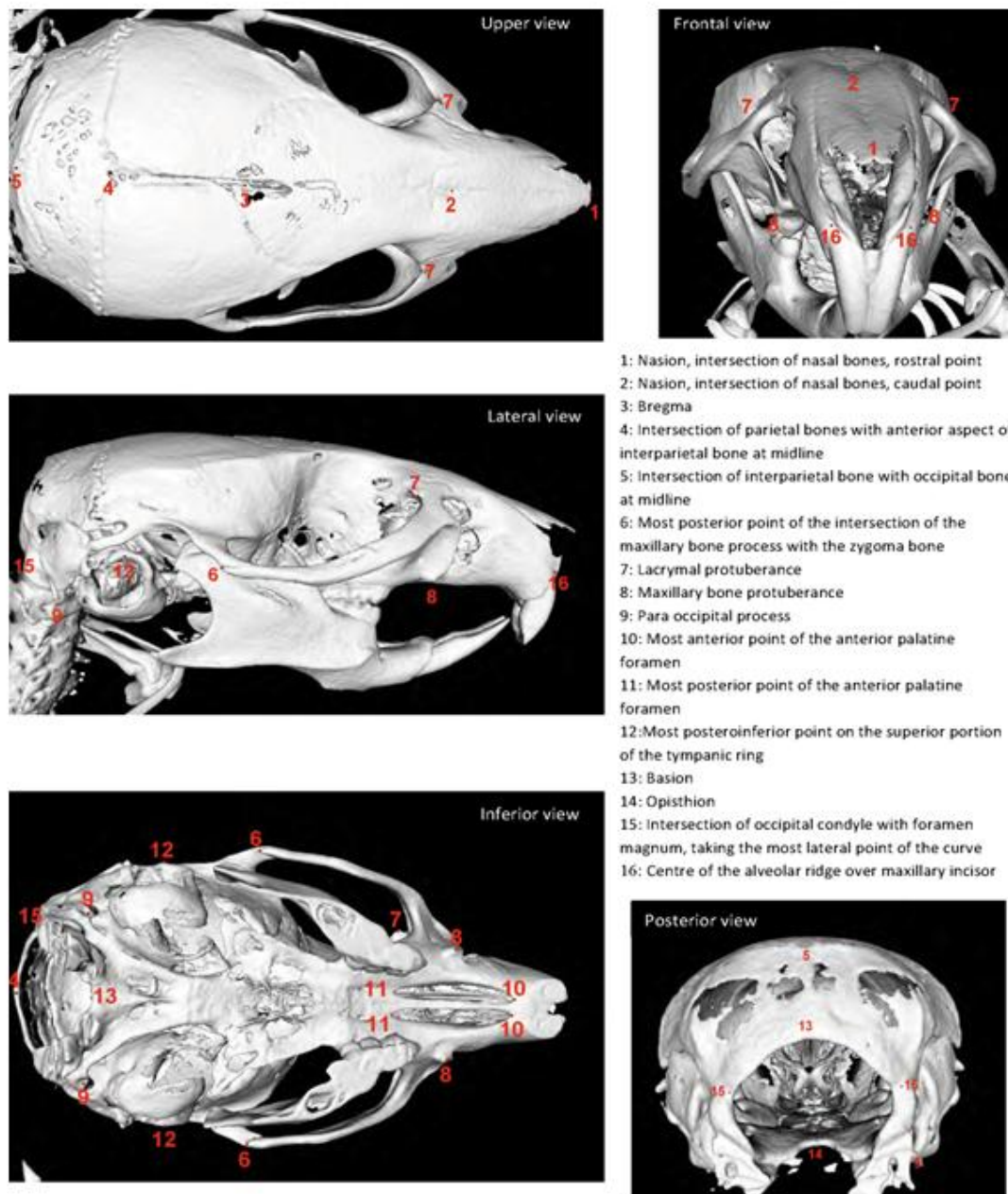


Figure S1: Description of the craniofacial anatomical landmarks used for X-Ray microtomographic analysis of Rsk mutant mice.
doi:10.1371/journal.pone.0084343.s001

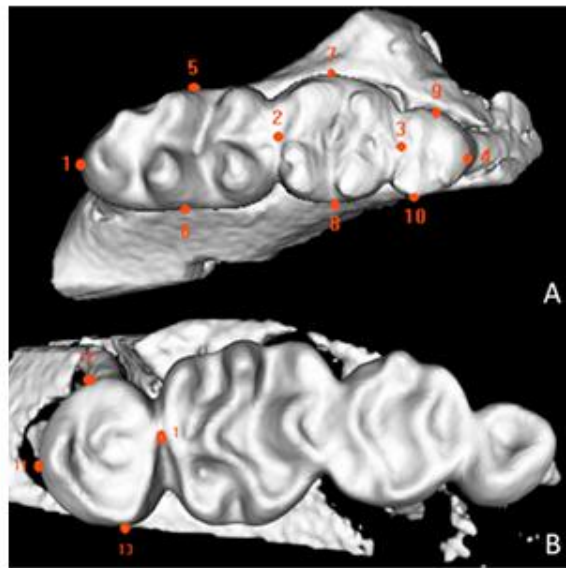


Figure S2: Molar landmarks used for the analysis of X-Ray tomography images.
doi:10.1371/journal.pone.0084343.s002

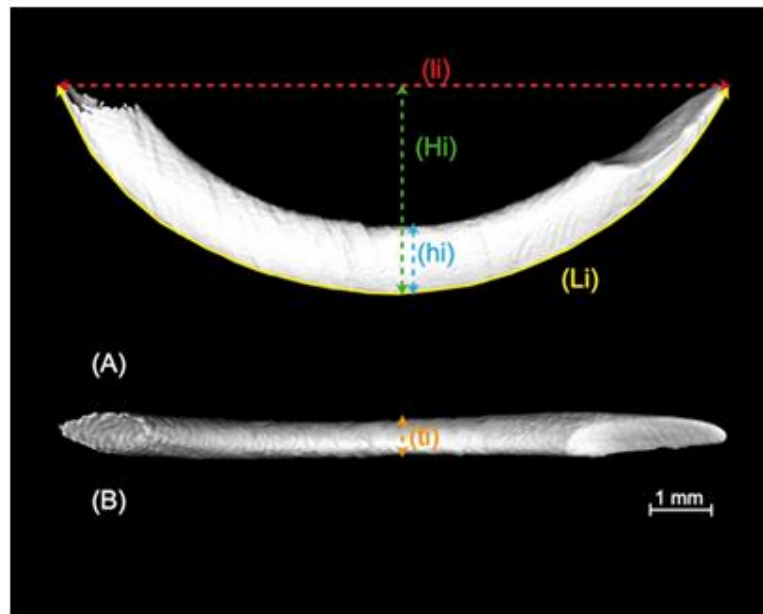


Figure S3: Three-dimensional isosurface rendering of a right mandibular incisor from a wild-type mouse, in lateral (A) and dorsal (B) views, depicting the distances measured for the morphometric analysis.
doi:10.1371/journal.pone.0084343.s003

WT #	M1 LR	M2 LR	M3 LR	Total LR	Total M1 + M2	Total M1 and M2 + ST
149	2	2	1	5	4	
730	2	2	1	5	4	
729	2	2	1	5	4	
727	2	2	1	5	4	
699	2	2	1	5	4	
154	2	2	1	5	4	
WT #	M1 LL	M2 LL	M3 LL	Total LL	Total M1 + M2	Total M1 and M2 + ST
149	2	2	2	6	4	
730	2	2	1	5	4	
729	2	2	1	5	4	
727	2	2	1	5	4	
699	2	2	1	5	4	
154	2	2	1	5	4	
Mutant #	M1 LR	M2 LR	M3 LR	ST LR	Total LR	Total M1 and M2 + ST
150	2	2	1		5	4
728	2	2	1		5	4
731	2	2	1		5	4
702	2	2	1	1	6	5
700	2	2	1		5	4
155	2	2	1	1	6	5
Mutant #	M1 LL	M2 LL	M3 LL	ST LL	Total LL	Total M1 and M2 + ST
150	2	2	1	1	6	5
728	2	2	1		5	4
731	2	2	1	1	6	5
702	2	2	1		5	4
700	2	2	1		5	4
155	2	2	1	1	6	5
WT #	M1 UR	M2 UR	M3 UR	Total UR	Total M1 + M2	Total M1 and M2 + ST
149	3	3	3	9	6	
730	3	3	2	8	6	
729	3	3	2	8	6	
727	3	3	2	8	6	
699	3	3	2	8	6	
154	3	3	3	9	6	
WT #	M1 UL	M2 UL	M3 UL	Total UL	Total M1 + M2	Total M1 and M2 + ST
149	3	3	3	9	6	
730	3	3	2	8	6	
729	3	3	2	8	6	
727	3	3	2	8	6	
699	3	3	1	7	6	
154	3	3	2	8	6	
Mutant #	M1 UR	M2 UR	M3 UR	ST UR	Total UR	Total M1 and M2 + ST
150	2	3	2	2	9	7
728	2	3	2	2	9	7
731	2	3	2		7	5
702	2	3	2		7	5
700	3	3	2		8	6
155	2	3	2	1	8	6
Mutant #	M1 UL	M2 UL	M3 UL	ST UL	Total UL	Total M1 and M2 + ST
150	2	3	2	1	8	6
728	2	3	2		7	5
731	3	3	3		9	6
702	3	3	3		9	6
700	3	3	2		8	6
155	2	3	2	2	9	7

Table S1 : Molar root numbers in WT and Rsk2-/- mice. UR: upper right. UL: upper left. LR: lower right. LL: lower left. M1: first molar. M2: second molar. M3: third molar. ST: supernumerary tooth.

GENE	Sequence	Vector	RNA polymerase
<i>Rsk1</i>	3097-2282	pCMV.SPORT6	T7
<i>Rsk2</i>	3025-2117	pT7T3D-Pacl	T3
<i>Rsk3</i>	5374-4403	pCMV.SPORT6	T7
<i>Rsk4</i>	4330-3405	pCMV.SPORT6	T7

Table S2: Templates for in situ hybridization

Primer	Sequence 5' to 3'
<i>RDH1 QF</i>	AACACGCAGAGCAATGAGGAG
<i>RDH1 QR</i>	TAGATGTGGCGAACCATGCC
<i>SP3 QF</i>	TCAAGTAGTCGCTAATGTGCCT
<i>SP3 QR</i>	GAACTCCCAGAGTCCCAAA
<i>POU6F2 QF</i>	GGACAGATTATTGGGACCATTCC
<i>POU6F2 QR</i>	GGTGTGATAGGCTGACTTGAAG
<i>NLRC5 QF</i>	GTGCCAAACGTCCTTTTCAGA
<i>NLRC5 QR</i>	AGTGAGGAGTAAGCCATGCTC
<i>EMX2 QF</i>	GAGGCTGATGCTACTTGTCAC
<i>EMX2 QR</i>	CTCACTGTCGCTTTCTGACTC
<i>PDE4A QF</i>	ACATTTCCAACACGTTCTAGAC
<i>PDE4A QR</i>	CCGGTGTGTACCAGCTTTTTC
<i>CFLAR QF</i>	GGTGAAGAGTGTCTTGATGAAG
<i>CFLAR QR</i>	CCCTGACGTTAGGTGCAGC
<i>AAK1 QF</i>	GCAATGGGGTAAAATGTGCC
<i>AAK1 QR</i>	TGTGCCCTGATAGGTCTCTCA
<i>MDM2 QF</i>	TGAAGTTGTTAAAGTCCGTTGGA
<i>MDM2 QR</i>	CTGCTGCTTCTCGTCATATAACC

Table S3: Primer sequences of genes analyzed by quantitative RT-PCR.

Annex 3

Control of the incisor number by Sprouty genes

Regulation of tooth number by fine-tuning levels of receptor-tyrosine kinase signaling

Cyril Charles^{1,2,*}, Maria Hovorakova^{3,*}, Youngwook Ahn⁴, David B. Lyons¹, Pauline Marangoni², Svatava Churava^{3,5}, Brian Biehs¹, Andrew Jheon¹, Hervé Lesot⁶, Guive Balooch⁷, Robb Krumlauf^{4,8}, Laurent Viriot², Renata Peterkova³ and Ophir D. Klein^{1,9,†}

SUMMARY

Much of our knowledge about mammalian evolution comes from examination of dental fossils, because the highly calcified enamel that covers teeth causes them to be among the best-preserved organs. As mammals entered new ecological niches, many changes in tooth number occurred, presumably as adaptations to new diets. For example, in contrast to humans, who have two incisors in each dental quadrant, rodents only have one incisor per quadrant. The rodent incisor, because of its unusual morphogenesis and remarkable stem cell-based continuous growth, presents a quandary for evolutionary biologists, as its origin in the fossil record is difficult to trace, and the genetic regulation of incisor number remains a largely open question. Here, we studied a series of mice carrying mutations in sprouty genes, the protein products of which are antagonists of receptor-tyrosine kinase signaling. In sprouty loss-of-function mutants, splitting of gene expression domains and reduced apoptosis was associated with subdivision of the incisor primordium and a multiplication of its stem cell-containing regions. Interestingly, changes in sprouty gene dosage led to a graded change in incisor number, with progressive decreases in sprouty dosage leading to increasing numbers of teeth. Moreover, the independent development of two incisors in mutants with large decreases in sprouty dosage mimicked the likely condition of rodent ancestors. Together, our findings indicate that altering genetic dosage of an antagonist can recapitulate ancestral dental characters, and that tooth number can be progressively regulated by changing levels of activity of a single signal transduction pathway.

KEY WORDS: FGF signaling, Sprouty genes, Incisor, Mouse

INTRODUCTION

Tooth number is highly variable among mammalian species because of adaptive changes that were selected during evolution. In many cases, evolution led to a reduction of tooth number in extant species compared with their ancestral forms. The laboratory mouse in particular has one of the most reduced mammalian dentitions. Like other rodents, mice have a single pair of ever-growing incisors in the upper and lower jaws (Fig. 1A-C). The ancestral dental formula of placental mammals includes three incisors, indicating that rodents have lost two pairs of upper and lower incisors during evolution. Unlike humans, mice do not replace their teeth, and the mouse incisor is considered to be an unreplaced deciduous tooth (Lockett, 1985; Moss-Salentijn, 1978). In contrast to rodents, the Lagomorpha

(rabbits and pika) have a pair of ever-growing incisors as well as a second pair of upper incisors located lingual (nearer the tongue) to the first pair.

The mechanism by which the number of incisors decreased during evolution is poorly understood because of a lack of transitional fossils. However, the study of incisor development in wild-type and mutant mice can potentially shed light on these evolutionary events. Mice carrying mutations in *Sostdc1* (wise, ectodin) (Munne et al., 2009; Murashima-Suginami et al., 2007), *Lrp4* (Ohazama et al., 2008) or *Di* (Danforth, 1958) have supernumerary upper or lower incisors that are located lingually to the normal incisor, in a configuration that is similar to Lagomorpha upper incisors. The detailed study of incisor development in *Sostdc1* mutants indicated that the supernumerary incisor corresponded to a replacement tooth (Munne et al., 2009). Splitting of the incisor placode has been observed in vivo in *Sostdc1*-follistatin double-null mice, in which there is a partial splitting of the placode leading to bifid incisors. In vitro studies using mandible explants have also shown that the main incisor placode is able to split and give rise to two incisors after activin or noggin treatments (Munne et al., 2010).

The normal mouse upper incisor, which is relatively large compared with the molars, has been documented to form through the fusion of six small primordia at early embryonic stages (Peterkova et al., 1993; Peterkova et al., 2006). Thus, previous studies suggest several potential mechanisms by which supernumerary incisors might arise in mice: failure of integration of the ancestral dental primordia (Hovorakova et al., 2011), development of a replacement tooth (Munne et al., 2009), splitting of a large placode into smaller elements (Munne et al., 2010) or development of a supernumerary germ (Sofaer, 1969).

¹Department of Orofacial Sciences and Program in Craniofacial and Mesenchymal Biology, University of California San Francisco, San Francisco, CA 94143, USA. ²Team 'Evo-devo of Vertebrate Dentition', Institut de Génétique Fonctionnelle de Lyon, ENS de Lyon, Université de Lyon, Université Lyon 1, CNRS, 69364 Lyon Cedex 07, France. ³Institute of Experimental Medicine, Academy of Sciences of the Czech Republic, 14220 Prague 4, Czech Republic. ⁴Stowers Institute for Medical Research, Kansas City, MO 64110, USA. ⁵Department of Anthropology and Human Genetics, Faculty of Science, Charles University, 12884 Prague 2, Czech Republic. ⁶Institut National de la Santé et de la Recherche Médicale UMR 977, Dental School, University of Strasbourg, Strasbourg F-67085, France. ⁷Department of Preventive and Restorative Dental Sciences, University of California San Francisco, San Francisco, CA 94143, USA. ⁸Department of Anatomy and Cell Biology, University of Kansas Medical Center, Kansas City, KS 66160, USA. ⁹Department of Pediatrics and Institute for Human Genetics, University of California San Francisco, San Francisco, CA 94143, USA.

*These authors contributed equally to this work

†Author for correspondence (ophir.klein@ucsf.edu)

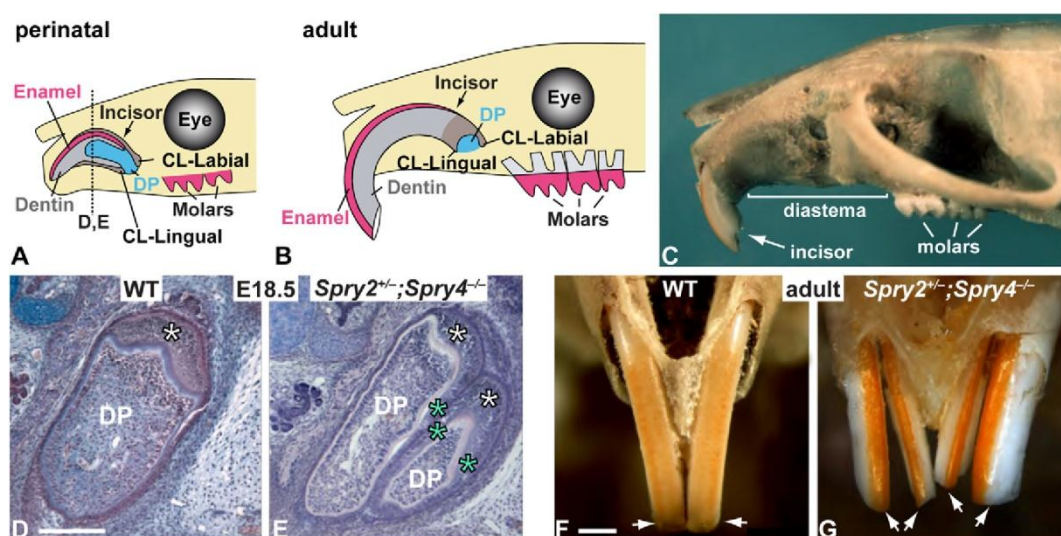


Fig. 1. Incisor duplication in *Spry2*^{+/-};*Spry4*^{-/-} mice. (A) Schematic of incisor in a perinatal mouse; dotted vertical black line indicates plane of section for D and E. (B) Schematic of incisor in an adult mouse. (C) Adult mouse skull showing the incisor, toothless diastema and molars. (D) Section of wild-type (WT) incisor at E18.5. (E) Section of *Spry2*^{+/-};*Spry4*^{-/-} incisor at E18.5. (F) Adult wild-type incisors in frontal view. (G) Incisor duplication in adult *Spry2*^{+/-};*Spry4*^{-/-} mutant mice. CL, cervical loop; DP, dental papilla. In D and E, white asterisks indicate labial ameloblasts and blue asterisks indicate ectopic ameloblasts. Arrows in F and G point to the incisors. Scale bars: 500 μ m.

Mammalian tooth morphogenesis is controlled by interactions between the oral epithelium and the neural crest-derived ectomesenchyme, and these interactions are mediated by signaling pathways, including the receptor-tyrosine kinase (RTK) pathway initiated by the secreted fibroblast growth factors (FGFs) (Pispa and Thesleff, 2003; Cobourne and Sharp, 2010). The sprouty (*Spry*) family of genes encodes proteins that are intracellular inhibitors of RTK signaling (Guy et al., 2003; Kim and Bar-Sagi, 2004). We have previously reported that mice carrying mutations in sprouty genes have dental abnormalities; in particular, *Spry2*^{+/-};*Spry4*^{-/-} mice have abnormal enamel deposition on the lingual surface of the incisors in their lower jaws (Klein et al., 2006; Klein et al., 2008; Boran et al., 2009; Peterkova et al., 2009; Caton et al., 2009). Here, we focus on the upper jaws of *Spry2*^{+/-};*Spry4*^{-/-} mice and show that loss of sprouty genes can increase the number of incisors by a subdivision of the single embryonic incisor anlage preceded by the subdivision of its gene expression domains. We also studied a dosage series of sprouty mutants to assess how fine-tuning levels of signaling affects the development of incisors and found that progressive changes in incisor number can occur as sprouty gene dosage is changed. The phenotype in sprouty loss-of-function mutants corresponds to the morphology of rodent ancestors, leading us to propose a new model for modification of incisor development during evolution.

MATERIALS AND METHODS

Mice

Mouse lines carrying mutant alleles of *Spry1* (Basson et al., 2005), *Spry2* (Shim et al., 2005), *Spry4* (Klein et al., 2008) and *Fgf10* (Min et al., 1998) were maintained on a mixed genetic background and genotyped as reported. For the study of dental development, we used age-matched CD1-K14-EGFP animals (Vaezi et al., 2002). In all other experiments, CD1 mice were used as wild-type controls. Noon of the day when a vaginal plug was detected was considered as embryonic day (E) 0.5. Because the *Spry2*^{+/-};*Spry4*^{-/-} incisor duplication was not

completely penetrant, we examined a large number of embryos (at least 20 mutants and 20 wild types between E12.5 and E14.5, and at least 12 mutants and 12 wild types for each time point between E15.5 and E17.5), and we selected the most representative for the figures on the study of dental development. For all other genotypes, at least five embryos per genotype were examined.

The pregnant mice were killed by carbon dioxide exposure followed by cervical dislocation. For 3D reconstructions, wet body weight of the fetuses was determined immediately after their removal from the uterus to be able to correctly compare age- and weight-matched embryos (Peterka et al., 2002).

The pK14-*Spry4* construct was made by replacing the wise cDNA of pK14-wise (Ahn et al., 2010) with the mouse *Spry4* cDNA (904 bases). The 3.8-kb K14-*Spry4* fragment was gel purified and injected into a CBA/J \times C57BL/10J one-cell zygote. A total of 40 K14-*Spry4* embryos between E14.5 and E18.5 were examined.

Epithelial-mesenchymal dissociation

Fresh embryos were dissected in Hanks' medium, and the developing incisor was isolated and incubated in dispase at 37°C for 30 minutes to 7 hours depending on the age of the embryo; the longest incubation periods were used only for late embryos with mineralized tissues. After dispase treatment, which disrupts the adhesion between epithelium and mesenchyme, the samples were transferred to PBS and the epithelium was carefully pulled out of the mesenchyme. The epithelium was then fixed in 4% paraformaldehyde. We have previously used this method, which enables direct visualization of the tooth germ from all sides, and have found that the morphologies observed with this method were consistent with 3D reconstructions (Prochazka et al., 2010).

3D reconstructions of the dental and adjacent epithelium

Mouse embryonic heads at E12.5-18.5 were fixed in Bouin-Hollande fluid and embedded in paraffin. Sixty heads were cut in series of 7 μ m frontal sections. The sections were stained with Hematoxylin-Eosin and Alcian Blue.

The specimens were ranked according to the chronological age, refined by body weight, of embryos. A succession of gradual stages of incisor development was determined on histological sections. For 3D

reconstructions of the epithelium of the developing incisor, we selected ten representative series of routinely stained frontal paraffin sections of *Spry2^{+/-};Spry4^{-/-}* mouse heads at E12.5–E17.5 and seven series of wild-type mouse heads. In all these specimens, the epithelium of the right and/or left upper incisor area was reconstructed.

Contours of the dental and adjacent oral epithelium were drawn from frontal histological sections using a Leica DMLB microscope (Leica Microsystems, Wetzlar, Germany) equipped with a drawing chamber at a magnification of $\times 320$. Apoptotic cells and bodies in the epithelium were recorded in the drawings. The digitalization of the serial drawings and correlation of successive images have previously been described (Lesot et al., 1996). Three-dimensional images were generated using VG Studio Max 2.0 software (VG Studio Max, Heidelberg, Germany).

Quantitative evaluation of proliferation and apoptosis

The area of dental epithelium was measured on each fifth frontal serial section using ImageJ (<http://rsb.info.nih.gov/ij/>). The measured area was delimited by the basement membrane, the oral surface of the epithelium, and the places where the thickness of the dental epithelium decreased to the thickness of the medially and laterally adjacent oral epithelium. The volume of dental epithelium was calculated as the mean of the area of dental epithelium multiplied by the length of the dental epithelium (corresponding to the number of sections with the thickened incisor epithelium multiplied by the section thickness 7 μm). The mitotic index was calculated as the percentage of cells in mitosis (from early metaphase to early telophase). The apoptotic rate was calculated as the number of observed apoptotic cells and bodies per 100 cells. For details, see Peterkova et al. (Peterkova et al., 2009).

In situ hybridization

After harvesting, embryos were fixed overnight in 4% paraformaldehyde. RNA in situ hybridizations were performed either on whole-mount embryos or on paraffin sections using standard protocols (Klein et al., 2006; Klein et al., 2008). Antisense, digoxigenin-labeled RNA probes were generated from full length *Fgf4* and *Shh* cDNAs (kind gifts from Drs Gail Martin, UCSF, San Francisco, CA, USA, and Andrew McMahon, Harvard University, Cambridge, MA, USA, respectively).

Quantitative RT-PCR

RNA was isolated from the incisor developing area at E12.5 and E13.5 using a Qiagen RNeasy Mini Kit. Expression was assessed quantitatively using GoTaq qPCR Master Mix (Promega) in a Mastercycler Realplex (Eppendorf), and transcript levels were normalized to the housekeeping gene glyceraldehyde-3-phosphate dehydrogenase (GAPDH). Results are expressed as normalized expression values (equal to $2^{-\Delta\text{Ct}}$). Primer sequences used for RT-qPCR are listed in Table S1 in the supplementary material.

Study of label-retaining cells

We crossed *Spry2^{+/-};Spry4^{-/-}* mice with *K5fTA;H2B-GFP* mice, in which expression of a doxycycline-repressible *H2B-GFP* transgene is controlled in the epithelium by the keratin 5 (*K5; Krt5* – Mouse Genome Informatics) promoter. All epithelial cells were uniformly labeled by GFP expression before doxycycline was added. In the presence of doxycycline, expression of *H2B-GFP* was repressed and, subsequently, the *H2B-GFP* label was diluted out in proliferating cells (Tumbar et al., 2004), resulting in isolated populations of label-retaining cells (LRCs; see Fig. S2 in the supplementary material). Mice carrying both *K5fTA* (Diamond et al., 2000) and *H2B-GFP* (Tumbar et al., 2004) alleles were genotyped by observation of GFP-fluorescent skin using a fluorescence dissecting microscope. Adult mice were fed a doxycycline-containing diet for 6–8 weeks. Dissection of the incisor and observations were made under a Leica MZ16F dissecting microscope equipped with a Leica EL600 light source.

Scanning electron microscopy

A Hitachi S-4300SE/N environmental scanning electron microscope (ESEM; Hitachi America, Pleasanton, CA, USA) operating at 20 kV under high-resolution image mode was used to image incisors. Prior to mounting on a metal stub for imaging, samples were embedded in epoxy resin and sectioned using an ultra-microtome (Leica, LLC).

RESULTS

Spry2^{+/-};Spry4^{-/-} mice have supernumerary incisors

The perinatal incisor (Fig. 1A), which appears as a tooth bud around embryonic day (E) 12, is unerupted. After eruption in the postnatal period, the incisor continues to grow for the rest of the animal's life because of the presence of stem cells in the cervical loops (CLs), the epithelial structures at the apical end of the incisors (Fig. 1B). Whereas the wild-type mouse always has a single upper incisor on each side of the jaw arch (Fig. 1C,D,F), approximately half of the *Spry2^{+/-};Spry4^{-/-}* mice had two upper incisors per half arch instead of one (Fig. 1E,G). The presence of two incisors per quadrant, each with enamel on both lingual and labial surfaces, is reminiscent of the incisor configuration of most non-rodent mammals.

The duplicated incisors in the mutant were located side by side and shared the same bone socket, suggesting that the development of the two incisors was not independent. Examination of embryonic sections at E18.5 allowed us to look at the relationship between the dental epithelium, called the enamel organ, and the ensheathed dental mesenchyme (papilla). In the *Spry2^{+/-};Spry4^{-/-}* mutants, we observed that the two incisors shared the same enamel organ split by an epithelial septum, each part accommodating a distinct dental papilla (prospective pulp). The septum was formed by a duplication of the layer of inner dental epithelium with interposed stratum intermedium cells, which participate in ameloblast differentiation.

In wild-type incisors, enamel-producing ameloblasts were only located on the labial (nearer the lip) side (white asterisk, Fig. 1D). In the mutant, the layer of ameloblasts also extended to the septum between the two incisors and to the lateral aspect of the lateral incisor (blue asterisks, Fig. 1E), although this was not reflected in the adult enamel pattern (Fig. 1G). We have previously reported that in lower incisors of *Spry2^{+/-};Spry4^{-/-}* mice, enamel is abnormally present on the lingual surface (Klein et al., 2008). We performed scanning electron microscopy (SEM) and found that *Spry2^{+/-};Spry4^{-/-}* mice also had lingual enamel in their upper incisors, and this enamel was normally organized (see Fig. S1 in the supplementary material).

Incisor growth is associated with the presence of stem cell niches in the CLs (Harada et al., 1999; Seidel et al., 2010; Parsa et al., 2010). We next set out to study the stem cell niches in the upper incisors of *Spry2^{+/-};Spry4^{-/-}* mutants, in order to determine whether the duplicated incisors in the mutants grow from the same stem cell population. We took advantage of label retention, which is a property of many stem cell populations and can serve as an indication of the presence of slow-cycling stem cells (Fuchs, 2009); we have previously used this approach to identify slowly cycling stem cells in the wild-type incisor (Seidel et al., 2010). We crossed *Spry2^{+/-};Spry4^{-/-}* mice with *K5fTA;H2B-GFP* mice and obtained LRCs as described previously (Seidel et al., 2010). In the wild-type adult mouse, the lingual CL contained one population of LRCs (see Fig. S2 in the supplementary material). In the mutant, the lingual part of the adult incisors contained a total of three stem cell niches (see Fig. S2 in the supplementary material). This result indicates that the maintenance of continuous growth of the two incisors was supported by multiple stem cell niches.

Incisor duplications in sprouty mutants arise following subdivision of the epithelium

To understand the origins of the incisor duplication, we investigated the development of the wild-type and *Spry2^{+/-};Spry4^{-/-}* mutant upper incisors between E12.5 and E17.5 using a combined analysis of dissociated epithelia, histological sections and 3D

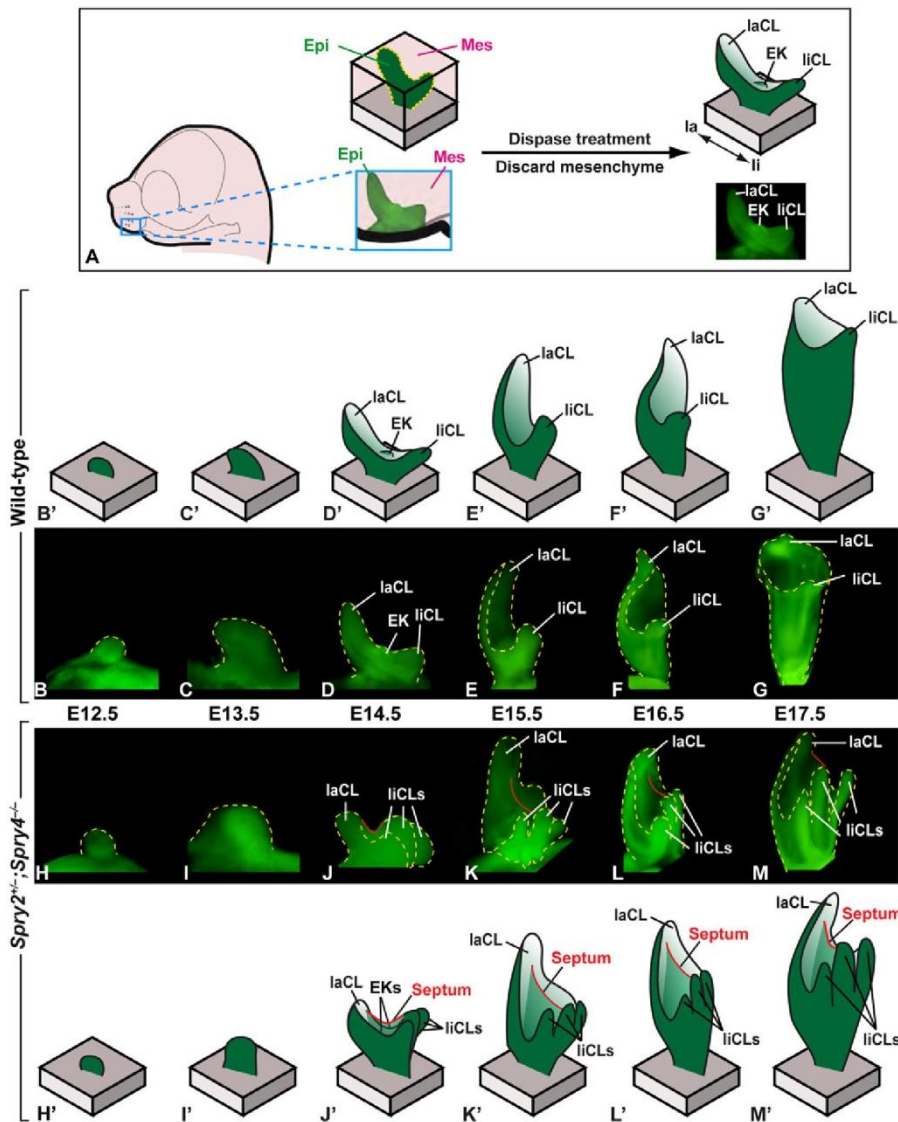


Fig. 2. Upper incisor development in wild-type and *Spry2^{+/-};Spry4^{+/-}* embryos. (A) Schematic of the epithelium-mesenchyme dissociation method. (B-G) Photographs of dissociated incisor epithelia in wild-type embryos from E12.5 to E17.5. (B'-G') Schematic of upper incisor development in wild-type embryos. (H-M) Photographs of dissociated incisor epithelia in *Spry2^{+/-};Spry4^{+/-}* embryos from E12.5 to E17.5. (H'-M') Schematic representation of upper incisor development in *Spry2^{+/-};Spry4^{+/-}* embryos. Yellow dashed lines outline the incisor epithelium; red line indicates position of septum. EK, enamel knot; Epi, epithelium; Mes, mesenchyme; la, labial; li, lingual; laCL, labial cervical loop; liCL, lingual cervical loop.

reconstructions. Tooth germs from closely staged embryos were dissected and the incisor dental epithelium was removed using dispase treatment (Fig. 2A) in order to enable visualization of the epithelium from all sides in a large sample of specimens. The 3D reconstructions documented detailed morphology of the incisor epithelium at different developmental stages.

At E12.5, the upper incisors of both wild-type and mutant embryos were at the early bud stage (Fig. 2B,H), and a well-formed bud was present at E13.5 (Fig. 2C,I). The cap stage started one day later, at E14.5 (Fig. 2D,J). The wild-type incisor cap normally contains the labial and lingual CLs and one enamel knot (Fig. 2D) (Kieffer et al., 1999); the latter is a transient signaling center that controls the morphology of the tooth by directing the growth of surrounding epithelium and mesenchyme (Vaahtokari et al., 1996). In contrast to the wild type, the *Spry2^{+/-};Spry4^{+/-}* incisor epithelium displayed a multiplication of the lingual CLs, such that three CLs were typically observed in the mutants (Fig. 2J). Additionally, in *Spry2^{+/-};Spry4^{+/-}* embryos we observed two enamel knots instead

of one, as well as a septum running from the labial CL to the middle CL located on the lingual side (Fig. 2J). This septum (red line in Fig. 2J) resulted from the splitting of the epithelium into two compartments, each one with its own enamel knot. At E15.5, the dental epithelium grew deeper into the mesenchyme, leading to a more elongated structure with the CLs on the top. The septum observed at E14.5 persisted as an epithelial demarcation between the two mesenchymal compartments at E15.5-17.5 (Fig. 2E-G,K-M).

Further examination by rotating the dissected epithelia (Fig. 3A) and analyzing 3D reconstructions (Fig. 4A-F) revealed the morphological origins of the incisor duplication. At E12.5, the wild-type and mutant incisor epithelia appeared similar (Fig. 3B,E, Fig. 4A,D). The first obvious morphological differences were observed at E13.5, at which point the late bud stage wild-type epithelium had a smooth-appearing surface (Fig. 3C, Fig. 4B), whereas a notch could be seen in mutant epithelium (Fig. 3F, Fig. 4E). A histological section through the incisor bud at E13.5 showed

that this notch was associated with an interruption of the regular arrangement of the inner epithelial cells that suggested an internal boundary between the cell population in the medial and lateral parts of the incisor bud (see Fig. S3 in the supplementary material). The location of the notch at E13.5 was the same as the future location of the septum, which was first visible at E14.5 (Fig. 3G) and persisted at later stages, dividing the papilla into two compartments (see Fig. S3 in the supplementary material). Thus, the earliest morphological change in the mutant embryos was a midline notch, first detectable at E13.5, and the two incisors observed in the jaw half of adult *Spry2^{+/-};Spry4^{-/-}* mice resulted from the development of two compartments within the budding dental epithelium, followed by formation of an epithelial septum that split the mesenchyme inside the enamel organ into two papillae.

Decreased cell death is associated with abnormal subdivision of the epithelium

To understand the cellular basis for the incisor duplication, we next analyzed epithelial cell proliferation, cell death and tissue volume. Apoptotic cells and bodies were labeled in drawings of the dental epithelium realized from frontal histological sections, and their distribution was represented on 3D reconstructions of the dental epithelium (Fig. 4A-F). The proportion of apoptotic elements and proliferative cells was calculated from sections. Although the size of wild-type and *Spry2^{+/-};Spry4^{-/-}* incisors did not differ (Fig. 4I) at E12.5, very little to no cell death, distributed throughout the epithelium, was detected in the mutant, representing a significant decrease from the wild type, which had apoptotic elements mostly present antero-labially in the dental epithelium (Fig. 4A,D,G). At E13.5, apoptotic elements were present in the central region in *Spry2^{+/-};Spry4^{-/-}* incisors as in the wild type, but the number of apoptotic elements was still significantly lower in mutants compared with wild-type embryos (Fig. 4B,E,G). At E14.5, the amount of cell death was similar in wild-type and *Spry2^{+/-};Spry4^{-/-}* mice (Fig. 4G), but the location of dying cells differed, as apoptosis was specifically concentrated along the central axis of the mutant incisor (Fig. 4C,F), corresponding to the area where the epithelial septum between the two duplicated papillae appears. This concentration along the midline was similar to the distribution of apoptotic cells one day earlier in wild-type mice and might reflect a failed attempt by the left and right parts of the incisor to fuse in the *Spry2^{+/-};Spry4^{-/-}* embryos. Interestingly, the only difference in proliferation was a small but significant increase in the mutant compared with wild type at E13.5 (Fig. 4H). Although the overall size of the incisor epithelium was similar at all three time points examined (Fig. 4I), the mutant epithelium was larger when viewed from the mesenchymal aspect, whereas the wild-type epithelium was submerged more deeply into the mesenchyme. Thus, the septum that separated the two dental papillae was correlated with a delay in the onset of cell death from E12.5 to E13.5, increased proliferation at E13.5 and a change in the location of apoptotic cells at E14.5.

Splitting of gene expression domains foreshadows the incisor duplication

To determine how loss of sprouty genes might affect incisor bud development, we assessed the expression pattern of sonic hedgehog (*Shh*), an early marker of tooth development. Initially, *Shh* is expressed in a single domain in the incisor area (Pispa and Thesleff, 2003). At E11.5, *Shh* expression appeared similar in wild-type and mutant specimens (Fig. 5A,B). At E12.5, the *Shh* expression domain was similar in wild-type and mutant embryos

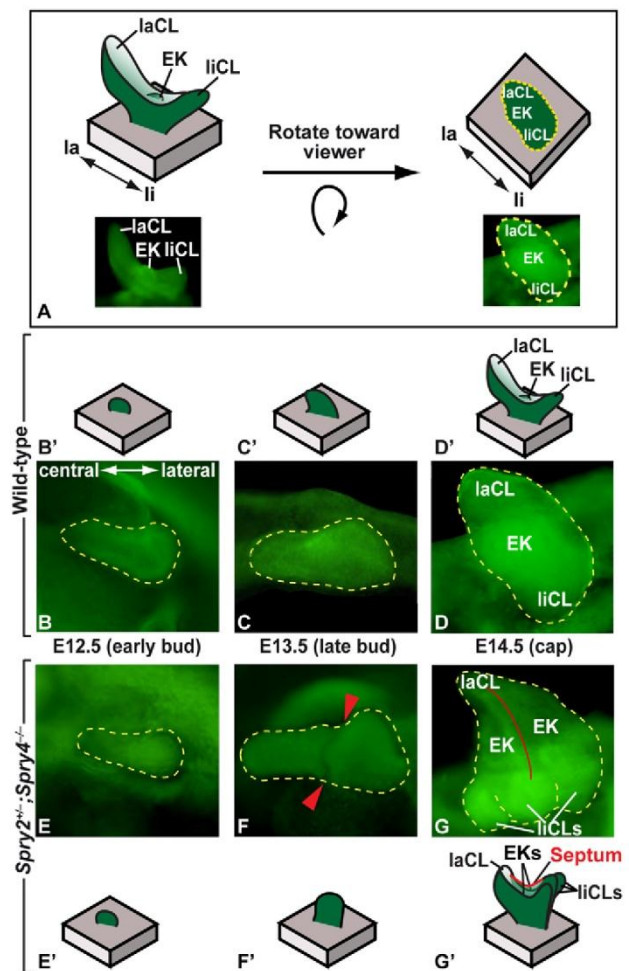


Fig. 3. Septum formation during incisor development in *Spry2^{+/-};Spry4^{-/-}* embryos. (A) Schematic of epithelium re-orientation. (B-D) Photographs of epithelia after re-orientation of wild-type embryos at E12.5, E13.5 and E14.5. (E-G) Photographs of epithelia of *Spry2^{+/-};Spry4^{-/-}* embryos at E12.5, E13.5 and E14.5. (B'-G') Schematics of epithelial development. Yellow dashed lines outline the incisor; red arrowheads in F point to notch; red line in G indicates septum. la, labial; li, lingual; EK, enamel knot; laCL, labial cervical loop; liCL, lingual cervical loop.

(Fig. 5C,D), but the *Shh* expression staining was more intense in the mutants, and this finding was confirmed by qPCR analyses (see Fig. S4 in the supplementary material). At E13.0, a time point at which morphological differences were not detected in the mutant, the domain of *Shh* expression was already widely split in the mutant mice (Fig. 5F). In wild-type embryos, a transient splitting of the early *Shh* expression domain can be observed in the lower as well as upper mouse incisor (Hovorakova et al., 2011), but this is followed by the presence of a single *Shh* domain at E13.5. However, in the present study, the split domain of *Shh* expression was identified in mutants but not controls at E13.5 (data not shown). These two separate domains of *Shh* expression in the mutant suggest that the decision to split into two teeth occurs at or before this time point.

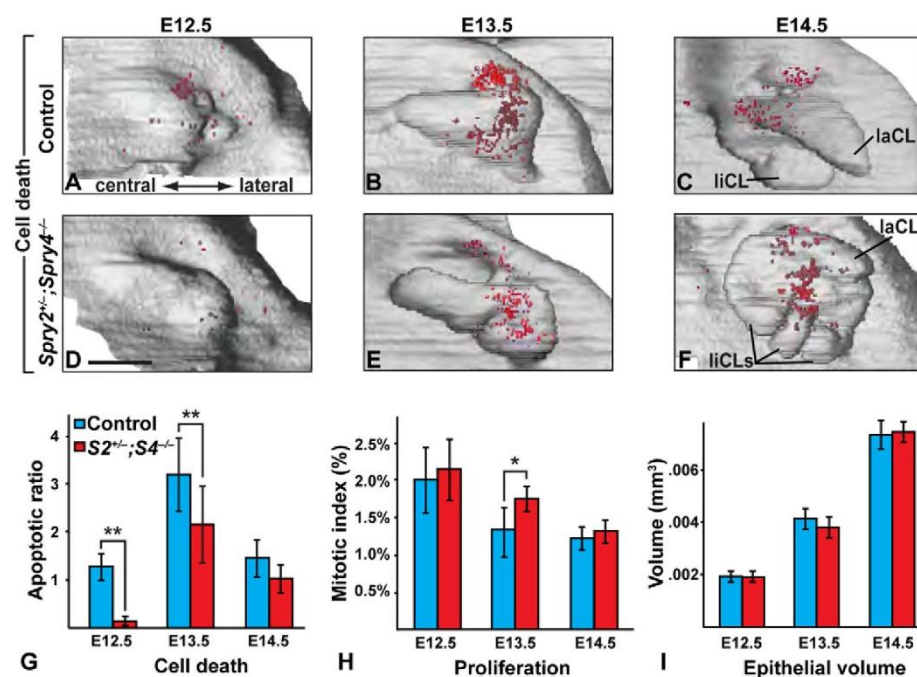


Fig. 4. Cell death and proliferation in incisors of control and *Spry2^{+/-};Spry4^{-/-}* embryos. (A-F) Three-dimensional reconstructions viewed from mesenchymal aspect and location of apoptotic elements (red dots) in epithelia of control (A-C) and *Spry2^{+/-};Spry4^{-/-}* embryos (D-F) at E12.5 (A,D), E13.5 (B,E) and E14.5 (C,F). Scale bar: 100 μ m. (G-I) Apoptotic rate (G), mitotic index (H) and epithelial volume (I) in control and *Spry2^{+/-};Spry4^{-/-}* embryos. Mean \pm s.e.m. are plotted. * P <0.05, ** P <0.01.

In our morphological analysis, we identified two raised structures as the likely enamel knots at E14.5 (Fig. 3G). We next assessed the expression of *Fgf4* and *Shh*, which are markers of enamel knots, to determine whether each compartment in the mutant has a bona fide, distinct enamel knot. In situ hybridization on dissected epithelia showed one domain of *Fgf4* and *Shh* expression in the wild type, located in the center of the incisor, whereas in the mutant, two *Fgf4* and *Shh* expression domains representing the two enamel knots were present, one on each side of the septum (Fig. 5G,H; data not shown). Thus, the mutant incisor had two distinct enamel knots at E14.5.

Loss of sprouty genes causes hypersensitivity to *Fgf10* in the dental epithelium

A previous study suggested that the lack of sprouty function leads to hypersensitivity of dental epithelial buds in the molar region to FGF signaling from the mesenchyme (Klein et al., 2006). To test for such hypersensitivity in the incisor of *Spry2^{+/-};Spry4^{-/-}* embryos, we measured the relative expression of *Etv5*, a marker of the FGF pathway (Roehl and Nüsslein-Volhard, 2001). The observed relative increase of *Etv5* at E12.5 and E13.5 indicated an upregulation of FGF signaling in the *Spry2^{+/-};Spry4^{-/-}* mutants (see Fig. S4 in the supplementary material). We have previously shown that, in both the early incisor and molar, *Spry1* is expressed in epithelium and mesenchyme, *Spry2* in epithelium and *Spry4* exclusively in the mesenchyme (Klein et al., 2006; Klein et al., 2008). qPCR analysis confirmed that *Spry2^{+/-};Spry4^{-/-}* mutants had half the dosage of *Spry2* and no expression of *Spry4* (see Fig. S4A,B in the supplementary material).

Fgf10 is expressed during incisor development from early stages to adulthood (Kettunen et al., 2000). Its expression around CLs regulates epithelial stem cell survival, which is essential for continuous incisor growth (Harada et al., 2002; Yokohama-Tamaki et al., 2006). We therefore produced *Spry2^{+/-};Spry4^{-/-}* mice lacking one *Fgf10* allele to test whether decreased FGF dosage would rescue

the incisor duplication phenotype. Whereas an incisor duplication was present in 43% of *Spry2^{+/-};Spry4^{-/-}* mice, compound mutants with a *Fgf10* null allele had a duplicated incisor in only 17% of specimens (see Fig. S5 in the supplementary material). Thus, a decrease in *Fgf10* dosage caused a decreased penetrance of the duplication, suggesting that the incisor duplication observed in *Spry2^{+/-};Spry4^{-/-}* mice resulted from hypersensitivity to FGF signaling. Interestingly, upregulation of *Fgf10* was detected by qPCR at E12.5 but not at E13.5 in the mutant, whereas *Fgf9* levels were unaltered (see Fig. S4A,B in the supplementary material), illustrating the importance of the proper dose and timing of activity of FGF signaling. This finding was reminiscent of the upregulation in *Fgf10* expression that we had previously observed in incisors from the lower mandibles of *Spry2^{+/-};Spry4^{-/-}* embryos (Klein et al., 2008).

Modulation of sprouty levels can lead to a phenotypic gradation in tooth number

The molecular regulation of tooth number is an important question in evolutionary biology (reviewed by Cobourne and Sharpe, 2010), and the phenotype in the *Spry2^{+/-};Spry4^{-/-}* mutant, which lacks three sprouty alleles, was particularly intriguing in that the incisor duplication was present in the upper but not lower jaw. This suggested to us that a subtle dosage response might exist between the level of FGF signaling and the number of teeth. Therefore, we produced a mouse with increased sprouty dosage in which *Spry4* was ectopically expressed in the epithelium under the control of the human keratin 14 promoter (*K14-Spry4^{GOF}*). There was significant variability among these embryos (see Fig. S6 in the supplementary material), but it was interesting to note that in one *K14-Spry4^{GOF}* embryo at E15.5, we observed fusion of left and right lower incisors along the midline (Fig. 6A-A''); we also observed in these mutants a case of lower incisor duplications (see Fig. S6 in the supplementary material). These data indicate that, in certain cases, increasing the expression of a signaling antagonist can lead to decreases in the number of teeth.

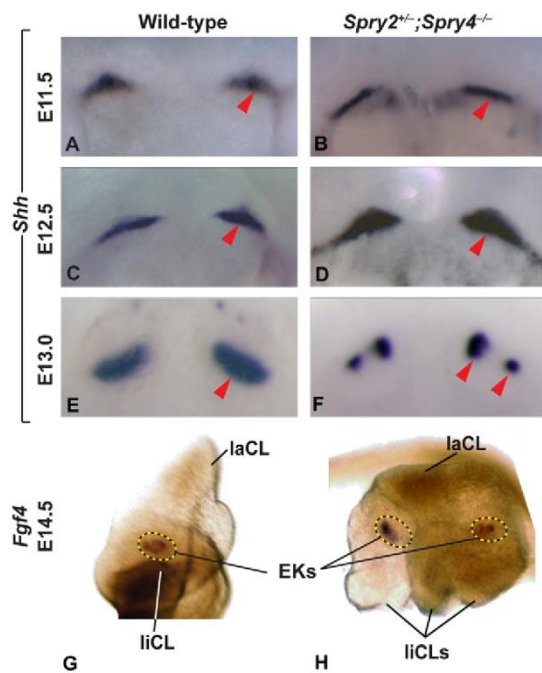


Fig. 5. In situ hybridization in incisors of wild-type and *Spry2*^{+/-};*Spry4*^{-/-} embryos. (A-F) Whole-mount RNA in situ hybridization for *Shh* in wild-type (A, C, E) and *Spry2*^{+/-};*Spry4*^{-/-} (B, D, F) embryos at E11.5, E12.5 and E13.0. Red arrowheads point to the left incisor expression domain. (G, H) Whole-mount RNA in situ hybridization for *Fgf4* in dissected incisor epithelia viewed from mesenchymal side of wild-type (G) and *Spry2*^{+/-};*Spry4*^{-/-} (H) embryos at E14.5. EK, enamel knot; laCL, labial cervical loop; liCL, lingual cervical loop.

We next produced a series of mice lacking different combinations of sprouty genes in order to progressively change the level of RTK signaling in the developing tooth. As described above, wild-type embryos have a single incisor in each dental quadrant (Fig. 6B-B''), and *Spry2*^{+/-};*Spry4*^{-/-} embryos had two upper incisors and one lower incisor (Fig. 6C-C''). Further decreases in sprouty dosage in *Spry1*^{-/-};*Spry4*^{+/-} and *Spry2*^{-/-};*Spry4*^{+/-} embryos led to two upper and two lower incisors in each quadrant (Fig. 6D-E''). Interestingly, the phenotypic gradation observed with the decrease of sprouty dosage involved not only the number of incisors but also their inter-relationship. In *Spry2*^{+/-};*Spry4*^{-/-} embryos, the two upper incisors were still in the same enamel organ (Fig. 6C'). In *Spry1*^{-/-};*Spry4*^{+/-} embryos, the two upper incisors were in the same enamel organ, but the enamel organ had two stalks joining the enamel organ with the oral epithelium (Fig. 6D'). In *Spry2*^{-/-};*Spry4*^{+/-} embryos, we identified specimens in which each duplicated upper incisor developed in its own enamel organ (Fig. 6E'; data summarized in Fig. 6F). A similar gradation from one to two teeth was seen in the lower incisors (Fig. 6B'', D'', E''), but in the case of the lower jaw, even in the double-null embryos the two incisors still developed in the same enamel organ. These data indicate that the tendency to increase tooth number in the lower jaw is less sensitive to sprouty dosage than in the upper jaw, as it occurred in the lower jaw only when four sprouty alleles were deleted versus three for the upper

jaw (Fig. 6F). Overall, in both upper and lower incisors, the decrease of sprouty dosage led to progressively more independent teeth in both upper and lower jaws.

DISCUSSION

We report that modification of sprouty gene dosage regulates the number of incisors. As sprouty gene dosage was increased or decreased, a spectrum of phenotypes was observed. These ranged from one central incisor to two separate incisors in two different enamel organs located side-by-side, which resembled the dentition of most non-rodent mammals. Our study of dental development in *Spry2*^{+/-};*Spry4*^{-/-} embryos indicates that sprouty genes control the integrity of the *Shh* expression domain. In these mutants, the duplication resulted from subdivision of the incisor enamel organ, which initially had a similar size to that of the control embryos, by an epithelial septum invading and splitting the mesenchyme into two papillae. This morphological splitting was associated with the persistent splitting of the *Shh* expression domain, with a delay in the onset of cell death at early stages and a later change in the location of apoptosis and increased proliferation. We also found that the sprouty genes antagonize the FGF pathway during regulation of incisor number by producing *Spry2*^{+/-};*Spry4*^{-/-} mutants in which one allele of *Fgf10* was inactivated.

The duplicated incisors belong to the same generation and are not replacement teeth

The supernumerary incisors reported in mutant mice have most often been located on the lingual side of the normal incisor (Danforth, 1958; Murashima-Suginami et al., 2007; Ohazama et al., 2008; Munne et al., 2009). The detailed analysis of one of these mutants (*Sostdc1*) showed that the supernumerary incisor developed on the lingual side of the normal one, and this tooth was considered to belong to a different tooth generation, corresponding to the revival of either the replacement incisor (Munne et al., 2009) or of a rudimentary lacteal incisor (Murashima-Suginami et al., 2007). The supernumerary incisor of *Lrp4*-null mice has been considered as having the same origin as the supernumerary incisor of *Sostdc1* mutants (Ohazama et al., 2010). In the sprouty mutants reported here, the concomitant developmental origin and the side-by-side organization of the two incisors indicate that they must be considered as the same tooth generation. To our knowledge, the only adult mutants reported to have an incisor phenotype similar to the *Spry2*^{+/-};*Spry4*^{-/-} mice are *Eda-tabby* (Sofaer, 1969) and the *Pax6-Sey* (small eye) homozygous mutants (Kaufman et al., 1995). In *Eda* mutants, only very rare cases of side-by-side upper incisor duplication have been reported (Sofaer, 1969); we did not detect this phenotype during our observation of 60 heterozygous and 80 null *Eda* mutants in previous studies (Charles et al., 2009a; Charles et al., 2009b). *Pax6* mutant rats, as *Pax6-Sey* mice, also exhibit supernumerary incisors, and it has been suggested that these incisors result from the total lack of fusion between two components of the epithelial incisor anlage separated by a cleft lip (Kriangkrai et al., 2006) and not from the secondary splitting of the incisor anlage as we have observed. Splitting of the incisor anlage might occur in *nestin-cre/K5-lacZfl-smad7* mice, but the splitting seemed to be a transient event, as the two incisors were fused at their base (Klopčic et al., 2007). The β -cat^{Δprx/lacZ} mice have two incisors belonging to the same generation, but in these mice only the lower incisors have been reported to be affected (Fujimori et al., 2010). Thus, the *Spry2*^{+/-};*Spry4*^{-/-} mice are the first in which supernumerary

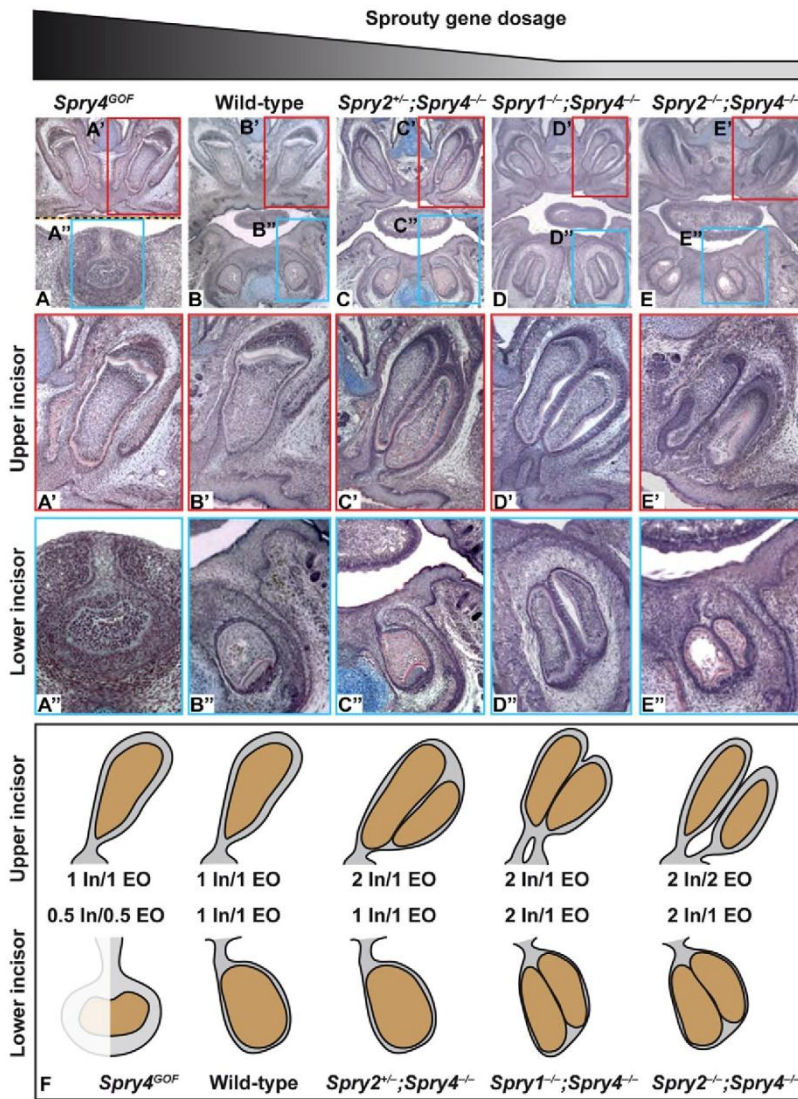


Fig. 6. Incisor phenotypes in a Sprouty gene dosage series. (A-E) Frontal histological sections of embryonic head at E15.5 (A) and E18.5 (B-E) showing the phenotype of upper and lower incisors in *K14-Spry4* (*Spry4^{GOF}*) (A), wild-type (B), *Spry2^{+/-};Spry4^{+/-}* (C), *Spry1^{+/-};Spry4^{+/-}* (D) and *Spry2^{+/-};Spry4^{+/-}* (E) embryos. (A'-E') High magnification of upper incisor. (A''-E'') High magnification of lower incisor. (F) Schematic with indication of the number of incisors and enamel organs for each genotype. EO, enamel organ(s); In, incisor(s). Dotted line in A indicates that this composite image is composed of upper and lower jaw images from different sections.

incisor development has been clearly shown in vivo to result from the secondary splitting of the incisor primordium and *Shh* expression domain after normal development at initial stages.

Splitting of the incisor primordium precedes the incisor duplication

In the sprouty dosage series reported here, we showed that the splitting of an anlage does not always occur as a sudden change but rather can also develop as a progressive process. The stable development of two incisors in the same enamel organ and the two independent incisors seen in *Spry2^{+/-};Spry4^{+/-}* and *Spry1^{+/-};Spry4^{+/-}* mice, respectively, might be facilitated by a varying degree of re-individualization of the ancestral primordia.

Etv5, which is known to be a downstream target of the FGF pathway (Roehl and Nüsslein-Volhard, 2001; Zhang et al., 2009), was upregulated in *Spry2^{+/-};Spry4^{+/-}* embryos (see Fig. S4 in the supplementary material), indicating increased FGF signaling in these mutants. Because *Shh* is necessary for the survival of tooth bud epithelial cells (Cobourne et al., 2001), the lower cell death

observed in the *Spry2^{+/-};Spry4^{+/-}* embryos at E12.5 might have resulted from the higher levels of *Shh* expression (see Fig. S4 in the supplementary material). Future studies will be needed to test our hypothesis that the splitting of the *Shh* expression domain in the mutant at E13.0 creates a *Shh*-free region in the placode; this might correspond to the region in which cell death is subsequently concentrated and where the septum appears, leading to the morphological splitting of the incisor.

We have previously reported that inactivation of sprouty genes leads to decreased apoptosis in a rudimentary diastema tooth bud (Peterkova et al., 2009), indicating that these genes perform similar functions in the incisor and molar regions. The transient splitting of some gene expression domains in the budding dental epithelium during a very short time period has also recently been shown in the early incisor region in both lower and upper jaws of wild-type embryos without any tooth anomalies (Hovorakova et al., 2011; Nakatomi et al., 2010). This splitting of the early *Shh* domain was followed by the presence of a single *Shh* expression domain at the incisor bud at E13.5 (Hovorakova et al., 2011). However, splitting

of the *Shh* expression domain leading to the development of a supernumerary lower incisor has been recently reported in β -cat ^{Δ Prx/lacZ} mice (Fujimori et al., 2010). In these embryos, the *Shh* expression domain splitting occurred at E13.0 and the first morphological evidence of the incisor duplication was noticed at E13.5. Together with our results, this study emphasizes that the integrity of *Shh* expression domain at the bud stage is crucial for the normal development of the mouse incisor. The developmental relationship between the early and later *Shh* expression domains (Hovorakova et al., 2011) and formation of the supernumerary incisors will require further investigation.

The absence of variability in the number of incisors in wild rodents suggests that incisor development is highly canalized. However, during our observation of wild-type embryos at E14.5 and E15.5, we found eight out of 55 specimens with a notch in the lingual CL, and two specimens even had a duplication of this CL (see Fig. S7 in the supplementary material). These specimens indicate that incisor development is not as highly canalized as it might seem when looking at adult mice, reflecting a degree of developmental plasticity that might explain the incomplete penetrance of the incisor duplication phenotype in *Spry2*^{+/-}; *Spry4*^{-/-} mice.

Activator-inhibitor balance allows a range of re-individualization of the ancestral tooth primordia

The fusion or separation of tooth primordia resulting in their respective joint or individual development has been proposed to depend on a balance between activators and inhibitors (Peterkova et al., 2002). In vitro modification of this balance by decreased concentration of noggin (considered to be an inhibitor) or increased concentration of activin (an activator) can lead to the development of two or three small incisors instead of the normal single thick incisor (Munne et al., 2010). In the present study, the decrease of sprouty gene dosage resulted in the splitting of the epithelial incisor anlage, providing an in vivo analog of the in vitro splitting (Munne et al., 2010). Previous studies on postnatal development of incisors in *Fgf3*^{-/-}; *Fgf10*^{-/-} mice showed that decreased FGF levels led to a single small incisor (Wang, X.-P., et al., 2007), which might develop from a smaller primordium. We can thus extrapolate the existence of a phenotypic gradation involving FGF signaling and sprouty genes, with a small incisor anlage in *Fgf3*^{-/-}; *Fgf10*^{-/-} embryos, a larger anlage in the wild type and a split incisor primordium in *Spry2*^{+/-}; *Spry4*^{-/-} embryos, which are hypersensitive to FGF10 signaling. The sprouty mutant series demonstrated such a gradation, from fusion of left and right lower incisors in one *K14-Spry4*^{GOF} specimen to two incisors in two enamel organs in *Spry1*^{-/-}; *Spry4*^{-/-} mice. The fusion of the left and right incisors as seen in the fused *K14-Spry4*^{GOF} specimen was also reported previously in mouse embryos with hypervitaminosis A (Knudsen, 1965). These mice showed a gradation of phenotypes ranging from normal to complete fusion of the two enamel organs (Knudsen, 1965), and similar observations were made in *p53* mutant embryos (Kaufman et al., 1997). In a study of *Bmp4*^{h Δ Prx1/ Δ lacZ} embryos, the mandibular *Shh* expression domains were fused in the midline, whereas in β -cat ^{Δ Prx/lacZ} embryos, two incisors developed, pointing to important differences in the roles of BMP and WNT/ β -catenin signaling in the regulation of incisor number in the mandible (Fujimori et al., 2010). In all these cases, we presume that the levels of activator and inhibitor of incisor development were modified, suggesting that in the sprouty series the incisor splitting was dosage dependant, with progressive splitting of the epithelial anlage as sprouty dosage was decreased.

The sprouty gene dosage series leads to the ancestral Glires phenotype

The number of upper incisors per quadrant varies from zero to five among extant mammals, and the genetic mechanisms underlying this variation are poorly understood. The progressive change in tooth number in the sprouty mutant series enabled us to explore the similarities between the incisor dental formulas (i.e. the number of incisors per quadrant) of sprouty mutants and wild Euarchothoglires, the group including rodents, rabbits and primates (Fig. 7A, node 1). Among Glires, the group that comprises rabbits and rodents (Fig. 7A, node 2), the number of incisors is reduced. This is particularly the case for rodents and Eurymilidae, a fossil family of rodent-related species, which together are called Simplicidentata (Fig. 7A, node 3) because they only possess one enlarged evergrowing incisor, considered to be the second deciduous incisor (dl²). Lagomorphs (rabbits and pikas) and the Mimotonidae family of Lagomorph-related fossil species are called Duplicidentata because they have two upper incisors (Fig. 7A, node 4); the enlarged evergrowing incisor typical of all Glires and a second, small tooth located behind the main incisor and considered to be the third permanent incisor (I³) (Lockett, 1985; Ooe, 1980). Almost all living Scandentia (treeshrews), Dermoptera (colugos) and primates, together named Euarchothonta (Fig. 7A, node 5), have two upper incisors. From the fossil record, it appears that the stem Euarchothoglires (e.g. *Purgatorius*) had at least three incisors (Fig. 7B), indicating that all extant species in this group have lost at least one incisor during evolution. The incisors in *Sostdc1* mutants (Fig. 7A') have many similarities with those of the Lagomorphs and Mimotonidae. In both cases, the incisors are placed one behind the other and appear to arise from two different dental generations (Munne et al., 2010), suggesting that *Sostdc1* might have played a role in the suppression of the permanent upper incisor in the dentition of rodents and Eurymilidae.

The two upper incisors of sprouty mutants belong to the same dental generation and are situated one next to the other, as is the case in most mammals. It is known that basal placental mammals (ancestors of Euarchothoglires) had up to five upper incisors per quadrant (Ji et al., 2002). How the number of incisors decreased during evolution is currently an open question. However, the studies of incisor development in wild-type embryos have produced morphological data suggesting that the decrease of incisor number during evolution was realized by the integration of the incisor primordia, potentially corresponding to rudiments of ancestral incisors (Peterkova et al., 1993). The progressive gradient of re-individualization of incisor primordia observed in our sprouty gene dosage series (Fig. 6A-E) might correspond to a reversal of how the fusion of these incisor primordia occurred during evolution. The ancestor of Glires possessed more incisors than extant rodents (Fig. 7B), and our results suggest that the loss of incisors during evolution of Glires might have occurred through the merging of dental germs.

Enlarged incisors have been positively selected during evolution and maintained in all Glires, perhaps because possessing enlarged incisors constitutes a functional advantage to cut or gnaw on hard plants. The main groups of Glires arose at the beginning of the Cenozoic, at about 60 Ma (Wang, Y., et al., 2007). It is thus likely that Glires diverged from other placental mammals near the close of the Cretaceous (Asher et al., 2005), meaning that the enlargement of the incisor took place during the Upper Cretaceous. The loss of sprouty gene function in the dosage series reported here leads to incisor phenotypes that resemble those of the earliest Glires, which might have been similar to the phenotype of the Euarchothoglires common ancestor.

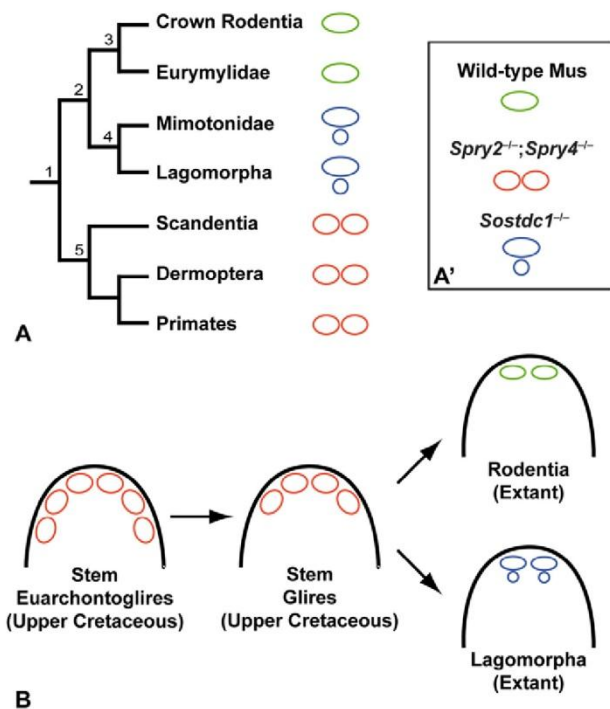


Fig. 7. Upper incisor evolution in Euarchontoglires.

(A) Phylogenetic tree of Euarchontoglires and schematic of the general upper incisor pattern of each taxon. Three patterns are indicated by color coding: one pair of incisors in Simplicidentata (green), two pairs of incisors (labial and lingual, each pair in tandem) in Duplicidentata (blue) and two pairs of incisors (frontals, each pair side by side) in Euarchonta (red). 1, Euarchontoglires; 2, Glires; 3, Simplicidentata; 4, Duplicidentata; 5, Euarchonta. (A') Upper incisor phenotypes of early mutants discussed in the text. (B) Schematic of incisor evolution in early Euarchontoglires showing the appearance of the three main incisor patterns.

Acknowledgements

We thank G. R. Martin for providing mice and for insightful observations and N. Strauli, D.-K. Tran and P. Mostowfi for technical assistance. We are grateful to W. v. Koenigswald for intellectual input, and to K. Seidel, C. Li and other members of the Klein laboratory for advice and discussion. This work was funded by a New Faculty Award II (RN2-00933) from the California Institute for Regenerative Medicine to O.D.K. and by the National Institutes of Health through the NIH Director's New Innovator Award Program, 1-DP2- OD007191, to O.D.K. Additional support was provided by the Grant Agency of the Czech Republic (CZ:GA ČR:GA 304/09/1579 and CZ:GA ČR:GA 304/07/0223), MSM of the Czech Republic (MSM0021620843) and Academy of Science of the Czech Republic (AV0Z50390512). Deposited in PMC for release after 12 months.

Competing interests statement

The authors declare no competing financial interests.

Supplementary material

Supplementary material for this article is available at <http://dev.biologists.org/lookup/suppl/doi:10.1242/dev.069195/-DC1>

References

Ahn, Y., Sanderson, B. W., Klein, O. D. and Krumlauf, R. (2010). Inhibition of Wnt signaling by Wise (Sostdc1) and negative feedback from Shh controls tooth number and patterning. *Development* **137**, 3221-3231.
Asher, R., Meng, J., Wible, J., McKenna, M., Rougier, G., Dashzeveg, D. and Novacek, M. (2005). Stem lagomorpha and the antiquity of Glires. *Science* **307**, 1091-1094.

Basson, M., Akbulut, S., Watson-Johnson, J., Simon, R., Carroll, T., Shakya, R., Gross, I., Martin, G., Lufkin, T., McMahon, A. et al. (2005). Sprouty1 is a critical regulator of GDNF/RET-mediated kidney induction. *Dev. Cell* **8**, 229-239.
Boran, T., Peterkova, R., Lesot, H., Lyons, D., Peterka, M. and Klein, O. D. (2009). Temporal analysis of ectopic enamel production in incisors from sprouty mutant mice. *J. Exp. Zool. B Mol. Dev. Evol.* **312B**, 473-485.
Catón, J., Luder, H. U., Zoupa, M., Bradman, M., Bluteau, G., Tucker, A. S., Klein, O. and Mitsiadis, T. (2009). Enamel-free teeth: Tbx1 deletion affects amelogenesis in rodent incisors. *Dev. Biol.* **328**, 493-505.
Charles, C., Pantalacci, S., Peterkova, R., Tafforeau, P., Laudet, V. and Viriot, L. (2009a). Effect of eda loss of function on upper jugal tooth morphology. *Anat. Rec.* **292**, 299-308.
Charles, C., Pantalacci, S., Tafforeau, P., Headon, D., Laudet, V. and Viriot, L. (2009b). Distinct impacts of Eda and Edar loss of function on the mouse dentition. *PLoS One* **4**, e4985.
Cobourne, M. and Sharpe, P. (2010). Making up the numbers: The molecular control of mammalian dental formula. *Semin. Cell Dev. Biol.* **21**, 314-324.
Cobourne, M., Hardcastle, Z. and Sharpe, P. (2001). Sonic hedgehog regulates epithelial proliferation and cell survival in the developing tooth germ. *J. Dent. Res.* **80**, 1974-1979.
Danforth, C. (1958). The occurrence and genetic behavior of duplicate lower incisors in the mouse. *Genetics* **43**, 140-148.
Diamond, I., Owolabi, T., Marco, M., Lam, C. and Glick, A. (2000). Conditional gene expression in the epidermis of transgenic mice using the tetracycline-regulated transactivators tTA and rTA linked to the keratin 5 promoter. *J. Invest. Dermatol.* **115**, 788-794.
Fuchs, E. (2009). Finding one's niche in the skin. *Cell Stem Cell* **4**, 499-502.
Fujimori, S., Novak, H., Weissenbock, M., Jussila, M., Goncalves, A., Zeller, R., Galloway, J., Thesleff, I. and Hartmann, C. (2010). Wnt/beta-catenin signaling in the dental mesenchyme regulates incisor development by regulating Bmp4. *Dev. Biol.* **348**, 97-106.
Guy, G., Wong, E., Yusoff, P., Chandramouli, S., Lo, T., Lim, J. and Fong, C. (2003). Sprouty: how does the branch manager work? *J. Cell Sci.* **116**, 3061-3068.
Harada, H., Kettunen, P., Jung, H.-S., Mustonen, T., Wang, Y. and Thesleff, I. (1999). Localization of putative stem cells in dental epithelium and their association with notch and FGF signaling. *J. Cell Biol.* **147**, 105-120.
Harada, H., Toyono, T., Toyoshima, K., Yamasaki, M., Itoh, N., Kato, S., Sekine, K. and Ohuchi, H. (2002). FGF10 maintains stem cell compartment in developing mouse incisors. *Development* **129**, 1533-1541.
Hovorakova, M., Prochazka, J., Lesot, H., Smrckova, L., Churava, S., Boran, T., Kozmik, Z., Klein, O., Peterkova, R. and Peterka, M. (2011). Shh expression in a rudimentary tooth offers new insights into development of the mouse incisor. *J. Exp. Zool. B Mol. Dev. Evol.* **316B**, 347-358.
Ji, Q., Luo, Z., Yuan, C., Wible, J., Zhang, J. and Georgi, J. (2002). The earliest known eutherian mammal. *Nature* **416**, 816-822.
Kaufman, M., Chang, H. and Shaw, J. (1995). Craniofacial abnormalities in homozygous Small eye (Sey/Sey) embryos and newborn mice. *J. Anat.* **186**, 607-617.
Kaufman, M., Kaufman, D., Brune, R., Stark, R., Armstrong, J. and Clarke, A. (1997). Analysis of fused maxillary incisor dentition in p53-deficient exencephalic mice. *J. Anat.* **191**, 57-64.
Kettunen, P., Laurikkala, J., Itäranta, P., Vainio, S., Itoh, N. and Thesleff, I. (2000). Associations of FGF-3 and FGF-10 with signaling networks regulating tooth morphogenesis. *Dev. Dyn.* **219**, 322-332.
Kieffer, S., Peterkova, R., Vonesch, J. L., Ruch, J. V., Peterka, M. and Lesot, H. (1999). Morphogenesis of the lower incisor in the mouse from the bud to early bell stage. *Int. J. Dev. Biol.* **43**, 531-539.
Kim, H. J. and Bar-Sagi, D. (2004). Modulation of signalling by Sprouty: a developing story. *Nat. Rev. Mol. Cell Biol.* **5**, 441-450.
Klein, O., Minowada, G., Peterková, R., Kangas, A., Yu, B., Lesot, H., Peterka, M., Jernvall, J. and Martin, G. (2006). Sprouty genes control diastema tooth development via bidirectional antagonism of epithelial-mesenchymal FGF signaling. *Dev. Cell* **11**, 181-190.
Klein, O., Lyons, D., Balooch, G., Marshall, G., Basson, M., Peterka, M., Boran, T., Peterkova, R. and Martin, G. (2008). An FGF signaling loop sustains the generation of differentiated progeny from stem cells in mouse incisors. *Development* **135**, 377-385.
Klopčič, B., Maass, T., Meyer, E., Lehr, H. A., Metzger, D., Chambon, P., Mann, A. and Blessing, M. (2007). TGF-beta superfamily signaling is essential for tooth and hair morphogenesis and differentiation. *Eur. J. Cell Biol.* **86**, 781-799.
Knudsen, P. (1965). Congenital malformations of upper incisors in exencephalic mouse embryos, induced by hypervitaminosis A. I. Types and frequency. *Acta Odontol. Scand.* **23**, 71-89.
Kriangkrai, R., Chareonvit, S., Yahagi, K., Fujiwara, M., Eto, K. and Iseki, S. (2006). Study of Pax6 mutant rat revealed the association between upper incisor formation and midface formation. *Dev. Dyn.* **235**, 2134-2143.
Lesot, H., Vonesch, J.-L., Peterka, M., Turecková, J., Peterková, R. and Ruch, J.-V. (1996). Mouse molar morphogenesis revisited by three-dimensional

- reconstruction. II. Spatial distribution of mitoses and apoptosis in cap to bell staged first and second upper molar teeth. *Int. J. Dev. Biol.* **40**, 1017-1031.
- Luckett, W. P. (1985). Superordinal and intraordinal affinities of rodents: developmental evidence from the dentition and placentation. In *Evolutionary Relationships Among Rodents* (ed. W. P. Luckett and J. L. Hartenberger), pp. 227-276. New York: Plenum.
- Min, H., Danilenko, D., Scully, S., Bolon, B., Ring, B., Tarpley, J., DeRose, M. and Simonet, W. (1998). Fgf-10 is required for both limb and lung development and exhibits striking functional similarity to *Drosophila* branchless. *Genes Dev.* **12**, 3156-3161.
- Moss-Salentijn, L. (1978). Vestigial teeth in the rabbit, rat and mouse; their relationship to the problem of lacteal dentitions. In *Development, function and evolution of teeth* (ed. P. M. Butler and K. A. Joysey), pp. 13-29. London: Academic Press.
- Munne, P., Tummers, M., Jarvinen, E., Thesleff, I. and Jernvall, J. (2009). Tinkering with the inductive mesenchyme: Sostdc1 uncovers the role of dental mesenchyme in limiting tooth induction. *Development* **136**, 393-402.
- Munne, P., Felszeghy, S., Jussila, M., Suomalainen, M., Thesleff, I. and Jernvall, J. (2010). Splitting placodes: effects of bone morphogenetic protein and Activin on the patterning and identity of mouse incisors. *Evol. Dev.* **12**, 383-392.
- Murashima-Suginami, A., Takahashi, K., Kawabata, T., Sakata, T., Tsukamoto, H., Sugai, M., Yanagita, M., Shimizu, A., Sakurai, T., Slavkin, H. et al. (2007). Rudiment incisors survive and erupt as supernumerary teeth as a result of USAG-1 abrogation. *Biochem. Biophys. Res. Commun.* **359**, 549-555.
- Nakatomi, M., Wang, X., Key, D., Lund, J., Turbe-Doan, A., Kist, R., Aw, A., Chen, Y., Maas, R. and Peters, H. (2010). Genetic interactions between Pax9 and Msx1 regulate lip development and several stages of tooth morphogenesis. *Dev. Biol.* **340**, 438-449.
- Ohazama, A., Johnson, E., Ota, M., Choi, H., Choi, H., Porntaveetus, T., Oommen, S., Itoh, N., Eto, K., Gritli-Linde, A. et al. (2008). Lrp4 modulates extracellular integration of cell signaling pathways in development. *PLoS One* **3**, e4092.
- Ohazama, A., Blackburn, J., Porntaveetus, T., Ota, M. S., Choi, H., Johnson, E., Myers, P., Oommen, S., Eto, K., Kessler, J. et al. (2010). A role for suppressed incisor cuspal morphogenesis in the evolution of mammalian heterodont dentition. *Proc. Natl. Acad. Sci. USA* **107**, 92-97.
- Ooe, T. (1980). Embryonic development of the incisors in the rabbit (*Oryctolagus cuniculus* L)-dental formula interpretation. *Mammalia* **44**, 259-275.
- Parsa, S., Kuremoto, K., Seidel, K., Tabatabai, R., Mackenzie, B., Yamaza, T., Akiyama, K., Branch, J., Koh, C., Al, Alam, D. et al. (2010). Signaling by FGFR2b controls the regenerative capacity of adult mouse incisors. *Development* **137**, 3743-3752.
- Peterka, M., Lesot, H. and Peterková, R. (2002). Body weight in mouse embryos specifies staging of tooth development. *Connect. Tissue Res.* **43**, 186-190.
- Peterkova, R., Peterka, M., Vonesch, J.-L. and Ruch, J.-V. (1993). Multiple developmental origin of the upper incisor in mouse: histological and computer assisted 3-D-reconstruction studies. *Int. J. Dev. Biol.* **37**, 581-588.
- Peterkova, R., Peterka, M., Viriot, L. and Lesot, H. (2002). Development of the vestigial tooth primordia as part of mouse odontogenesis. *Connect. Tissue Res.* **43**, 120-128.
- Peterkova, R., Lesot, H. and Peterka, M. (2006). Phylogenetic memory of developing mammalian dentition. *J. Exp. Zool. B Mol. Dev. Evol.* **306**, 234-250.
- Peterkova, R., Churava, S., Lesot, H., Rothova, M., Prochazka, J., Peterka, M. and Klein, O. (2009). Revitalization of a diastemal tooth primordium in *Spry2* null mice results from increased proliferation and decreased apoptosis. *J. Exp. Zool. B Mol. Dev. Evol.* **312B**, 292-308.
- Pispa, J. and Thesleff, I. (2003). Mechanisms of ectodermal organogenesis. *Dev. Biol.* **262**, 195-205.
- Prochazka, J., Pantalacci, S., Churava, S., Rothova, M., Lambert, A., Lesot, H., Klein, O., Peterka, M., Laudet, V. and Peterkova, R. (2010). Patterning by heritage in mouse molar row development. *Proc. Natl. Acad. Sci. USA* **107**, 15497-15502.
- Roehl, H. and Nüsslein-Volhard, C. (2001). Zebrafish *pea3* and *erm* are general targets of FGF8 signaling. *Curr. Biol.* **11**, 503-507.
- Seidel, K., Ahn, C., Lyons, D., Nee, A., Ting, K., Brownell, I., Cao, T., Carano, R., Curran, T., Schober, M. et al. (2010). Hedgehog signaling regulates the generation of ameloblast progenitors in the continuously growing mouse incisor. *Development* **137**, 3753-3761.
- Shim, K., Minowada, G., Coling, D. and Martin, G. (2005). *Sprouty2*, a mouse deafness gene, regulates cell fate decisions in the auditory sensory epithelium by antagonizing FGF signaling. *Dev. Cell* **8**, 553-564.
- Sofaer, J. (1969). Aspects of the tabby-crinkled-downless syndrome I. The development of Tabby teeth. *J. Embryol. Exp. Morphol.* **22**, 181-205.
- Tumbar, T., Guasch, G., Greco, V., Blanpain, C., Lowry, W., Rendl, M. and Fuchs, E. (2004). Defining the epithelial stem cell niche in skin. *Science* **303**, 359-363.
- Vahtokari, A., Aberg, T., Jernvall, J., Kerwen, S. and Thesleff, I. (1996). The enamel knot as a signaling center in the developing mouse tooth. *Mech. Dev.* **54**, 39-43.
- Vaezi, A., Bauer, C., Vasioukhin, V. and Fuchs, E. (2002). Actin cable dynamics and Rho/Rock orchestrate a polarized cytoskeletal architecture in the early steps of assembling a stratified epithelium. *Dev. Cell* **3**, 367-381.
- Wang, X.-P., Suomalainen, M., Felszeghy, S., Zelarayan, L., Alonso, M., Plikus, M. V., Maas, R., Chuong, C.-M., Schimmang, T. and Thesleff, I. (2007). An integrated gene regulatory network controls stem cell proliferation in teeth. *PLoS Biol.* **5**, 1324-1333.
- Wang, Y., Meng, J., Ni, X. and Li, C. (2007). Major events of Paleogene mammal radiation in China. *Geol. J.* **42**, 415-430.
- Yokohama-Tamaki, T., Ohshima, H., Fujiwara, N., Takada, Y., Ichimori, Y., Wakisaka, S., Ohuchi, H. and Harada, H. (2006). Cessation of Fgf10 signaling, resulting in a defective dental epithelial stem cell compartment, leads to the transition from crown to root formation. *Development* **133**, 1359-1366.
- Zhang, Z., Verheyden, J. M., Hassell, J. A. and Sun, X. (2009). FGF-regulated *Etv* genes are essential for repressing *Shh* expression in mouse limb buds. *Dev. Cell* **16**, 607-613.

Files in this Data Supplement:

Supplemental Figure S1 -

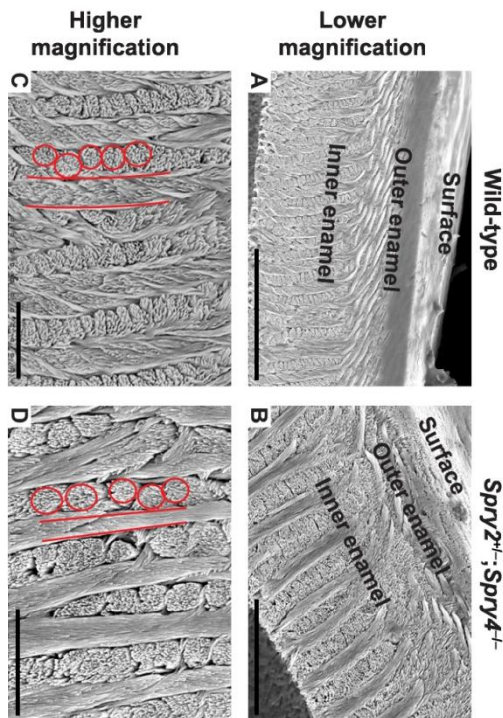


Fig. S1. Environmental scanning electron micrograph of incisor enamel microstructure in wild-type and *Spry2*^{+/-};*Spry4*^{-/-} mice. (A-D) The ectopic lingual enamel of a *Spry2*^{+/-};*Spry4*^{-/-} mouse (B,D) is compared with the labial enamel of a wild-type mouse (A,C). Red lines and circles outline the enamel prisms; \diamond outer enamel \diamond and \diamond inner enamel \diamond indicate the two constitutive layers of enamel. Scale bars: in A, 50 μ m; in B, 25 μ m; in C, 10 μ m; in D, 10 μ m.

Supplemental Figure S2 -

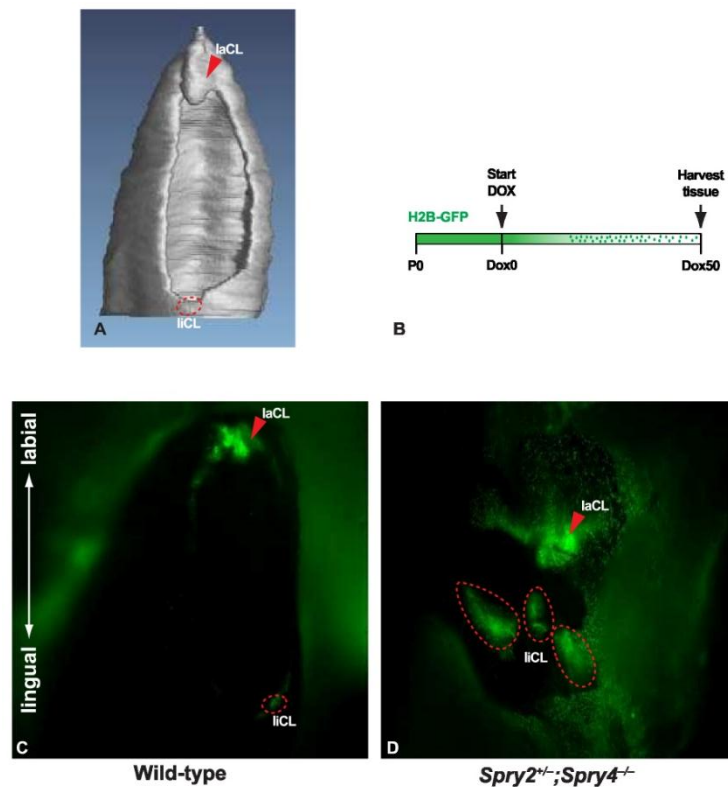


Fig. S2. Multiplication of lingual cervical loops containing label-retaining cells in *Spry2*^{+/-};*Spry4*^{-/-} mice. (A)

Three-dimensional reconstruction of an adult proximal incisor, indicating location of labial and lingual cervical loops. (B) Time-course for treatment of K5tTA;H2B-GFP mice with doxycycline (DOX). P0, postnatal day 0; Dox0, day of first DOX treatment; Dox50, day 50 of DOX treatment. (C,D) Label-retaining cells (LRCs) in wild-type (C) and *Spry2*^{+/-};*Spry4*^{-/-} (D) incisors. Arrowheads point to the population of LRCs on the labial side and dashed circles indicate the populations of LRCs on the lingual part of the tooth. laCL, labial cervical loop; liCL, lingual cervical

loop.

Supplemental Figure S3 -

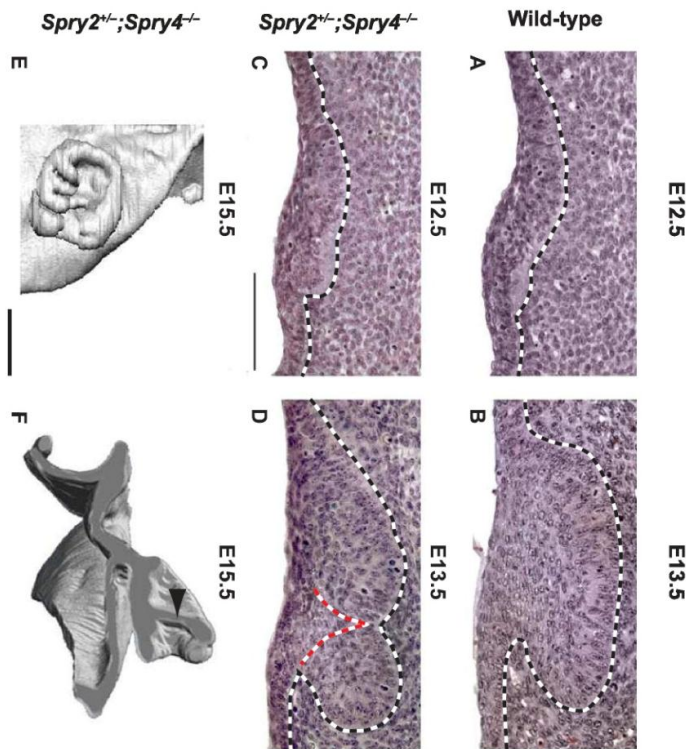


Fig. S3. Subdivision of the developing upper incisor in *Spry2^{+/-};Spry4^{-/-}* mice. (A-D) Frontal histological sections show the incisor placodes of wild-type (A) and mutant (C) mice at E12.5 and the incisor bud of wild-type (B) and mutant (D) mice at E13.5. Internal boundary between two cell populations in the epithelium of *Spry2^{+/-};Spry4^{-/-}* incisor is indicated by red dashed line. Black dashed lines indicate demarcation between epithelium and mesenchyme. (E,F) Three-dimensional reconstructions of the dental epithelium in *Spry2^{+/-};Spry4^{-/-}* embryo at E15.5. The 3D model shown from the mesenchymal aspect with anterior part on the top of the figure (E) has been rotated, semi-frontally sectioned and viewed from posterior aspect (F) to visualize the protruding epithelial septum (black arrowhead). Scale bars: 100 μm.

Supplemental Figure S4 -

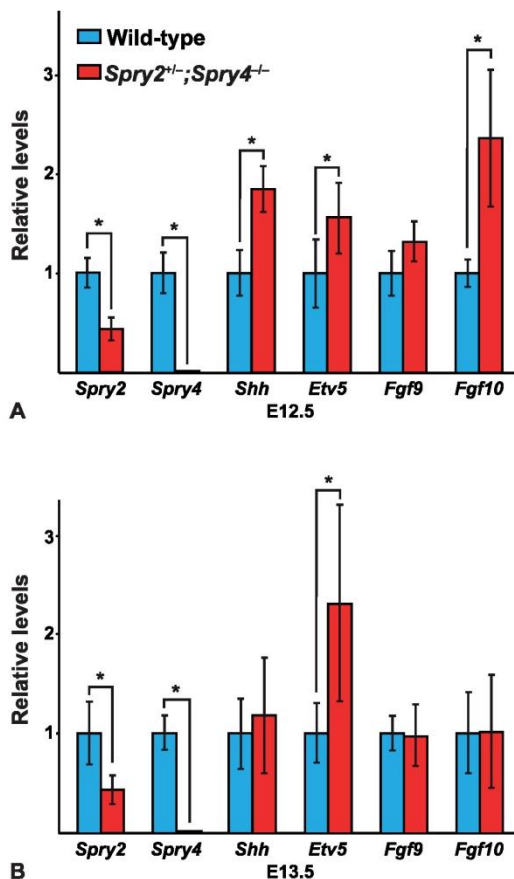
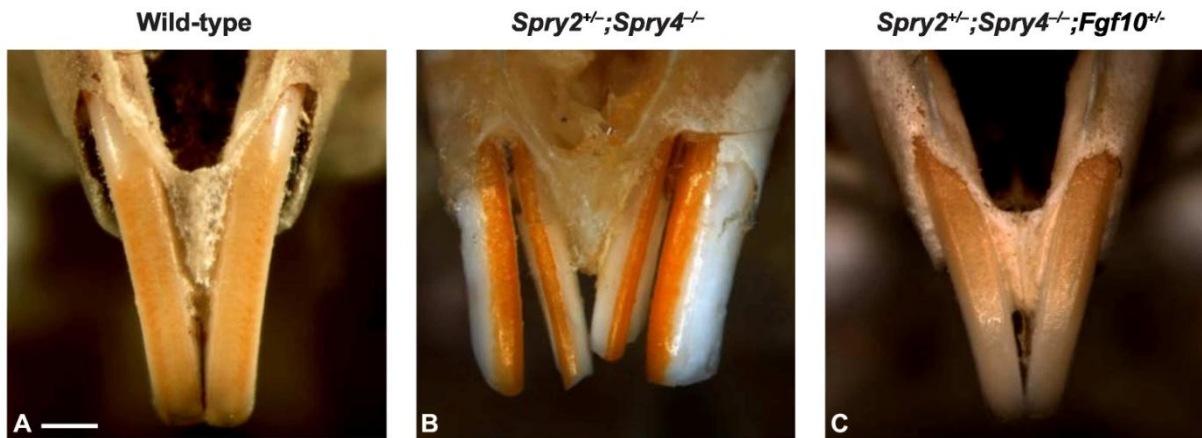


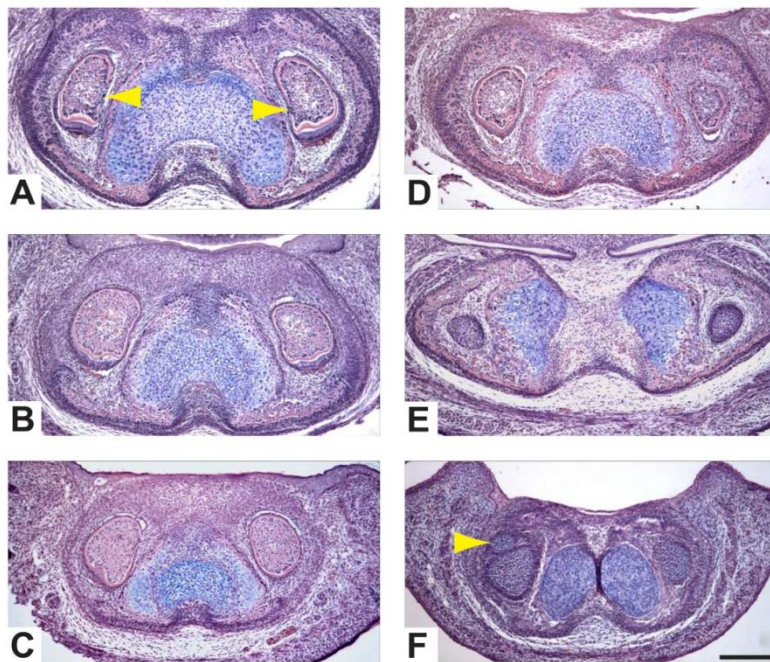
Fig. S4. Quantitative RT-PCR of FGF pathway components and target genes. (A,B) Quantitative RT-PCR of FGF pathway components and target genes of wild-type and *Spry2^{+/-};Spry4^{-/-}* at E12.5 (A) and E13.5 (B). Error bars represent s.d. * $P < 0.005$.

Supplemental Figure S5 –

Fig. S5. Rescue of the incisor duplication phenotype in *Spry2*^{+/-};*Spry4*^{-/-};*Fgf10*^{+/-} mice. (A-C) In the wild-type (A), all mice have a single pair of incisors, whereas 43% of *Spry2*^{+/-};*Spry4*^{-/-} mice (B) have duplicated incisors. In *Spry2*^{+/-};*Spry4*^{-/-};*Fgf10*^{+/-} mice (C), only 17% of mice have duplicated incisors.



	Wild-type	<i>Spry2</i> ^{+/-} ; <i>Spry4</i> ^{-/-}	<i>Spry2</i> ^{+/-} ; <i>Spry4</i> ^{-/-} ; <i>Fgf10</i> ^{+/-}
<i>One incisor</i>	50/50 (100%)	17/30 (57%)	10/12 (83%)
<i>Two incisors</i>	0/50 (0%)	13/30 (43%)	2/12 (17%)



Supplemental Figure S6 –

Fig. S6. Lower incisor phenotypic range of K14-S4^{GOF} mice. (A) Milder phenotype, with a break in the medial side of the incisors (yellow arrowheads). **(B-E)** Typical phenotype, showing small incisors and impaired ameloblast differentiation. **(F)** One case of unilateral supplementary small incisor (yellow arrowhead) and impaired ameloblast differentiation. Scale bar: 200

µm.

Supplemental Figure S7 -

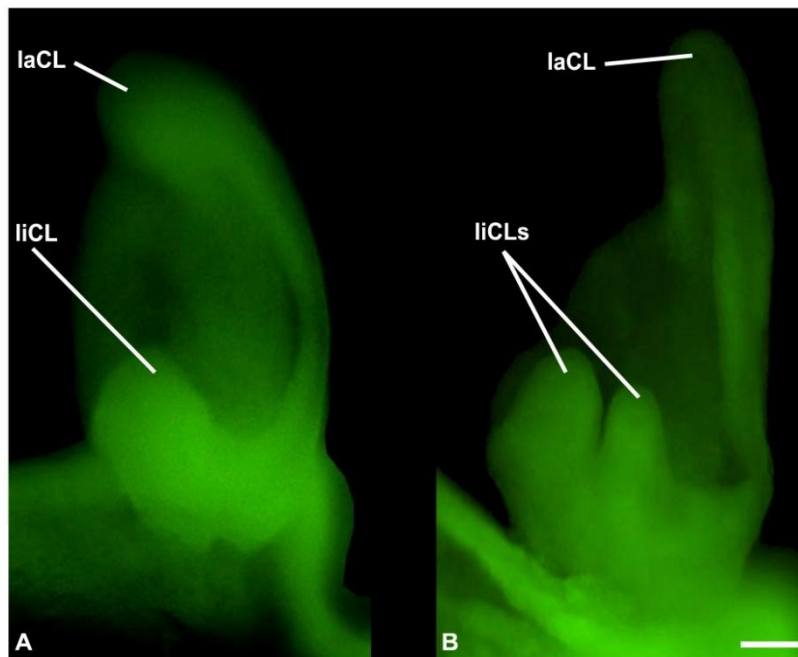


Fig. S7. Lingual cervical loop duplication in wild-type embryos at E15.5. (A) Most frequent embryonic incisor morphology with one lingual cervical loop. (B) Embryonic incisor with a duplication of the lingual cervical loops. laCL, labial cervical loop; liCL, lingual cervical loop. Scale bar: 50 μ m.

Supplemental Table S1 -

Table S1. Primer sequences for quantitative RT-PCR

Gene	Primer sequences
<i>Spry2</i>	F - GCAGTGCCTCTGCTCAGCCC R - ACCCGGCCTGTTCACTCGGT
<i>Spry4</i>	F - CCCGTGAGTAGCAGGATGGAGAAGG R - CTGGAGGATGGCGTGATGAGCGGAC
<i>Shh</i>	F - TTACGTCCCGGAGACCGCGT R - GTGGGCCCGAGTCGTTGTG
<i>Etv5</i>	F - GACCCTGCACAGCCGTTCCC R - CGTCCCCACCGTCCAAACC
<i>Fgf9</i>	F - ACCTCGGCATGAACGAGAAG R - TCTCCTTCCGGTGCCACATGTTT
<i>Fgf10</i>	F - CCGAGGACGGAGCGAGGACA R - CGGCAGGTGGGGAAAGGCTG
<i>L19</i>	F - ATGTATCACAGCCTGTACCTG R - TTCTGGTCTTCTCTCTTG

Annex 4

Collection numbers of natural history museums specimens

Species	Source	Collection number
<i>Bathyergus suillus</i>	MNHN	2298
<i>Heliophobius argenteocinereus</i>	MNHN	7088
<i>Gerbillus sp.</i>	MNHN	CG-1992-1887
<i>Geomys bulleri</i>	NHM	93-3-6-22i
<i>Geomys bursarius</i>	NHM	7-7-7-1808i
<i>Myotomys unisulcatus</i>	MRAC	34234
<i>Parotomys brantsii</i>	MRAC	34236
<i>Otomys irroratus</i>	MRAC	34402
<i>Microtus arvalis</i>	MNHN	CG-1903-704
<i>Eliurus minor</i>	MNHN	CG-1957-783
<i>Nesomys rufus</i>	MNHN	CG-1957-784

- MNHN: Muséum National d'Histoire Naturelle, Paris, France
- NHM: National History Museum, London, UK
- MRAC: Muséum Royal d'Afrique Centrale, Tervuren, Belgium